Ruamāhanga Catchment Groundwater Modelling

C. Moore
M. Toews
M. Gyopari
D. Mzila

GNS Science Report 2016/162
October 2017

GNS SCIENCE
TE PŪ AO

DISCLAIMER

BIBLIOGRAPHIC REFERENCE

Moore, C.[1]; Gyopari, M.[2]; Toews, M.[1] Mzila, D.[3] 2017. Ruamāhanga Catchment Groundwater Modelling, *GNS Science Consultancy Report* 2016/162. 189 p.

[1] GNS Science
[2] Earth in Mind Ltd
[3] Greater Wellington Regional Council

CONTENTS

FIGURES

TABLES

APPENDICES

APPENDIX FIGURES

APPENDIX TABLES

EXECUTIVE SUMMARY

Groundwater and surface water flow and groundwater contaminant transport models have been developed for the Wairarapa Valley as an integral component of the Greater Wellington Regional Council Collaborative Modelling Project (termed the 'Ruamāhanga CMP'). The models are linked to surface water, contaminant loading, contaminant transport and soil moisture balance models which together provide an integrated modelling system designed to simulate water and contaminant fluxes between the land surface, groundwater and surface water environments. The modelling system provides a tool for exploring the groundwater and surface water quality implications of various land and water management scenarios to assist decision making.

The groundwater modelling study had the following objectives:

- Construction of groundwater and surface water flow models for the Wairarapa plains which are linked to a contaminant transport groundwater model, using the previously developed FEFLOW model as a foundation;
- The models should be calibrated over a range of climatic and abstraction conditions using measured groundwater levels, stream flows and other 'real-world' water balance measurements;
- The models should accurately simulate the connections between surface water and groundwater;
- Contaminant loadings (nitrate) to groundwater from land use and from surface waters should be simulated by the model. The models should be able to closely match the observed nitrate concentration spatial patterns in groundwater;
- Contaminant transfers from groundwater to surface water and vice versa should be represented;
- The groundwater models should be able to 'speak' to other models which form part of the CMP (for instance the IRRICALC recharge and water demand model and the Source surface water model)
- The study should incorporate methodologies that seek to optimisation and reduce the uncertainly of the models predictions. An analysis of the uncertainty of the models should also be undertaken.

Modelling of Wairarapa Valley groundwater system has utilised the United States Geological Survey three-dimensional groundwater modelling code MODFLOW. This code is able to interface with the other models used in the CMP. The groundwater contaminant transport model (MT3DMS) was also used with MODFLOW to simulate the transport of nutrients in groundwater.

Three separate but interdependent models provided inputs to the groundwater models:

- IRRICALC — a soil moisture balance model which calculates rainfall runoff, aquifer recharge and irrigation water demand.
- TOPNET — a surface water routing hydrological model for simulating river flows in the hill country feeding into the plains.
- OVERSEER — a farm nutrient budget model for simulating nutrient loadings into groundwater and in surface runoff.

The groundwater model was also linked to the SOURCE surface water contaminant transport model.

The MODFLOW-based modelling system significantly advances the functionality of previous models for the Wairarapa Valley constructed using FEFLOW (2010). These earlier models were focussed upon accurately representing the geological environment and simulating groundwater flows and balances, including the connectivity to surface water. However, the FEFLOW models did not simulate stream/river flow rates nor contaminant transport through surface water and groundwater — both essential requirements for the NPS-FM and whaitua limit setting processes. Unlike the FEFLOW models, the MODFLOW models also have significantly enhanced capability in terms of interfacing with other models (as listed above) to allow more accurate and holistic surface water-groundwater simulation and contaminant transport (in surface water and groundwater). They also employ more robust and state-of-art calibration and uncertainty analysis technologies.

Two MODFLOW/MT3DMS models were constructed for the Wairarapa Plains: The ‘northern model’ covers an area of 425 km^2 and incorporates the middle catchment of the Ruamāhanga River and its tributaries — the Waiohine, Waingawa and Waipoua rivers. The ‘southern model’ covers an area of 680 km^2 and incorporates the lowland catchments of the Tauherenikau and Ruamāhanga rivers, Lake Wairarapa and Lake Onoke. The models were based upon a previously developed conceptual geological interpretation of the groundwater system, and the FEFLOW model parameterisation. Deviations from this model occurred only to the extent that this deviation was informed by measurements.

Surface water flow simulation was facilitated using the MODFLOW Streamflow routing (SFR) package. SFR is able to handle surface water runoff inputs and surface water abstractions (both provided by IRRICALC). SFR was calibrated to observed river and stream flows and relied upon flow inputs provided by TOPNET at the model boundaries.

Model calibration involved adjusting model parameter values until the model outputs match the historical measurements of groundwater levels, concentrations, and surface water flows. The aim of calibration is to ensure that the model can simulate the status quo, and on that basis then make more reliable predictions of the future. The northern and southern models were initially calibrated for the period 1992 to 2007 using 7-day stress periods (inputs and outputs were averaged over 7 days). Calibration targets were groundwater levels, measured surface water flow losses and gains, and measured spring and stream flows.

Summary of Calibration results

Overall, the model simulated outputs matched the measured data reasonably well, with correlation coefficient (R-squared) values over 0.9 and 0.8 for the north and south models respectively. Model to measurement mismatches can be explained with reference to the model uncertainty analysis.

The simulated surface water flows closely matched the measured surface water flows at the surface water gauging sites in terms of the overall pattern of high and low flows. This was the case for both groundwater spring fed streams, e.g., Tilsons Creek and Papawai Stream and the large losing and gaining streams, e.g., Ruamāhanga River and Waiohine River.

Flow duration curves were also used to show how well the range of flows are simulated. For most of the gauging sites the modelled flow duration curves matched measured (actual) flows. for most gauging sites.

While only the stream flows were used as calibration targets, the mean annual low flow, the flow duration curves and the number of days below the partial and full restriction flows were also analysed for reporting purposes. While improved fits to these additional reporting measures would be expected by including these measures as calibration targets in the calibration process, that groundwater simulation models are most reliable when assessing differences rather than absolutes. Therefore, these metrics can be estimated most robustly in the context of assessing relative impacts.

The ability to simulate groundwater-surface water interaction is another main objective of the model development listed above, and is important when assessing stream depletion impacts from groundwater pumping. The simulated flows between groundwater and surface waterways match the spatial and temporal pattern of measured losses and gains well. Of interest is the interaction with the lake in the south model. The simulated flows indicate groundwater seeping into the lake along the western and southern lake margins.

The simulated groundwater levels reflect the measured groundwater levels and their relative responses to climatic and pumping stresses. In general model to measurement fits for groundwater levels are better in the north model than in the south. The model to measurement misfit result in part from the model layer structure adopted and the assignment of flow conditions assigned to that layer structure. For example, in the south model it appears that the magnitude of some of the simulated water level fluctuations are larger than the measured, which may indicate unconfined aquifer conditions occur to a greater depth than simulated. Reasons for this greater range of water level fluctuations in some wells could also be attributed to nearby groundwater abstractions that were not included in the model. It is recommended that future work with these models investigate these issues further.

Measured nitrate concentrations vary significantly over short distances, including within the same model grid cell, making it impossible to match all measured nitrate concentrations well. Despite the challenging nature of these observations the model outputs capture the spatial and depth trend in measured nitrate values. Residual model to measurement misfit in these nitrate values are accounted for in the uncertainty analyses discussed in Section 7.

As expected the calibrated model simulates some parts of the system very well, and less well in others. This range of model to measurement fits is experienced in all groundwater models, and occurs because the model cannot include all of the real-world complexity.

For scenario testing the remaining model to measurement misfit in the calibrated model will be accounted for in two ways. Scenario testing will assess the relative changes in flows and levels from these base flow conditions. These estimated <u>differences</u> in flows are more straightforward to estimate than absolute values of flows and levels, because to some extent the misfit errors cancel each other out. Secondly, the model to measurement misfit will be accounted for in the uncertainty analyses accompanying selected model scenario outputs.

Uncertainty analysis

The advantage of the complex model adopted in this study, is that while all model simulated flows and groundwater levels have uncertainty associated with them; this uncertainty is able to be robustly quantified.

The degree to which the model parameters were able to be estimated through the calibration process, and the remaining parameter uncertainties were analysed. One contributor to this parameter uncertainty is the degree of model to measurement misfit described above.

However, model parameter uncertainty also occurs because variations in the strata and the flow system below the ground can never be perfectly known on the basis of sparsely distributed well data. To address this incomplete knowledge, we have described the reliability of model parameters. Parameter error was quantified using a Bayesian linear uncertainty analysis.   We have also described the extent to which the model calibration reduced the parameter uncertainty.

To the extent that calibrated model parameters have uncertainty associated with them, so will the model scenario outputs simulated on the basis of these parameters. The impact that these uncertainties may have on future scenario simulations can be quantified for selected scenarios on the basis of the parameter uncertainty analysis described in this report.

1.0 INTRODUCTION

This report documents the groundwater modelling component of the collaborative modelling project (CMP) for the Wairarapa Valley.

The overall purpose of this groundwater modelling is to contribute a robust technical foundation for the development of a sustainable groundwater management policy for the Wairarapa region. The groundwater models developed for this project build upon earlier groundwater modelling work undertaken by Greater Wellington Regional Council (Gyopari and McAlister, 2010a, 2010b and 2010c). In particular, the comprehensive geological, hydrogeological and conceptual interpretations have been carried through from the earlier work and form the basis of the new models. Furthermore the model construction and parameterisation of the earlier FEFLOW models are used as the foundation of the current model development.

The previous FEFLOW modelling carried out by Greater Wellington (Gyopari and McAlister 2010a, b, c) had a strong focus on developing the geological conceptualisation of the groundwater system — this has not been revisited. It is important to note that the extensive geological analysis invested in the FEFLOW models is regarded to be the best interpretation that currently exists. For this reason, these former models are the foundation of the current model development, and are only altered where data supports this adjustment.

The new CMP 'MODFLOW and MT3D models' represent a step change in groundwater model simulation capability in a number of ways. Most importantly, they expand the functionality of the earlier models in terms of their ability to simulate stream flows, surface water and groundwater interaction (including with lakes) and are able to simulate groundwater and surface water transport and associated water quality impacts. Furthermore, the new CMP models employ significantly more robust calibration methodologies, including the use of distributed parameters, and incorporate parameter uncertainty analyses. The CMP models are also integrated with a number of other models, and are designed to provide a more robust coupled climate — land use – surface water – groundwater simulation framework for integrated testing of various land management and climatic scenarios.

This report provides documentation of the model purpose and objectives (Section 2), model construction and calibration (Sections 3, 4, and 5), and model limitations and associated parameter uncertainty (Section 6). Section 7 briefly summarises the model calibration and uncertainty analysis and describes future scheduled work on the model.

Appendix 1 contains a description and analysis of the physical characteristics of the Wairarapa plains in terms of physiography, surface water and groundwater. The conceptualisation of the groundwater environment is also described. Appendix 1 generally represents a synthesis of the work carried out for the 2010 greater Wellington groundwater study (Gyopari and McAlister, 2010a, 2010b and 2010c).

Appendix 2 contains a summary of the programs written to support the model calibration and integration with other models in the CMP.

Appendix 3 contains plots of model output and measurement comparisons for groundwater levels and stream flows.

2.0 GROUNDWATER MODELLING PURPOSE AND OBJECTIVES

The purpose of this groundwater modelling project is to produce a robust simulation tool to assist in the management of the groundwater and surface water resources in the Wairarapa Valley with respect to both quantity and quality.

Principal objectives of the groundwater modelling study are as follows:

- Construction of a numerical groundwater flow and contaminant transport models for the groundwater system using an appropriate model code to a level of complexity consistent with the models purpose and available information.
- Calibration of the model to historic long-term transient climatic and abstraction stresses using observed groundwater level, stream flows and water balance targets. The model should robustly simulate the connection between surface water and groundwater, groundwater levels and stream flows.
- Simulation of the movement of contaminant loadings to groundwater from land use and from surface waters and calibrate to measured nitrate concentrations.
- Simulation of nitrate movement to surface waters.
- Simulation of the relative changes to surface water flow and groundwater levels in response to changes in climate, resource developments and water management. This component of work is being undertaken in the scenario testing phase of the project.
- Dynamically integrate and couple the groundwater model with other models to both facilitate receipt of inputs to the groundwater models, and conversely, to provide inputs to other models.
- Undertake parameter uncertainty analysis and quantify the extent to which the calibrated model has reduced the parameter uncertainties, and assess how these uncertainties may impact the predictive capacity of the model.
- Quantify regional and sub-regional water balances and their long-term seasonal variability in response to changes in climate and abstraction stresses.
- Identify the limitations and critical model assumptions.

3.0 MODEL CONSTRUCTION

3.1 MODEL CODE SELECTION

A number of numerical computer codes can simulate groundwater flow, each with inherent strengths and weaknesses. To meet the objectives of this study, important considerations when selecting a suitable model code were:

- Requirement to provide a framework that could be used to represent both regional and local-scale features in one integrated model and incorporate important features at both scales. It is intended that where local-scale features are at very fine scale, the framework needed to be able to support nested local models (e.g. hot-spot models).
- Ability to represent complex and irregular geology and complex aquifer conditions.
- Ability to accurately simulate the interaction between groundwater and surface water and couple this model with a surface water simulation model.
- Ability to simulate surface water flows and groundwater level responses to climate and abstraction stresses.
- Ability to facilitate coupling with other models (such as a surface water, contaminant loading and recharge/abstraction models).
- Ability to simulate transport of land based nutrient loadings through the groundwater environment, and the discharges of these nutrient loads from groundwater to surface water.

The United States Geological Survey (USGS) three-dimensional finite difference groundwater flow modelling code MODFLOW-2005 (Harbaugh, 2005) was selected because it meets the above criteria when used in conjunction with the three-dimensional groundwater transport model MT3DMS (Zheng and Wang, 1999). Because of its open source nature of these codes, they are highly amenable to integrating with other models through development of custom-built scripts.

MT3DMS (implemented within MODFLOW) can be used to simulate changes in concentrations of miscible contaminants in groundwater by considering advection, dispersion, diffusion (and some basic chemical reactions) with various types of boundary conditions and external sources or sinks.

3.2 COUPLING MODFLOW AND MT3DMS WITH EXTERNAL MODELS

Several external models have either provided input into, or received inputs from, the MODFLOW and MT3DMS models. The connections between these models are depicted in Figure 3.1. Pre-processing and the writing of a number of small utility programs were written to take outputs from the external models and put them into the format required for running MODFLOW and MT3DMS. A summary of each link to the external model, the processing required and a reference to the scripts used is described below. Appendix 2 contains the code written for the utility programs.

The four principal MODFLOW/MT3DMS interfacing models are:

- IRRICALC — a soil moisture balance, rainfall runoff and irrigation demand model (Aqualinc, 2016).
- TOPNET — a hydrological model for simulating catchment water balance and river flow (https://one.niwa.co.nz/display/HYPRO/TOPNET+++Model).

- SOURCE — a surface water contaminant transport and flow routing model (http://ewater.org.au/products/ewater-source/source-overview/).
- OVERSEER — a farm nutrient budget model and management tool (http://overseer.org.nz/).

IRRICALC was used to calculate rainfall recharge, rainfall runoff or 'quick flow', and irrigation water demand. Irrigation demand modelling relied on irrigated area and surface water and groundwater consents data bases (CMP Aqualinc report, 2016). The IRRICALC water demand, recharge and runoff outputs were then imported to MODFLOW (WELLS and SFR packages).

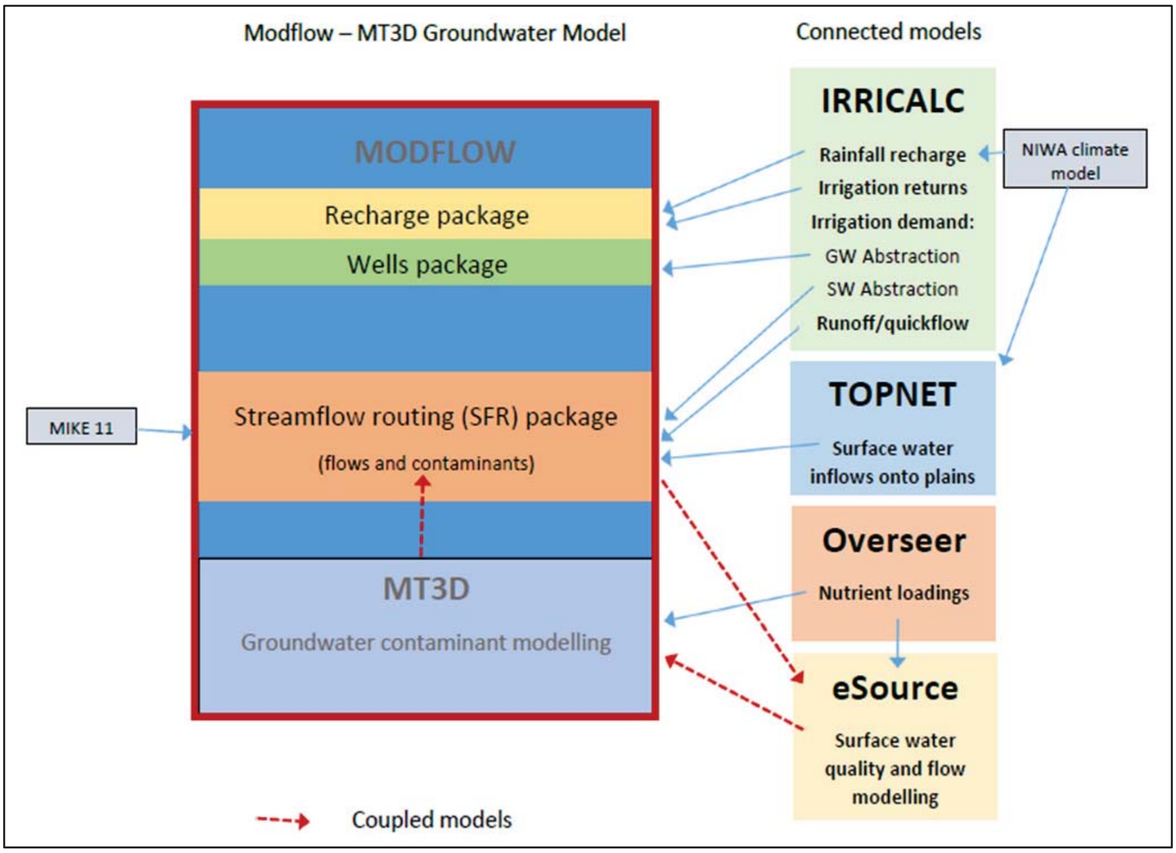

Figure 3.1 Integration of MODFLOW and MT3DMS with other models. Customised transfer scripts were developed to transfer data between models (see Appendix 1)

MT3DMS simulates contaminant transport processes in groundwater and fluxes between surface water and groundwater. The SOURCE model (CMP Jacobs report, 2016) was used to simulate contaminant transport processes within surface water channels. MODFLOW/ MT3DMS also provide groundwater-surface water nutrient load fluxes to SOURCE. A Python script was written to process budget and concentration files from the MODFLOW/MT3DMS models and writes outputs tailored to SOURCE requirements (Appendix 1).

TOPNET (CMP NIWA report, 2016) provided the surface water inflows to the SFR boundaries at the edges of the groundwater flow model where rivers and streams enter. Within the groundwater model the surface water system was simulated using the MODFLOW stream ('SFR') package in parallel with the SOURCE model. Surface water flows within the MODFLOW model domain are influenced by surface water abstractions (simulated using SFR diversions) and by groundwater-surface water exchanges (simulated by MODFLOW/SFR).

The OVERSEER model provided the nutrient loadings for irrigated areas to MT3DMS which simulates transport of nutrients into the groundwater system and subsequent discharge to the surface water environment (CMP MPI report 2016).

3.3 TWO MODEL DOMAINS: NORTH AND SOUTH MODELS

The groundwater system for the Wairarapa Valley is defined by the occurrence of late Quaternary and Holocene alluvial sediments (Appendix 1). The northern and southern sub-regional flow systems (described in Appendix 1, Figure A4.10) are represented by two separate groundwater models (Figure 3.2). The reason why a single model was not created relates to practical constraints concerning the large size of the groundwater system and the need to incorporate an adequate degree of complexity and workable model run times. The two models represent separate groundwater basins with negligible groundwater flow occurring between them. Groundwater in the northern model is discharged to surface water prior to it flowing into the southern model domain. Flows in the Ruamāhanga River, where it crosses from the northern to southern models, carries all groundwater discharge and surface water discharge from the northern domain. The Ruamāhanga River therefore represents the hydraulic connection between the models (this is the only surface water channel to cross the boundary).

The northern model domain covers an area of 425 km^2 and incorporates the middle catchment of the Ruamāhanga River and its tributaries – the Waiohine, Waingawa and Waipoua rivers. Tiffen Hill represents an up-faulted block of greywacke basement within the model domain (modelled as an internal inactive area).

The southern model covers an area of 680 km^2 and incorporates the lowland catchments of the Tauherenikau and Ruamāhanga rivers, Lake Wairarapa and Lake Onoke. Te Maire ridge consists of an uplifted greywacke basement block and is represented as an area of very low permeability (modelled as an internal inactive area). The domain is 42.5 km in length, extending from the southern edge of the Waiohine Plains to the coast at Lake Onoke. The maximum width of the modelled catchment is approximately 30 km, extending from the base of the Tararua Range to the eastern hills incorporating the Martinborough terraces and the Huangarua Valley.

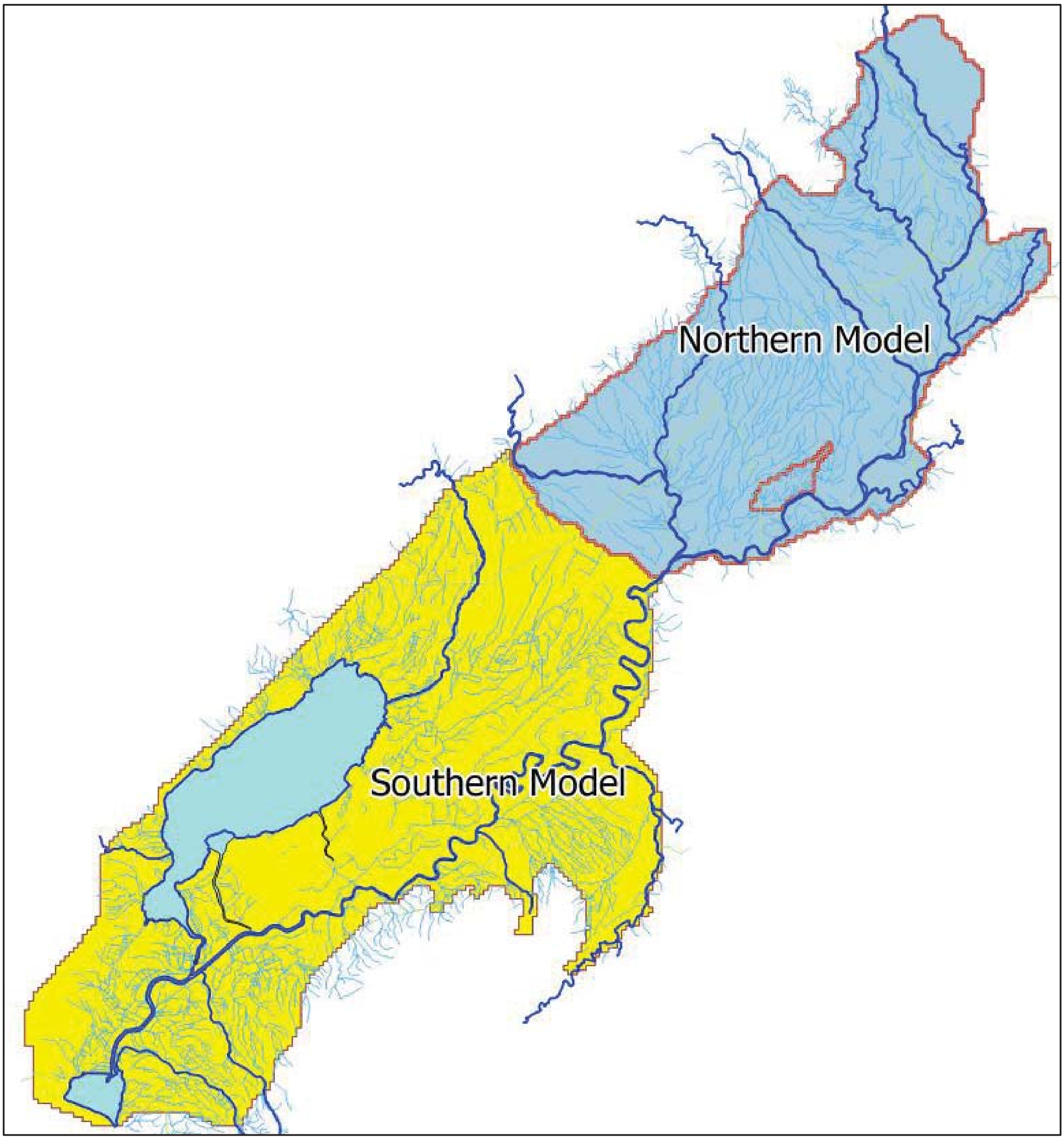

Figure 3.2 Northern and southern groundwater model domains for the Wairarapa Valley.

3.4 GRID AND LAYER DESIGN — NORTHERN AND SOUTHERN MODELS

The northern and southern models retain the fundamental layer structure and geometry of the previous FEFLOW models (Gyopari and McAlister, 2010a, 2010b and 2010c) to honour their geological interpretation and conceptualisation.

The northern MODFLOW model structurally represents a fusion of the FEFLOW Upper and Middle valley models. The southern model is equivalent to the FEFLOW Lower Valley model. FEFLOW had requirements concerning the simulation of vertical flow and the need to use additional layers within aquiclude units. It was however possible to rationalise the number of layers in the MODFLOW models whilst retaining the same hydrostratigraphic units and layer geometry.

The layer surfaces were based upon the suite of geological cross sections developed for the FEFLOW models (Gyopari and McAlister, 2010a, 2010b and 2010c, see also Appendix 1). Where there were no bore log data, layer surfaces were extrapolated to maintain consistency with the conceptual hydrogeological model. Each layer surface was modelled externally using ArcMap prior to importing into the model. The process of developing model layers was essentially an iterative one of using the cross sections as a control and tailoring the surfaces to maintain consistency with the conceptual model and the geological interpretation of the catchment.

The ground surface was modelled using a combination of LIDAR data and the 20-m contour topographic map digital dataset. The base of the model coincides with the interpreted lower boundary of the Q8 alluvial sediments and represents the base of the groundwater flow system.

Both the northern and southern models have been set up with a finite difference grid size of 250 m^2. This is an appropriate size to enable the representation of the irregular geological boundaries and simulate a sufficient spatial resolution for recharge, contaminant loadings and abstractions.

3.4.1 Northern Model: MODFLOW Layer Configuration

Figure 3.3 shows the active domain for the northern model which covers an area of approximately 425 km^2 with a grid spacing of 250 m and five layers (about 6,800 cells per layer; 33,900 active cells in total). Internally, the uplifted greywacke basement block of Tiffen hill is represented by an inactive grid area. The major Masterton and Carterton faults, recognised as representing partial regional barriers to groundwater flow, have been simulated using the MODFLOW WALL package with an effective thickness of 1 m. The northern most Masterton fault has been assigned an initial hydraulic conductivity of 0.1m/day, whilst Carterton Fault is recognised as being more permeable and is consequently assigned a hydraulic conductivity of 6 m/d (approx. 10–30 times less than the formation hydraulic conductivity). These values were derived from the previous FEFLOW model calibrations and will undergo further calibration testing in this model.

The models five layers correspond to the hydrostratigraphic units shown in Table 3.1. The layer surfaces were transferred and merged from the equivalent FEFLOW model slices for the Middle and Upper valleys (MV and UV, respectively). Since the UV FEFLOW model had a much simpler layer structure, consistent layer thicknesses simulated in the MV area were extended into the LV. This is not envisaged to be a significant problem since the layer divisions below Layer 1 in the UV model are somewhat arbitrarily placed in the fan gravel sequence because no distinct deeper aquifer horizons are identifiable.

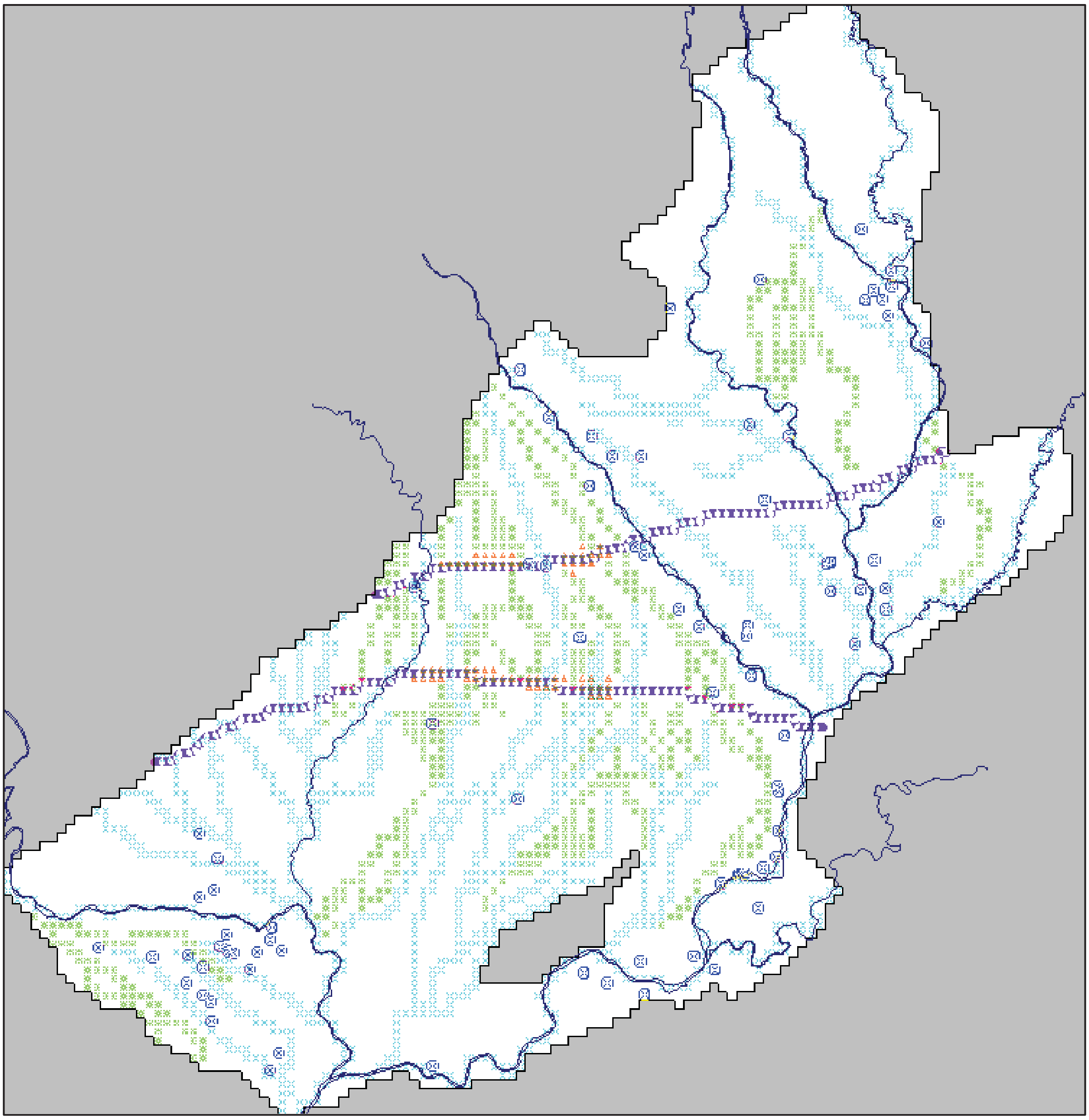

Figure 3.3 Northern model domain showing boundaries, no flow areas (shaded grey) and semi permeable walls representing the Carterton and Masterton regional flow 'barriers' (purple symbols). Other boundary conditions are also shown (SFR = blue symbol; water race injection wells = green symbol; abstraction bores = blue circles; drains/wetlands = orange symbol along faults).

Table 3.1 Northern model layer structure and equivalent FEFLOW model layers to show data source for MODFLOW model.

MODFLOW layer	Unit	FEFLOW Middle Valley layer	FEFLOW Upper Valley layer
1	Q1 Aquifers (where present). Fan gravels elsewhere	1, 2	1
Base L1 source:		Slice 3	Slice 2
2	Q2–4 aquifers in sub basins, fan gravels elsewhere.	3, 4	2
Base L2 source:		Slice 5	Slice 3
3	Q5 Aquitard – central Parkvale area, fan gravels elsewhere.	5, 6	Not explicitly modelled
Base L3 source:		Slice 7	Extend MV layer thickness into UV area.
4	Q6 Gravels – Aquifer in sub basins, fan gravels elsewhere.	7, 8	3
Base L4 source:		Slice 9	Slice 4
5	Q7–8 – Aquifers in sub basins, fan gravels elsewhere.	9	4
Model base source:		Slice 10	Slice 5

3.4.2 Southern Model MODFLOW Layer Configuration

Figure 3.4 shows the active domain for the southern model which covers an area of 680 km^2 with a grid spacing of 250 m and eight layers (about 10,800 cells per layer; 86,560 active cells in total). The model has eight layers which correspond to the hydrostratigraphic units shown in Table 3.2. The layers were transferred from the equivalent FEFLOW LV model slices indicated.

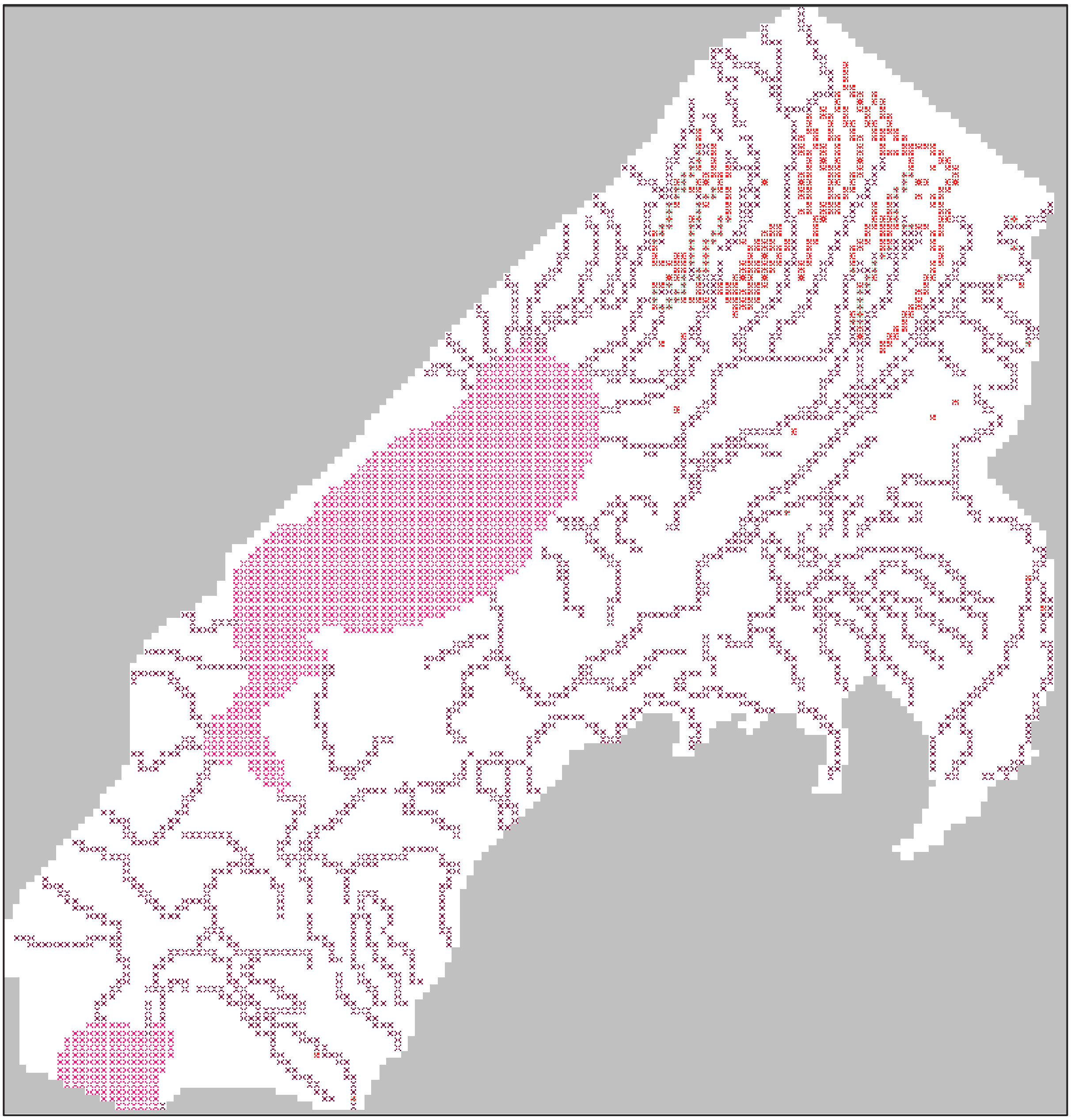

Figure 3.4 Southern model domain showing boundaries, no flow areas (shaded grey). Boundary conditions shown are SFR (purple cross symbol), lake (pink symbol) and water race injection wells (red symbol).

Table 3.2 Southern model layer structure and equivalent FEFLOW model layers to show data source for MODFLOW model.

MODFLOW layer	Unit	FEFLOW Lower Valley layer
1	**Q1 Aquifers:** Ruamāhanga, Huangarua, Tauherenikau. **Q1 aquitard:** Holocene lake sediments – Lake basin. Q2–8 fan gravels: Tauherenikau fan, Huangarua Valley, Martinborough Terraces, Onoke area.	1, 2
Base L1 source:		Slice 3
2	**Q1 Aquifers:** Ruamāhanga, Huangarua. **Q1 aquitard:** Holocene lake sediments – Lake basin. Q2–8 fan gravels: Tauherenikau fan, Huangarua Valley, Martinborough Terraces, Onoke area.	3, 4, 5
Base L2 source:		Slice 6
3	**Q1 Aquifers:** Ruamāhanga, Huangarua. Q2–8 fan gravels: Tauherenikau fan, Huangarua Valley, Martinborough Terraces, Onoke area.	6, 7
Base L3 source:		Slice 8
4	**Q3 Aquitard:** Ruamāhanga, Lake Basin, Onoke. Q2–8 fan gravels: Tauherenikau fan, Huangarua Valley, Martinborough Terraces, Onoke area.	8, 9, 10
Base L4 source:		Slice 11
5	**Q4 Aquifer:** Ruamāhanga, Lake Basin. Q2–8 fan gravels: Tauherenikau fan, Huangarua Valley, Martinborough Terraces, Onoke area.	11
Base L5 source:		12
6	**Q5 Aquitard:** Ruamāhanga, Lake Basin, Onoke. Q2–8 fan gravels: Tauherenikau fan, Huangarua Valley, Martinborough Terraces, Onoke area.	12, 13, 14
Base L6 source:		15
7	**Q6 Aquifer:** Lake basin. Q2–8 fan gravels: Tauherenikau fan, Huangarua Valley, Martinborough Terraces, Onoke area.	15
Base L7 source:		16
8	**Q7and aquitard**: Lake basin. Q2–8 fan gravels: Tauherenikau fan, Huangarua Valley, Martinborough Terraces, Onoke area.	16, 17
Model base source:		Slice 18

3.5 BOUNDARY CONDITIONS

3.5.1 Rivers and Spring-Fed Streams — SFR Boundaries

The MODFLOW Streamflow-Routing Package (SFR version 2) was used to simulate the rivers, streams and spring-fed drainage system. The SFR package was employed for this project since it is designed to route streamflow through a network of channels and budget for diversions to and from stream segments (i.e., surface water abstractions, water race diversions out of the channel, or input into the channel from overland flow). SFR can calculate stream depth using a variety of methods. The method chosen uses a rectangular stream cross sectional area and Manning's roughness coefficient to compute water depth. The SFR package can also be used to route flow to and from the Lake package (used to model Lake Wairarapa and Lake Onoke).

The SFR network of streams is divided into segments that have uniform or linearly changing properties (for example; streambed elevation, thickness, and conductance, and stream depth and width). Each segment can also be associated with tributary flows or a specified inflow or outflow (only at the top of the segment) and diversions (only at the bottom of the segment). Generally, the main Wairarapa rivers have been divided into segments approximately 2 km in length, although this varies depending upon the location of tributary inflows. Some smaller streams have significantly longer segments where they are considered to exhibit relatively uniform properties over long distances. The northern model has 110 stream segments and these occupy a total of 1677 SFR model cells (or reaches), while the southern model has 165 segments and 2580 SFR model cells/reaches.

The SFR package requires the stream bed elevation to be defined at the start and end of each segment. This was achieved using a surface water model MIKE11 which was set up for the previous FEFLOW models using channel geometries derived from GWRC river cross section surveys. Cross sectional surveys at about 100 m intervals are carried out about every five years – the most recent dataset was used for the MIKE11 models.

Figure 3.5 and Figure 3.6 show the SFR segments for the northern and southern flow models respectively. Hydraulic continuity between the northern and southern models is achieved through adding the measured Ruamāhanga River flows to the top segment on the Ruamāhanga River in the southern model.

The external models which are coupled to the SFR package in this CMP project to provide various water budget components are:

- TOPNET (TOPNET report ref): This model provides inflows to the SFR segments at the model boundaries.
- IRRICALC (Aqualinc, 2016): This model provides inflows from overland runoff and diversions for surface water abstractions.

Note that at the time of model development the released version of MT3DMS did not calculate solute transport through the surface water system, only from surface water into groundwater, and throughout the groundwater system. However, a new version of MT3DMS that does calculate solute transport through the surface water system (as the SOURCE model does) is now available for future model versions.

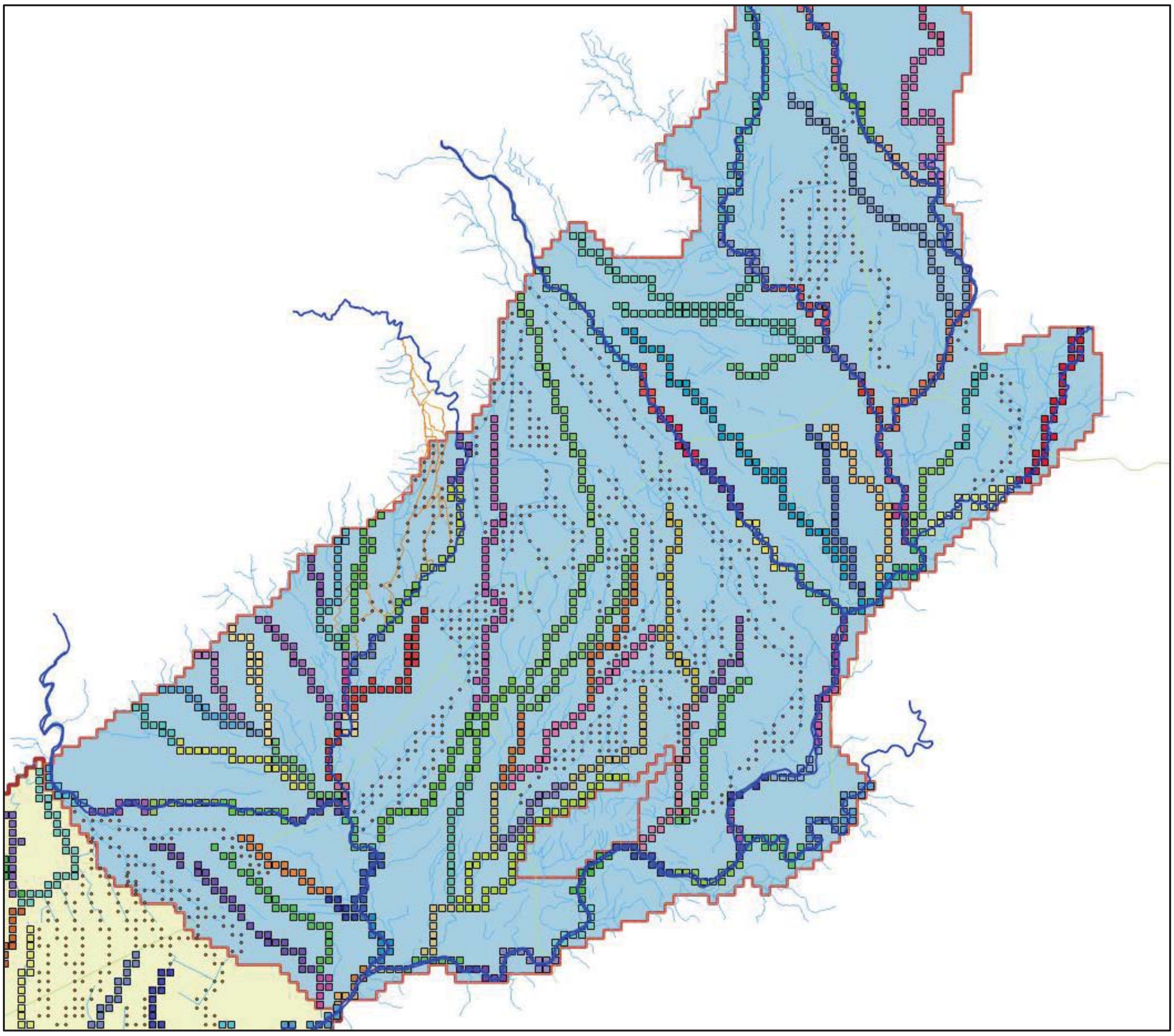

Figure 3.5 SFR1 segments (squares, each segment represented by a different colour) for the northern model for main rivers as well as minor stream and spring-fed drainage systems. Small dots show locations of water race injection wells

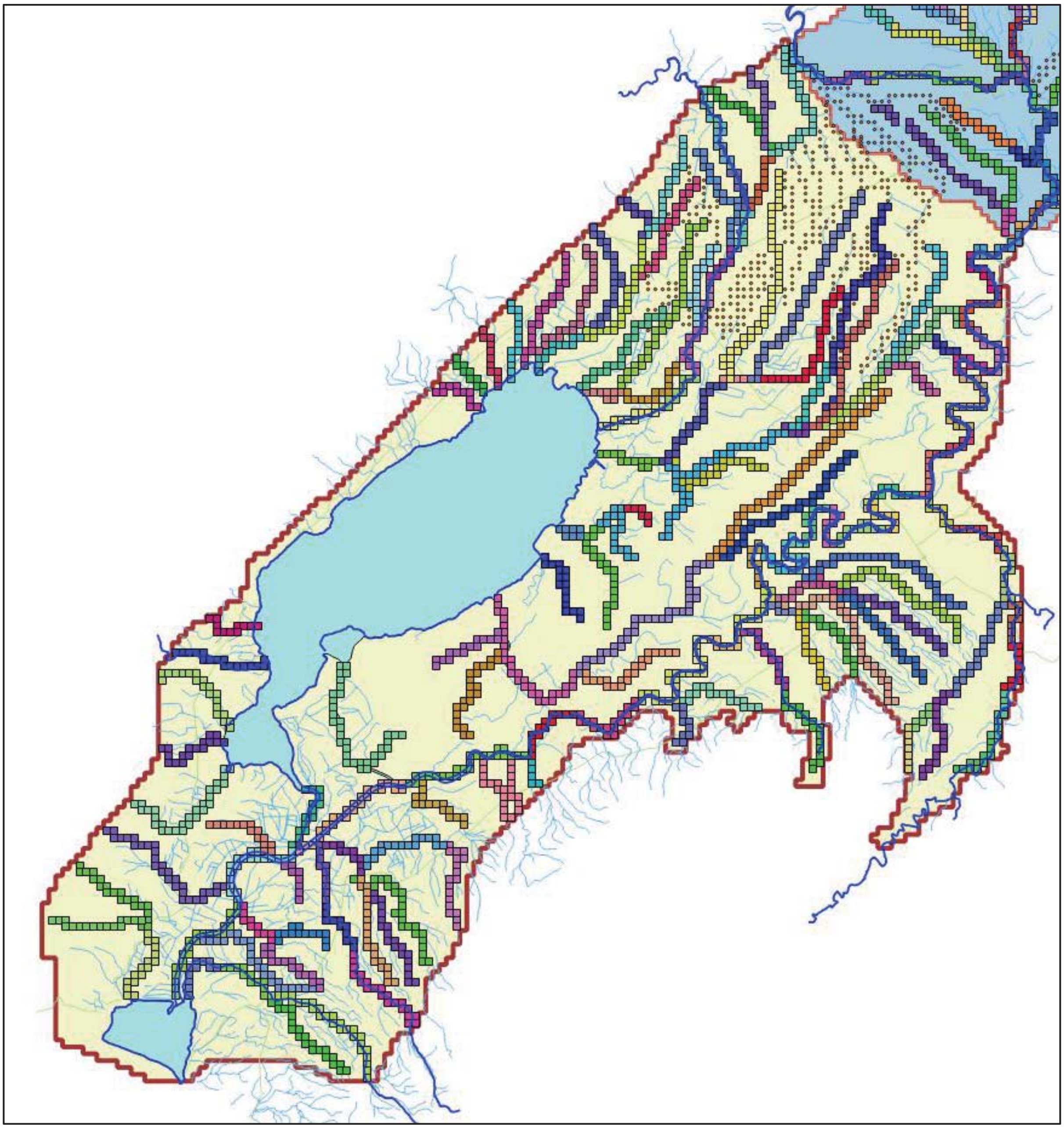

Figure 3.6 SFR1 segments for the southern model for main rivers as well as minor stream and spring-fed drainage systems.

3.5.2 Pumping and Water Race Injection Wells

The MODFLOW WELLS package has been used to simulate both abstraction wells and injection wells to represent recharge from the water race network. There are two types of abstractionwells in the models – irrigations and public water supply wells. The latter have been simulated based upon actual abstraction records provided by operating authorities. Irrigation wells are placed at their recorded locations, depths. Abstraction rates for consented irrigation wells have been provided by the IRRICALC model which has been coupled to the input files for the WELLS package.

The water race injection wells have been placed in layer 1 along the mapped channel networks. It has been assumed that approximately 50% of the flow in the water races (based upon consented rates of flow) leaks through the channel bed to recharge groundwater.

3.5.3 Lake Boundaries

Lakes Wairarapa and Onoke in the southern model have been simulated using the MODFLOW Lake (LAK3) package (Figure 3.4). The lake boundary condition is a head-dependent boundary condition which simulates flow of water into or out of the aquifer whilst taking into account a bed conductance term. The model computes the head for the lake taking into consideration surface water (from SFR) and groundwater inflows and outflows, evaporation and rainfall. The SFR and groundwater exchange fluxes have also been provided for use in the coupled the hydrodynamic ELCOM lakes model (CMP — Allen report, 2016)).

Lake Wairarapa was set up in MODFLOW using a fixed head condition (due to controlled lake levels) of 1.023 m masl, and a bed conductance of 50 m/day. Lake Onoke has a stage fixed at mean sea level (0 m) and the same bed conductivity. Because lake levels were not used as a calibration target in the model these parameter values were not adjusted in the calibration process.

3.5.4 Faultline Wetlands — Drains Boundaries

Drain boundaries have been used in areas of known diffuse groundwater discharge along the Masterton and Carterton Faults (see Figure 3.3). Initial bed conductance values used in all drains cells is 1.2 x 10^5 m^2/day. The base elevations of the drains have been taken from either LIDAR or estimated from topographic maps.

3.6 Hydraulic Property Zonation — Initial Calibration Approach

Development of a hydraulic property zonation framework for both models has maintained consistency with the conceptual hydrogeological model. The previous FEFLOW hydraulic property zones have been used in the MODFLOW models as base parameters, and then are adjusted, where supported by data, during model calibration (Section 5).

3.6.1 Northern Model

Figures 3.7A–E and Figure 3.8 show these FEFLOW model zones for hydraulic conductivity and storage respectively. These have been transferred directly from the previous FEFLOW model (Gyopari and McAlister, 2010a, 2010b and 2010c) as a first estimate prior to further calibration work. Table 3.3 contains the initial hydraulic conductivity parameters assigned to the zones.

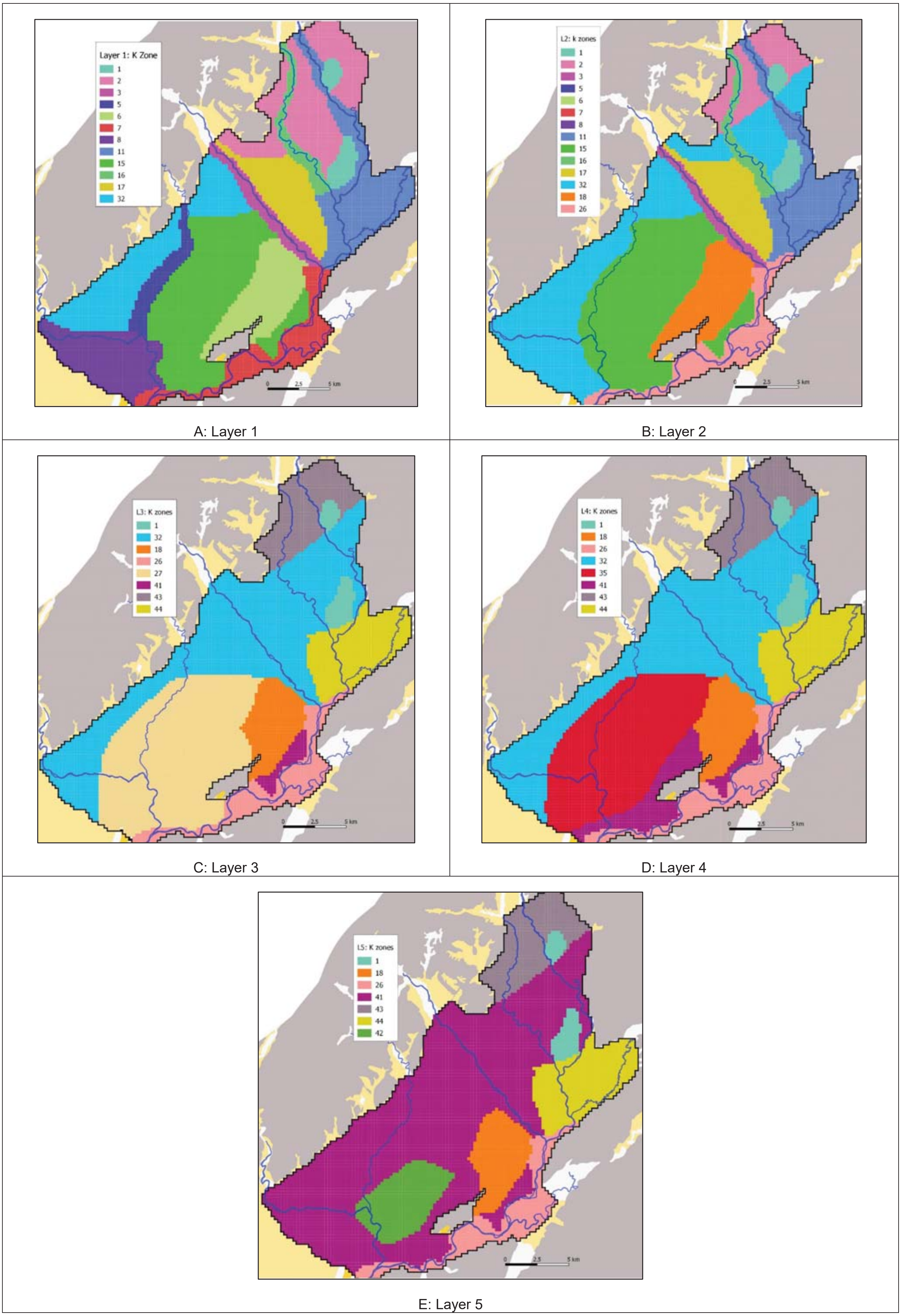

Figure 3.7 Hydraulic conductivity zonation for the northern model (numbers = zone identification numbers)

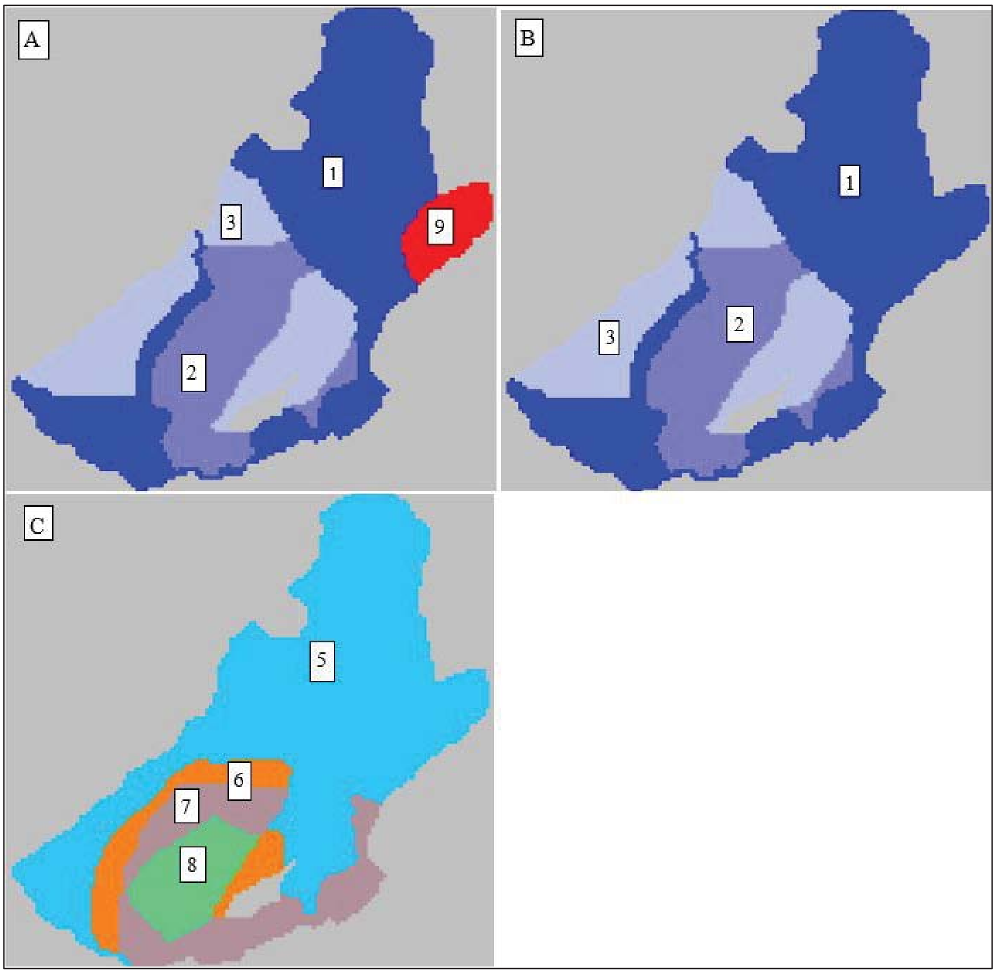

Figure 3.8 Storage zones for northern model — A: Layers 1–2; B: Layer 2; C: Layer 4–5.

Table 3.3 Initial hydraulic conductivity and storage parameters assigned to northern model zones.

Zone No.	Horizontal hydraulic conductivity Kx and Ky (m/day)	Vertical hydraulic conductivity Kz (m/day)	Specific storage Ss (v/v)	Specific yield Sy (v/v)	Porosity (v/v)
1	1.00	0.100	1.3E-4	0.15	0.01
2	10.00	0.200	1.3E-3	0.05	0.01
3	270.00	0.800	6E-4	0.1	0.01
4	106.60	0.794	-	-	-
5	-	-	2E-5	-	0.01
6	20.00	0.001	3.5E-5	-	0.01
7	328.00	2.300	5E-5	-	0.01
8	320.00	2.300	7E-6	-	0.01
11	80.00	0.006	-	-	-
15	60.00	0.001	-	-	-
16	150.00	0.200	-	-	-
17	50.00	0.033	-	-	-
18	20.00	0.080	-	-	-
26	328.00	0.100	-	-	-
27	0.00	0.001	-	-	-
32	5.00	0.001	-	-	-
35	105.00	0.800	-	-	-
41	10.00	0.040	-	-	-
42	20.00	0.040	-	-	-
43	4.00	0.100	-	-	-
44	20.00	0.100	-	-	-

3.6.2 Southern Model

Figure 3.9 and Figure 3.10 show the initial parameter zones for hydraulic conductivity and storage respectively. Again, these have been transferred directly from the previous FEFLOW model (Gyopari and McAlister, 2010a, 2010b and 2010c), and provide the initial model parameter values for the model, which are then subsequently adjusted during model calibration using distributed parameters (Section 5).

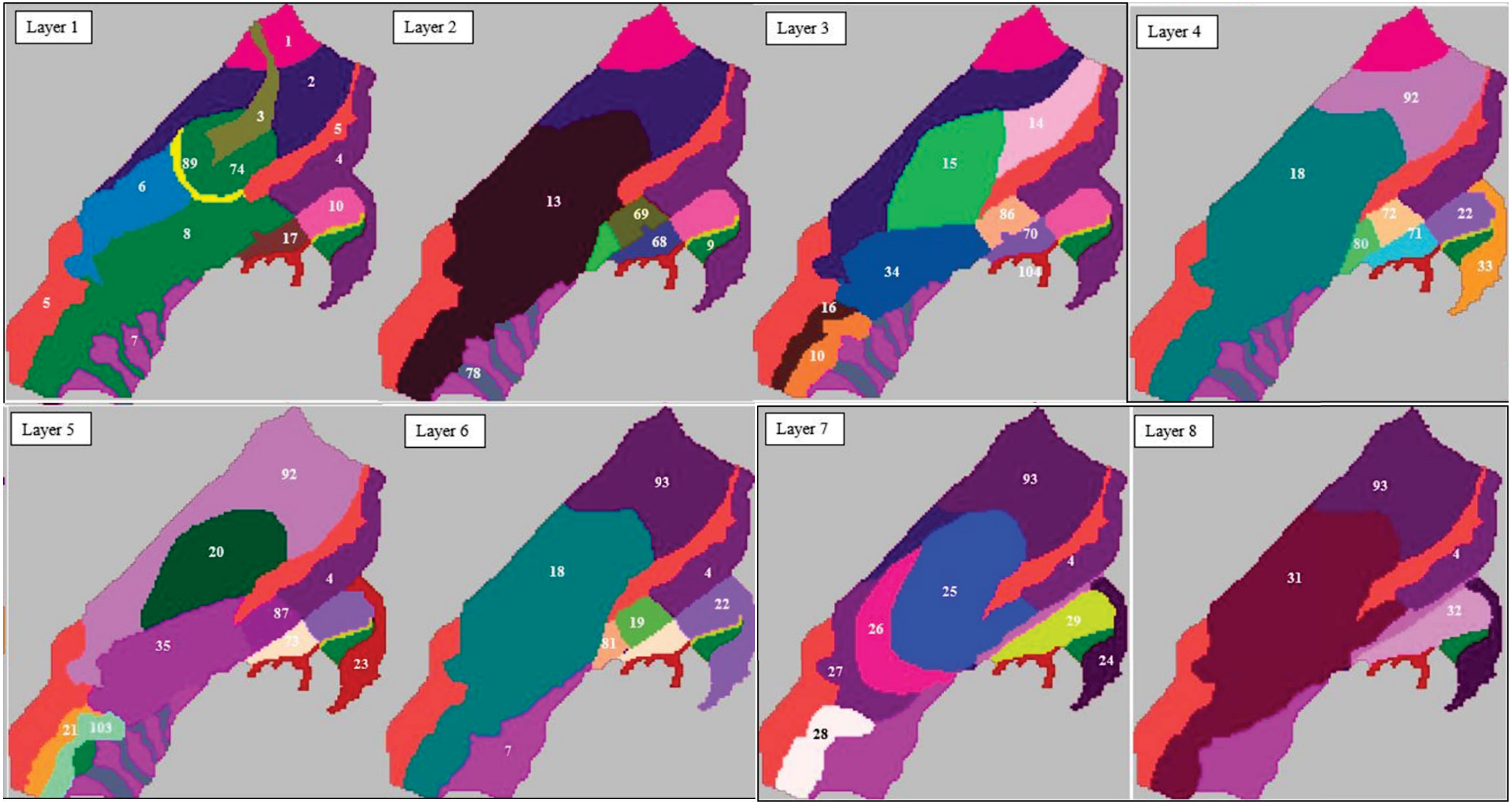

Figure 3.9 Southern model — initial hydraulic conductivity zones.

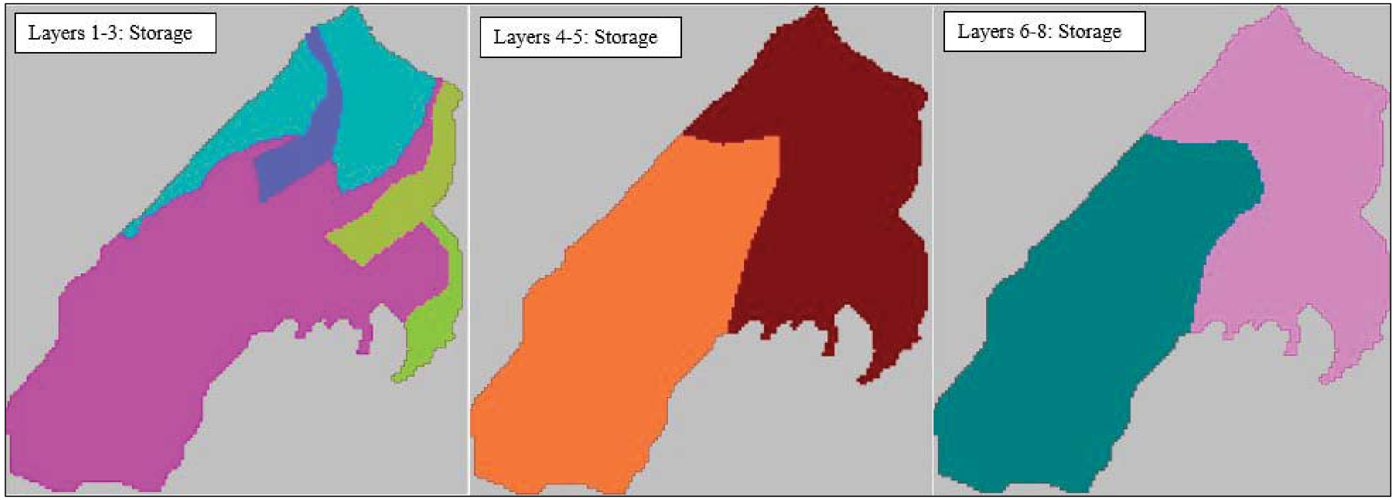

Figure 3.10 Southern model — initial storage zones.

3.7 RAINFALL AND IRRIGATION RECHARGE

Groundwater recharge has been externally modelled on a 500 m^2 grid using the IRRICALC daily soil moisture balance model (CMP Aqualinc report, 2016). This model was coupled to the MODFLOW RECHARGE package and the calculated recharge was distributed onto the model grid.

Figure 3.11 shows the annual average recharge pattern for the Wairarapa Plains calculated by IRRICALC. There is a strong west to east recharge gradient ranging from about 800–1,000 mm/yr on the western side of the plains against the Tararua Range to 180–200 mm/yr on the eastern side which reflects the high rainfall gradient. The annual average rainfall on the western side of the valley is 1,000 mm and therefore the calculated recharge in this area represents about 50–60% of rainfall. On the drier eastern side of the valley rainfall recharge is estimated to be about 25% of rainfall.

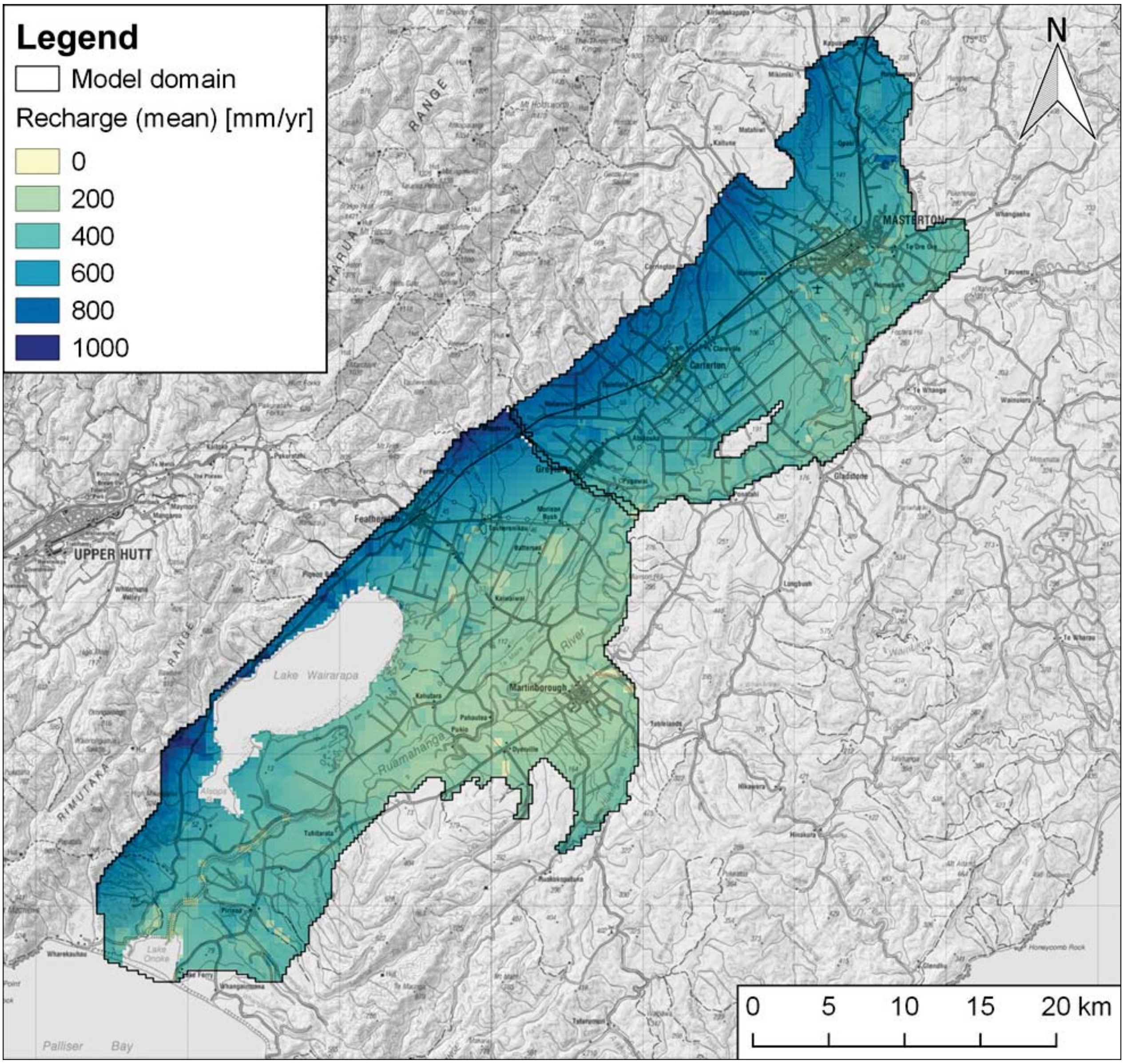

Figure 3.11 Calculated rainfall recharge using IRRICALC in mm/year.

Figure 3.12 and Figure 3.13 show the recharge time series for northern and southern models respectively.

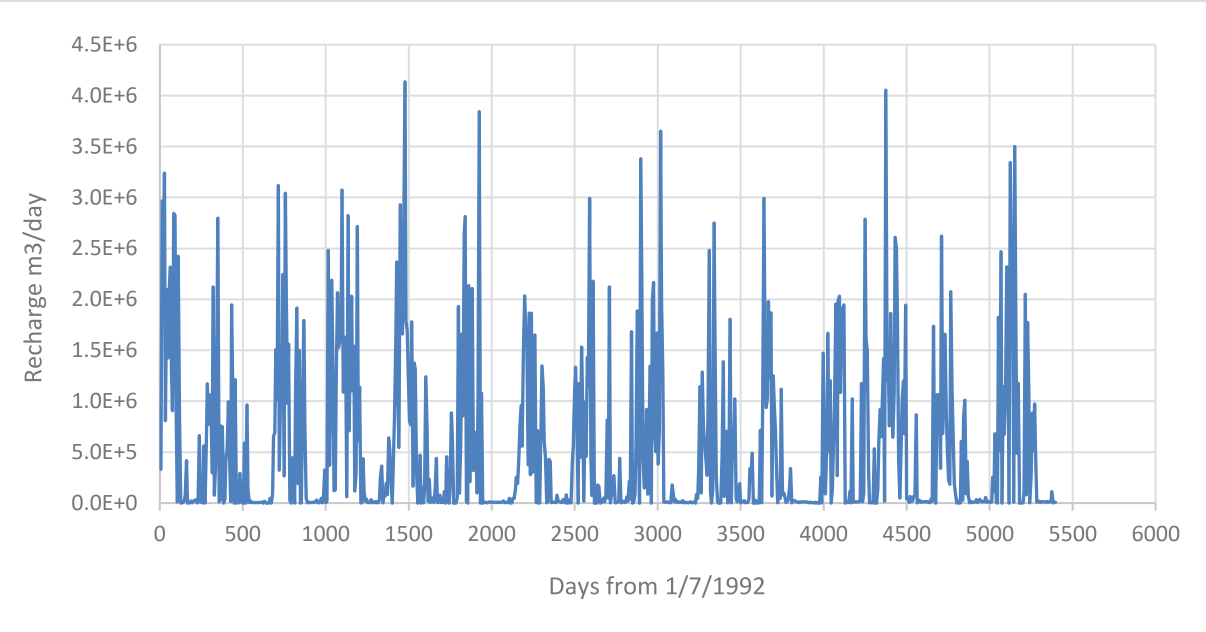

Figure 3.12 Calculated groundwater recharge for the northern model using IRRICALC (Aqualinc, 2016).

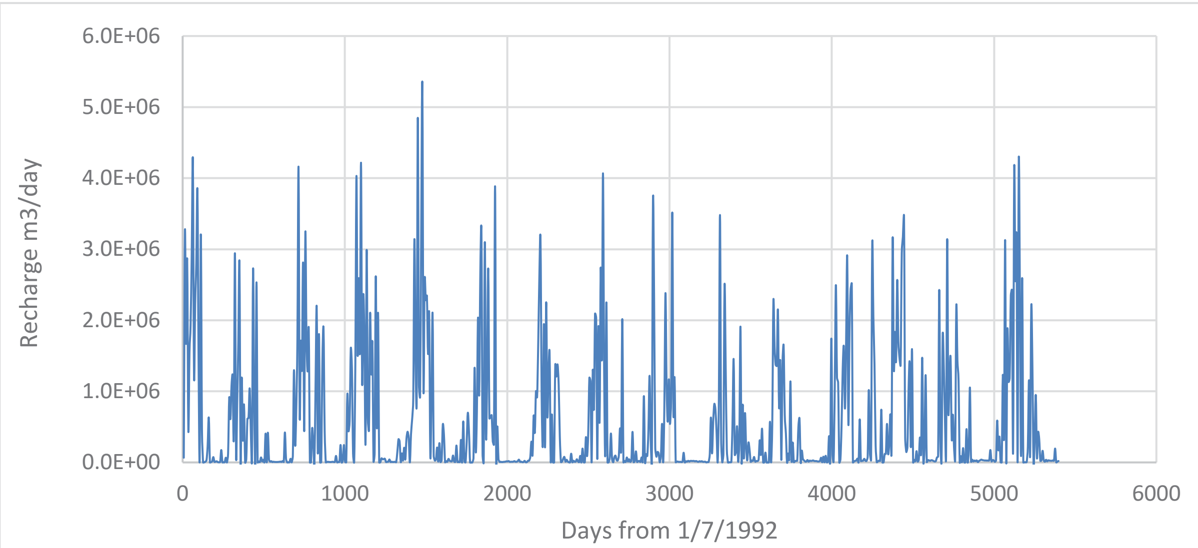

Figure 3.13 Calculated groundwater recharge for the southern model using IRRICALC (Aqualinc, 2016).

4.0 CONTAMINANT TRANSPORT MODEL DEVELOPMENT

4.1 GENERAL

The groundwater transport model was developed using the transport modelling software MT3DMS. MT3DMS is a post simulator to MODFLOW that uses the groundwater flow results from the MODFLOW outputs, and combines this flow with additional transport processes, to simulate solute transport for multiple species.

MT3DMS can be used to simulate solute fluxes in groundwater that accumulate at the stream bottom, and flow into any of the supported MODFLOW head-dependant flux boundary packages (e.g. lakes). At the time of model development MT3DMS could be used with any of the standard MODFLOW packages, except for the SFR package. However, a new version of MT3DMS, ‘MT3D-USGS’ (Bedekar et al., 2016) has been released in September 2016 which can route solute through the surface water system as defined by the SFR package. This new version requires that the MODFLOW-NWT version is used to run the MODFLOW simulation. In any future versions of the model it is recommended that this new version be used. Furthermore, the new version of MT3DMS also can be used to calculate solute transport through the surface water system (as the SOURCE model does).

It should be noted that the model does not have the capability to simulate the transport of multiple forms of nitrogen, but only of nitrate. To simulate all forms of nitrogen would require reactive transport modelling software such as PHT3D, which couples MT3DMS with a chemical reaction software PHREEQC to undertake the full suite of reaction equations (Prommer and Post, 2010). The significant computational requirements of reactive transport software, particularly the very long model run times, mean that this software is not an option for the Ruamāhanga regional groundwater models which cover such a large region. However, such software could be used for future investigations of “hot-spots”. On this note, it is important to understand that the model grid resolution (cell size) used in this project dictates that this model is not adequate to serve as an effective tool for addressing issues related to local or site specific issues, but rather should be used for exploring larger scale nutrient flux issues across the modelled area.

4.2 NITRATE FLUXES INTO THE MODEL

Nitrate inputs enter the model via rainfall recharge and river losses to groundwater. These nitrate fluxes entering the model in rainfall recharge were calculated as part of the CMP SOURCE model development (CMP Jacobs report, 2016) using outputs from the OVERSEER model (CMP MPI report, 2016) in combination with climate and soil databases. These nitrate fluxes were calculated by OVERSEER as an average annual value and converted to a nitrate concentration in rainfall recharge for use in this model by dividing the nitrate flux by the average annual recharge rate calculated by IRRICALC (Aqualinc, 2016).

The nitrate input into the north and south models are depicted in Figure 4.1 in terms of the nitrate nitrogen load and as a nitrate concentration in rainfall recharge in Figure 4.2. The nitrate concentration in rainfall recharge (Figure 4.2) is calculated using the recharge values depicted in Figure 3.10 and the nitrate load values in Figure 4.1. Interestingly, the recharge trend across the Wairarapa Valley (e.g., higher recharge rates in the west and lower recharge rates towards the east), results in a distribution of recharge nitrate concentrations (Figure 4.2) that is almost the reverse of the calculated nitrate loads depicted in Figure 4.1. However, this concentration distribution is reasonably consistent with the measured nitrate nitrogen as shown in Figure 4.3.

The nitrate concentrations of surface water also provided nitrate fluxes into the groundwater model where these surface water ways lose water into groundwater. These river and stream concentrations were assigned based on long term measurements of nitrate concentrations. The average calculated surface water concentration was significantly lower than that in the rainfall recharge, with an average concentration of 0.0005 kg/m^3.

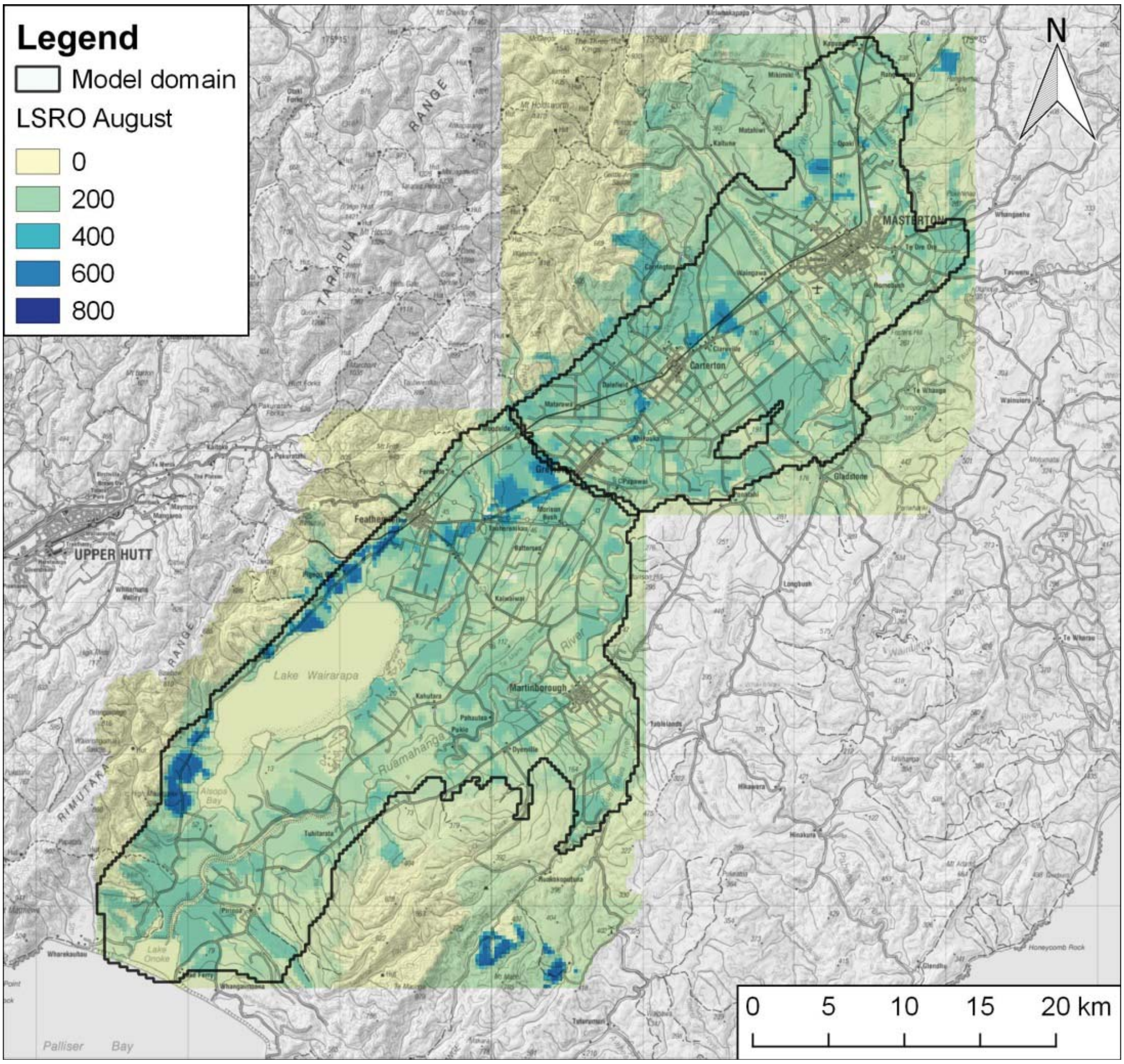

Figure 4.1 Nitrate load in kg/year as estimated by OVERSEER and distributed by SOURCE (CMP Jacobs report, 2016).

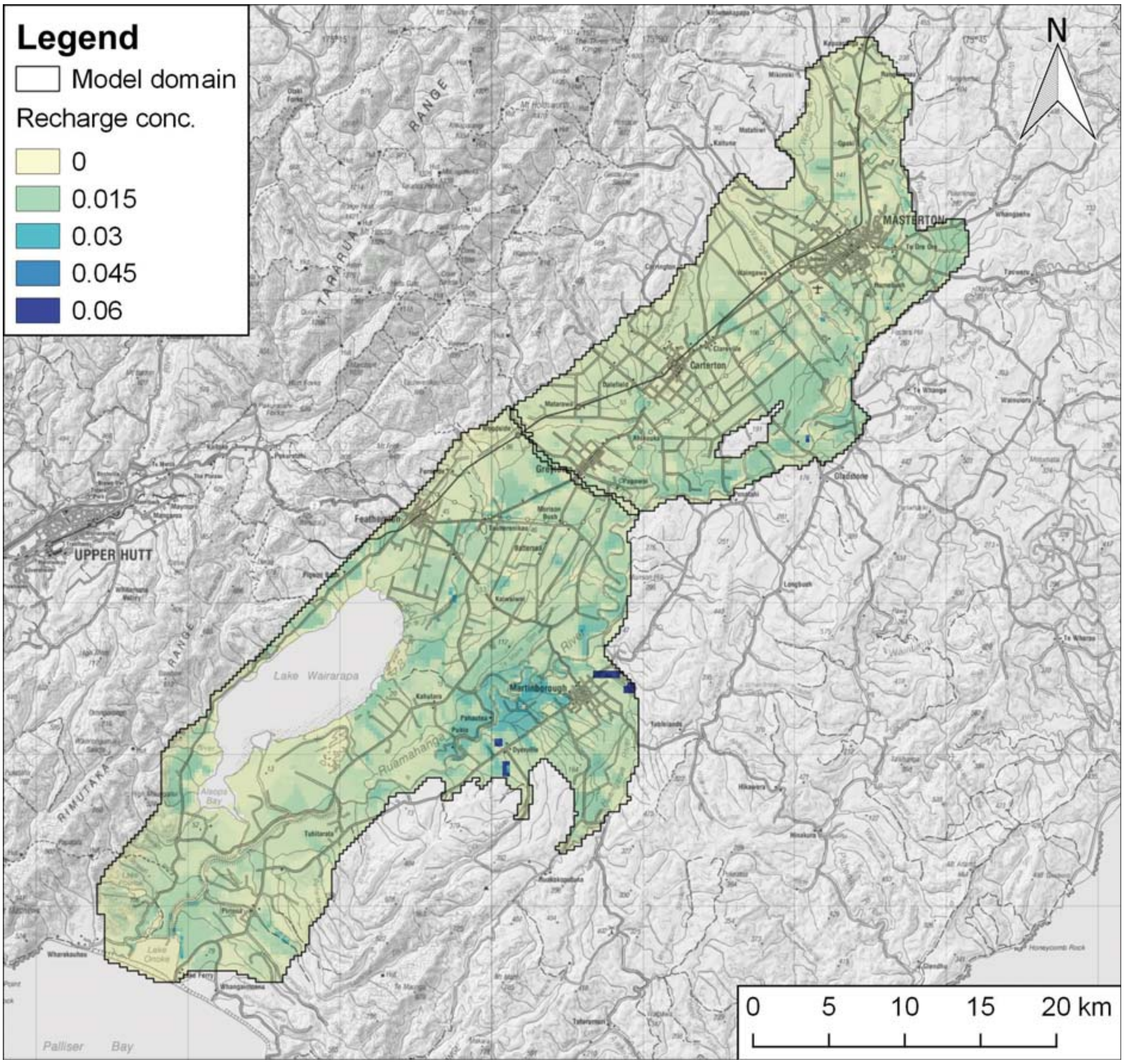

Figure 4.2 Nitrate concentration (kg/m^3) in rainfall recharge percolating through the soil and unsaturated strata above the aquifers derived using the recharge values depicted in Figure 3.11 and the nitrate loads depicted in Figure 4.1.

4.3 TRANSPORT MODEL CALIBRATION TARGETS

The calibration targets used are the average groundwater nitrate concentrations over the past 10 years (Figure 4.3). While there is significant variation in concentrations, on average the observed concentrations are highest in the shallow layers and lower in the deeper model layers (Figure 4.4).

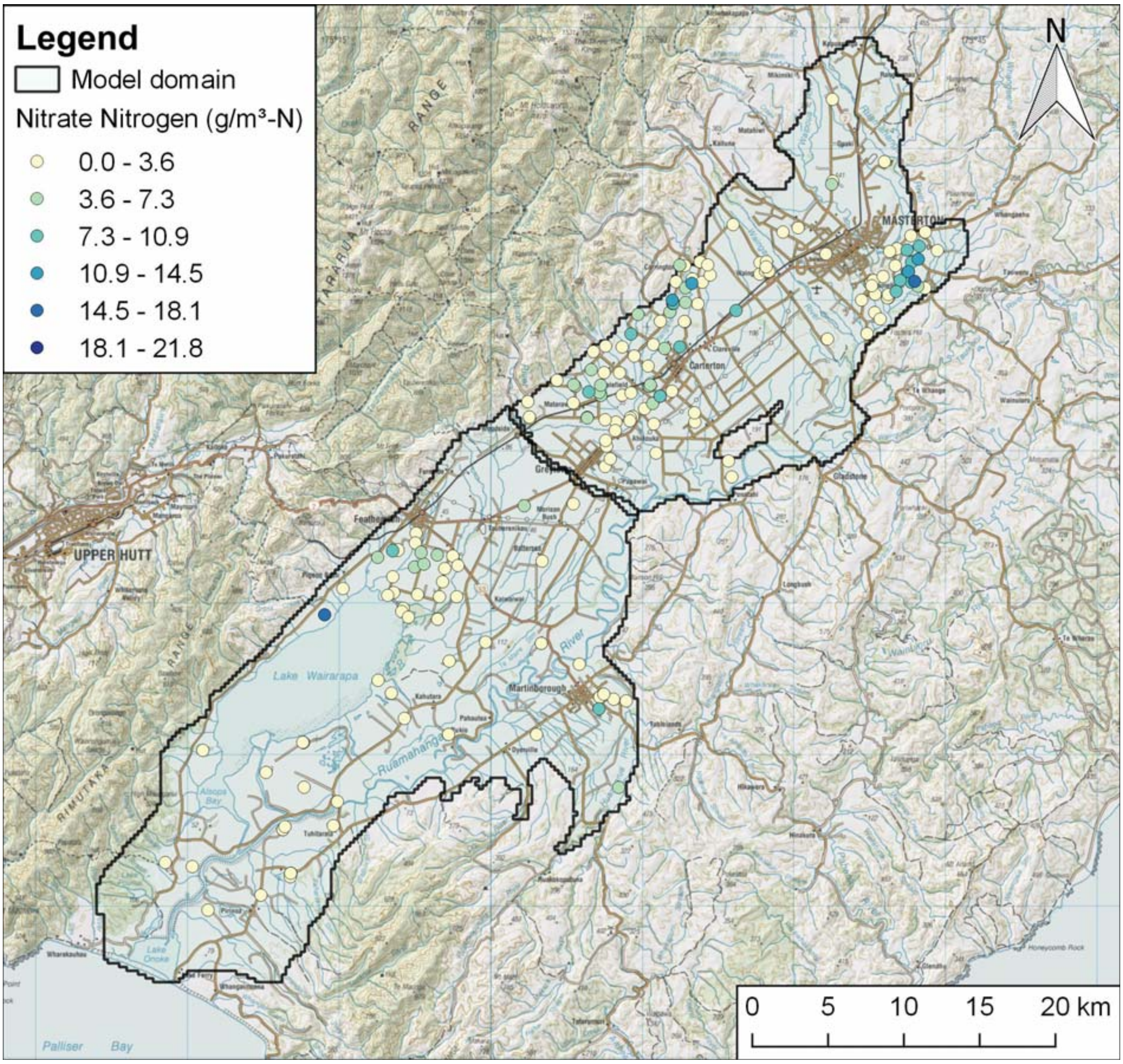

Figure 4.3 Groundwater nitrate nitrogen concentration distribution in the Wairarapa Valley.

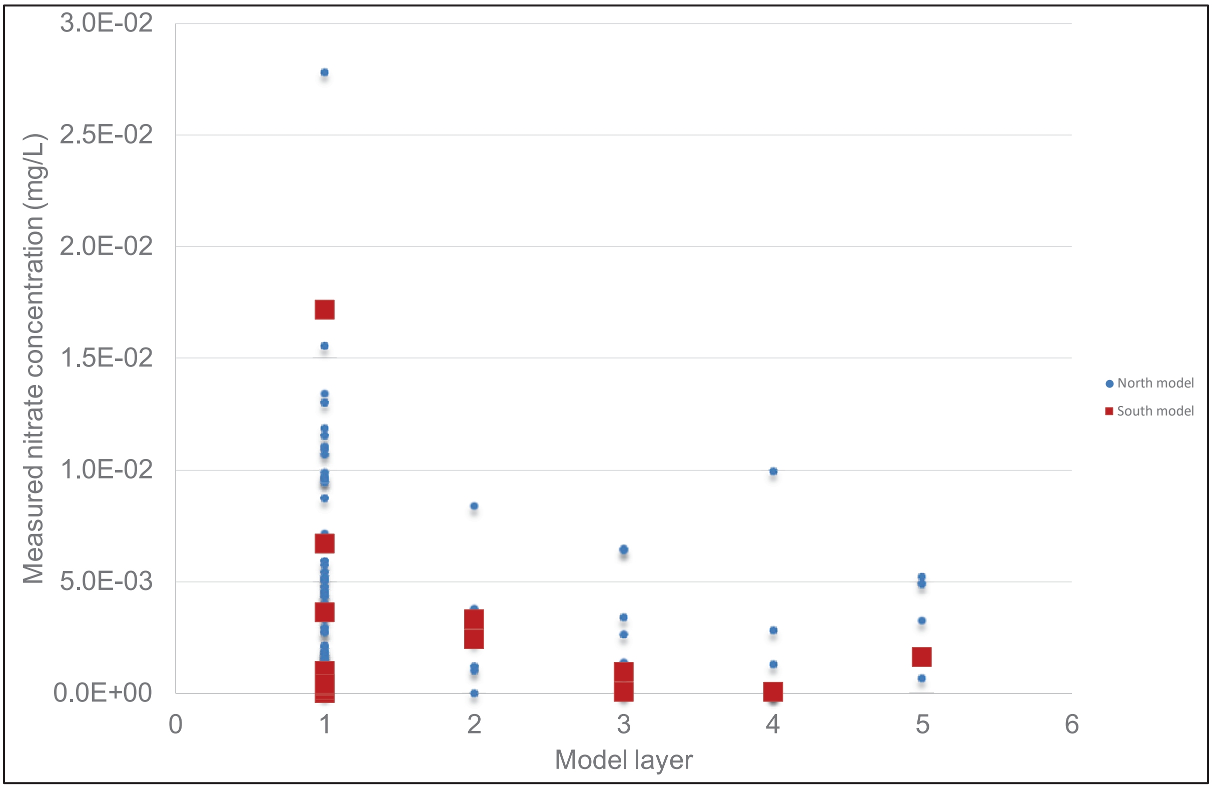

Figure 4.4 Groundwater nitrate nitrogen concentration distribution with depth in the northern model.

The observed trend of shallow bores having higher nitrate values than deeper bores is evident in both the north and south model layers. However, on average nitrate concentrations within the southern area appear to be lower than in the northern area. These lower average nitrate concentrations in the southern model area may indicate more denitrification occurs within the southern model.

4.4 DENITRIFICATION POTENTIAL

Denitrification processes are key removal process for nitrate concentrations in groundwater. These processes are typically lumped together and represented as a first order decay rate in regional groundwater models, to present these denitrification processes.

Four conditions are required for denitrification processes to occur, namely anoxic or low oxygen conditions; provision of a suitable electron donor; microbial consortia capable of carrying out denitrification; and sufficient nitrate (Korom, 1992 in Close et al., 2016). Of these four, the redox status of groundwater alone can be used to provide a good indicator of where denitrification can occur (Close et al., 2016) as the necessary microbes are typically present. Combining redox status with groundwater flow paths and nitrate concentrations, allows us to assess whether denitrification is likely to occur in a particular area of an aquifer.

Close et al. (2016) describes the series of redox reactions that occur in groundwater systems that successively utilise O_2, NO_3, Mn (IV), Fe(III), SO_4, and CO_2 as electron acceptors. Because there is a decrease in energy available to the microbes from each successive electron acceptor, these redox reactions typically follow this sequence. Therefore, where reducing conditions occur, we can expect that concentrations of O_2 will be low, NO_3 will be low and the soluble forms of Mn will be high and Fe may also be high etc. The distributions of O_2, NO_3, Mn and Fe for the Wairarapa Valley are shown in Figures 4.5 to 4.7, and indicate that some denitrification is likely to occur in the lower valley area around Lake Wairarapa.

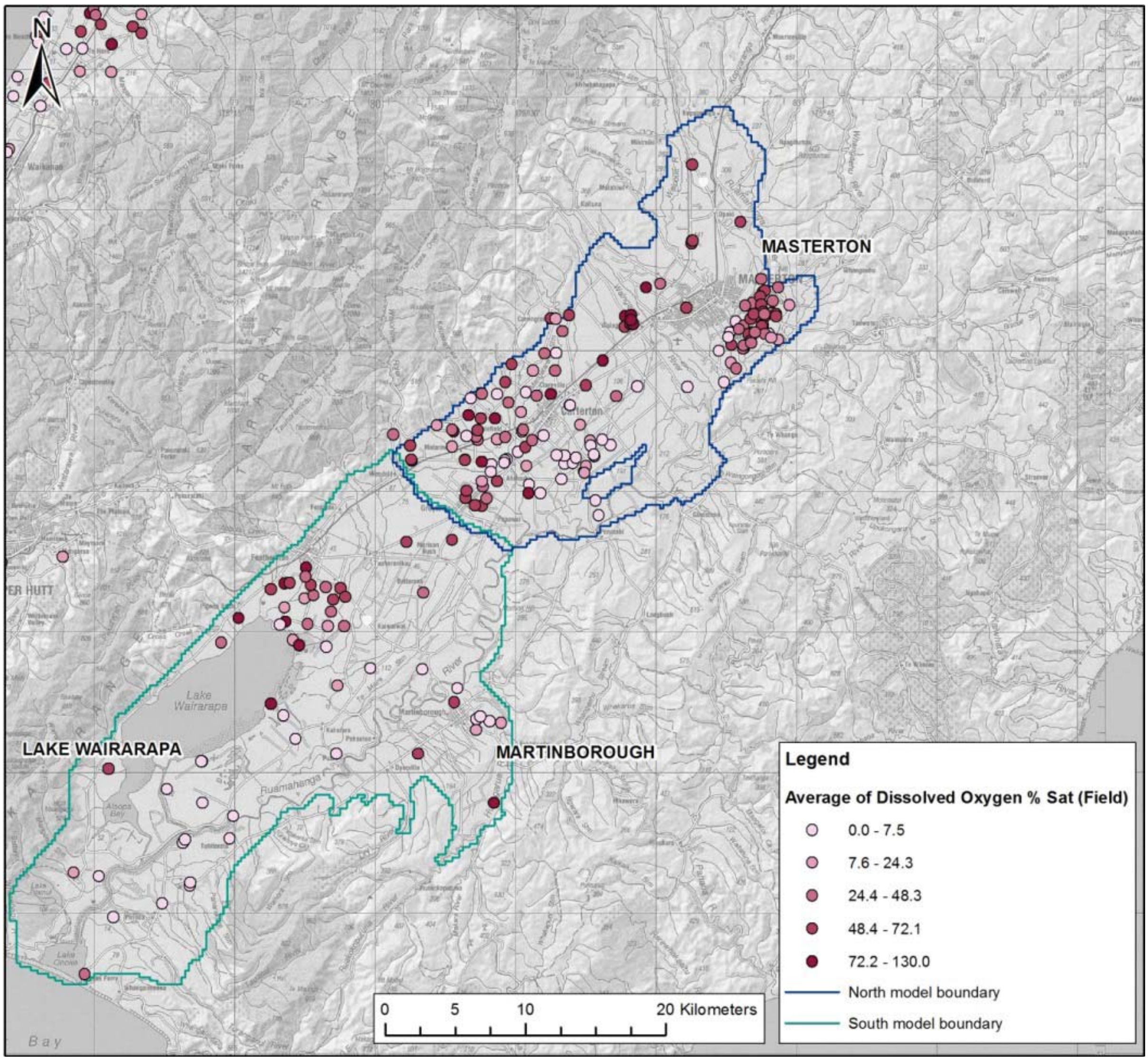

Figure 4.5 Groundwater dissolved oxygen concentration distribution in the Wairarapa Valley.

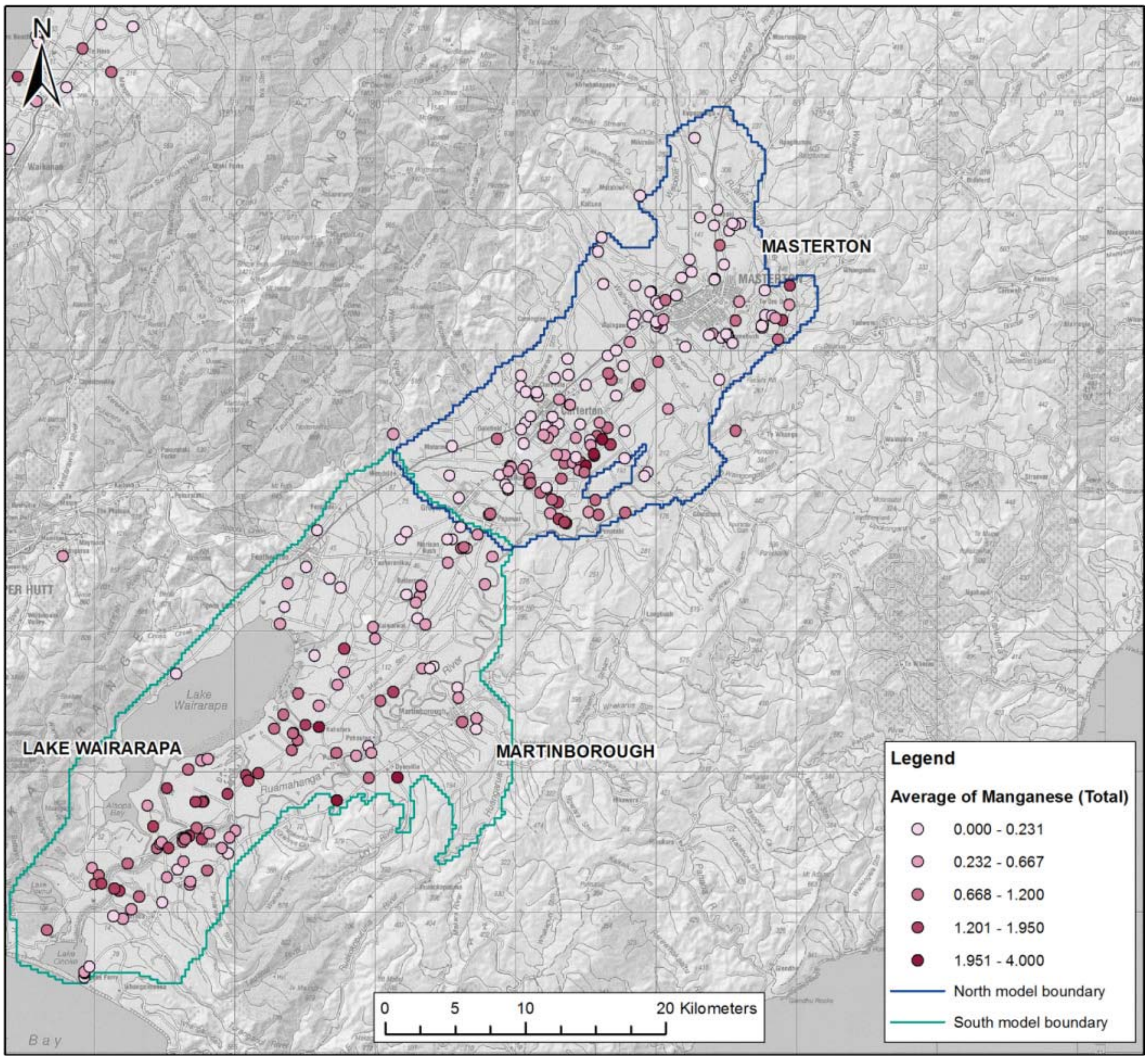

Figure 4.6 Groundwater total manganese concentration distribution in the Wairarapa Valley.

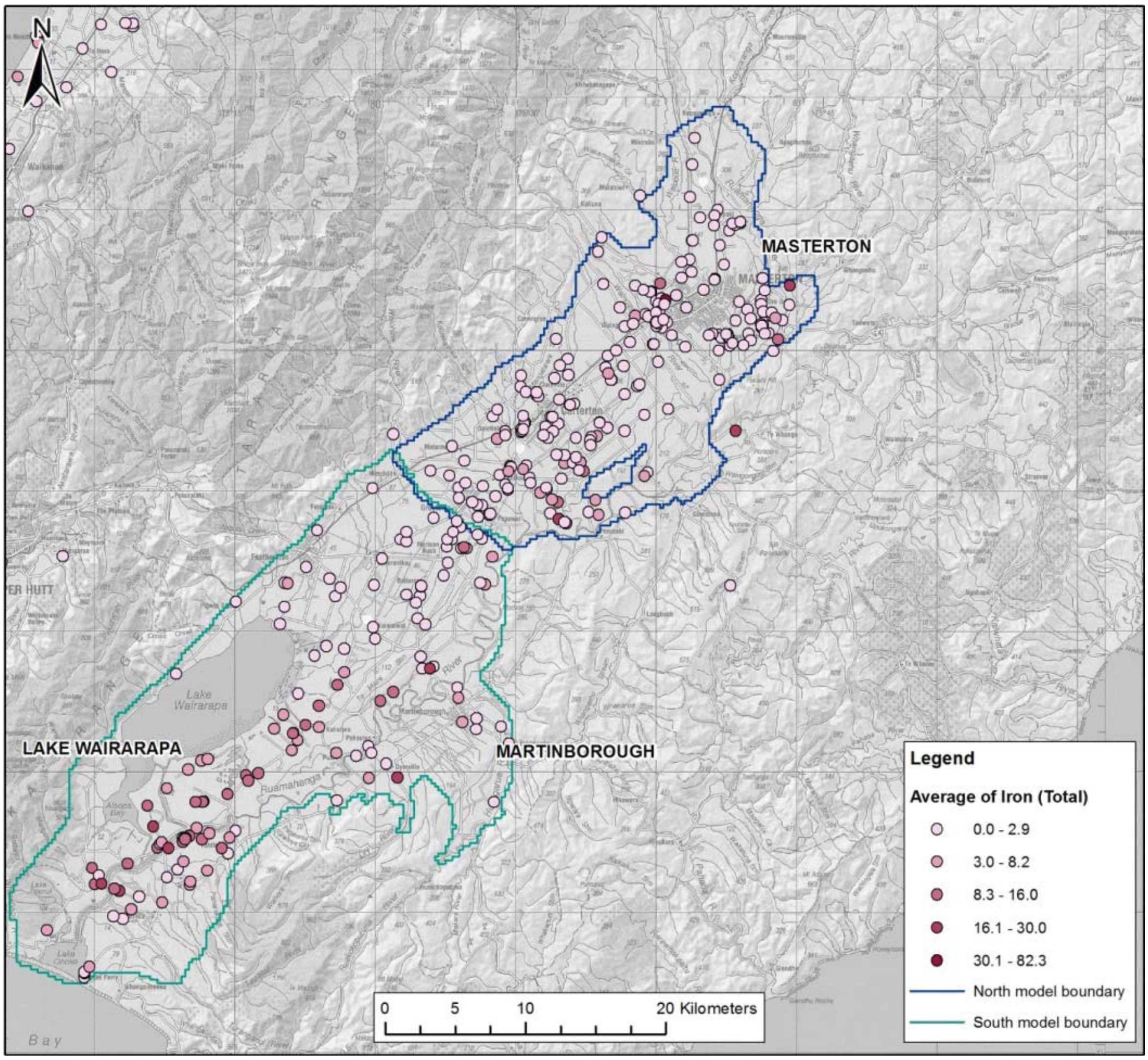

Figure 4.7 Groundwater iron concentration distribution in the Wairarapa Valley.

4.5 TRANSPORT MODEL CALIBRATION PARAMETERS

The transport model inherits the flow regime from the flow model, and hence the same model parameters that are adjusted in the flow model calibration are considered as calibration parameters for the transport model. In addition, denitrification, and dispersity are considered additional model calibration parameters that are adjusted during the transport model calibration. Note that in this modelling project, because we were calibrating to a steady state concentration of nitrate, based on a long-term average input of nitrate, the model calibration process is insensitive to porosity values and their variation. Therefore, these porosity values cannot be estimated through the calibration process, and are not discussed further in this report.

Unlike the aquifer hydraulic parameters of hydraulic conductivity and storage (Section A4.8, Appendix 1) that are informed from aquifer pumping tests, there is little prior field information on dispersivity and denitrification rates for the Ruamāhanga areas, and so literature values were used as prior parameter estimates. At the time of completion of this modelling report, a subsequent analysis of the redox potential of groundwater within the Ruamāhanga area has become available, which has been undertaken as part of a GNS led and GWRC cofounded research programme (Smart Models for Aquifer Management), and these analyses are presented in Section 5.

5.0 MODEL CALIBRATION

5.1 OVERVIEW

Model calibration involves adjusting model parameter values until the model outputs match the historical measurements of system state that have been provided. The aim of calibration is to ensure that the model can simulate the status quo, and on that basis then make more reliable predictions of the future.

In this project groundwater levels, stream flows, simultaneous river gaugings and groundwater concentrations were used as calibration targets, for the period 1992 to 2007. The model calibration in this project comprised a number of stages, as follows.

- The original FEFLOW model's recharge inputs, boundaries (rivers/lakes/wells), layer structures and aquifer properties the model were converted to the MODFLOW software platform.
- This converted model was calibrated and extended as follows:
  - Recharge and abstraction flux estimates were updated using IRRICALC estimates of both groundwater recharge and soil water demand (Aqualinc).
  - Representation of surface water ways as surface water boundaries in the MODFLOW SFR package was undertaken to allow stream flow rates to be simulated (incorporating TOPNET flow inputs and IRRICALC surface water abstraction and runoff fluxes).
  - The groundwater transport model (MT3DMS model) was added to the calibration suite to simulate the observed groundwater nitrate concentrations. Nutrient loadings calculated from the OVERSEER model and Jacobs estimates of the spatial distribution of these loadings (as depicted in Figure 4.1), plus the surface water nitrogen concentrations were used.
  - A range of scripts were written to automate the conversion of IRRICALC and TOPNET and the SOURCE outputs into MODFLOW and MT3D inputs, so that future model scenario work could be streamlined. These scripts are included in Appendix 2.
  - The resulting uncertainty of parameter estimates were analysed.

Typically, model calibration is evaluated using a range of metrics, such as:

- model to measurement fits;
- random distribution of residuals;
- parameter credibility and identifiability;
- uncertainty quantification.

Model to measurement fits and residuals are discussed later in Section 5. Parameter identifiability and uncertainty quantification are discussed in Section 6.

5.1.1 A note on model verification versus calibration and uncertianty analysis

The Australian Groundwater Modelling Guidelines (Barnett et al., 2012) discuss the traditional process of model verification, where this involves comparing the predictions of the calibrated model to a set of measurements that were not used to calibrate the model. This guideline document suggests that a formal verification process should only be attempted where a large quantity of surplus calibration data is available and it is possible to set aside a number of key observations that could otherwise be used for calibration. They note that this process of choosing not to use some data, and reserving it for verification, may not make the best use of available data. One of the authors of this document goes further and states that the process of model validation is largely superseded by the use of formal uncertainty analysis methods (e.g., see attached the “A Note on Model Validation” section in the widely cited USGS report; Doherty and Hunt, 2010). The authors of this report support this approach, and hence the analysis of model to measurement fits along with uncertainty analysis (discussed in Section 6) is used in place of model validation.

5.2 MODEL CALIBRATION WITH PEST

Estimation of model parameters through calibration was undertaken using PEST software (Doherty, 2016). BeoPEST (Schreüder, 2009), a parallel processing version of PEST, was used to reduce computational times.

In addition to the constraints on the parameter estimation process imposed by specifying parameter bounds and initial values, Tikhonov regularisation constraints in the form of preferred parameter values was adopted. This regularisation approach results in deviations from the preferred parameter value condition only to the extent that is necessary to adequately match field data.

In the case of hydraulic properties, the preferred parameter values were those derived from the original FEFLOW model as is now described. This provides a means to ensure both numerical stability of the parameter estimation processes but also to ensure that our “expert knowledge” derived from the initial FEFLOW model is communicated to the current model calibration.

5.3 CALIBRATION MODEL PARAMETERS

The model calibration for hydraulic parameters utilised the zones of constant parameter value estimated from initial FEFLOW model calibration. These zoned parameter fields were then multiplied by the spatially distributed pilot points depicted in Figure 5.1.

The initial zone parameter values were used as the Tikhonov regularisation preferred values. Preferred values were assigned to every pilot-point parameter, the value of which is dependent on the geological unit being represented, and provides a credibility constraint in terms of representing the relative difference in hydraulic conductivity between different units.

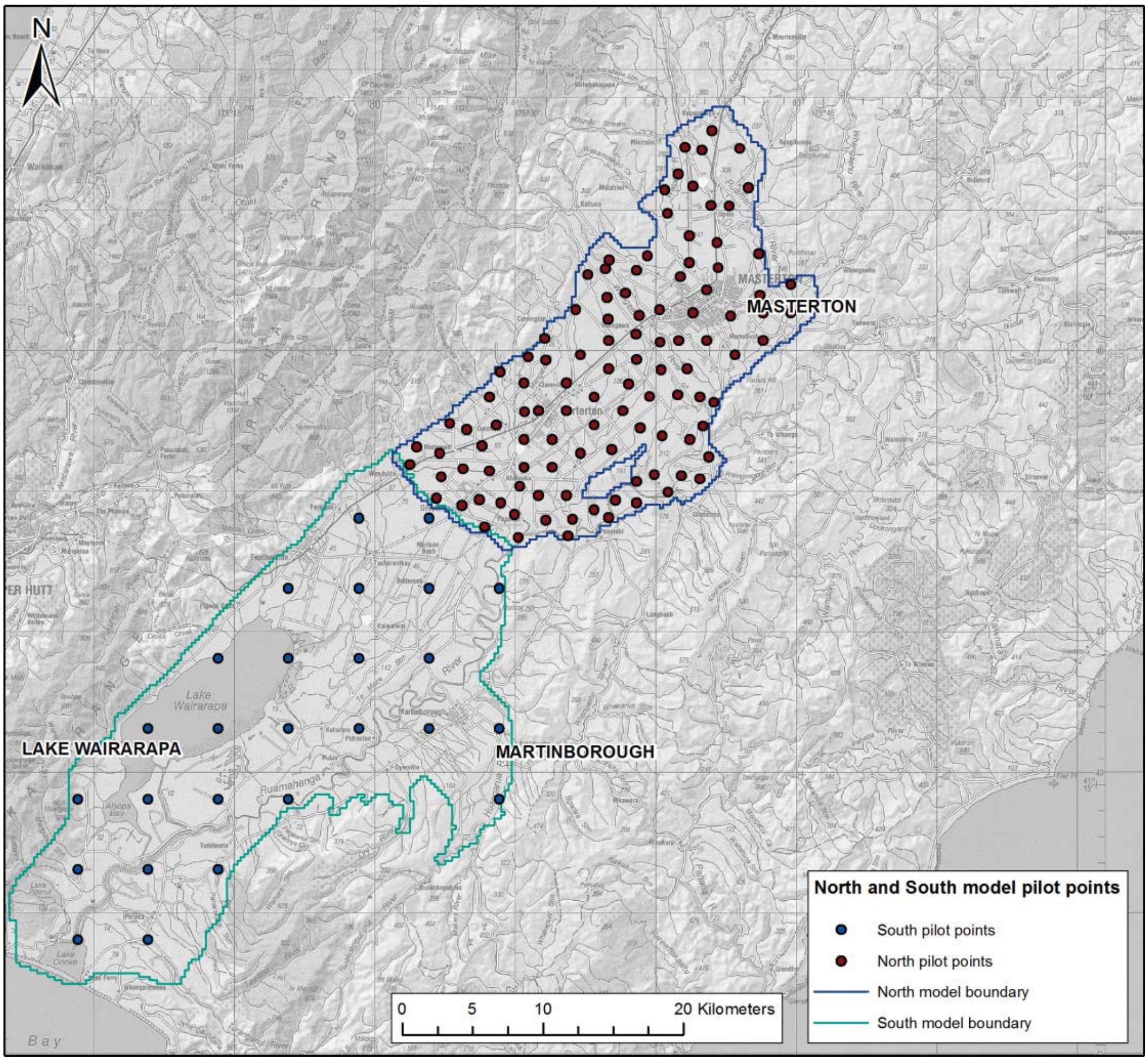

Figure 5.1 Location of pilot point multiplier parameters used in the north and south model calibration.

5.3.1 Hydraulic Properties – Hydraulic Conductivity, Storage and Porosity

The calibrated parameter fields from the north model are depicted in Figure 5.2 for the north model and in Figure 5.3 and Figure 5.4 for the south model. Evidence of the initial parameter zonation (refer to Section 3) can be seen in all the property fields. The new estimated parameters vary only slightly from the original fields, and only to the extent necessary to achieve more acceptable model to measurement matches, reflecting the agreed CMP agreed modelling approach for this project.

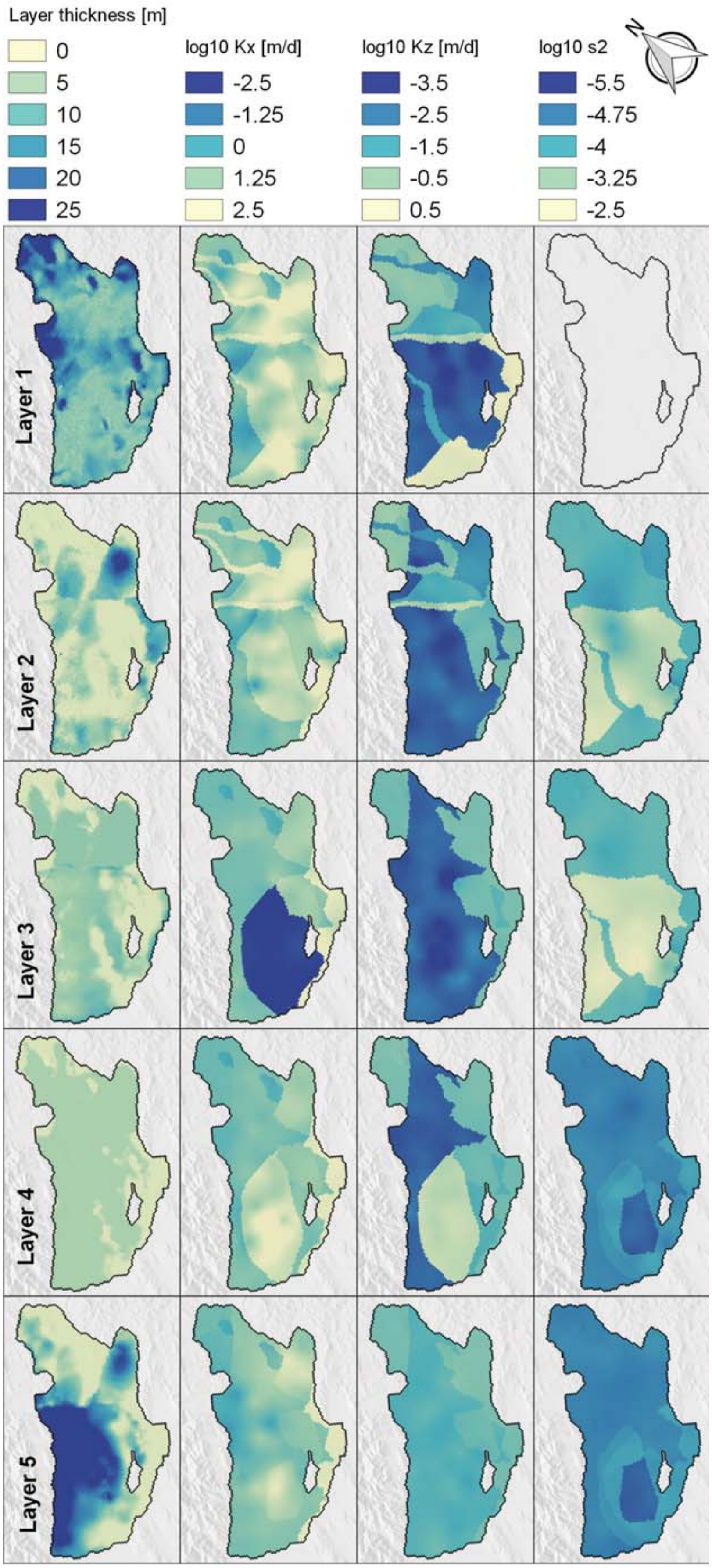

Figure 5.2 Calibrated hydraulic parameter fields from the north model calibration.

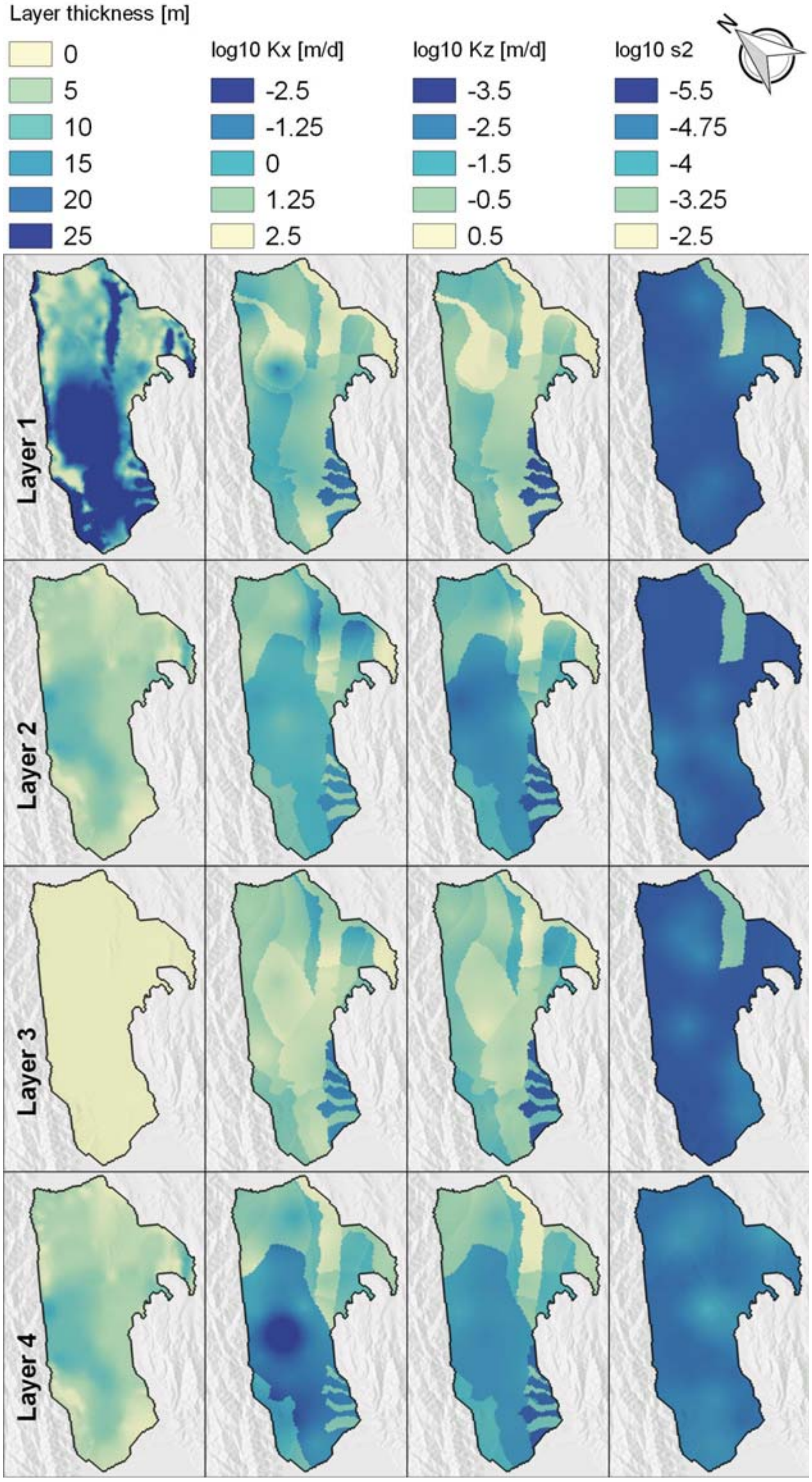

Figure 5.3 Calibrated hydraulic parameter fields from the south model calibration (layers 1–4).

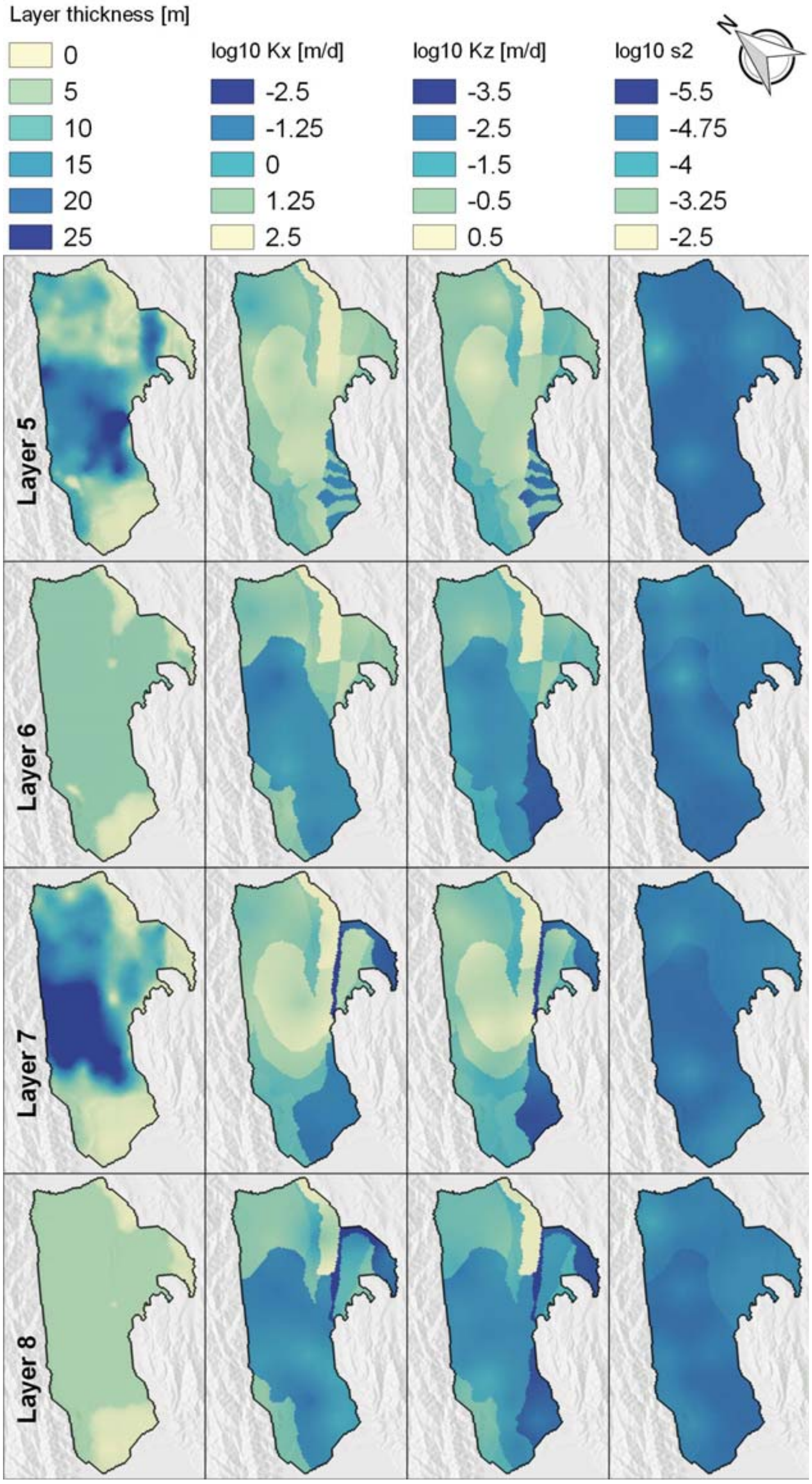

Figure 5.4 Calibrated hydraulic parameter fields from the south model calibration (layers 5–8).

5.4 DENITRIFICATION RATES

The denitrification rates were modelled as a first order decay rate. The resulting distribution of these denitrification rates were constant for layer 2 and below in both the north and south model, while in layer 1 denitrification rates had slightly greater variability within the north model. These denitrification rates ranged from very low (<0.000005 day^{-1}) up to 0.005 day^{-1}, and are within the denitrification ranges reported in Close (2017).

While the general patterns of measured nitrate concentrations were matched with depth, these denitrification rates are based on only a limited groundwater data set, and an approximate estimate of the land-use nitrate flux. Therefore, the information available to estimate the denitrification rates within the model, is insufficient to estimate the spatial distribution of denitrification rates with reliability; this is discussed in Section 6.

A current research programme (GNS led and GWRC co-funded research programme Smart Models for Aquifer Management) has been exploring how to define these denitrification rates using parallel lines of information related to the redox potential of groundwater. It is anticipated that future modelling work will be able to include this information in the model conceptualisation and calibration. These redox potential maps are included in Figure 5.5. Areas of low redox potential (oxic zones) are shown to occur in the North model area, and these areas can be expected to have low denitrification rates. Reducing zones, which are associated with higher denitrification rates, are more widespread within the South model area.

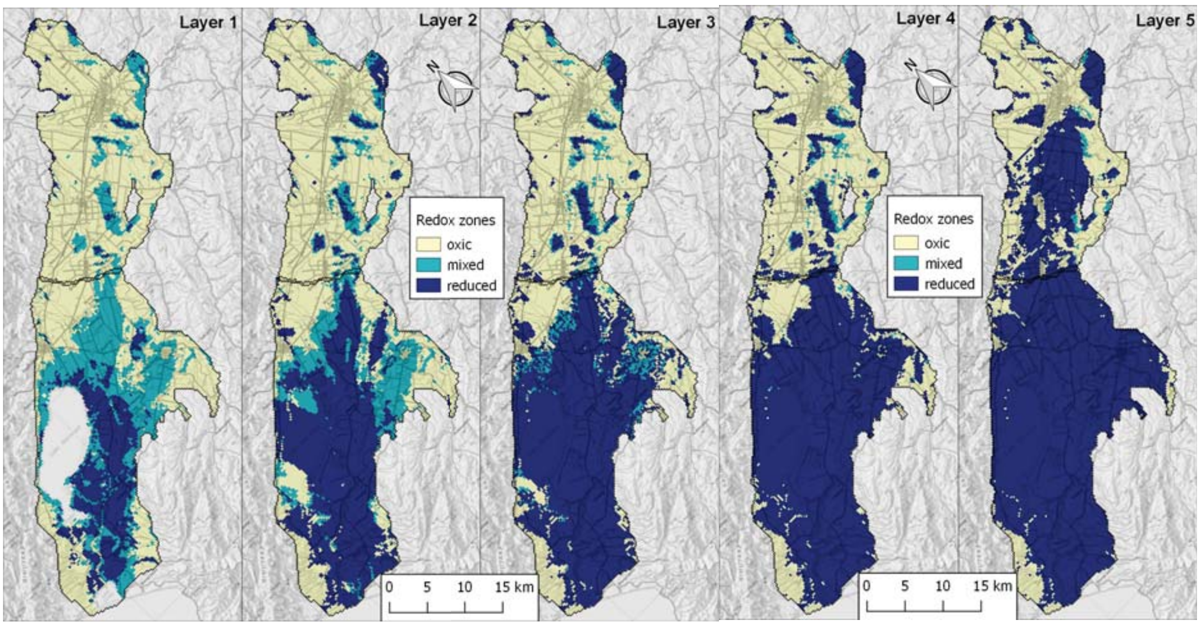

Figure 5.5 Redox zones which are correlated with likely denitrificaion rate ranges in the north and south model (from GNS led and GWRC co-funded research programme Smart Models for Aquifer Management, compiled by ESR-Murray Close).

5.5 DISPERSION

Dispersion is a lumped parameter used to account for the fine scale variations in groundwater velocity that occur because of variations in aquifer hydraulic conductivity, which results in the spreading of a solute. Three dispersivity coefficients are used: one for longitudinal dispersivity, which represents dispersion along the primary flow axis, and two for transverse dispersivity values, which represent dispersion in the horizontal and vertical directions normal to the axis of flow. MT3DMS allows the user to specify the longitudinal dispersivity for each model layer and to set the transverse horizontal and transverse vertical dispersivity values as a fraction of the longitudinal dispersivity.

For regional models with coarse discretization, as in the Ruamāhanga model, the dispersion term is often not estimated and instead is held constant, as dispersion relationships at the kilometre and greater scale essentially serve as a 'fudge' parameter. Sanford (2010), makes an argument for omitting dispersion altogether in such large-scale models, illuminating its lack of relevance for regional models.

We have adopted a longitudinal dispersion rates of 250 m, and a transverse and vertical ratio of 25 and 2.5 respectively, but a sensitivity analysis indicated that the model results were not sensitive to this parameter, at the model scale. As a consequent we subsequently adopted Sandfords strategy in this modelling work, and worked with a fixed dispersivity.

5.6 MODEL OUTPUTS, CALIBRATION TARGETS AND MODEL TO MEASUREMENT FITS

The transient groundwater flow model uses the following observations as calibration targets:

- groundwater levels;
- stream flows;
- loss gauging's as calibration targets.

Nitrate concentrations are used as calibration targets for the transport model.

5.6.1 Model Output Patterns of Piezometric Head, Concentration and Horizontal and Vertical Fluxes

An overview of the model simulated head distribution, flow patterns and nitrate concentrations are shown in Figure 5.6 for the north model, and Figure 5.7 and Figure 5.8 for the south model, for each model layer. The circles in each plot are the locations of the relevant calibration targets (groundwater levels and concentrations).

The first column in these plots depicts the hydraulic head distribution in each model layer. It can be seen that these general flow patterns are consistent with those indicated by the piezometric flow patterns derived from the measured data depicted in Appendix A, Figure A4.10. The sparse coverage of calibration targets is also clear from these plots, particularly in the deeper model layers. This sparse coverage is one of the main causes of the predictive uncertainty that is discussed in Section 6.

The second column depicts the calibrated nitrate concentrations in each model layer. These plots are generally consistent with the spatial trend of both the recharge nitrate concentrations, shown in Figure 4.2, and the measured observations depicted in Figure 4.3. These figures also show the declining concentrations with depth that were summarised in Figure 4.4. Once again, the sparse nature of the calibration targets can be seen, particularly with deeper model layers. Note that there are no concentration calibration targets in the south model below layer 5.

The third and fourth columns depict the average horizontal and vertical flux components within each model layer. In the horizontal flux column, the north model plots depict significant flow along the faults and river systems in the shallow model layers. Of interest is the very low flux in layer 3 which is associated with the very low hydraulic conductivity (inherited from the FEFLOW model and based on the geological interpretation of the strata in this region, refer to Section 9). In the Southern model, most flow occurs around surface water ways in the shallow model layers.

In the vertical flux column, the red shading indicates areas where the movement of fluxes is upwards between layers and the green–blue shading indicates areas of downwards flow (i.e., the first plot is between layer 1 and 2, the second between 2 and 3 etc.). The north model pattern of vertical fluxes indicates downwards fluxes are generally occurring to the west of the model domain, and upwards fluxes to the east of the model domain. This pattern is evident in all model layers. In the south model, most of the central and southern areas of the model domain are indicating predominant upwards flow, with downwards flow occurring around the margins of the model domain, particularly in the northern area.

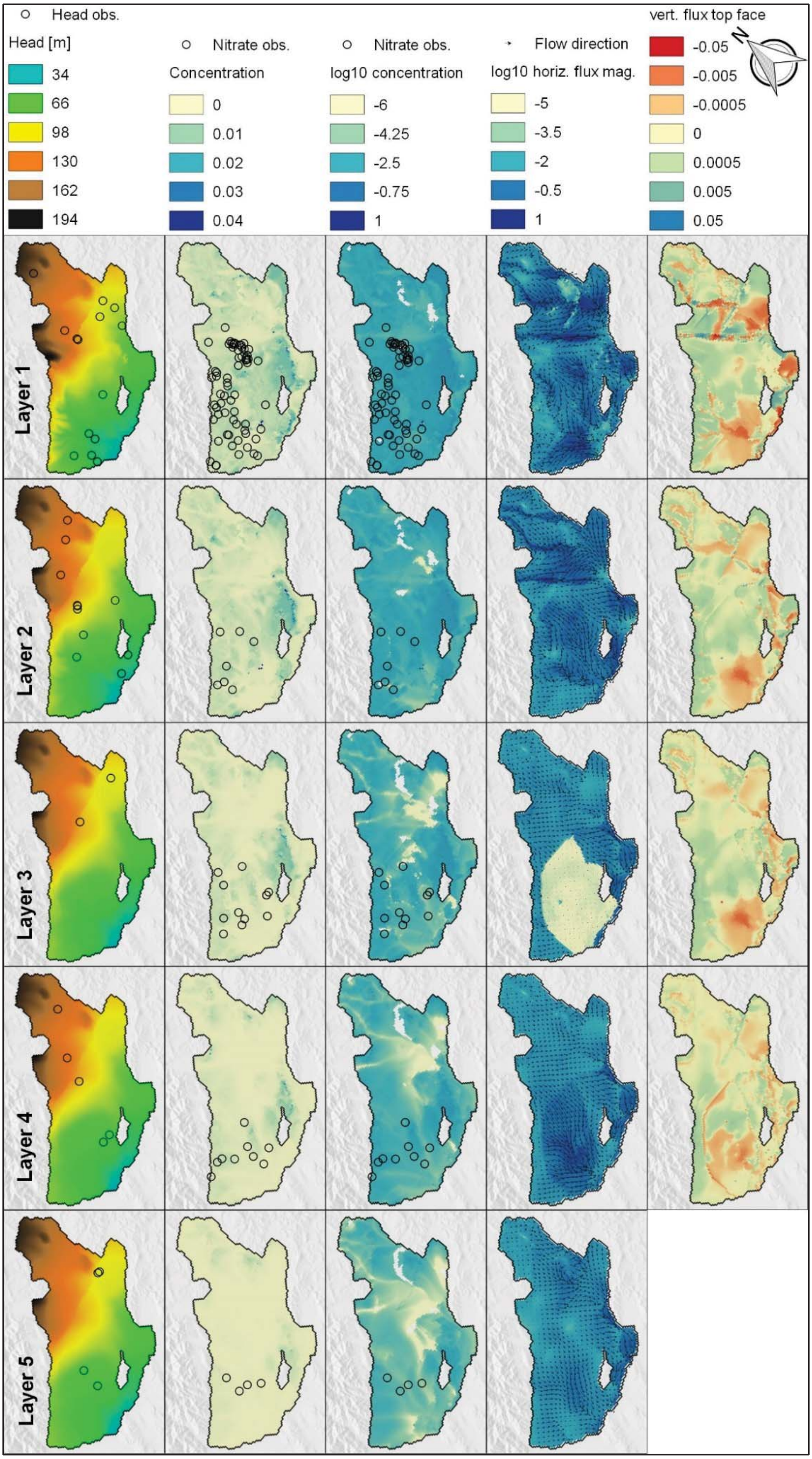

Figure 5.6 Calibrated piezometric, concentration and flux model outputs from the north model calibration.

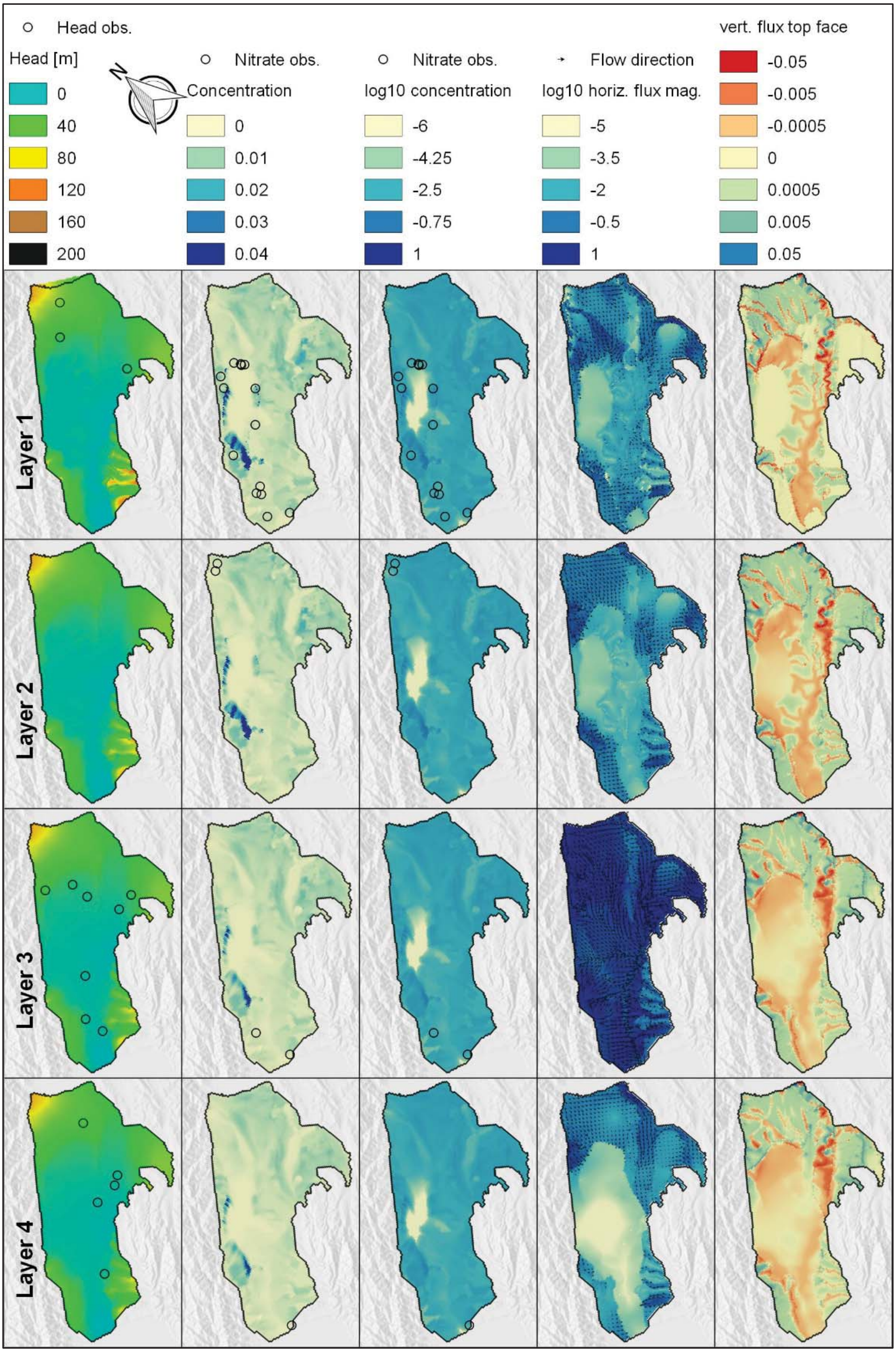

Figure 5.7 Calibrated piezometric, concentration and flux model outputs from the south model calibration (layers 1–4).

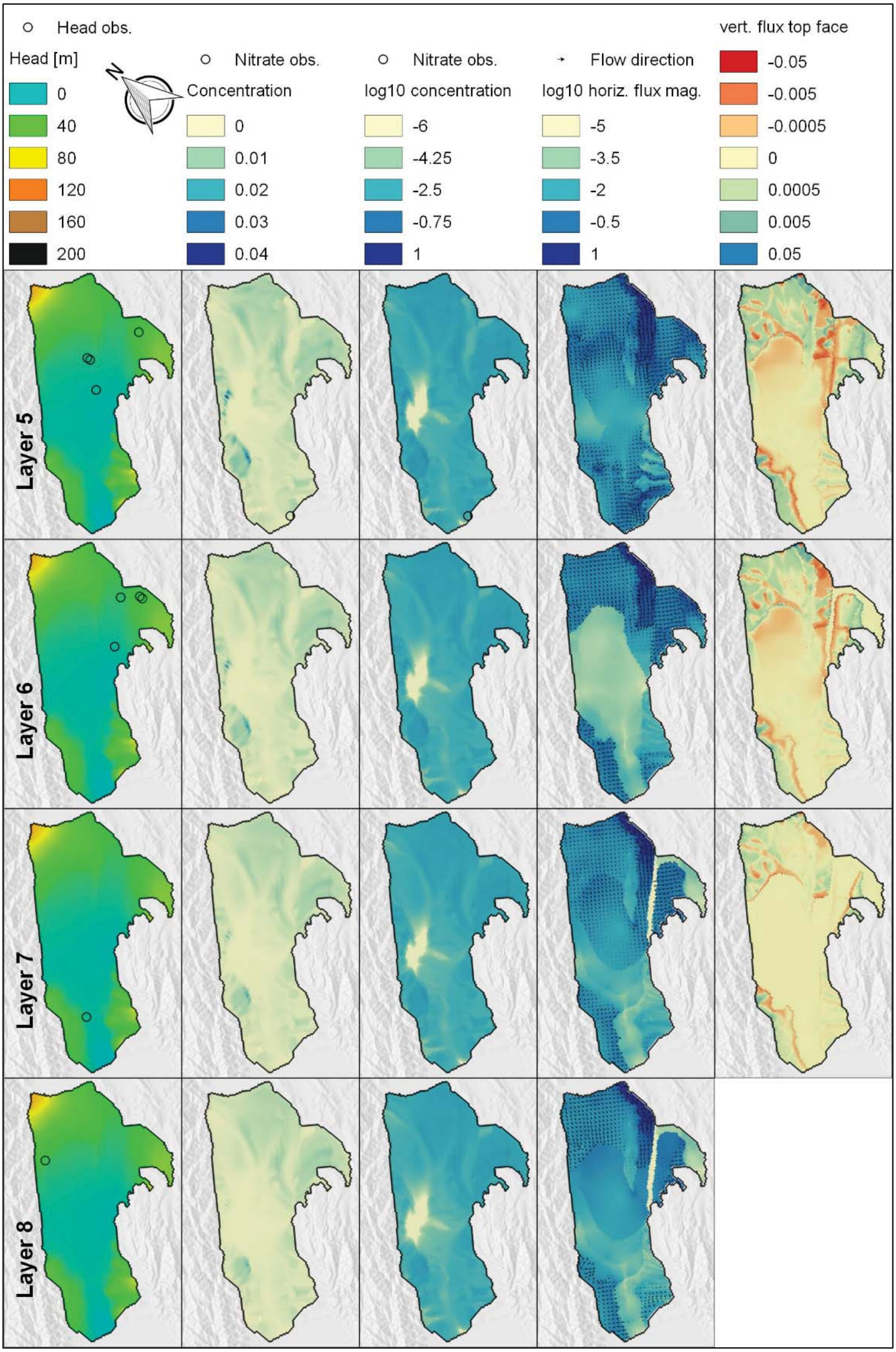

Figure 5.8 Calibrated piezometric, concentration and flux model outputs from the south model calibration (layers 5–8).

5.6.2 Modelled and Measured Groundwater Levels

The locations of groundwater levels are shown in Figure 5.9 and Figure 5.10 for the north and south model, respectively. Selected plots showing measured and modelled values for these calibration targets are shown in Figure 5.11 and Figure 5.12, respectively, and a complete set of these plots is in Appendix A8 and A9.

The simulated groundwater levels reflect the measured relative responses to climatic and pumping stresses reasonably well. In general, model to measurement fits for groundwater levels are better in the north model than in the south model. The model to measurement misfit in these wells is similar to that of the original FEFLOW model.

While the relative responses are reasonably well matched, potential causes of a degree of model to measurement misfit may be the result of the model layer structure. For example, in the south model it appears that the magnitude of some of the simulated water level fluctuations are larger than the measured. This may be due to the layer type assignment in the model — layer 1 was unconfined, but deeper layers were assigned a confined layer type. However, if unconfined conditions are occurring in the second and third model layers then a specific yield values instead of a specific storage values could be used in the simulation calculations which would result in smaller groundwater level fluctuations.

Similarly, some model to measurement misfit in the north model may be attributed to the same cause. For example, the plot for well S26/0030 indicates a much larger groundwater fluctuation that was able to be simulated. Reasons for this could also be attributed to nearby groundwater abstractions that were not included in the model. It is recommended that future work with these models investigate these issues further.

Model to measurement fits could also be improved by the use of a of greater density or numbers of pilot point parameters, as while there is a greater density of observations than pilot points, there is sometimes tension between fitting one water level over the other if the aquifer is reasonably heterogeneous. However, more pilot points were not adopted in this project, as the model run times for this model are long, and hence this option was not possible in the project time frame. Another often neglected reason for such model to measurement misfit can be attributed to the robustness of the measurements, as was recently discussed in Lundquist et al. (2015). These model-to-measurement misfits contribute to the model uncertainty and are accounted for in the uncertainty analysis described in Section 6.

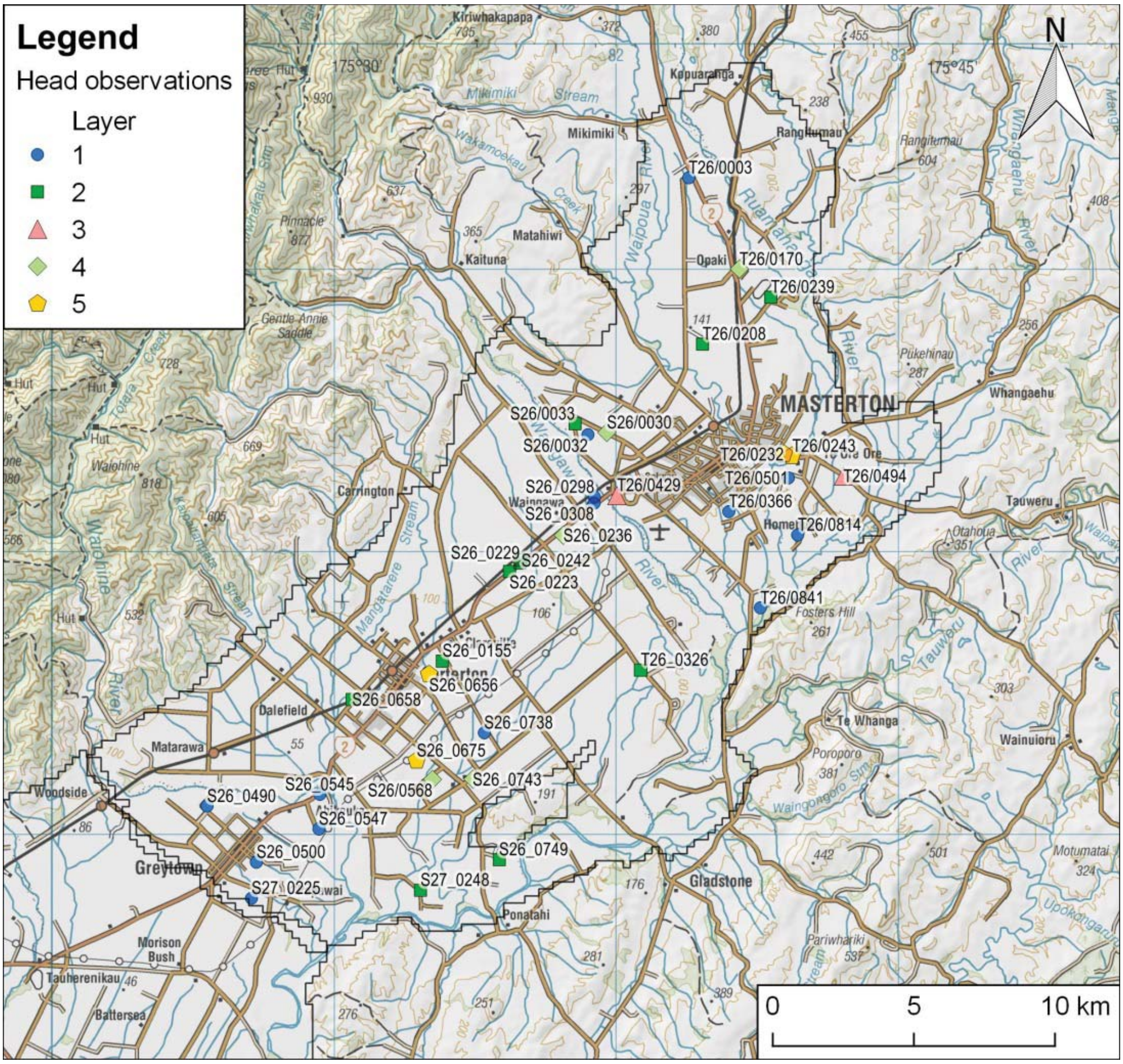

Figure 5.9 Location of groundwater level monitoring sites used in the north model calibration.

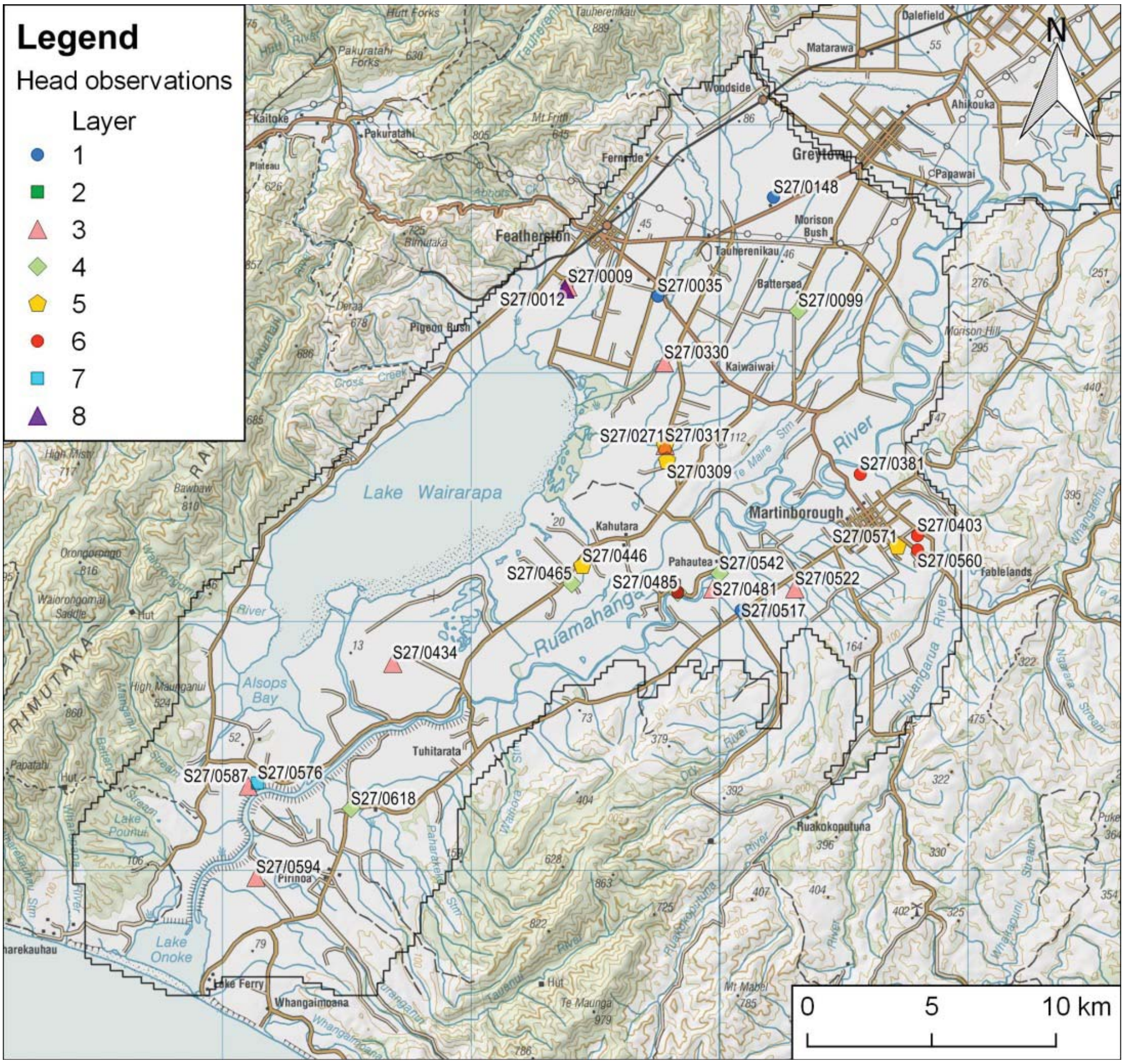

Figure 5.10 Location of groundwater level monitoring sites used in the south model calibration.

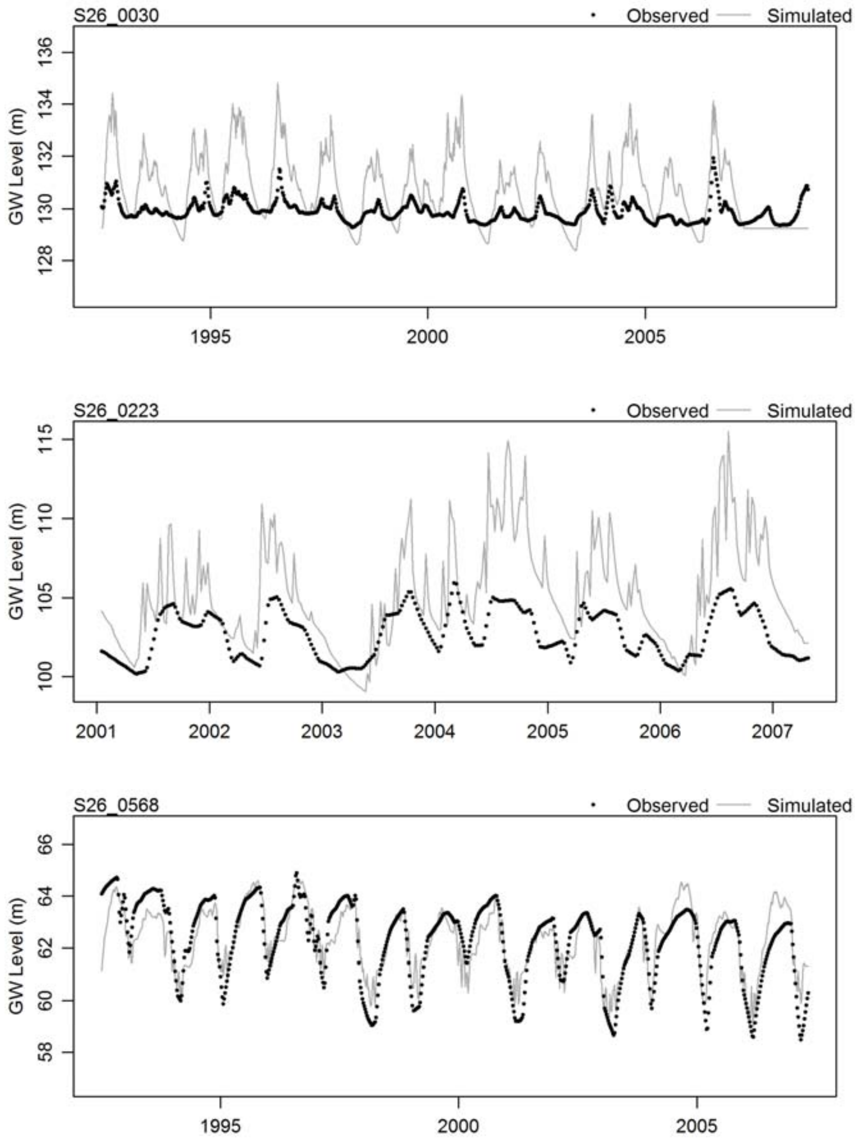

Figure 5.11 Selected modelled and measured groundwater levels in the north model for wells S26/0223, S26/05658 and S26/0030 (refer to Appendix A8 for a complete set of monitoring well modelled-measured groundwater level plots).

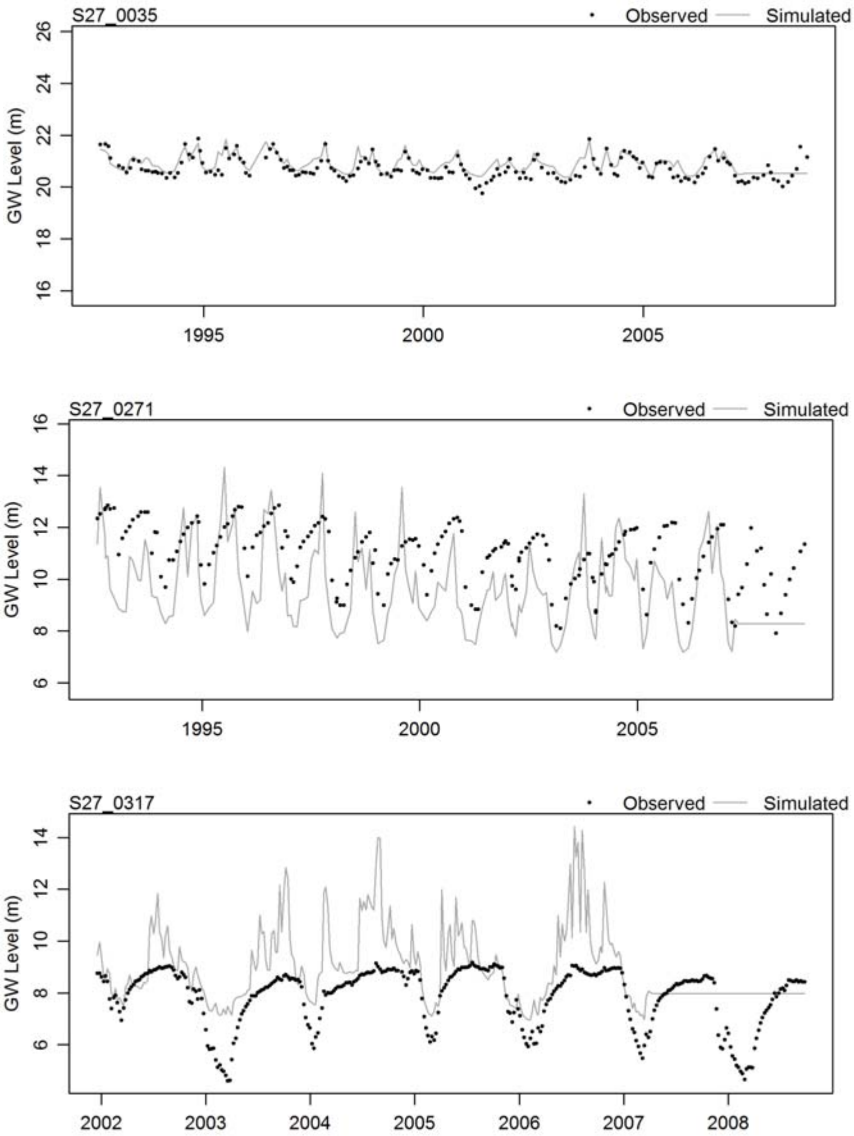

Figure 5.12 Selected modelled and measured groundwater levels in the south model for wells S27/0035, S27/0271 and S27/0317 (refer to Appendix A9 for a complete set of monitoring well modelled-measured groundwater level plots).

5.6.3 Stream Flows

Locations of stream flows recording sites are shown in Figure 5.13 and Figure 5.14 for the north and south models, respectively. The measured and modelled values for these calibration targets are shown in Figure 5.15 and Figure 5.17 and Appendices A10 and A11. These stream flows are also plotted as flow duration curves in Figure 5.16 and Figure 5.18, and in Appendices A12 and A13 respectively. The previous FEFLOW model did not simulate stream flows, but as discussed in Section 3 the representation of the rivers in the MODLFOW stream flow routing package (SFR package) has allowed these flows to be simulated in the current model version.

The model to measurement misfit of flows at the surface water gauging sites in both the north and the south models reflect the overall pattern of high and low flows. In the north model the simulated flows for both the largely groundwater spring fed streams, e.g., Tilsons Creek and Papawai Stream and the large losing and gaining streams, e.g., Ruamāhanga River and Waiohine River are matched equally well. A number of smaller intermittently gauged streams were also used as calibration targets with similarly good history matching results. In the south model the model simulation match to the gauged surface water flow sites were again similarly good.

The flow duration curves show how well the absolute magnitude of flows is matched over time rather than the temporal fluctuations. For most of the gauging sites the model to measured matches to flow duration curves are good.

In addition to these graphs in Figures 5.15 to 5.18, the model to measured fit was assessed in two other ways. Firstly, the correspondence of mean annual low flow between modelled and measured data was assessed, based on a 7-day time step (this was necessary because of the model time steps adopted in calibration). Secondly, correspondence between the duration of stream low flow periods simulated by the model and as measured (based on a 7-day time step) was explored. These figures are presented in a series of tables in Appendix A14. Table A14.1 and Table A14.2 list the mean annual low flow comparisons. Table A14.3 and Table A14.4 show the number of days where the simulated flow went below the partial and full flow restriction level for a number of sites for each year in the model calibration period for both modelled and measured data.

It is important to note that the mean annual low flow, the flow duration curves and the number of days below the partial and full restriction flows were not used in the model as calibration targets, and have only been requested later in the project for reporting purposes. Better fits to these measures could be expected by including these measures as calibration targets in the calibration process.

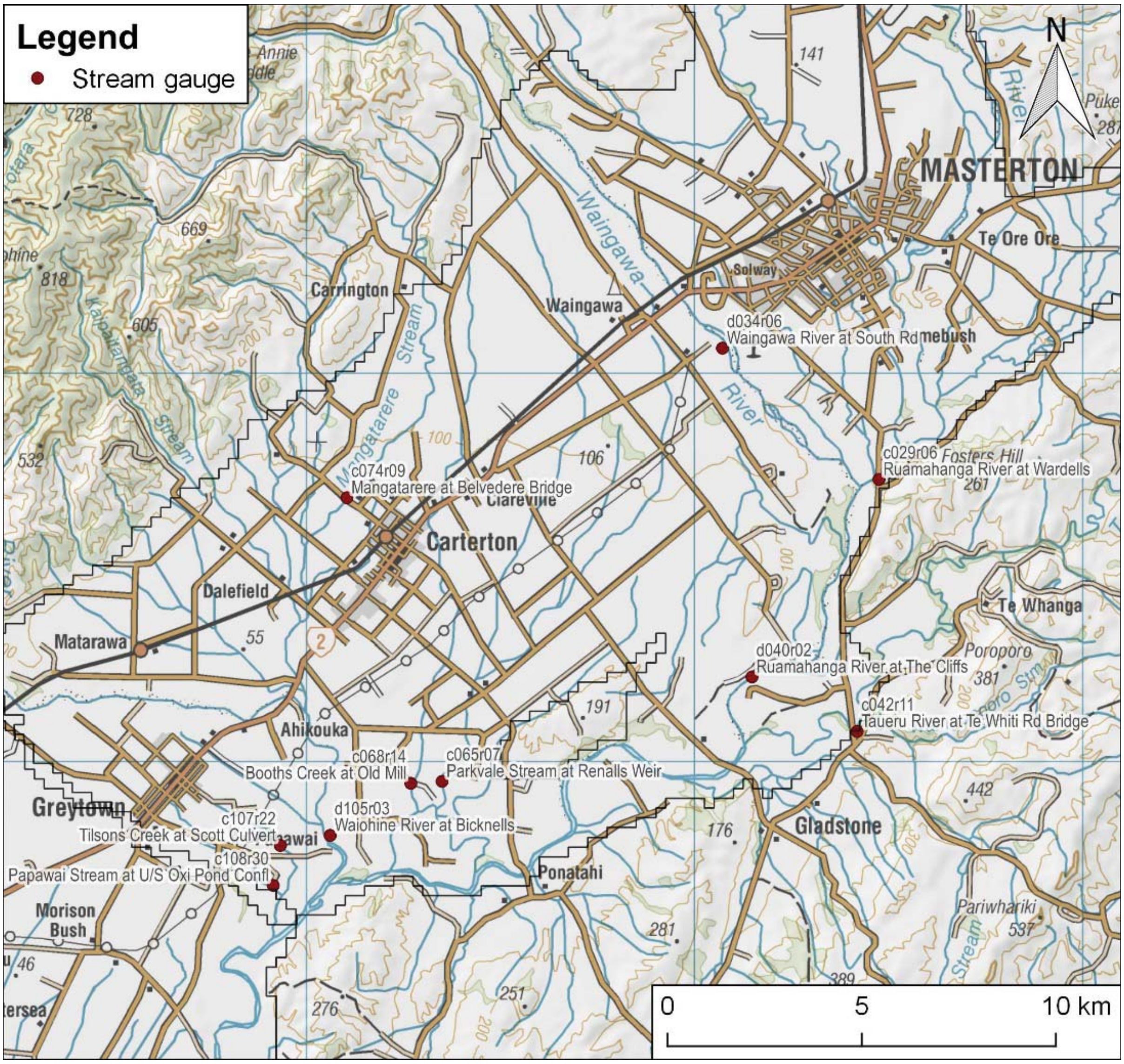

Figure 5.13 Location of surface water gauging sites used in the north model calibration.

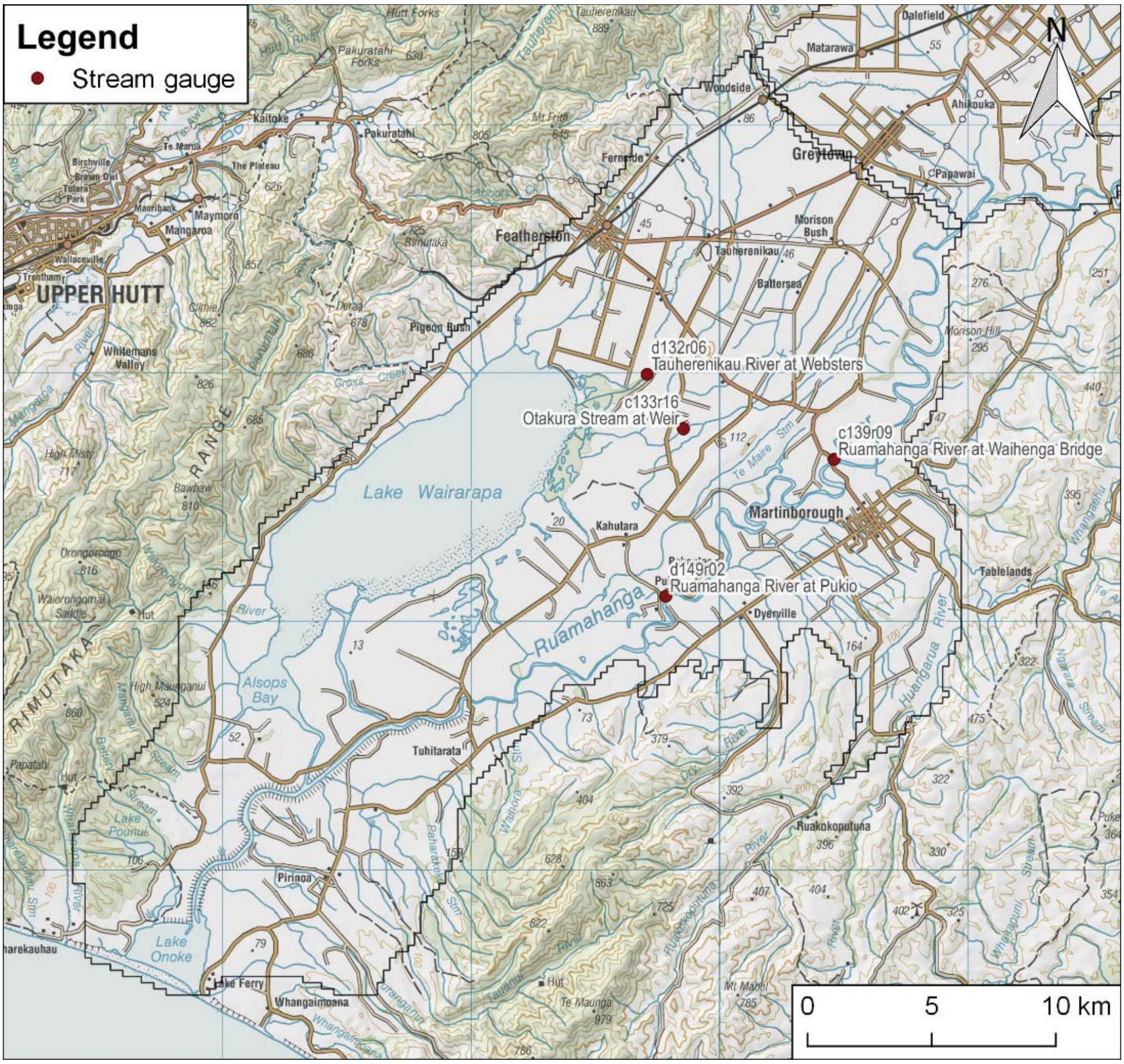

Figure 5.14 Location of surface water gauging sites used in the south model calibration.

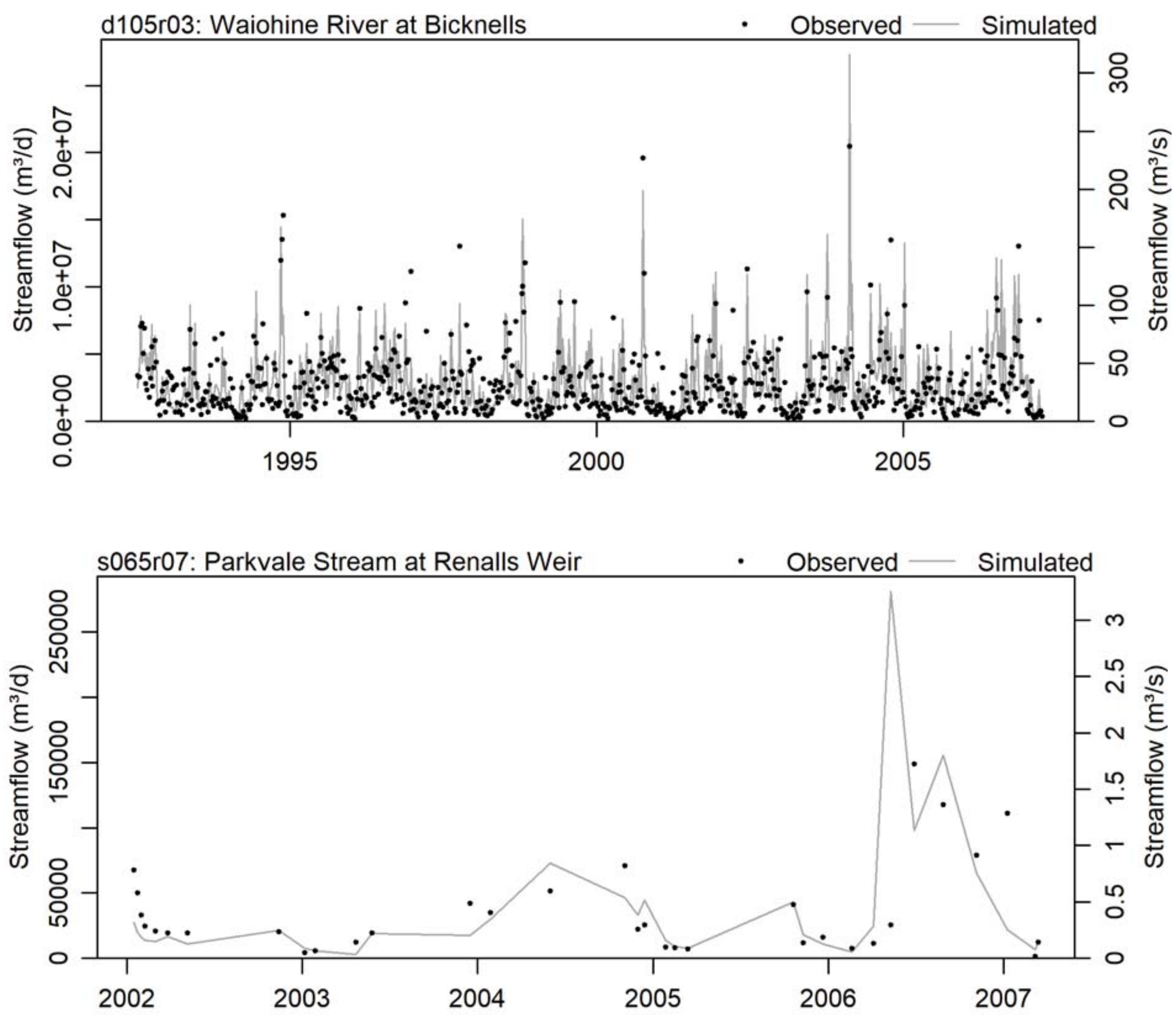

Figure 5.15 Selected modelled and measured surface water flows in the north model. Refer to Appendix A10 for complete set of model to measured surace water flow time series for the north model.

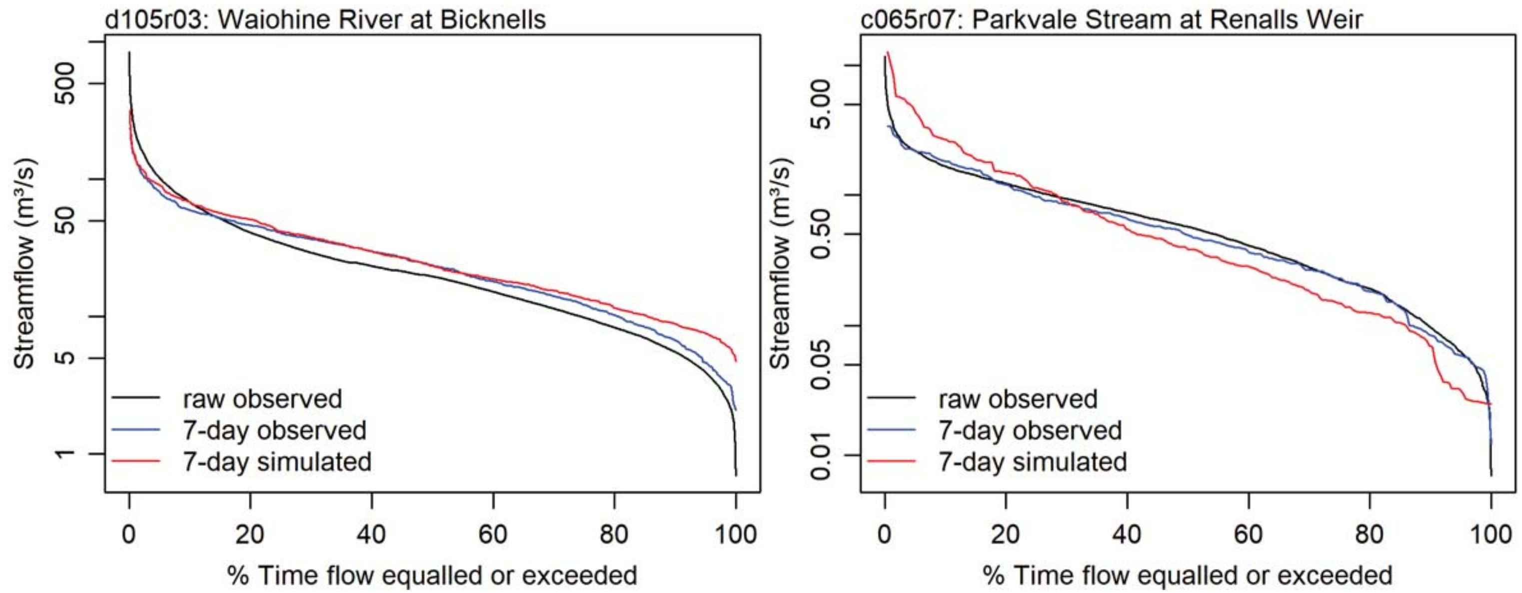

Figure 5.16 Selected flow duration curves for modelled and measured surface water flows in the north model based on a 7 day time step, and for raw daily data. Refer to Appendix A12 for complete set of model to measured flow duration curves for the north model.

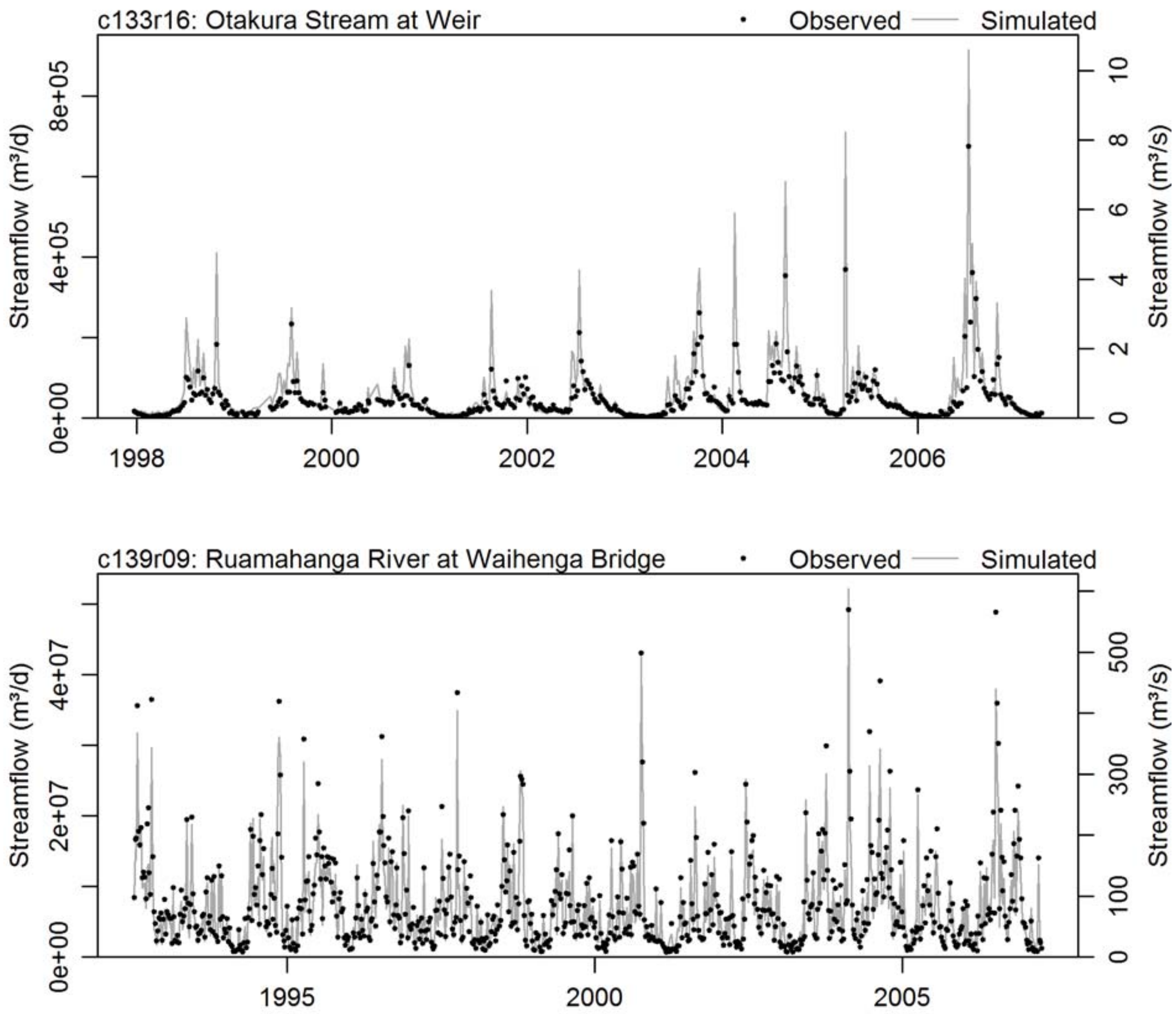

Figure 5.17: Selected modelled and measured surface water flows in the south model. Refer to Appendix A11 for complete set of model to measured flow duration curves for the south model.

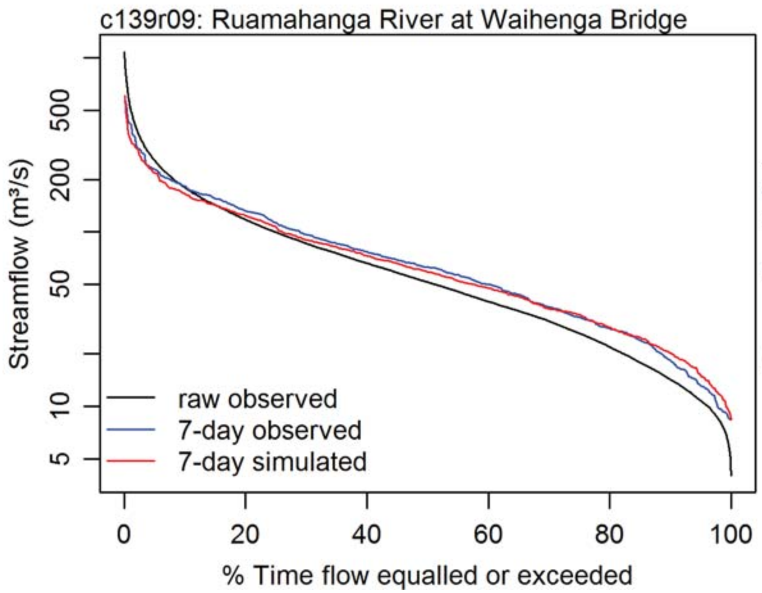

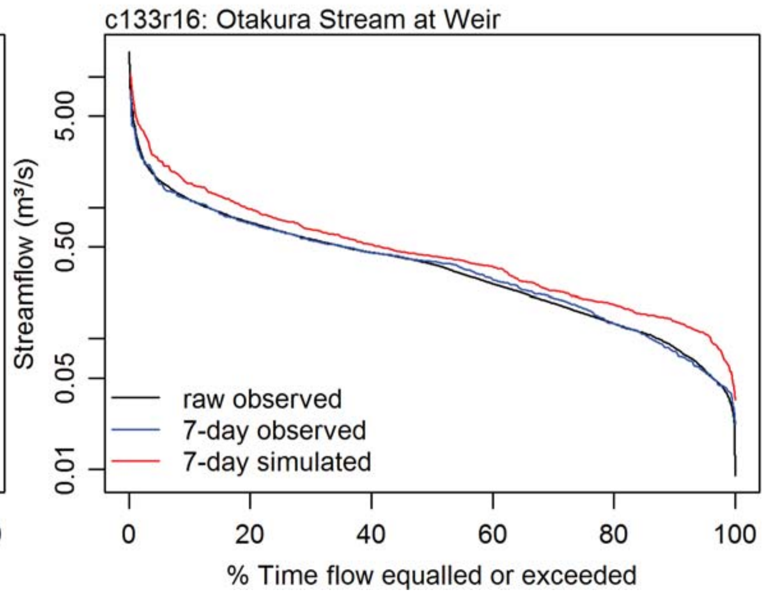

Figure 5.18 Selected flow duration curves for modelled and measured surface water flows in the south model based on a 7 day time step, and for raw daily data.Refer to Appendix A13 for complete set of model to measured flow duration curves for the south model.

5.6.4 Stream Losses and Gains

The simulated average losses and gains from the surface water ways are depicted in Figure 5.19, and Figure 5.22 for the north and south models, respectively. The river gain loss patterns are consistent with the recognised patterns depicted in Figure 5.9.

The match to the measured river losses and gains from simultaneous gaugings is also shown in Figure 5.20 for the north model, and locations where the simultaneous gaugings were taken is shown in Figure 5.21. While the absolute values of losses and gains are not always matched exactly, the pattern of measured losses and gains is well simulated. This level of fit is considered acceptable given the approximate nature of these measurements.

Figure 5.22 depicts the simulated average river gain loss patterns for the south model and once again these are consistent with the previously recognised patterns depicted in Figure 5.1. The match to the measured river losses and gains from simultaneous gaugings is also shown in Figure 5.23 for the south model and locations where the simultaneous gaugings were taken is shown in Figure 5.24. As for the north model this level of fit is considered acceptable given the approximate nature of these measurements.

Of interest is the interaction with the lake in the south model (the Lake was represented as drains in the FEFLOW model). The simulated flows indicate groundwater seeping into the lake along the western and southern lake margins.

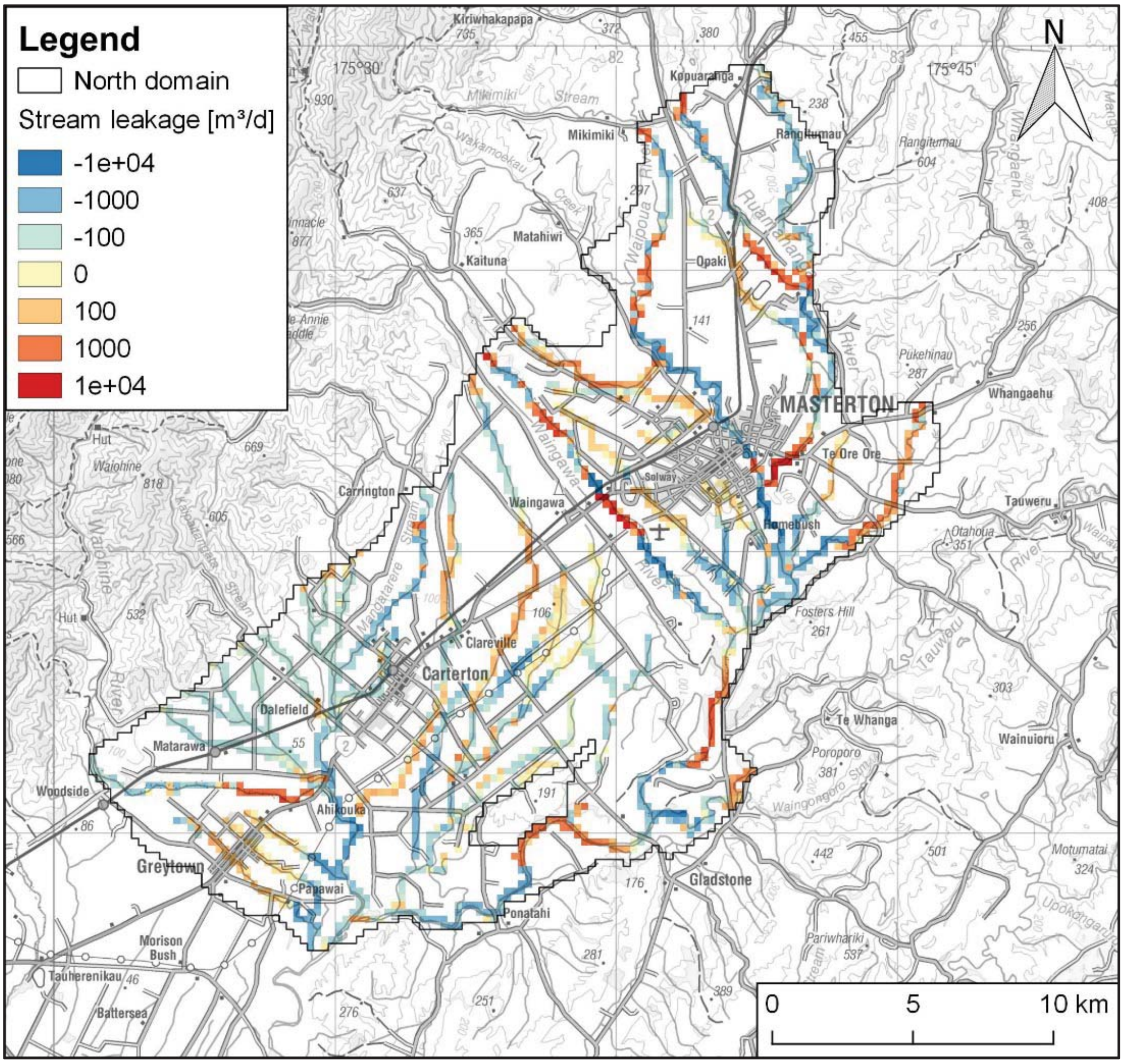

Figure 5.19 Modelled losing and gaining stream reaches in the north model (in this figure negative values indicate a loss from the aquifer or gaining streams, positive is a gain to the aquifer and so losing streams).

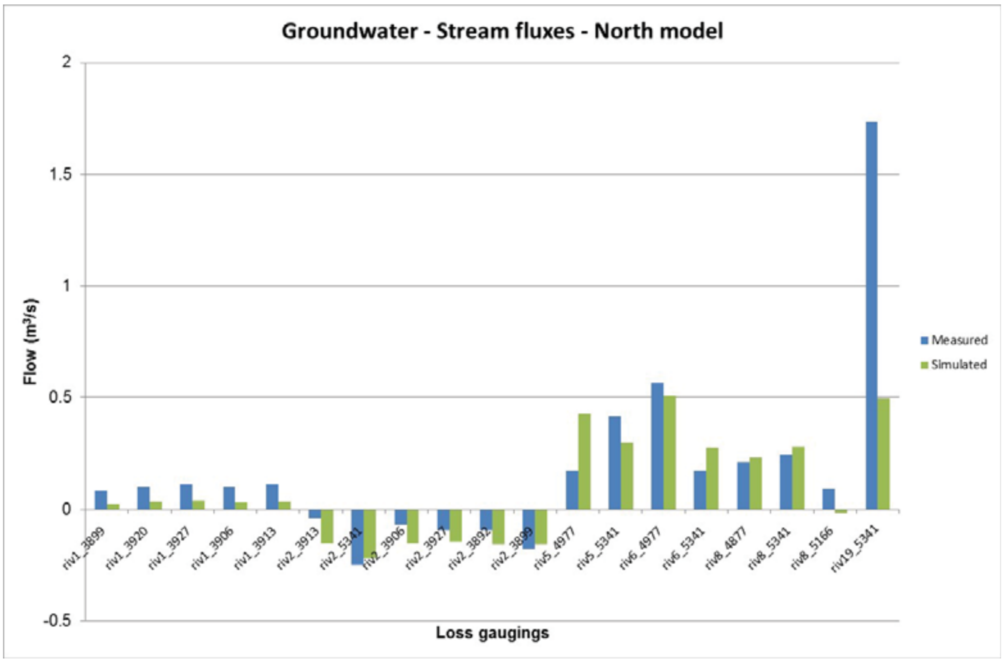

Figure 5.20 Measured and simulated surface water losses and gains for selected river reaches in the north model for various observation times (in this figure negative values indicate a loss to the stream, and positive is a gain to the stream).

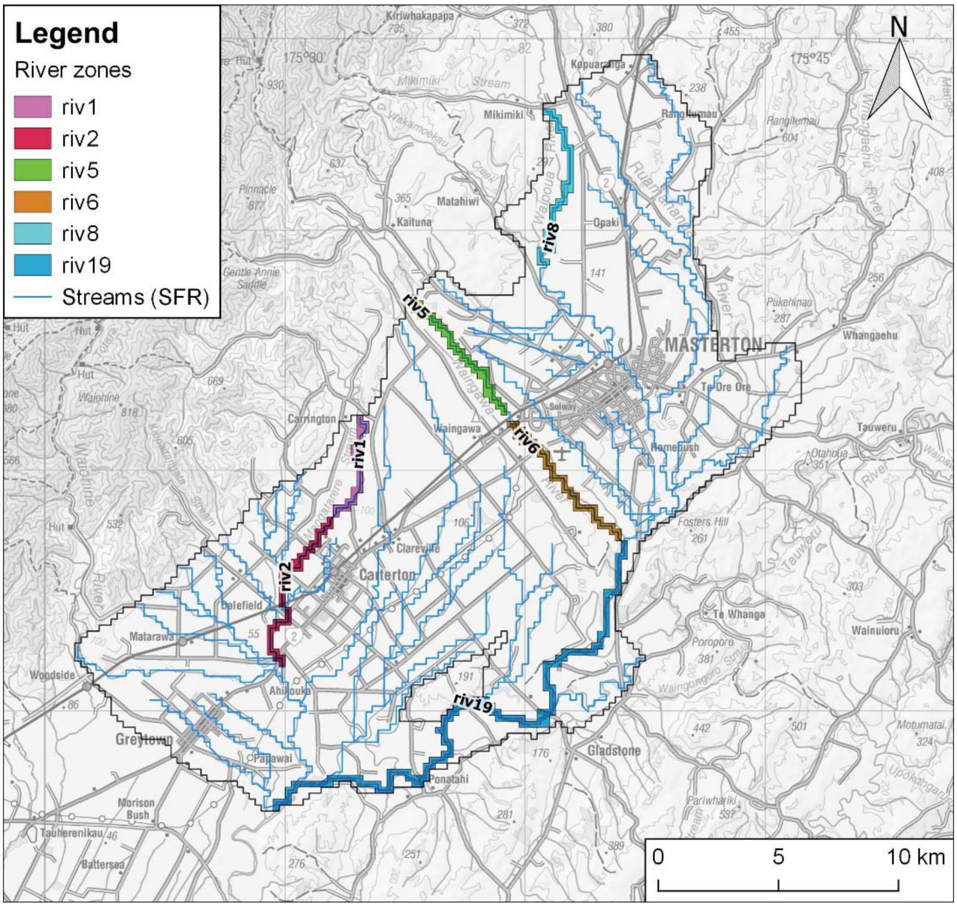

Figure 5.21 Location of reaches over which simultaneous guagings calculated aquifer – surface water fluxes in the north model are compared in Figure 5.20.

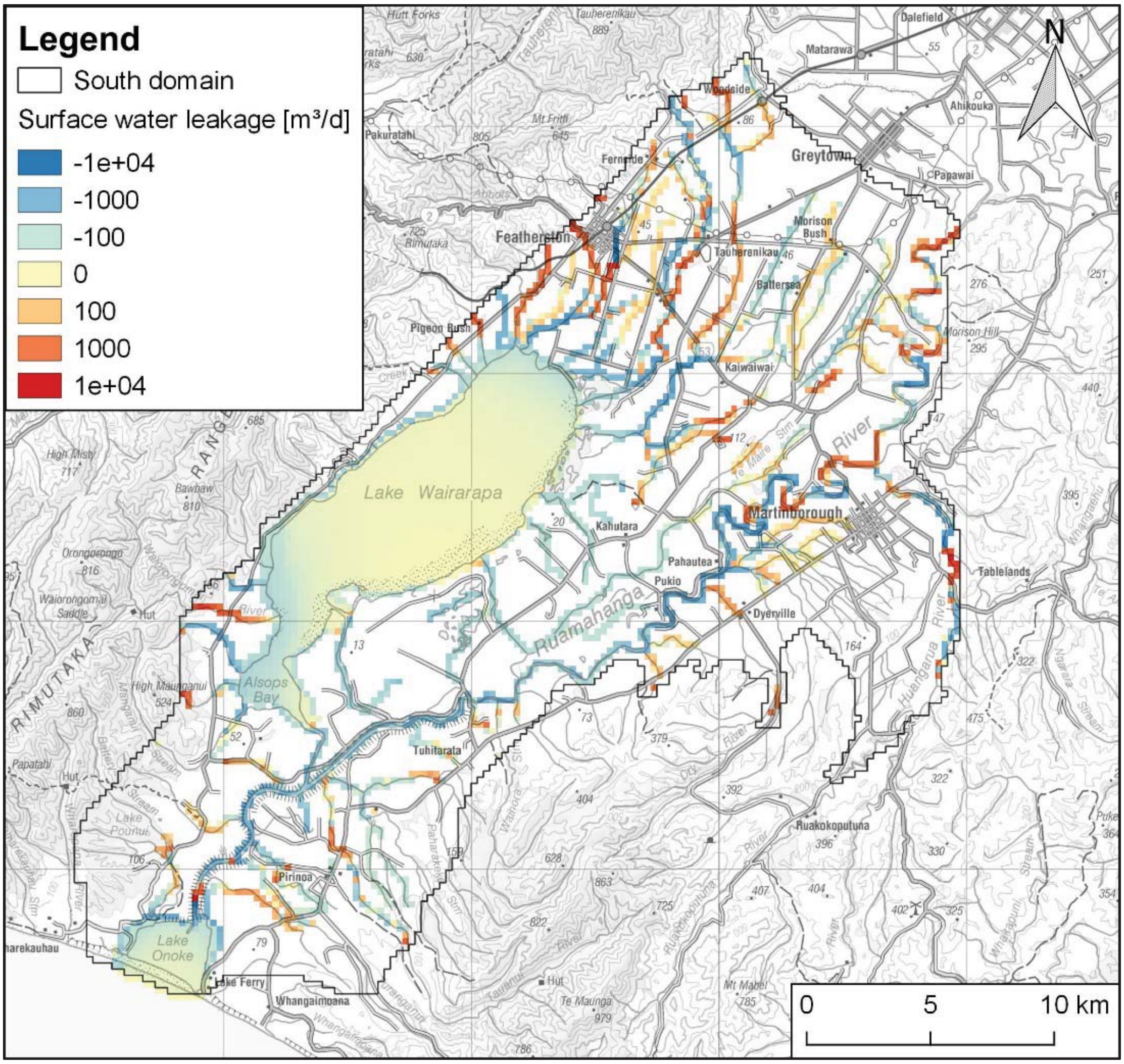

Figure 5.22 Modelled losing and gaining stream reaches in the south model (in this figure negative values indicate a loss from the aquifer or gaining streams, positive is a gain to the aquifer and so losing streams).

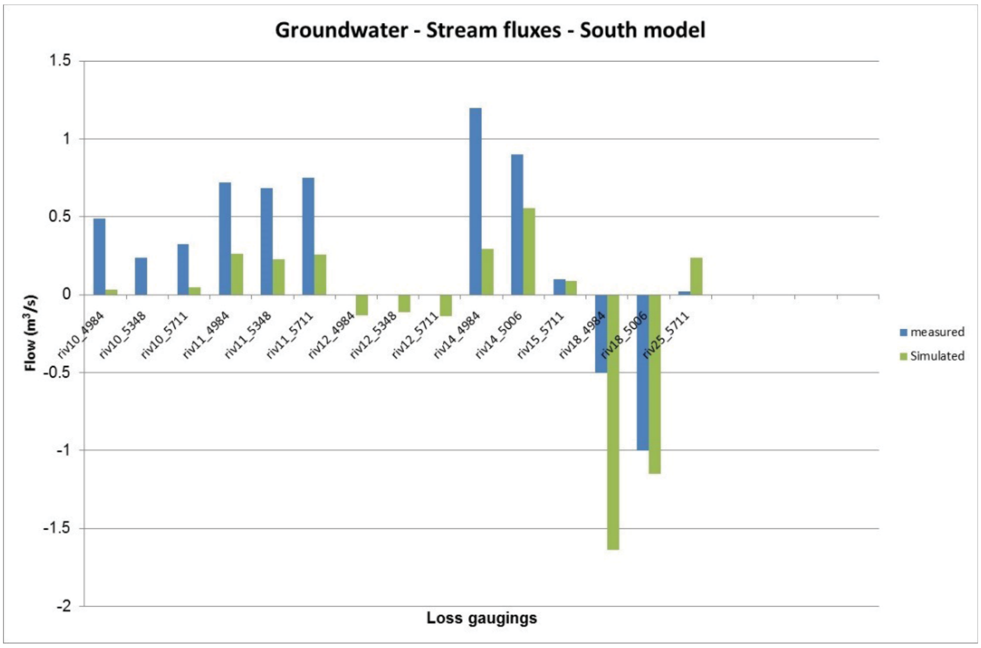

Figure 5.23 Measured and simulated surface water losses and gains for selected river reaches in the south model for various obvervation times (in this figure negative values indicate a loss to the stream, and positive is a gain to the stream).

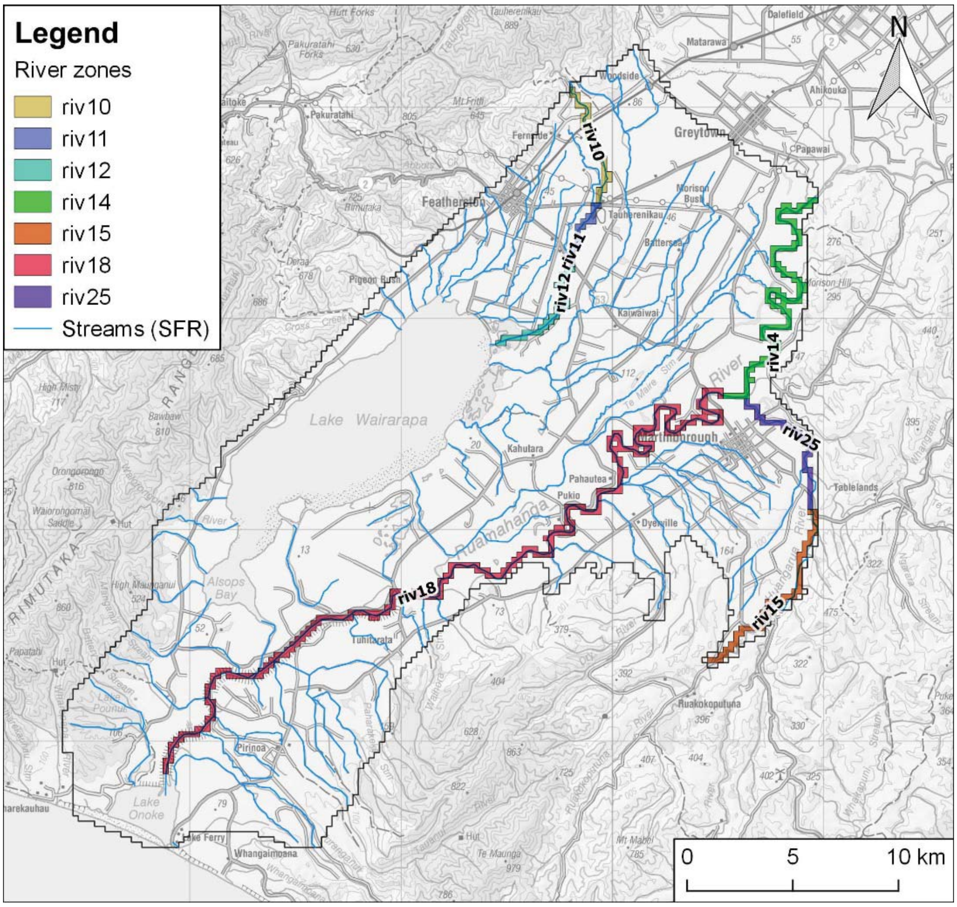

Figure 5.24 Location of reaches over which simultaneous guagings calculated aquifer – surface water fluxes in the south model are compared in Figure 5.23.

5.6.5 Water Budgets for the North and South Models and Groundwater Management Zones

The simulated water budget for the north and south models are given in Table 5.1 and Table 5.2, respectively. These tables indicate that generally higher fluxes are moving through the aquifer system than was estimated in A6.5. In a large part, this is driven by the greater rainfall recharge values provided by IRRICALC compared to the previous FEFLOW model values, and commensurate greater simulated river flow losses and gains. In terms of the latter, observed flow losses and gains from concurrent gaugings are only available for extreme low flows and therefore it is entirely possible the modelled mean fluxes are significantly different to these. The calibration of the models to stream flows provides additional confidence in the new water balance simulation. From these water balance components, it is clear that the amount of storage available within the aquifers has remained similar to the previous FEFLOW models (Gyopari and McAlister, 2010a, 2010b and 2010c).

Table 5.1 Simulated average water balance for the northern groundwater model.

	In (m3/day)	**Out (m3/day)**
Rainfall recharge	545852	
River flow loss/groundwater recharge	658925	
Water race loss	39533	
River flow gain/ groundwater discharge		1201337
Abstraction		44722
Totals	1244310	1246059

Table 5.2 Simulated average water balance for the southern groundwater model.

	In (m3/day)	**Out (m3/day)**
Rainfall recharge	587760	
River flow loss/groundwater recharge	924644	1483706
Water race recharge (Moroa)	20926	
River flow gain/groundwater discharge		
Abstraction		38399
Lake Wairarapa discharge (and Onoke)	70139	138345
Inflow from northern model boundary	54363	
Totals	1657832	1660449

The water budgets for the GWRC groundwater management zones depicted in Figure 5.25 are summarised in Table 5.3 and Table 5.4 for the north and south models, respectively. Note that the water management zones do not cover the entire model domain, and hence an additional column has been added to these tables. These values are tabled as they provide the foundation for the current allocation rules.

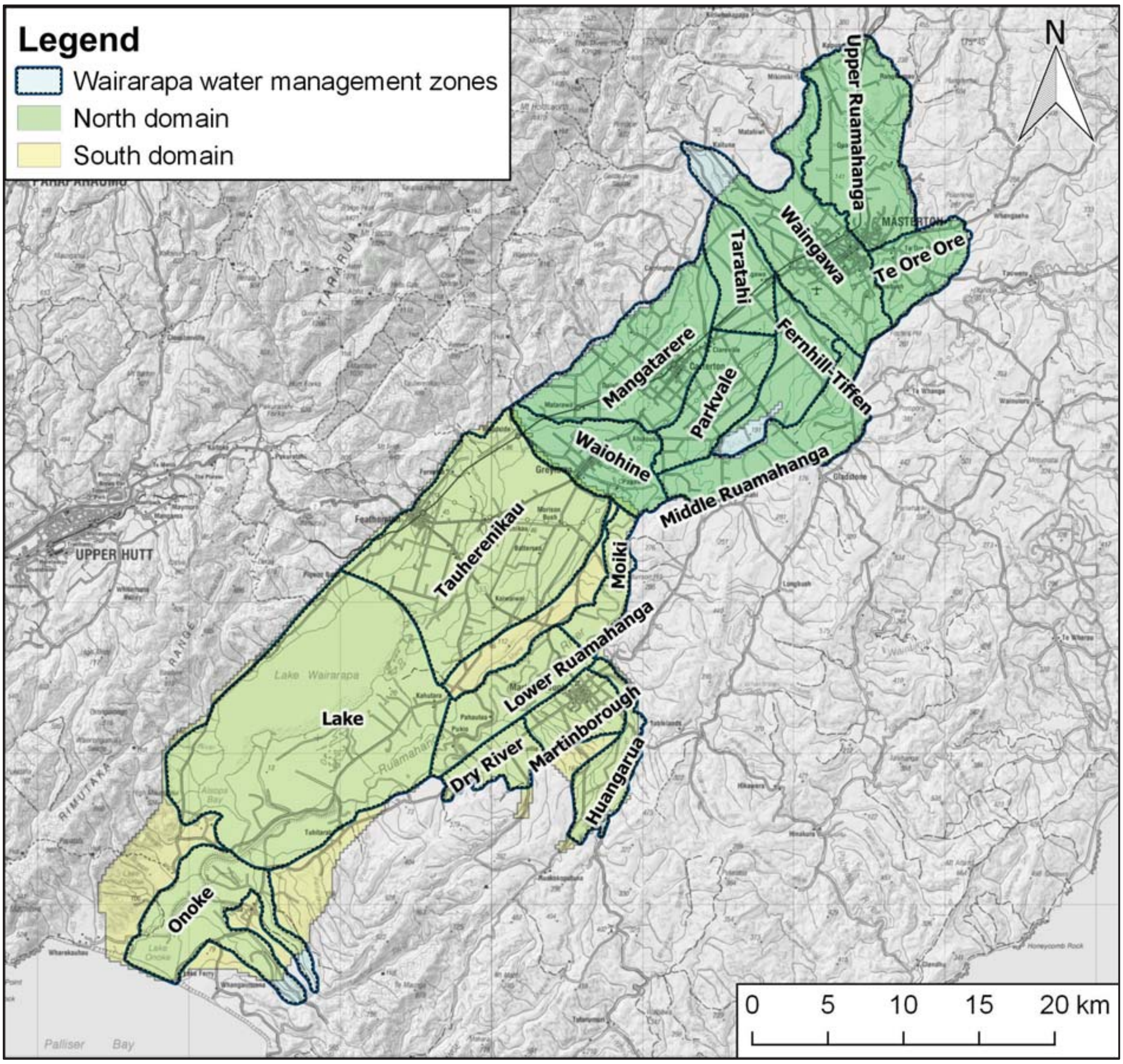

Figure 5.25 Groundwater management zones used by GWRC.

Table 5.3 Simulated average water balance for the northern model groundwater management zones used by GWRC (m^3/day).

	IN	U. Ruamahanga	Te Ore Ore	Waingawa	Taratahi	Parkvale	Fernhill-Tiffen	M. Ruamahanga	Mangatarere	Waiohine	Outside
From Zone	U. Ruamahanga		5,671	124,366	—	—	—	—	—	—	—
	Te Ore Ore	629		99,231	—	—	—	—	—	—	—
	Waingawa	83,003	3,971		67,907	—	81,223	3,689	—	—	—
	Taratahi	—	—	85,514		33,789	4,862	—	4,253	—	—
	Parkvale	—	—	—	174		4,692	8,898	22,232	11,016	—
	Fernhill-Tiffen	—	—	84,984	1,973	9,811		13,629	—	—	—
	M. Ruamahanga	—	—	615	—	1,025	401		—	2,264	937
	Mangatarere	—	—	—	4,628	27,206	—	—		44,745	—
	Waiohine	—	—	—	—	1,116	—	53	3,398		—
	Outside	—	—	—	—	—	—	1,081	—	—	
Stream leakage		76,954	126,535	214,054	13,018	12,556	2,386	143,553	23,343	18,968	—
Recharge		100,682	21,130	87,458	47,831	38,954	29,776	32,520	133,045	54,313	144
Wells		7,773	8,470	—	5,720	2,244	4,972	924	4,824	4,575	—
Total IN		269,041	165,777	696,222	141,250	126,700	128,311	204,347	191,095	135,881	1,081

	OUT	U. Ruamahanga	Te Ore Ore	Waingawa	Taratahi	Parkvale	Fernhill-Tiffen	M. Ruamahanga	Mangatarere	Waiohine	Outside
To Zone	U. Ruamahanga		629	83,003	—	—	—	—	—	—	—
	Te Ore Ore	5,671		3,971	—	—	—	—	—	—	—
	Waingawa	124,366	99,231		85,514	—	84,984	615	—	—	—
	Taratahi	—	—	67,907		174	1,973	—	4,628	—	—
	Parkvale	—	—	—	33,789		9,811	1,025	27,206	1,116	—
	Fernhill-Tiffen	—	—	81,223	4,862	4,692		401	—	—	—
	M. Ruamahanga	—	—	3,689	—	8,898	13,629		—	53	1,081
	Mangatarere	—	—	—	4,253	22,232	—	—		3,398	—
	Waiohine	—	—	—	—	11,016	—	2,264	44,745		—
	Outside	—	—	—	—	—	—	937	—	—	
Stream leakage		136,170	63,769	445,130	12,386	78,222	17,749	191,308	103,588	129,687	—
Wells		3,301	2,827	12,665	558	2,374	789	7,935	12,003	2,239	—
Total OUT		269,509	166,455	697,589	141,361	127,606	128,935	204,485	192,170	136,493	1,081

		U. Ruamahanga	Te Ore Ore	Waingawa	Taratahi	Parkvale	Fernhill-Tiffen	M. Ruamahanga	Mangatarere	Waiohine	Outside
IN-OUT		-4.68E+02	-6.78E+02	-1.37E+03	-1.11E+02	-9.06E+02	-6.23E+02	-1.38E+02	-1.08E+03	-6.12E+02	-2.37E-01
Percent error		-1.74E-01	-4.08E-01	-1.96E-01	-7.87E-02	-7.13E-01	-4.85E-01	-6.74E-02	-5.61E-01	-4.50E-01	-2.19E-02

Table 5.4 Simulated average water balance for the southern model groundwater management zones used by GWRC (m^3/day).

	IN	Huangarua	Martinborough	Dry River	Moiki	L. Ruamahanga	Tauherenikau	Lake	Onoke	Outside
From Zone	Huangarua		23,108	—	—	10,879	—	—	—	49,040
	Martinborough	17,478		18,808	—	29,959	—	—	—	—
	Dry River	—	3,285		—	56,072	—	—	—	—
	Moiki	—	—	—		87,712	—	—	—	102,874
	L. Ruamahanga	—	0	—	—		—	7,958	—	759
	Tauherenikau	—	—	—	1,683	—		42,223	—	67,561
	Lake	—	—	—	—	4,786	5,664		2,651	22,583
	Onoke	—	—	—	—	—	—	6,720		2,784
	Outside	25,577	33,127	7,913	159,239	15,763	86,550	64,371	63,910	
Constant		—	—	—	—	—	22,043	—	—	76,175
Stream leakage		92,133	6,903	26,591	72,044	47,303	200,705	46,158	39,857	78,773
Recharge		16,366	11,328	9,413	12,821	21,179	187,661	157,093	49,851	122,048
Wells		—	—	—	—	—	20,924	—	—	—
Lake seepage		—	—	—	—	—	—	20,751	16,352	—
Total IN		151,554	77,752	62,725	245,787	273,654	523,547	345,273	172,621	522,597
	OUT	Huangarua	Martinborough	Dry River	Moiki	L. Ruamahanga	Tauherenikau	Lake	Onoke	Outside
To Zone	Huangarua		17,478	—	—	—	—	—	—	25,577
	Martinborough	23,108		3,285	—	0	—	—	—	33,127
	Dry River	—	18,808		—	—	—	—	—	7,913
	Moiki	—	—	—		—	1,683	—	—	159,239
	L. Ruamahanga	10,879	29,959	56,072	87,712		—	4,786	—	15,763
	Tauherenikau	—	—	—	—	—		5,664	—	86,550
	Lake	—	—	—	—	7,958	42,223		6,720	64,371
	Onoke	—	—	—	—	—	—	2,651		63,910
	Outside	49,040	—	—	102,874	759	67,561	22,583	2,784	
Constant		—	—	—	—	—	1,864	—	—	41,974
Stream leakage		66,133	273	130	54,055	259,005	407,282	241,334	135,825	24,175
Wells		3,506	11,492	3,715	1,317	6,345	9,441	1,228	978	378
Lake seepage		—	—	—	—	—	—	70,461	30,800	3,825
Total OUT		152,667	78,010	63,201	245,957	274,066	530,054	348,707	177,107	526,802
IN-OUT		-1.11E+03	-2.59E+02	-4.76E+02	-1.71E+02	-4.12E+02	-6.51E+03	-3.43E+03	-4.49E+03	-4.20E+03
Percent error		-7.32E-01	-3.32E-01	-7.56E-01	-6.94E-02	-1.51E-01	-1.24E+00	-9.90E-01	-2.57E+00	-8.01E-01

5.6.6 Nitrate Concentration

The nitrate concentration monitoring bores utilised as calibration targets for the transport model are shown in Figures 5.26 and 5.27 for the north and south models, respectively. The nitrate concentrations vary significantly over short distances, including within the same model grid cell. For this reason, we have decided to compare the average measured and modelled nitrate values per model layer as shown in Figure 5.28. Figure 5.28 indicates that the general spatial and depth trend in nitrate vales are captured by the models. Model to measurement misfit in these nitrate values are accounted for in the uncertainty analyses discussed in Section 6.

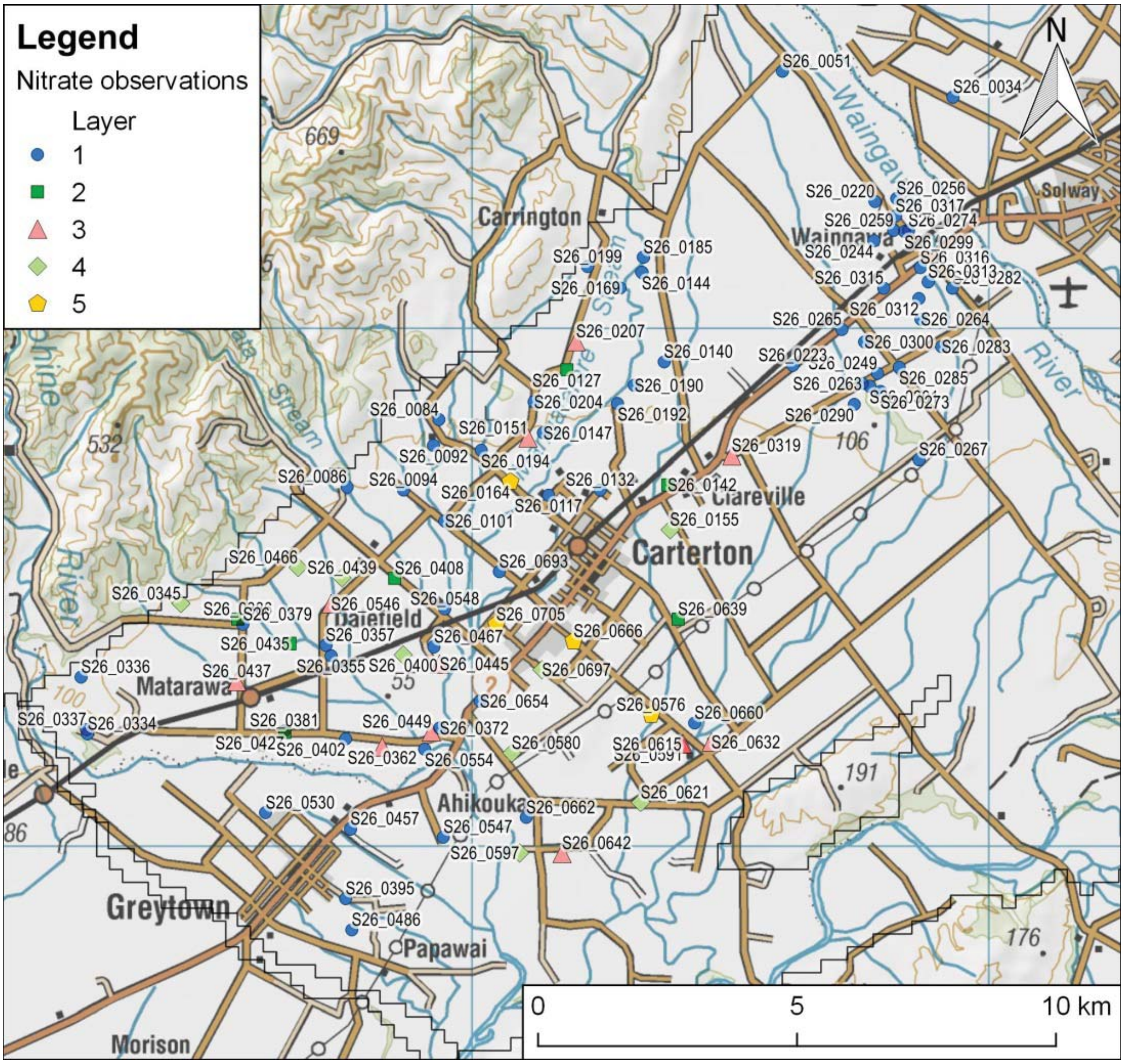

Figure 5.26 Location of groundwater nitrate concentration sites used in the north model calibration.

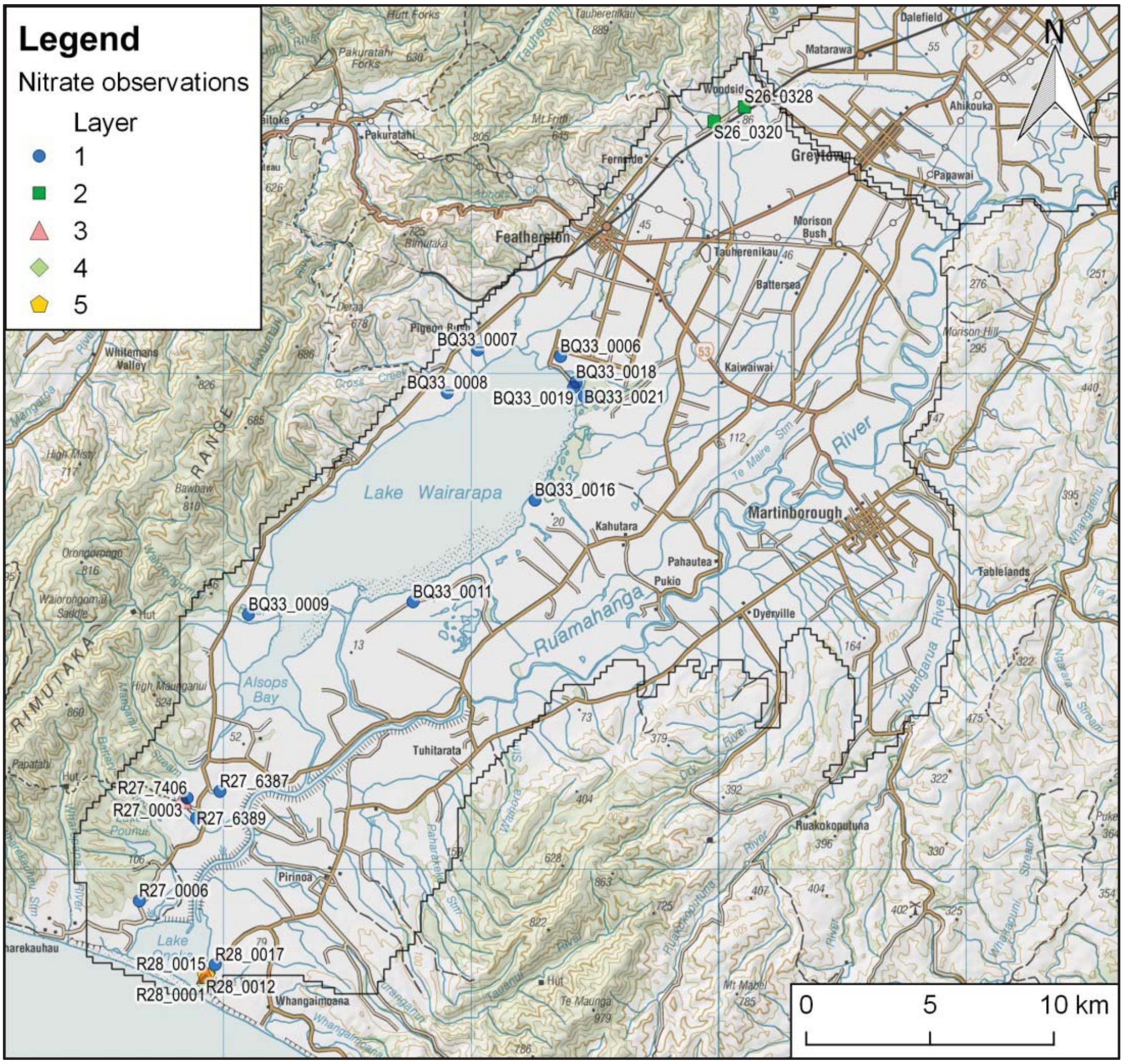

Figure 5.27 Location of groundwater nitrate concentration sites used in the north model calibration.

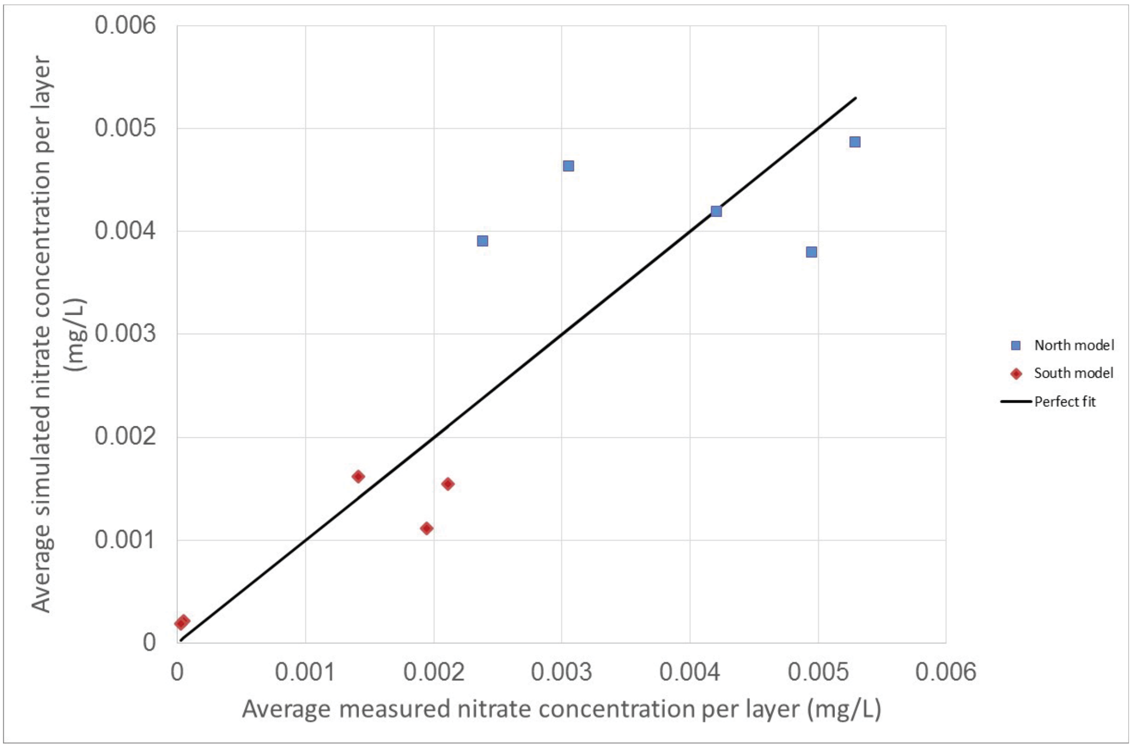

Figure 5.28 Location of groundwater nitrate concentration sites used in the south model calibration.

6.0 MODEL LIMITATIONS, PARAMETER IDENTIFICATION AND PARAMETER UNCERTAINTY

Model parameter uncertainty analysis involves describing the range of model parameter values and their combinations that provide model outputs which are consistent with measurements and have credible values when compared with expert opinion. It also must account for the model limitiations. Model predictive uncertainty explores the model predictive outputs consistent with the range of credible parameter values identified in the parameter uncertainty analysis. This report addresses parameter uncertainty only and this is described in this section; predictive scenario uncertainty analysis is scheduled to be explored in future modelling work.

The Australian Groundwater Modelling Guidelines (Barnett et al., 2012) advocate open and clear reporting of uncertainty to provide the decision-maker with the capacity to place model outputs in the context of risk to the overall project objectives. The uncertainty analyses undertaken in this section describe the combined outcome of prior parameter uncertainties, measurement inaccuracies, and the model limitations on parameter uncertainty.

6.1 LINEAR BAYESIAN UNCERTAINTY ANALYSIS

We have adopted a linear Bayesian parameter uncertainty analysis for this report to describe the uncertainty of the calibrated model parameters. This analysis incorporates the following components:

- The sensitivities of model outputs to all model adjustable parameters (e.g. sensitivity analyses).
- The innate uncertainties of model parameters (‘prior uncertainty’), as derived from expert knowledge, some of which incorporates spatial hydraulic property variability knowledge (refer to geostatistical analyses in section 6.2.1;
- The extent to which this “prior uncertainty” derived from expert knowledge was reduced through the model calibration process.

The theoretical basis for the linear Bayesian uncertainty analysis is discussed in Doherty (2015) and implemented by utility programs that support the PEST suite of software (Doherty, 2016). This method was selected for the current study because the numerical burden of linear uncertainty analysis is small compared with that of nonlinear uncertainty analysis, especially in highly parameterized contexts, such as was required in this model. Furthermore, while linear uncertainty analyses are more approximate that a non-linear analysis (e.g. Monte Carlo analyses), at this stage of the project, where the emphasis is on describing parameter uncertainty rather than predictive uncertainty, this is an appropriate uncertainty analysis method as it has other advantages:

- The analysis can be readily extended to include “parameters” which would not normally be estimated through model calibration, including model boundary conditions such as the TOPNET inflows, the nitrate flux inputs, and the recharge.
- The analysis can determine the dimensions of the calibration solution and null spaces, which provide a bulk indication of the degree of parameter correlation. By describing the extent of the calibration solution space the analysis also determines how many unique combinations of parameters can be estimated based on the available data. This can be compared with the number of parameters being estimated;

- The analysis can be used to describe parameter identifiability, which describes the extent to which a unique parameter estimate has been achieved through the calibration process (this varies from 0 to 1)
- The analysis can also be used to rapidly describe the relative parameter uncertainty reduction that was achieved through the calibration process.

Future work which will be completed under the GNS led and GWRC co-funded Smart Models for Aquifer Management research programme, will also use this linear analysis method to assess:

- the contributions made to the uncertainties of predictions of interest by different parameters and/or groups of parameters;
- the worth of existing data, or as-yet-uncollected data, in reducing parameter and predictive uncertainty.

6.2 PRIOR PARAMETER UNCERTAINTY ESTIMATES

Prior parameter uncertainty estimates were generally decided with a groundwater modelling team caucus, with the exception of the TOPNET model stream inputs to the model boundary. The uncertainty of these TOPNET model stream flow inputs were provided by NIWA. A summary of the prior parameter uncertainty values is now given and is summarised in Table 6.1.

6.2.1 Hydraulic properties

The geology of the Wairarapa Plains is exceedingly complex and the sediment sequence has been disrupted by complex tectonic deformation in the form of faulting and folding. The unconsolidated alluvial sediments that contain the aquifer system are also highly variable, on both microscopic and macroscopic scales. The fluvial depositional environment and active tectonism have produced a highly heterogeneous groundwater flow system comprising a mixture of coarse permeable gravels and less permeable sands and silts. The model has, necessarily, greatly simplified the complex geological environment and a suite of assumptions have been made regarding the three-dimensional geometry of broadly characterised units based upon available information and knowledge of the later Quaternary structural and depositional history of the plains. The model calibration attests to the validity of these assumptions and the leaky interconnected nature of the shallow groundwater environment. The model can therefore only reliably provide useful information at a sub-regional scale and will be unable to accurately simulate small areas (for example, at a farm scale) in detail. The model parameterisation of this sub-regional scale is however still uncertain, as characterised below.

6.2.1.1 Geostatistical analysis of hydraulic properties

Groundwater flow is strongly controlled by the spatial distribution and variation of hydraulic properties. In order to reveal the spatial structure of these hydraulic properties in the Ruamāhanga aquifer system, a preliminary geostatistical analysis was conducted using available hydraulic property data provided from the GWRC database (a spatial plot of the hydraulic conductivity data is depicted in Figure A4.17). The output of this analysis was then used to provide constraints to parameter uncertainty analyses discussed in this section.

This geostatistical analysis comprised a variogram analyses. The variogram describes how hydraulic properties are likely to vary spatially (i.e. their spatial auto-correlation structure).

Parameter groups comprising pilot point parameters were all assigned a full covariance matrix based on these variograms. All variograms are exponential, and specified by the equation:

$\Upsilon(h)=C(0)[1 - \exp(h/a)]$

In the above equation, Υ is the semi-variance, h is distance and C(0) is the overall variance of the hydraulic property in question, this being equal to the sill of the variogram. The range of an exponential variogram is often characterized as 3a.

The hydraulic conductivity variogram derived from the pumping tests undertaken in the Ruamāhanga is depicted in Figure 6.1. The variogram sill for the hydraulic properties used in the model were around 0.45 for log transformed data (the variogram sill describes the semi-variance value at which the variogram curve flattens off and is equivalent to variance of the hydraulic property). The variogram range used in the model was around 3500 m (the variogram range is the distance at which the variogram curve flattens and indicates the distance at which hydraulic parameters are no longer spatially correlated).

Despite the vertical hydraulic conductivity and storage property values being much lower than the hydraulic conductivity, the analyses of the semi-variance of the log of these properties were similar to that depicted in Figure 6.1.

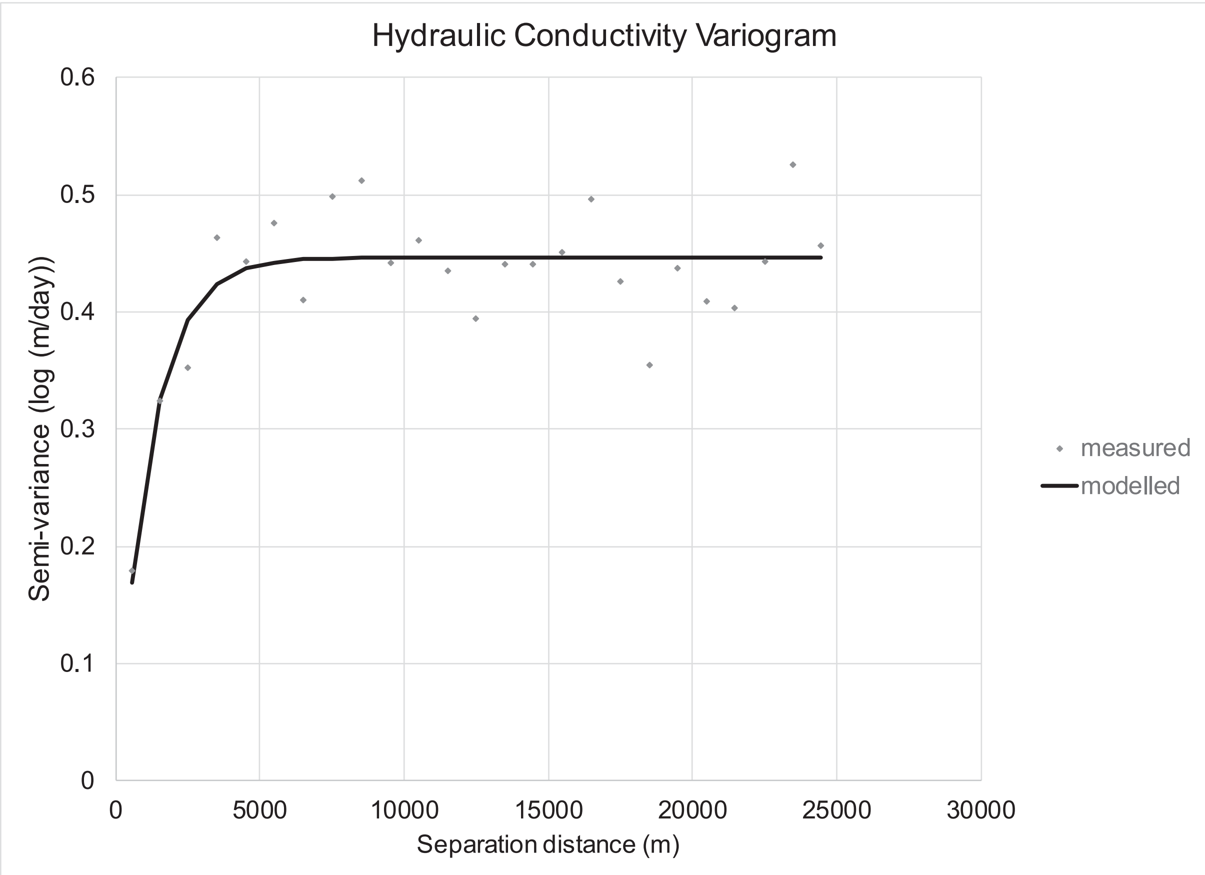

Figure 6.1 Semi-variogram for hydraulic conductivity values (log transformed) in the Ruamāhanga model.

6.2.2 Surface water inflows to the model domain and stream bed conductance

The TOPNET stream flow inputs into the model were associated with multiplier parameters, so that these inflows could be scaled upwards or downwards if data within the model calibration data-set supported these adjustments. The uncertainties for these stream multiplier parameters were analysed by NIWA (pers. Comm. Christian Zammit) who provided time series for each surface water ID number (REC number) at the 5th, 25th, 50th, 75th and 95th percentiles. For the linear analyses a standard deviation term was used to summarise the observed percentiles in the NIWA analysis; the standard deviation summarises the deviation of flows (in the log domain) from the 50th percentile flow time series.

6.2.3 Rainfall recharge

Assumptions and estimates have been made when assigning hydraulic parameters to soil properties for rainfall recharge modelling. The recharge calculations are highly sensitive to assumed rainfall runoff coefficients and broad assumptions over the entire catchment have been made in the absence of more detailed rainfall runoff modelling. Runoff is also sensitive to soil moisture condition and whether the soil is saturated – the recharge modelling does not account for this. The IRRICALC modelling also assumes that a proportion of the irrigated water returns to groundwater. Details of this assumption are contained in the CMP Aqualinc report (2016). These factors were all considered collectively in the uncertainty analysis.

NIWA's uncertainty analysis (CMP NIWA report 2017) assumes a rainfall rate uncertainty of 10%. Rainfall recharge estimates propagate this uncertainty through the soil water balance models used to calculate rainfall recharge. Additional errors relating to inaccuracies of soil maps and the soil property values assigned to these soils, and to the soil moisture model result in an increase in rainfall recharge errors. For the uncertainty analysis, we conservatively estimated an error of up to 33% for the multipliers on rainfall recharge. A spatial correlation structure was again assumed for this error, which was estimated to have a variogram range of 3500m. Currently, a research programme (GNS led and GWRC co-funded Smart Models for Aquifer Management) is exploring the likely magnitude of these combined errors and their spatial correlation structure, and so future work in this region could provide an update to this estimated error structure.

6.2.4 Nitrate flux estimates and denitrification rates

The groundwater model simulates nitrate concentrations in groundwater and nitrate fluxes between surface water and groundwater. These nitrate fluxes were calculated for a number of sites, using OVERSEER, as an average annual value and were converted to a nitrogen concentration of the recharge flux by dividing the nitrate nitrogen flux by the average annual recharge rate (calculated by IRRICALC).

The nitrate inputs used in the model are based on a small number of sites for which OVERSEER model runs have been undertaken for selected farm types. These nitrate flux model outputs have then extrapolated to the model domain on the basis of the land-use map, soil maps and rainfall gradients, plus a number of assumptions as part of the eSource component of the Ruamāhanga CMP. Both the OVERSEER model output and the extrapolation of these outputs result in significant uncertainty in the estimate of nitrate inputs to the model. Acurate quantification of the nitrate discharges for model calibration purposes was therefore not possible.

The model does not have the ability to simulate the transport of multiple forms of nitrogen, but only nitrate-nitrogen. Therefore, denitrification processes are used to represent changes to the concentration of nitrate in this regional model in conjunction with dilution processes.

The uncertainty around the multiplier parameters scaling the nitrate flux inputs to the model is difficult to estimate, and ideally this analysis would be undertaken as part of the Overseer analyses and their extrapolation to modelled area (undertaken as part of the eSource modelling). The uncertainties in nitrate input are also correlated with errors in the estimated denitrification rates (and porosity values when modelling transient nitrate concentrations). For the purposes of this parameter uncertainty analysis we have been estimated these nitrate input scaling parameters to have a standard deviation of 33%, and also to have a spatial correlation range of around 3500m.

Denitrification rates cited in Close (2017) range over 2 orders of magnitude, within a zone of expected redox potential. We have adopted a standard deviation of 0.125 (in the log domain) to account for this range plus potential inaccuracies in the mapping of redox potential. Current work in the GNS led, GWRC co-funded research programme (Smart Models for Aquifer Management) is formally assessing the uncertainty associated with the estimation of denitrification rates.

6.2.5 Abstractions

Complete records for historical groundwater abstraction are not available. For model calibration, abstractions have been calculated using the IRRICALC water demand and soil moisture balance model. There are many assumptions associated with the demand and abstraction modelling (Aqualinc, 2016). Soil parameters, individual irrigation practices and estimates of irrigated area contribute to uncertainty around estimated historical water usage. There are also many ‘permitted takes’ (generally less than 20 m^3/day) in the catchment for domestic and stock supply. These have not been incorporated into the model but are assumed to be relatively minor in magnitude when compared to the large consented groundwater abstractions.

The uncertainty for the outputs of the IRRICALC model were not provided. Therefore, we have assumed a standard deviation of the multiplier parameters on abstraction rates as 10%, for the purposes of the parameter uncertainty analysis discussed herein. All other non-irrigation abstractions were also assigned a multiplier standard deviation of 10%.

6.2.6 Water race recharge

Another form of recharge is also assumed in the models – leakage from the extensive water race network. It is assumed the approximated 50% of the flow in the water races is returned to groundwater (representing a recharge source). This is based upon generalised assessments and near-surface geological conditions. Water race returns however represent a very small proportion of the water balance for the groundwater system.

Water race uncertainty was estimated on the basis of little data, and therefore a large standard deviation on the multiplier parameters of 15% has been assumed.

Table 6.1 Standard deviations assigned independently to each parameter within each respective parameter group. Note that these are applied to the log (to base 10) of each parameter for the purpose of linear analysis.

Parameter	Standard deviation ascribed to each parameter within group to reflect prior parameter uncertainties
Hydraulic properties (Hydraulic conductivity, river bed conductance, and storage properties)	0.67
TOPNET inputs to model	Varies from 0.32 to 1.21
Water race recharge (m3/day)	0.15
Abstractions (m3/day)	0.1
Rainfall recharge (m/day)	0.33
Nitrate flux	0.33
Denitrification rate	0.125

6.3 CALIBRATION DATA SET AND MODEL AND PARAMETERISATION LIMITATIONS

Groundwater head calibration targets: Groundwater level monitoring bores tend to be unevenly distributed and associated with the shallow groundwater system. There is sparse monitoring of deeper groundwater particularly in the more marginal alluvial fan areas. This is regarded to be one of the largest contributors to model uncertainty for simulated groundwater level outputs. This data sparseness has been incorporated into the parameter uncertainty analysis

Flow calibration targets: Surface water flows (river, springs and streams) are not uniformly characterised and groundwater-surface water fluxes tend to be focussed on low flow conditions. Groundwater exchanges with larger rivers, such as the Ruamāhanga River, are not well quantified due to the difficulties associated with obtaining accurate flow gaugings on the plains. The concurrent flow gauging database is limited in both the number of gaugings and the number of gauging locations. It therefore provides only low flow snapshots of groundwater–surface water connections. Many of the spring systems do not have accurate flow monitoring data for model calibration. This is mainly due to the springs having a number of channels distributed over a wide area. Many groundwater discharges also probably lose a significant amount to evapotranspiration around wetland areas. Accurate quantification of the discharges for model calibration purposes has therefore proven difficult. This data sparseness has also been incorporated into the parameter uncertainty analysis

Parameterisation: Distributed pilot point parameters were used as a parameter calibration device. In general, the more pilot points used the better the fit that can be achieved. A large number of pilot points were not adopted in this project, as the model run times for these models are long, and hence this option was not possible in the project time frame. Increasing the spatial representation of parameters would benefit future work with this model.

Model complexity: The Australian Groundwater Modelling Guidelines (Barnett et al., 2012) define model complexity as the degree to which a numerical model resembles the physical hydrogeological system. The guidelines state that level of detail encapsulated within a model should be chosen, based on the modelling objectives (resource management policy decisions in this project), the availability of quality data, and knowledge of the groundwater system of interest, and its complexity. A complex model is based on a significant amount of field observation data and a strong conceptual understanding of the groundwater system. Where the resource management policy decisions are sensitive to the system complexity detail, a complex model can provide greater information regarding the risks associated with such decisions. A complex model also avoids additional model simplification bias and errors. However, the development of such models requires a considerable investment of time, skills and data to develop.

A complex model was selected by the modelling team because of the wide range of model objectives as outlined in the introduction of this report. A sufficiently detailed conceptual understanding of the catchment has been developed and a large volume of data exists to support the development and calibration of a complex model.

6.4 PARAMETER IDENTIFIABILITY

As already discussed, groundwater model calibration adjusts parameters values until model outputs are consistent with measurements such as groundwater levels and concentrations, and stream flows. In areas of the model where measurements are plentiful, the estimation of parameter values is more reliable than in areas where measurements are scarce. Where there is no data these estimates are based on expert opinion. This range of parameter estimability and its associated uncertainty can be expressed most simply by a parameter identifiability value.

Doherty and Hunt (2009) define the identifiability of a parameter as the square of the cosine of the angle between a parameter and its projection onto the calibration solution space. This ranges between zero and one. These can be estimated using the IDENTPAR utility available in Doherty (2015). If a parameter has an identifiability of zero, then no model output that is employed in the calibration process is sensitive to that parameter. If a parameter has an identifiability of one, then it is uniquely estimable on the basis of the calibration dataset. Its estimation will be accompanied by uncertainty; however, this uncertainty arises only from contamination of the calibration dataset by measurement/structural noise, and not from a deficit of information in the calibration dataset.

If a parameter has an identifiability that is between zero and one, this indicates that information pertinent to that parameter resident in the calibration dataset is shared between this parameter and at least one other parameter. Because the parameter has a non-zero projection onto the calibration null space, it cannot be estimated uniquely.

The parameters relating to denitrification rates, and the nitrate flux, have parameter identifiability values of near zero and hence cannot be estimated uniquely on the basis of the available data. The other model parameters explored have varying levels of identifiability and these are now discussed.

6.4.1 Identifiability of hydraulic properties

Figure 6.2 and Figure 6.3 map the identifiability of hydraulic properties in the North and South model respectively. These range between zero and one. Parameters with an identifiability of zero are completely inestimable through the calibration process because they lie in the calibration null space. Parameters with an identifiability of 1 are completely estimable as they lie entirely in the calibration solution space.

A quick glance at these figures indicates that some of the hydraulic properties within Layer 1 in the north model have been estimated with the greatest reliability. There are also high parameter identifiability values for hydraulic conductivity in layer 5 of the North model. In general, the hydraulic properties within the south model have lower identifiability values, indicating parameter values are less well estimated. Unsurprisingly, identifiabilities are highest where observation data density is greatest.

These maps are important and indicate that while in some locations parameter values are well estimated, the propensity for parameter correlation, non-uniqueness and uncertainty in parameter estimates is high for these models, and particularly so for the south model. These results are typical for regional groundwater models, which have a large propensity of model uniqueness. It is important to note that the use of a distributed parameterisation device, such as the pilot points employed in this model, which are used to both extract maximum information from data, and to explicitly represent parameter detail for which predictions may be sensitive to, provide realistic parameter uncertainty analyses using the Bayesian linear uncertainty analysis. This is in contrast to a lumped parameterisation, such as zones of constant parameter value (as with the original FEFLOW model), where a single parameter value is assigned to a spatially defined zone. When lumped parameterisations are used in a model, an additional component of uncertainty analysis is required, which explicitly quantifies the model simplification error. The reader us referred to White et al, (2014), for a more detailed discussion on the issue of model simplification error.

These results indicate that predictive simulations made by this model should be considered only in a relative sense. If future model predictive simulations are to be assessed within a risk context, then these model outputs should be accompanied by an uncertainty analysis.

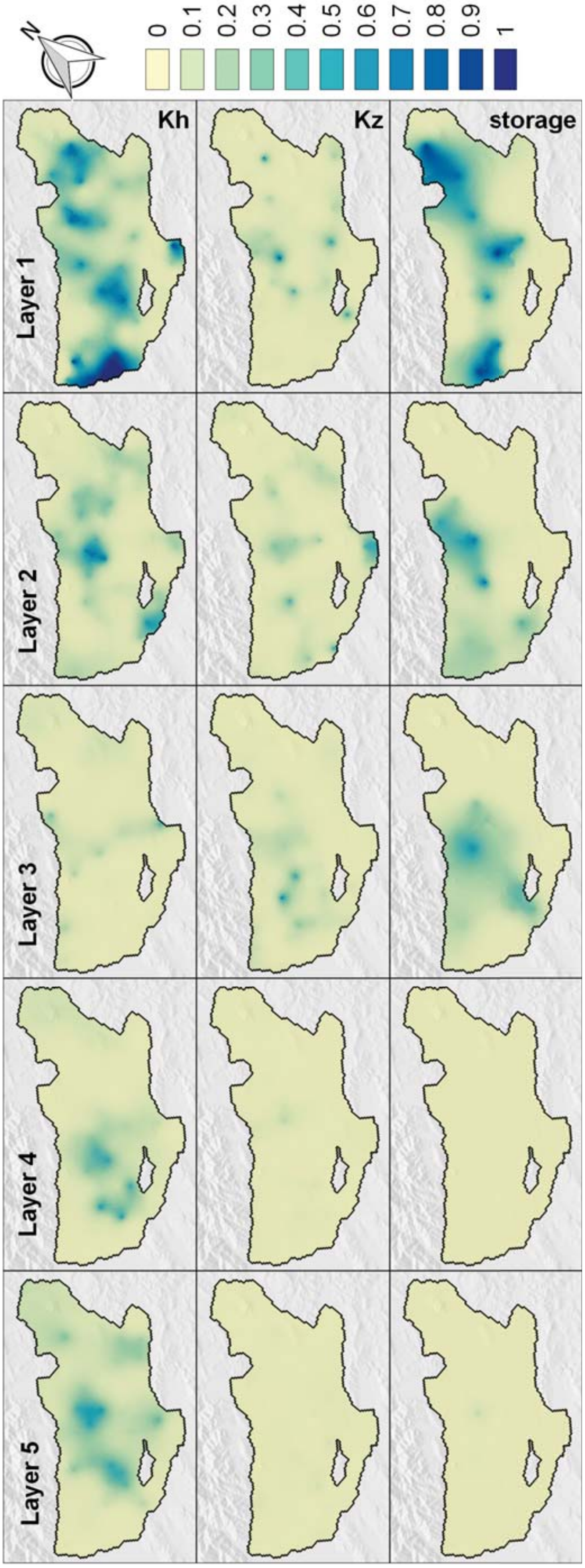

Figure 6.2 Identifiability of hydraulic properties in the north model. Note that storage refers to specific yield in model layer 1 and specific storage in all other model layers.

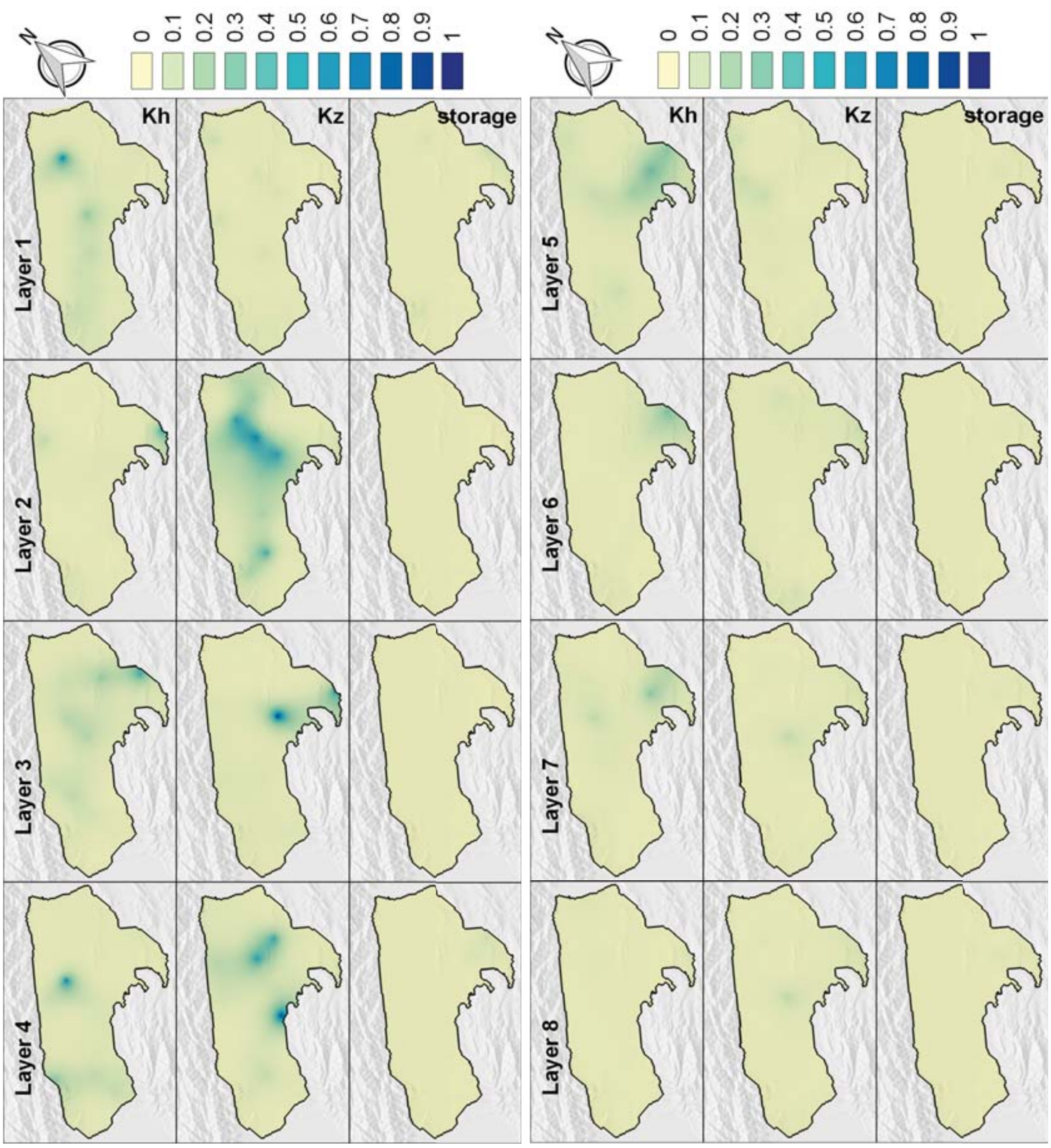

Figure 6.3 Identifiability of hydraulic properties in the south model. Note that storage refers to specific yield in model layer 1 and specific storage in all other model layers.

6.4.2 Identifiability of stream-bed conductance, and model boundary stream inflows

Figure 6.4 and Figure 6.5 map the identifiability of the stream bed conductance parameters and the stream multiplier parameters for the north and south model respectively. Again, identifiabilities are highest where observation data density (e.g. stream flow data and groundwater level data) is greatest.

While some stream inflow and stream bed conductance parameters are well estimated, there are still large areas of the model domain where stream parameterisations must be considered non-unique and uncertain. Once again, these results indicate that predictive simulations should be considered only in a relative sense or if within a risk context, then these model outputs need to be accompanied by an uncertainty analysis.

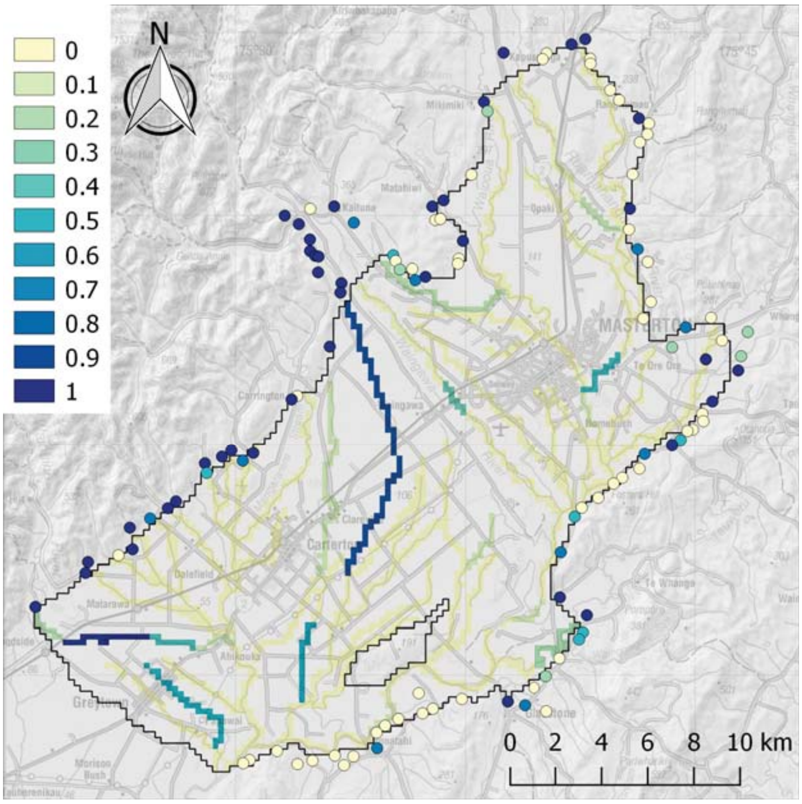

Figure 6.4 Identifiability of stream bed conductance parameters and TOPNET model stream multipliers (circles) in the north model.

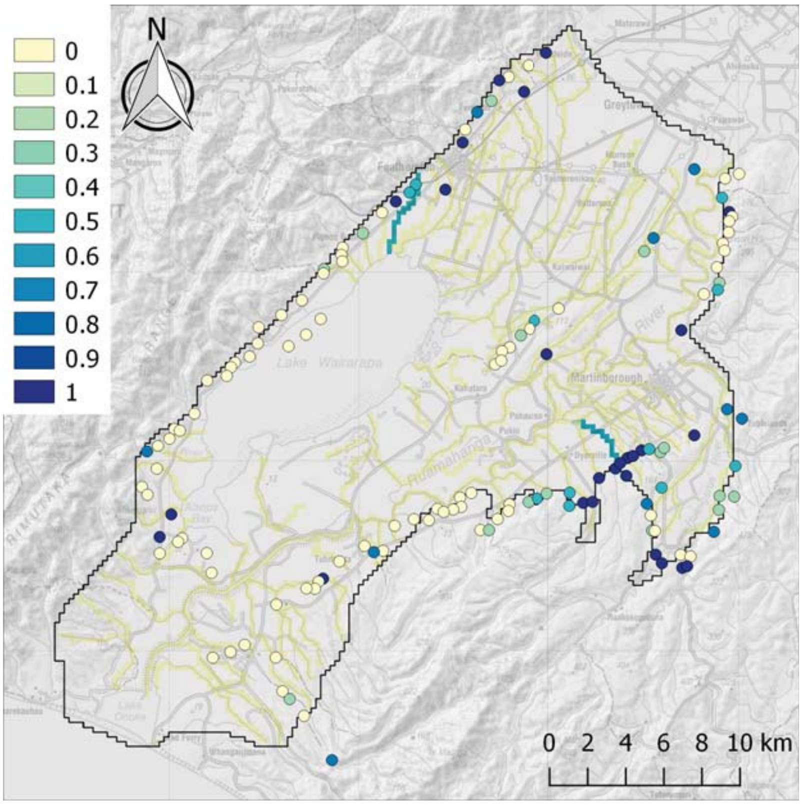

Figure 6.5 Identifiability of stream bed conductance parameters and TOPNET model stream multipliers in the south model.

6.4.3 Identifiability of recharge estimates

The identifiability of the recharge array multipliers is depicted in Figure 6.6 and Figure 6.7 for the north and south models respectively. These higher identifiability values are again consistent with greater density of monitoring data wells and surface water gauging sites.

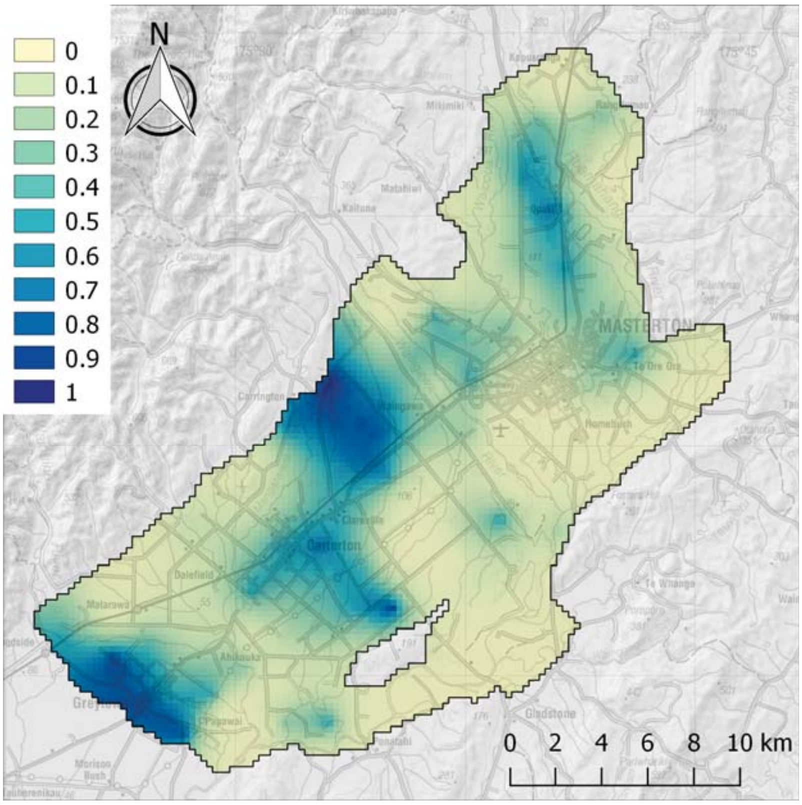

Figure 6.6 Identifiability of recharge multiplier parameters in the north model.

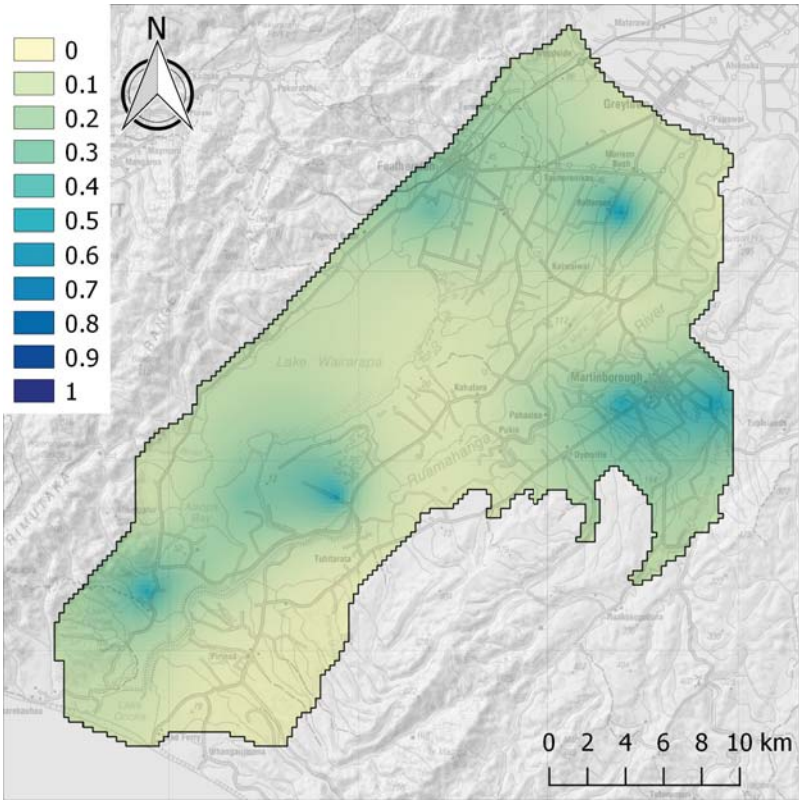

Figure 6.7 Identifiability of recharge multiplier parameters in the south model.

6.5 CONTRIBUTIONS TO PARAMETER UNCERTAINTY FROM FIXED MODEL INPUTS AND OBSERVATIONS

Like identifiability, the relative uncertainty variance reduction of a parameter is a number between zero and one. For the i'th parameter it is calculated as:

$$r_i = \frac{\left(\sigma_{ip}^2 - \sigma_{ic}^2\right)}{\sigma_{ip}^2}$$

where

σ^2_{ip} is the prior uncertainty variance of parameter i; and

σ^2_{ic} is the posterior (i.e. post-calibration) uncertainty variance of parameter i.

This statistic takes more explicit account of the presence of measurement/structural noise in the calibration dataset than does identifiability; it also takes greater account of prior parameter spatial correlation. The maps plotted depict the magnitude of parameter uncertainty reduction that has been achieved via the model calibration process.

6.5.1 Hydraulic property parameter uncertainty reduction

Figure 6.8 and Figure 6.9 map the parameter uncertainty reduction of hydraulic properties in the North and South model respectively (where parameter variance is being used to quantify uncertainty). As discussed above, these range between zero and one, and they exhibit a similar pattern to those shown in the parameter identifiability maps.

The greatest parameter uncertainty reduction achieved through calibration process occurs in areas where there are a greater number of observations, e.g. where there is information with which to reduce the prior parameter uncertainty. The information in these maps combined with the prior parameter uncertainty descriptions outlined in Table 6.1, can be combined to provide the post calibration parameter uncertainty values which are used in any predictive uncertainty analysis.

At first glance these plots are sobering, indicating there are large areas of the model that have parameters values that are not well estimated via the calibration process. However, these values are typical for regional groundwater models, and knowing the extent to which parameter estimates are uncertain, and their location, enables a realistic assessment of risks associated with the decision-making process.

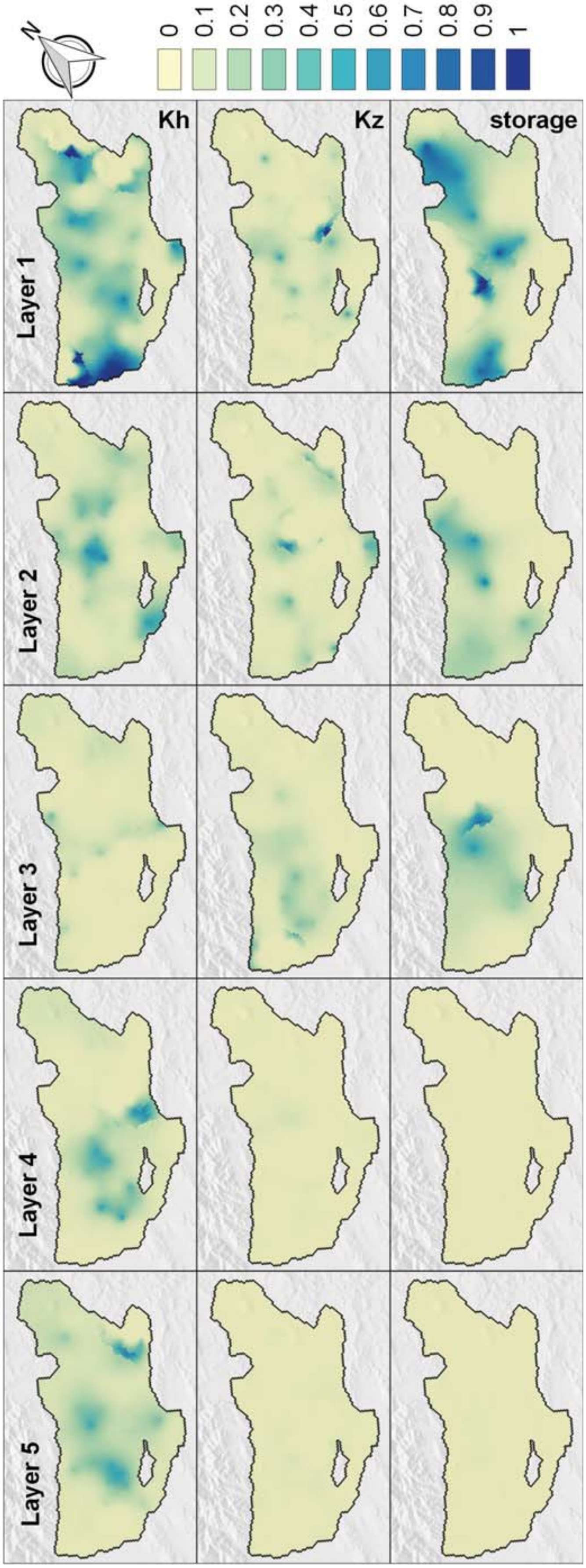

Figure 6.8 Relative parameter uncertainty variance reduction of recharge multiplier parameters in the North model.

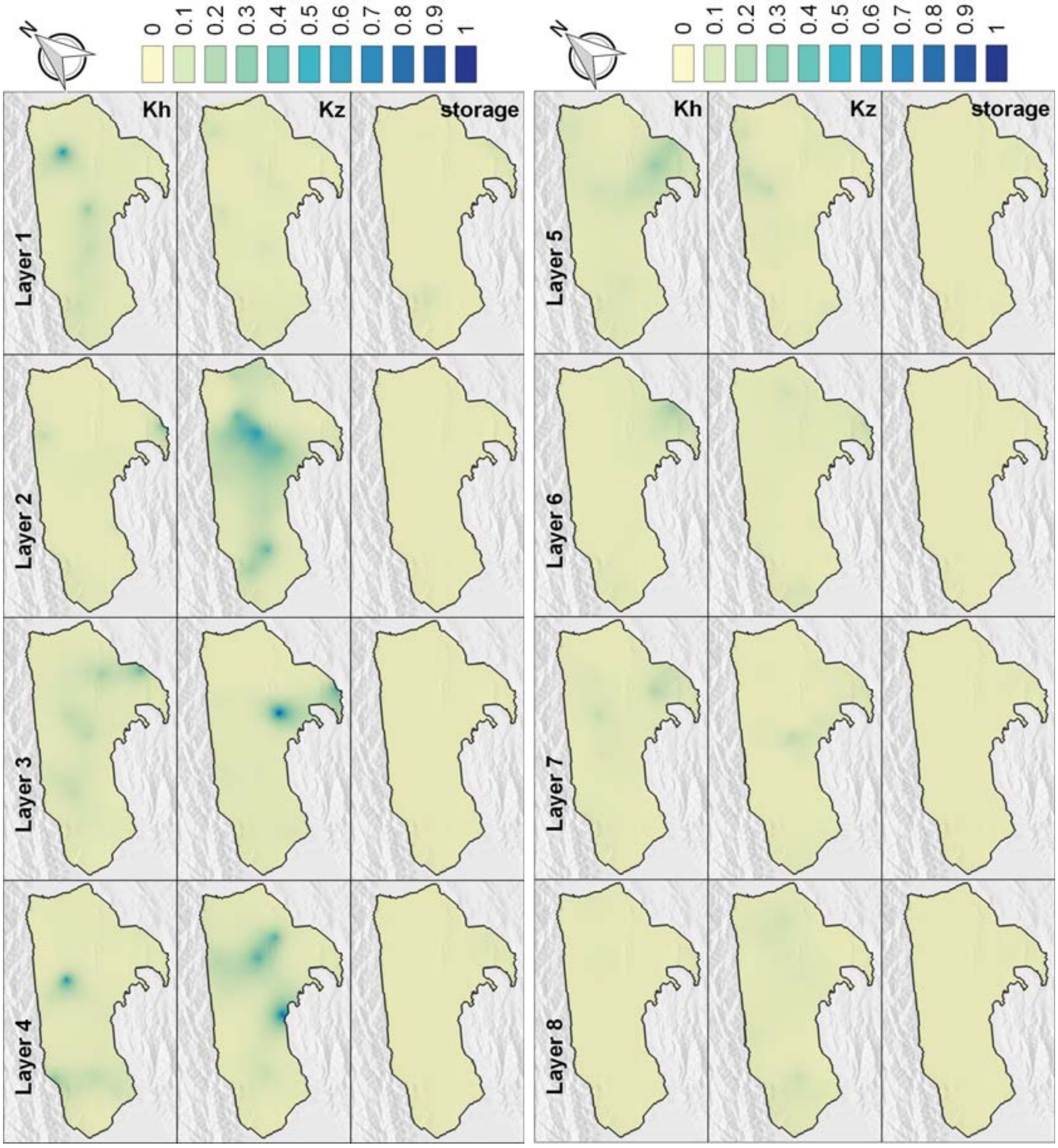

Figure 6.9 Relative parameter uncertainty variance reduction of recharge multiplier parameters in the South model.

6.5.2 Stream-bed conductance, and model boundary stream inflows parameter reduction

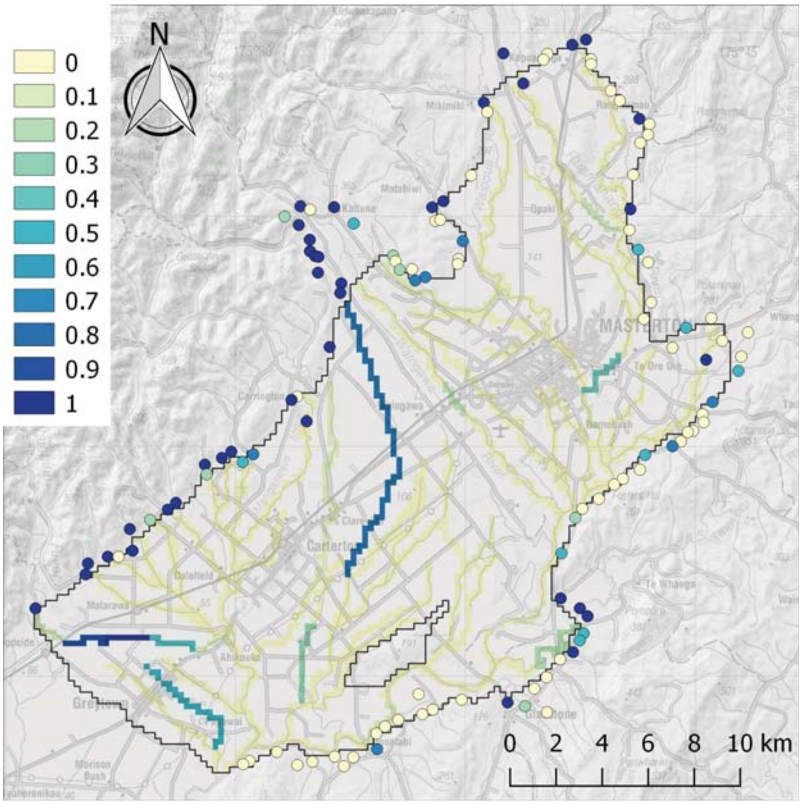

Figure 6.10 Relative parameter uncertainty variance reduction of stream bed conductance parameters and TOPNET model stream multipliers in the north model.

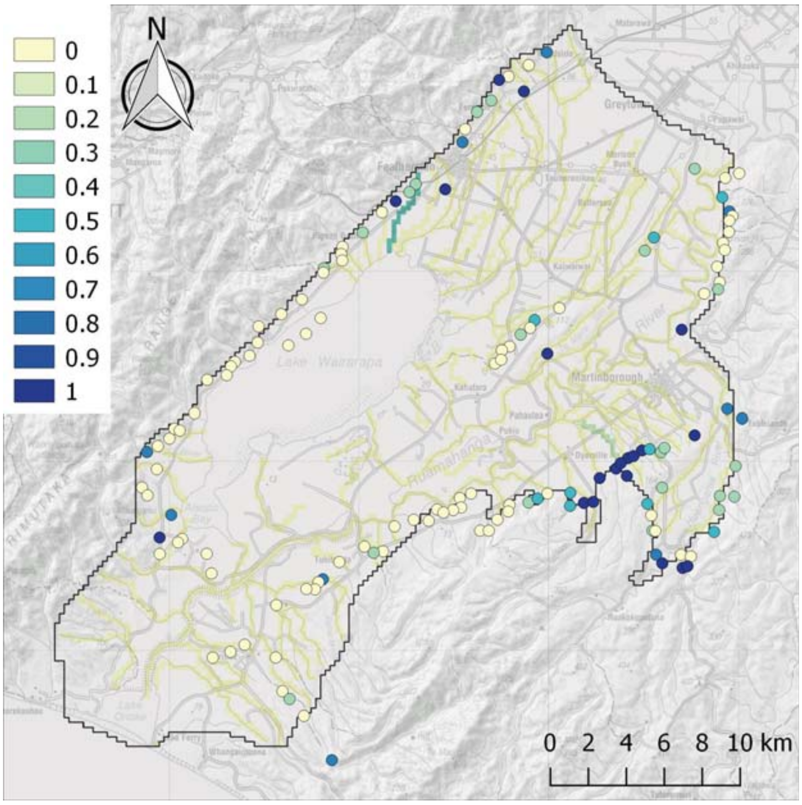

Figure 6.11 Relative parameter uncertainty variance reduction of stream bed conductance parameters and TOPNET model stream multipliers in the south model.

6.5.3 Recharge Parameter uncertainty reduction

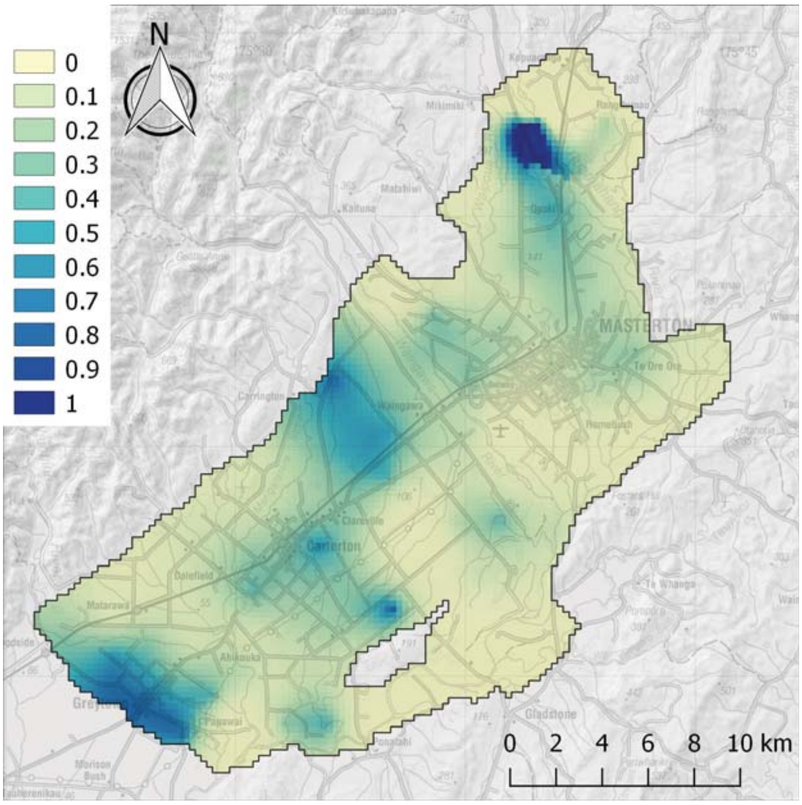

Figure 6.12 Relative parameter uncertainty variance reduction of recharge multiplier in the north model.

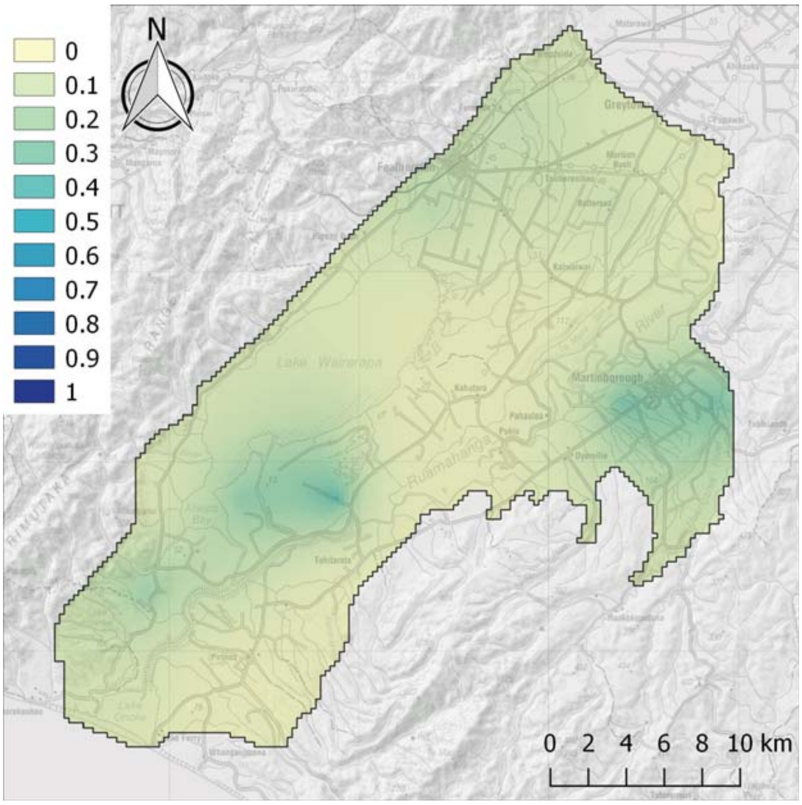

Figure 6.13 Relative parameter uncertainty variance reduction of recharge multiplier in the north model.

6.6 SUMMARY

While the model to measurement fits described in Section 5 provide a pleasing level of correspondence, the analysis in this section indicates that there are a number of parameter combinations that could provide equally good fits to the measured data. These alternative equally likely parameter combinations would likely also result in a range of different predictive simulation outputs. The identifiability and parameter uncertainty variance reduction plots shown in this section are typical for regional groundwater models. These results emphasise the importance of using expert knowledge within the model as far as is possible in these regional modelling contexts, as there will be seldom sufficient data to achieve widespread parameter uncertainty reduction beyond that encapsulated in expert knowledge, via the calibration process.

The results also indicate that the model is best used in a relative sense; in fact, it is generally accepted that models are better at predicting changes than absolutes. This is because defects resulting from model construction will often “cancel out” as the value of a prediction pertaining to one simulation time is subtracted from its value at another simulation time, in order to predict the change in system behaviour precipitated by alterations to human management of that system.

For the above reasons, it is recommended that the current models are best used in a relative sense. Where the risks associated with a proposed model-based environmental management option are being considered explicitly, then it is recommended that the predictive simulations exploring this option are accompanied by a predictive uncertainty analysis.

7.0 SUMMARY AND FUTURE WORK

The groundwater and surface water flow and groundwater contaminant transport models described in this report have been developed for the Wairarapa Valley as an integral component of the Greater Wellington Regional Council (GWRC) Collaborative Modelling Project (termed the 'Ruamāhanga CMP'), in a collaboration with other consultants and GWRC staff.

The models are linked to surface water, contaminant loading, contaminant transport and soil moisture balance models which together provide an integrated modelling system designed to simulate water and contaminant fluxes between the land surface, groundwater and surface water environments. The modelling system provides a tool for exploring the groundwater and surface water quality implications of various land and water management scenarios to assist decision making. The MODFLOW and MT3D flow and transport models in this modelling system are the focus of this report. These models derive some of their inputs from three other models, TOPNET, IRRICALC and OVERSEER, details of which can be obtained from other reports in the Ruamāhanga CMP.

The groundwater modelling component of this project had a number of objectives which included extending the previously developed FEFLOW groundwater simulation models of the Wairarapa Valley (Gyopari and McAlister 2010 a,b,c). Most significantly, in terms of the simulation capacity, the new models can now simulate surface water flows and the movement of contaminant loadings through the integrated surface and groundwater system, which the existing FEFLOW models were unable to do. These model developments represent a step change in model simulation capability, which is essential for providing decision support for the limit setting process under the National Policy Statement for Fresh Water Management (NPS-FM), and for the Whaitua limit setting processes alike.

Overall, the model simulated surface water flows, and groundwater levels and concentration data provide reasonable fits to measurements. The correspondence between modelled and measured data had a correlation coefficient (r-squared) values of above 0.9 and 0.8 for the north and south models respectively. The calibrated model parameter confidence ranges are easily calculated on the basis of the prior parameter standard deviation and variance terms and the reduction in these values achieved via calibration as described in Section 7 of this report.

The uncertainty analyses (using metrics of parameter identifiability and parameter variance reduction) indicated that while the calibration process achieved significant reduction in parameter uncertainties in some areas, many parameter estimates have significant residual uncertainty, caused by a sparse distribution of monitoring data, which is typical for regional groundwater models.

To address this incomplete knowledge, any predictive simulations made with this model should be considered in a relative sense only, or where the magnitude of model outputs are important, then these predictive simulations should be accompanied by a predictive uncertainty analysis which accounts for the parameter uncertainties calculated for this model.

A current research programme (GNS led and GWRC co-funded Smart Models for Aquifers Management, 'SAM') is scheduled to undertake the further work to extend the capability of this model even further. This work includes:

- A non-linear predictive uncertainty analysis on selected scenarios.

- Integrating estimates of potential denitrification zones into the model based on linear discriminant analyses of water quality and assessments of uncertainty in denitrification rate estimates.
- Assessment of uncertainty of linked model inputs provided to the groundwater model.
- Use of streamlined and nested model components within the current model structure for greater predictive reliability of more local scale predictions such as spring flows, and groundwater levels.
- Implement new version of MT3DMS so that solute transport through the surface water system can also be simulated.

8.0 REFERENCES

Aqualinc. 2016. Groundwater recharge and irrigation demand modelling. Ruamāhanga collaborative modelling project. Prepared for Greater Wellington Regional Council.

Bakker, M.; Post, V.; Langevin, C.D.; Hughes, J.D.; White, J.T.; Starn, J.J.; Fienen, M.N. 2016. Scripting MODFLOW Model Development Using Python and FloPy. Groundwater. doi:10.1111/gwat.12413.

Barnett et al, 2012, Australian groundwater modelling guidelines, Waterlines report, National

Water Commission, Canberra.

Begg, J.; Brown, L.; Gyopari, M.; Jones. A. 2005. *A review of Wairarapa geology – with a groundwater bias.* Institute of Geological and Nuclear Sciences Client Report 2005/159.

Bedekar, V.; Morway, E.D.; Langevin, C.D.; Tonkin, M. 2016. MT3D-USGS version 1: A U.S. Geological Survey release of MT3DMS updated with new and expanded transport capabilities for use with MODFLOW: U.S. Geological Survey Techniques and Methods 6–A53, 69 p., http://dx.doi.org/10.3133/tm6A53.

Close, M.E.; Abrahama, P.; Humphriesa, B.; Lilburne, L.; Cuthill, T.; Wilsonc, S. 2016. Predicting groundwater redox status on a regional scale using linear discriminant analysis. Journal of Contaminant Hydrology 191 19–32.

Close, M.E., 2017. Review of Denitrification Rates in Groundwater Systems. ESR client report for Environment Southland. ESR report number CSC 16008.

Dann, R., V. Bidwell, S. Thomas, T. Wöhling, and M. Close. 2010. Modeling of Nonequilibrium Bromide Transport through Alluvial Gravel Vadose Zones All rights reserved. No part of this periodical may be reproduced or transmitted in any form or by any means, electronic or mechanical, including photocopying, recording, or any information storage and retrieval system, without permission in writing from the publisher. . Vadose Zone J. 9:731–746. doi:10.2136/vzj2009.0127

Doherty, J., 2015. Calibration and uncertainty analysis for complex environmental models. Published by Watermark Numerical Computing, Brisbane, Australia. 227pp. ISBN: 978-0-9943786-0-6. Downloadable from www.pesthomepage.org.

Doherty, J. 2016. PEST user manual part I and II. Watermark Numerical Computing, Brisbane, Australia.

Doherty, J. and Hunt, R.J., 2009. Two statistics for evaluating parameter identifiability and error reduction. Journal of Hydrology. 366, 119–127.

Doherty, J.E., and Hunt, R.J., 2010, Approaches to highly parameterized inversion—A guide to using PEST for groundwater-model calibration: U.S. Geological Survey Scientific Investigations Report 2010–5169, 59 p.

Gyopari, M.; McAlister, D. 2010a. *Wairarapa Valley groundwater resource investigation: Upper Valley catchment hydrogeology and modelling.* Greater Wellington Regional Council Technical Publication GW/EMI-T-10/74.

Gyopari, M.; McAlister, D. 2010b. *Wairarapa Valley groundwater resource investigation: Middle Valley catchment hydrogeology and modelling.* Greater Wellington Regional Council Technical Publication GW/EMI-T-10/73.

Gyopari, M.; McAlister, D. 2010c. *Wairarapa Valley groundwater resource investigation: Lower Valley catchment hydrogeology and modelling.* Greater Wellington Regional Council Technical Publication GW/EMI-T-10/75.

Harbaugh, A.W. 2005. MODFLOW-2005, The U.S. Geological Survey modular ground-water model—the Ground-Water Flow Process: U.S. Geological Survey Techniques and Methods 6–A16.

Keenan, L. 2009. *Mean annual low flow statistics for rivers and streams in the Wellington region*. Unpublished internal report (WGN_DOCS#715651), Greater Wellington Regional Council.

Korom SF (1992) Natural denitrification in the saturated zone: A review. Water Resources Research 28: 1657–1668

Lundquist, J. D., N. E. Wayand, A. Massmann, M. P. Clark, F. Lott, and N. C. Cristea (2015), Diagnosis of insidious data disasters, Water Resour. Res., 51, 3815–3827, doi:10.1002/2014WR016585.

Middlemis, M. 2001. *Murray Darling Basin Commission groundwater flow modelling guideline.* Aquaterra Consulting Limited. Project No. 125, Final Guideline – Issue 1, January 2001.

Morgenstern, U. 2005. *Wairarapa Valley groundwater – residence time, flow pattern and hydrochemistry trends.* GNS Science Report 2005/33.

Niswonger, R.G.; Prudic, D.E. 2005. Documentation of the Streamflow-Routing (SFR2) Package to include unsaturated flow beneath streams—A modification to SFR1: U.S. Geological Survey Techniques and Methods, Book 6, Chap. A13, 47 p.

Prommer, H.; Post, V.E.A. 2010. A Reactive Multicomponent Model for Saturated Porous Media, Version 2.0, User's Manual, http://www.pht3d.org.

Prudic, D.E. 1989. Documentation of a computer program to simulate stream-aquifer relations using a modular, finite-difference, ground-water flow model: U.S. Geological Survey Open-File Report 88–729, 113 p.

Schreüder, W. 2009. Running BeoPEST: In: Preceedings of the 1st PEST Conference, Potomac, MD, November 1–3.

Sanford, W. 2011. Calibration of models using groundwater age. Hydrogeology Journal, 19(1),13-16 DOI 10.1007/s10040-010-0637-6

Zheng, Chunmiao; Wang, P. Patrick. 1999. "MT3DMS: A modular three-dimensional multispecies transport model for simulation of advection, dispersion, and chemical reactions of contaminants in groundwater systems; documentation and user's guide," Contract Report SERDP-99-1, U.S. Army Engineer Research and Development Center, Vicksburg, MS.

APPENDICES

This page is intentionally left blank.

A1.0 THE WAIRARAPA VALLEY — PHYSIOGRAPHY AND CLIMATE OVERVIEW

The Wairarapa plains encompass an area of about 1,200 km^2 and incorporates the shallow extensive alluvial fans and floodplains of the Ruamāhanga River and its tributaries flowing out of the Tararua Range to the west, Lake Wairarapa, the Martinborough terraces and Lake Onoke at the coast. The plains are bounded to the northwest by the Tararua Range and to the southeast by the Haurangi Range (Figure A1.1). The principal population centres are Greytown, Carterton, Masterton and Martinborough. Lake Wairarapa is the dominant surface water feature in the catchment covering an area of 78.4 km^2. Agriculture is the dominant land use. Of the defined land-uses dairy is the dominant activity, followed by beef, arable cropping and sheep and beef.

Sheltered by the Tararua Range, the Wairarapa plains experience a dry, warm climate. Typical maximum summer daytime temperatures range between 20 and 28°C, and sometimes rise above 30°C. High summer temperatures may be accompanied by strong dry 'foehn' winds from the northwest. Winters are generally mild in the north of the region and cooler in the south where frosts are common. Typical maximum winter temperatures range from 10 to 15°C.

The ranges shelter the plains from the predominant westerly winds resulting in higher temperatures and a very steep rainfall gradient from west to east as shown by the annual average rainfall map in Figure 1.2. The highest annual rainfall of 1,500–2,000 mm occurs close to the ranges, reducing to 600–700 mm on the eastern side of the valley around Martinborough. However, in southerly and easterly airflow conditions, rainfall is greater due to reduced orographic effect because there are no, or only low, ranges for moist air to cross.

Variations in climate occur from year to year and also over longer periods of decades, centuries or millennia. The 'El Niño Southern Oscillation' (ENSO) is the primary driver of natural climate variability that affects New Zealand's precipitation in the two- to seven-year cycle. El Niño is defined by sustained differences in Pacific Ocean surface temperatures when compared with the average value. The accepted definition is a warming or cooling of at least 0.5°C averaged over the east-central tropical Pacific Ocean. When this happens for five months or longer, it is called an El Niño or La Niña episode. Typically, the episodes occur at irregular intervals of 2–7 years and last nine months to two years. El Niño (ENSO warm phase) is associated with more frequent southwest airflows over New Zealand. This leads to cooler conditions than normal, more rain in western areas, and can cause drought in eastern areas such as the Wairarapa. Conversely, La Niña (ENSO cool phase) conditions lead to more frequent northeast winds. This can cause drought on the Wairarapa plains due to the sheltering effect of the eastern hill country. Although both La Nina and El Nino can cause low seasonal rainfall in the Wairarapa, overall El Niño has a greater influence due to the enhancement of westerly conditions. In general, in the Wairarapa an El Niño episode increases the chance of low summer rainfall; conversely, if a La Niña episode occurs, the chance of low autumn rainfall increases. Some of the most severe droughts of the last few decades in the Wairarapa (e.g., 2002/03, 1997/98, 1977/78) occurred during El Niño episodes, although there have also been notable droughts during La Niña (e.g., 2007/08, 2000/01).

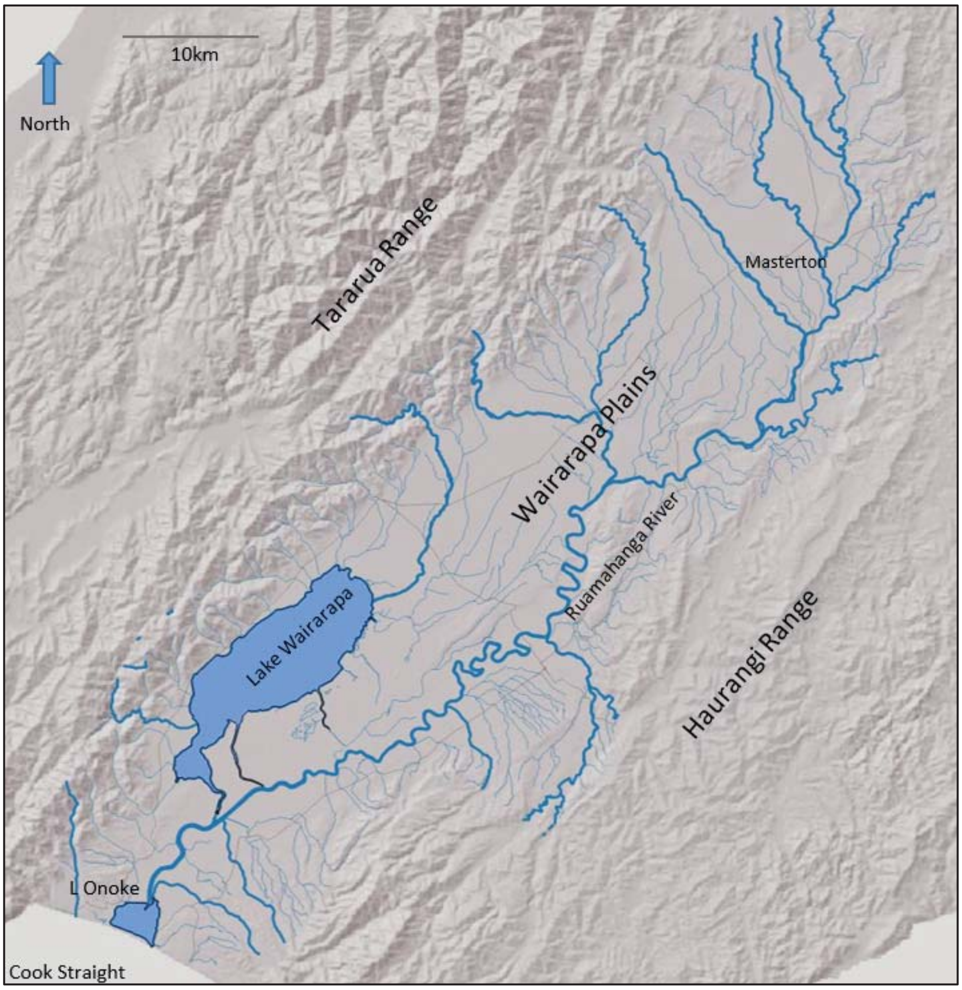

Figure A1.1 Wairarapa Valley and main physiographic features.

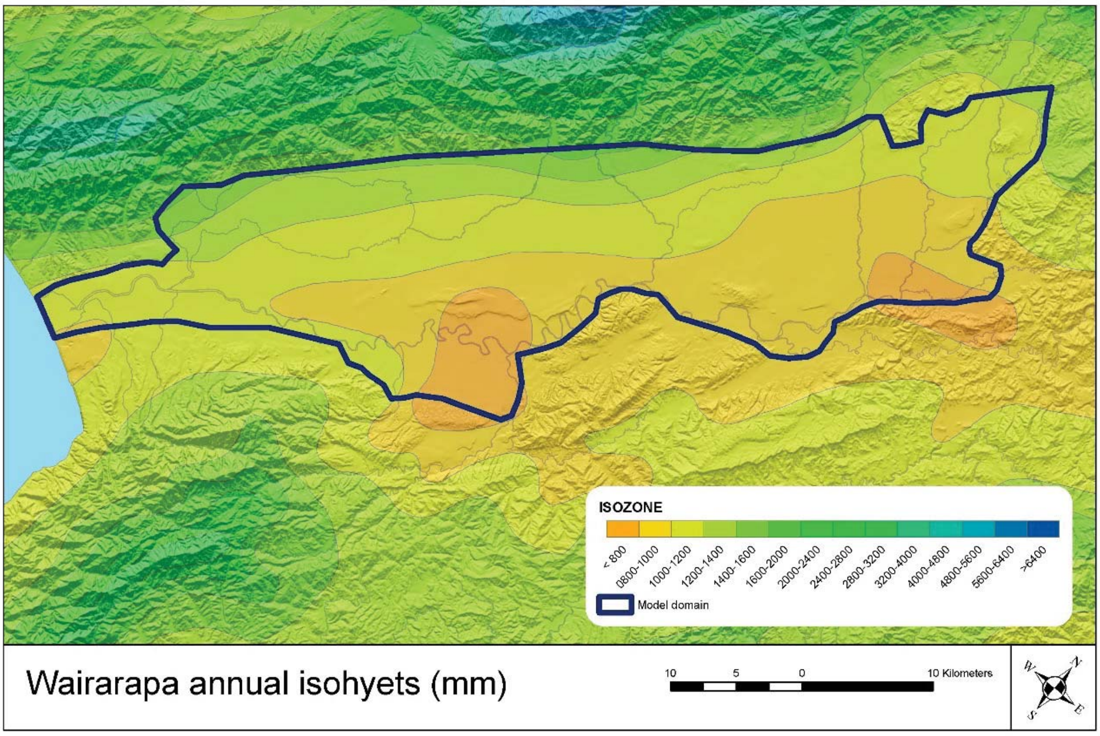

Figure A1.2 Annual rainfall isohyets for the Wairarapa plains.

A2.0 SURFACE WATER ENVIRONMENT

Figure A2.1 shows the principal surface water features of Wairarapa Valley associated with the Ruamāhanga River and its main tributaries (from north to south): the Waipoua, Waingawa, Waiohine (including the Mangatarere Stream) and Huangarua. Lake Wairarapa is the dominant surface water feature occupying the southern part of the valley, which receives much of its inflow from the Tauherenikau River.

Flows in the Ruamāhanga River, its tributaries and the Tauherenikau River are monitored by GWRC at gauges located in the foothills, a short distance before each waterway emerges onto the plains. Flow in the Ruamāhanga River is also measured on the plains at Wardell's Bridge, Gladstone and Waihenga. Flow monitoring sites are shown in Figure A3.1 and flow statistics for these sites are contained in Table A 2.1.

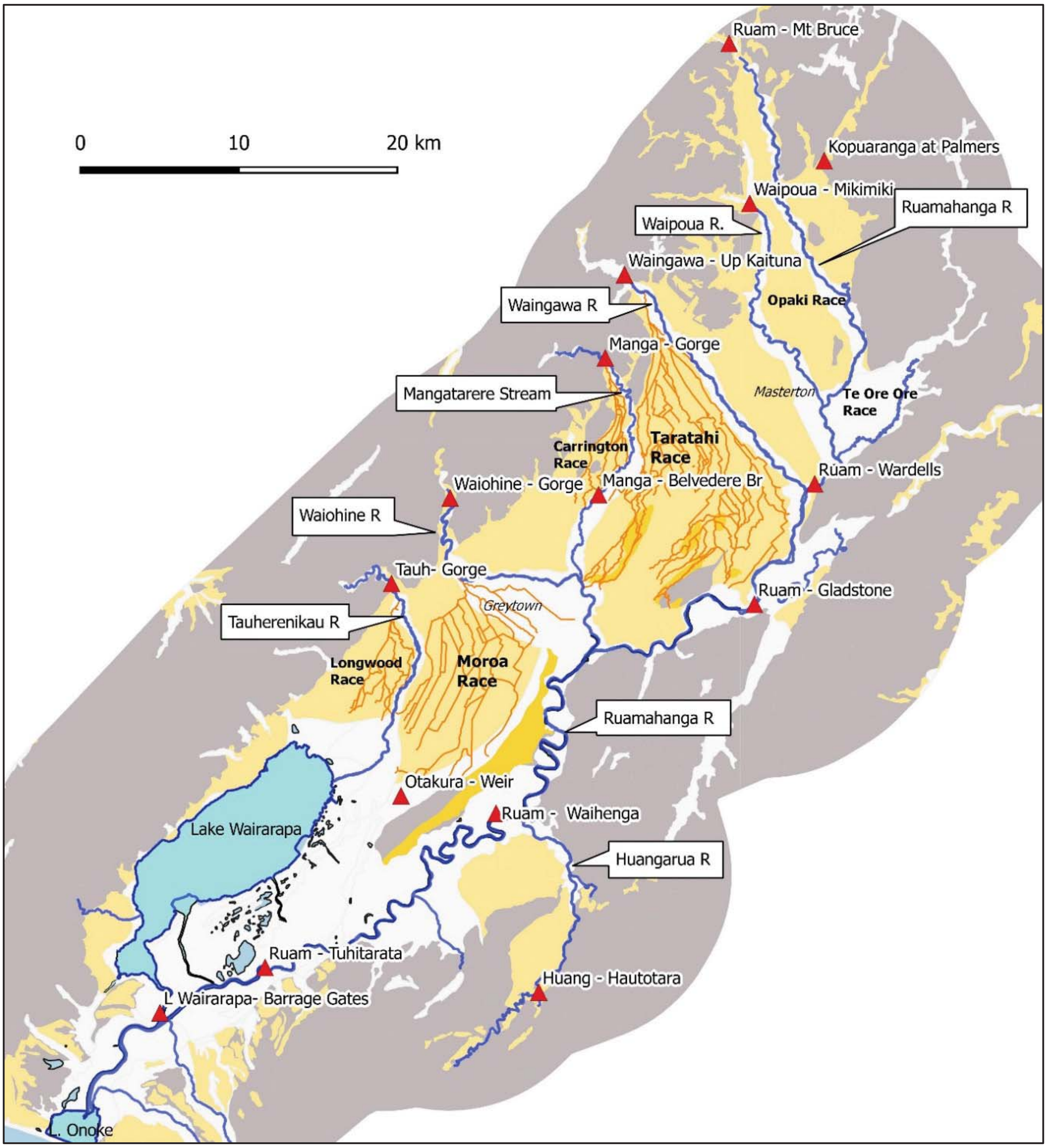

Figure A2.1 Wairarapa Valley natural drainage system — principal rivers, streams and lakes. Surface water gauging sites (red triangles) and water race networks (orange network) also shown.

Table A2.1 Flow statistics for major waterways in the Wairarapa Valley.

River and gauge site	Catchment area above flow site (km2)	Mean flow (m3/s)	Median flow (m3/s)	Mean annual low flow (m3/s)	Maximum recorded flood (m3/s)
Ruamāhanga River at Wardells (upstream of Waingawa River)	637	23.8*	12.5*	2.7*	844
Ruamāhanga River at Waihenga	2340	85.34	50.3	8.77	1903
Waingawa River at Kaituna	79	10.2	5.1	1.2	426
Waipoua River at Mikimiki	80.3	6.0	3.7	0.31	355
Kopuaranga River at Palmers	100.3	2.6	1.2	0.28	60
Whangaehu River at Waihi	36.6	0.54	0.16	0.018	80
Waiohine River at Gorge	180	24.5	13.0	3.0	1558
Mangatarere Stream at Gorge	33	1.9	0.84	0.13	122
Tauherenikau River at Gorge	112	9.17	4.94	1.1	670
Huangarua River at Hautotara	140	-	-	0.19	514

*Flow statistic likely to be affects by upstream abstraction of water.

A2.1 RUAMĀHANGA RIVER

The Ruamāhanga River is the principal drainage system for the Wairarapa Valley (Figure A2.1). The river originates in the northeastern Tararua Range near Mt Dundas (1,500 metres above mean sea level) and flows south through the Wairarapa Valley to Lake Onoke, which discharges to the sea. The river is about 162 kilometres long with a catchment area of approximately 3430 square kilometres. It has major tributaries rising from the Tararua Range – including the Waipoua, Waingawa and Waiohine rivers, and from the northern and eastern Wairarapa hills – the Kopuaranga, Whangaehu, Tauweru and Huangarua rivers.

The Ruamāhanga River emerges onto the Wairarapa Plains at Mt Bruce, about 21 km north of Masterton. In general, the upper reach of the river has a wide, semi-braided form, although it narrows to a single-thread channel in places, particularly where it is confined by bluffs. As the river flows past Masterton it has an incised single channel, with beaches on the inside of river bends.

Immediately downstream of the Waingawa River confluence the Ruamāhanga River steepens and changes to a wide braiding channel (Figure A2.2). Through this reach the river alternates between semi-braided and single-thread form with gravel beaches. The width also varies, narrowing from over 100 metres near Gladstone to around 60 metres upstream of the Waiohine River confluence.

Downstream of the Waiohine River confluence the river has a strong meander pattern, with a single channel and extensive gravel beaches in the river bends. However, downstream of Pahautea, the effects of river control works become more apparent: the river is confined between stopbanks, with less frequent shingle beaches and less meandering. From Tuhitarata to Lake Onoke high stopbanks confine the river, meanders have been cut off, and the gravel beaches are largely absent.

Long term flow monitoring on the Ruamāhanga River occurs at Wardell’s Bridge and Waihenga Bridge (just below the Huangarua confluence). At Wardell’s Bridge the mean flow is about 24 m^3/sec whilst further downstream at Waihenga Bridge, tributary and groundwater inflows result in an increased mean flow of about 85 m^3/sec.

Figure A2.2 Ruamāhanga River near Carters Bush during winter 2008.

A2.2 WESTERN TRIBUTARIES OF THE RUAMĀHANGA RIVER

On the Wairarapa Plains, the major tributaries that enter the Ruamāhanga River from the west are sourced in the Tararua Range and its foothills. Rivers flowing out of the Tararua Range are characteristically sediment-charged. As they emerge into the Wairarapa Valley the sudden reduction in stream gradient causes deposition of sediment load resulting in the formation of large coalescing alluvial fans (up to 300 metres thick in some places).

A2.2.1 Waipoua River

The Waipoua River is the first major western tributary of the Ruamāhanga River in the Wairarapa Valley, with a catchment area of 149 km^2. The river originates in the Blue Range within the eastern Tararua Range and emerges onto the Wairarapa plains about 18 km north of Masterton before flowing across the plains to join the Ruamāhanga River at Masterton. In the reach, upstream of Masterton there is significant gravel accumulation and during times of low flow the river often disappears below bed level. The mean flow of the Waipoua River is about 6.0 m^3/sec (Table A3.1).

A2.2.2 Waingawa River

The Waingawa River rises in the Tararua Range between Mt Arete and Mt Girdlestone and is approximately 36 km in length. The catchment has a total area of 146 km^2, of which 119 km^2 is in the Tararua Range. In the foothills, the river is joined by a major tributary – the Atiwhakatu

Stream — it then crosses the Wairarapa Plains in an unusually straight easterly direction down the alluvial fan for 16 km to its confluence with the Ruamāhanga River. The mean flow of the Waingawa River (measured at Kaituna in the foothills before the river emerges onto the plains) is 10.2 m^3/sec and an estimated 7-day mean annual low flow (MALF) of 1.72 m^3/sec at the Ruamāhanga confluence. On the plains, a number of faults cut across the river channel and tectonic activity appears to frequently displace the river course. It is evident from prominent channel patterns observed on LIDAR imagery that the river has migrated through the Masterton area and probably merged with the Waipoua River since the last glaciation.

A2.2.3 Waiohine River and Mangatarere Stream

The Waiohine River has a catchment area of 378 km^2, originates at the drainage divide of the Tararua Range south of Mt Arete. It emerges onto the Wairarapa plains at the Waiohine Gorge where it has a mean flow of 24.5 m^3/sec (Table A 2.1). From here, it flows a further 20 km in an easterly direction to the Ruamāhanga River confluence about 5 km east of Greytown. Approximately 6 km upstream of the confluence, the Mangatarere stream joins the Waiohine River. The mean annual 7-day low flow in the Waiohine River at the gorge and at the Ruamāhanga confluence has been estimated to be 3.57 and 3.55 m^3/sec respectively. Concurrent flow gaugings indicate that the Waiohine River loses about 15–25% of its flow to groundwater upstream of the Mangatarere confluence during periods of low flow. This water enters the shallow alluvial groundwater system to later discharge into the Papawai, Tilsons and Muhunoa streams on the Greytown-Waiohine plain. The combined mean outflow from this spring system is estimated to be in the order of 1.5 m^3/sec (1,500 L/sec).

The Waiohine River's main tributary, Mangatarere Stream, is a small single-channel, gravel-bed river (Figure A2.3). It drains a catchment of 90 km^2, of which 56 km^2 lies in the foothills of the Tararua Range. The Mangatarere Stream has a mean flow of 1.9 m^3/sec at the gorge and estimated mean annual 7-day low flow at the Ruamāhanga River confluence of 0.37 m^3/sec. The low flows at the end of the catchment incorporate the inputs from spring-fed tributaries (principally Beef Creek, Enaki Stream and Kaipaitangata Stream). The Mangatarere Stream loses flow to groundwater in its upper reaches and is known to run dry in the vicinity of Andersons Line; although a short distance downstream, the river begins to gain baseflow from groundwater and contributions from small (often spring-fed) tributaries. During dry periods, the flow at the Waiohine confluence is often greater than at the gorge.

Figure A2.3 Mangatarere Stream at Belvedere Road during summer low flow. This is the gaining section of stream below Anderson Line. When this photo was taken in 2008 the stream was dry upstream at Andersons Line. Note the wide active stream bed indicating high flows at certain times of the year.

A2.3 EASTERN TRIBUTARIES OF THE RUAMĀHANGA RIVER

A2.3.1 Huangarua River

A major tributary of the Ruamāhanga River is the Huangarua River with the confluence about 1.8 km north of Martinborough. The Huangarua River starts at the confluence of two other tributary rivers – Ruakokoputuna River and Makara River – which join and become the Huangarua River at the Hautotara Bridge. The total catchment area of the Huangarua River is 311 km^2.

The 7-day MALF at the Ruamāhanga confluence has been estimated at 360 L/sec (Keenan, 2009). There is evidence that surface water and groundwater abstractions may have significantly influenced the low flow conditions in this river which are estimated to have dropped by about 10% over the last decade.

A2.3.2 Other Rivers Draining the Haurangi Range in the East

Several small streams and rivers flow off the Haurangi Range to join the lower section of the Ruamāhanga River. The most significant of these are Dry River near Martinborough and Tauanui and Turanganui rivers in the Onoke area. The Tauanui River joins the Ruamāhanga River about 9 km upstream of Lake Onoke. The Turanganui River once flowed into the Ruamāhanga River through a broad gravel delta but has now been artificially diverted south for about 1.5 km and flows directly into Lake Onoke.

The Dry River drains a small catchment (36 km^2) in the northern Haurangi Range and joins the Ruamāhanga River about 6 km southwest of Martinborough. Dry River also has a high gravel load and lives up to its name, often flowing below bed level during dry periods.

The eastern catchments of these rivers have different rainfall patterns and geological characteristics than western tributaries. The eastern tributaries tend to have lower flows (during dry periods), lower gravel loads, poorer water quality and higher suspended sediment and nutrient concentrations.

A2.4 TAUHERENIKAU RIVER

The Tauherenikau River is the only major drainage system in the Wairarapa Valley that is not a tributary of the Ruamāhanga River. It originates in the main Tararua Range near Mt Hector, and emerges onto the Wairarapa Plain north of Featherstone. It then flows across the alluvial plain to discharge into Lake Wairarapa. The Tauherenikau River is relatively steep and takes a short and direct course to Lake Wairarapa. On the plains, it is initially a steep, semi-braided river with a wide channel partly bounded by terraces. Downstream of SH2 the gradient levels out and the river is less confined but also less braided. Below the Martinborough Road bridge the river has a single-thread form that actively wanders across the gravel bed. The river carries a high sediment load and gravel is extracted from reaches in the vicinity of both the SH2 and Martinborough Road bridges. In the mid-1950s the lower section of the Tauherenikau River between the Martinborough Road bridge and Lake Wairarapa was straightened. The new channel is confined within stop banks and the bed is elevated above the surrounding plains.

Keenan (2009) reports that the 7-day MALF at the gorge, just upstream of where the river emerges onto the plains, is 1.32m^3/sec. At the river mouth (lake shore) the MALF drops to 0.31m^3/sec showing that the river loses flow to groundwater for its entire course across the plains — mostly in the middle reach between SH2 and SH53. The flow losses possibly feed the sub-parallel Docks Creek spring fed stream system. There are no major tributaries to the river on the plains, and there is only one major abstraction — the Longwood water race.

A2.5 LAKES WAIRARAPA AND ONOKE

Lake Wairarapa is the dominant feature of the lower part of the Wairarapa plains covering an area of about 78 km^2 (Figure A2.1). The lake is shallow (mostly less than 2.5 m deep) and some 18 km long by 6 km wide. It receives the majority of its inflow from the Tauherenikau River with small contributions from several small streams along the western shores and occasional flood flows from the Ruamāhanga River. There is anecdotal evidence that the lake also receives inflows via discrete springs on the lake bed and it seems probable that groundwater also discharges to the lake through the Tauherenikau River delta gravels. The hydrochemical characteristics of the lake provide evidence that it may also receive discharge from deep confined aquifers. Ongoing water conductivity profiling investigations by GWRC have also shown evidence of lake bed spring discharge.

Between 1964 and 1974 major flood control works around the lake involved the diversion of the Ruamāhanga River away from the lake under normal flow conditions and the construction of the Oporua spillway and barrage floodgates at the outlet to the lake (Figure A2.1). Over 1,200 ha of wetlands around the lake shore were drained at this time.

The exit from Lake Wairarapa to Lake Onoke is regulated by tidal barrage gates operated by GWRC under a resource consent provided for under the National Water Conservation Order for Lake Wairarapa. As a result, the lake level is artificially regulated. Some natural fluctuations in lake level are caused by rainfall, inputs from inflowing rivers and the effects of wind. The mean lake level is 0.64 m amsl (recorded at Burlings).

Lake Onoke is a 650-ha brackish barrier lake at the mouth of the Ruamāhanga River. It is separated from the beach by a 3-km long gravel spit which is breached by rising lake levels or, now more commonly, cut artificially to reduce the danger of flooding to nearby farmland. For long periods the lake is tidal, but in southerly conditions during a low river flow, the exit to the sea becomes blocked. The level of Lake Onoke can rise to such a height that there can be backflow through the barrage gates into Lake Wairarapa.

A2.6 WATER RACES

The Wairarapa Valley has an extensive network of gravity-fed water races that divert water from the main rivers into a system of unlined channels. The water is used principally for stock water supply and limited irrigation. Water races were constructed in the first half of the 20th century by local government authorities and are still administered by them under consent from GWRC. The races distribute water across catchment boundaries and probably contribute to some groundwater recharge in more permeable fan areas. The races receive spring discharges in low-lying areas and are integrated into natural drainage and spring-fed channels.

Figure A2.1 shows the four main water race systems in the Wairarapa Valley– the Moroa (sourced from the Waiohine River), the Longwood (sourced from the Tauherenikau River), the Taratahi (sourced from the Waingawa River) and the Carrington (sourced from the Mangatarere Stream). There are other smaller water race systems in the northern part of the valley – such as the Opaki race north of Masterton and the Te Ore Ore race (also shown on Figure A2.1). The complex network of water race channels often link in with existing natural waterways, agricultural drainage systems, springs and wetlands rendering it very difficult to distinguish natural spring discharge from race water.

A2.6.1 Moroa Race

The largest and most extensive water race in the lower valley area is the Moroa Water Race. The race diverts water from the Waiohine River upstream of the Railway Bridge at a maximum consented rate of 450 L/s. A minor amount of the take flows north into the Greytown area. The Moroa Water Race links into the Battersea Drain system and the Otakura stream both of which are partially spring-fed and partially sustained by the water race and surface runoff.

A2.6.2 Longwood Race

The Longwood Water Race has an extensive channel network between Featherstone and the Tauherenikau River (Figure A2.1). The water is sourced from the Tauherenikau River at the foot of the Tararua Range at a maximum consented rate of 200 L/s.

A2.6.3 Taratahi Race

The Taratahi Water Race diverts water from the Waingawa River downstream from the confluence of the Atiwhakatu River at a consented rate of up to 482 L/s. The race system extends southwards through the Taratahi area combining with spring flows from the Masterton and Carterton faults. The race then flows southward as a network of channels through the Parkvale area and merging with the natural Parkvale spring system before eventually discharging to the Ruamāhanga River.

A2.6.4 Carrington Race

The Carrington Water Race is fed from the Mangatarere Stream and is consented to take up to 113 L/s. It comprises a channel network extending southwards through the alluvial fan area west of the Mangatarere Stream (see Figure A2.1). The race system discharges water back to the Mangatarere Stream between Andersons Line and Brooklyn Road, particularly during wetter periods (the channels will also receive surface water runoff). The volumes of this discharge have not been quantified.

A2.6.5 Opaki Race

To the north of Masterton, the small Opaki Water Race diverts water from the Ruamāhanga River where the Mokonui Fault crosses, about 3.5 km upstream of the Kopuaranga River confluence (Figure A2.1). Water is diverted from the river at a permitted maximum rate of 250 L/s and maximum daily rate of 14,688 m^3. The Opaki Water Race network extends westwards from the river over the fan area north of Lansdowne Hill and any water remaining in the race discharges into the Waipoua River at several points.

A2.6.6 Te Ore Ore Race

The Te Ore Ore Water Race diverts water from the Ruamāhanga River immediately west of Lansdowne Hill near Masterton before the river enters the Te Ore Ore Plain. This intricate race network extends across the eastern part of the plain and links to the Whangaehu River at several locations. A water permit authorises the diversion of water into the race from the Ruamāhanga River at a rate of 250 L/s and 21,600 m^3/day.

A3.0 GEOLOGY

A3.1 REGIONAL GEOLOGICAL SETTING

A comprehensive review of the geology of the Lower Wairarapa Valley has been undertaken with assistance from Quaternary Geologistat GNS Science. The detail of this work is provided in previous reports (Gyopari and McAlister, 2010a, 2010b and 2010c), upon which the following summary is based.

The broad floodplains and alluvial fans of the Wairarapa Valley are underlain by thick unconsolidated sedimentary deposits which fill a major a structural depression orientated NE–SW and extending for 80 km along the southern foothills of the Tararua Ranges (Figure A3.1). The sediment-filled depression, or 'groundwater basin', is enclosed by the basement greywacke bedrock (Torlesse) formations of the fringing Tararua Ranges to the north and west, and the Aorangi Mountains and hills ('Eastern Wairarapa Hills') of Pleistocene/Late Tertiary marine strata to the east.

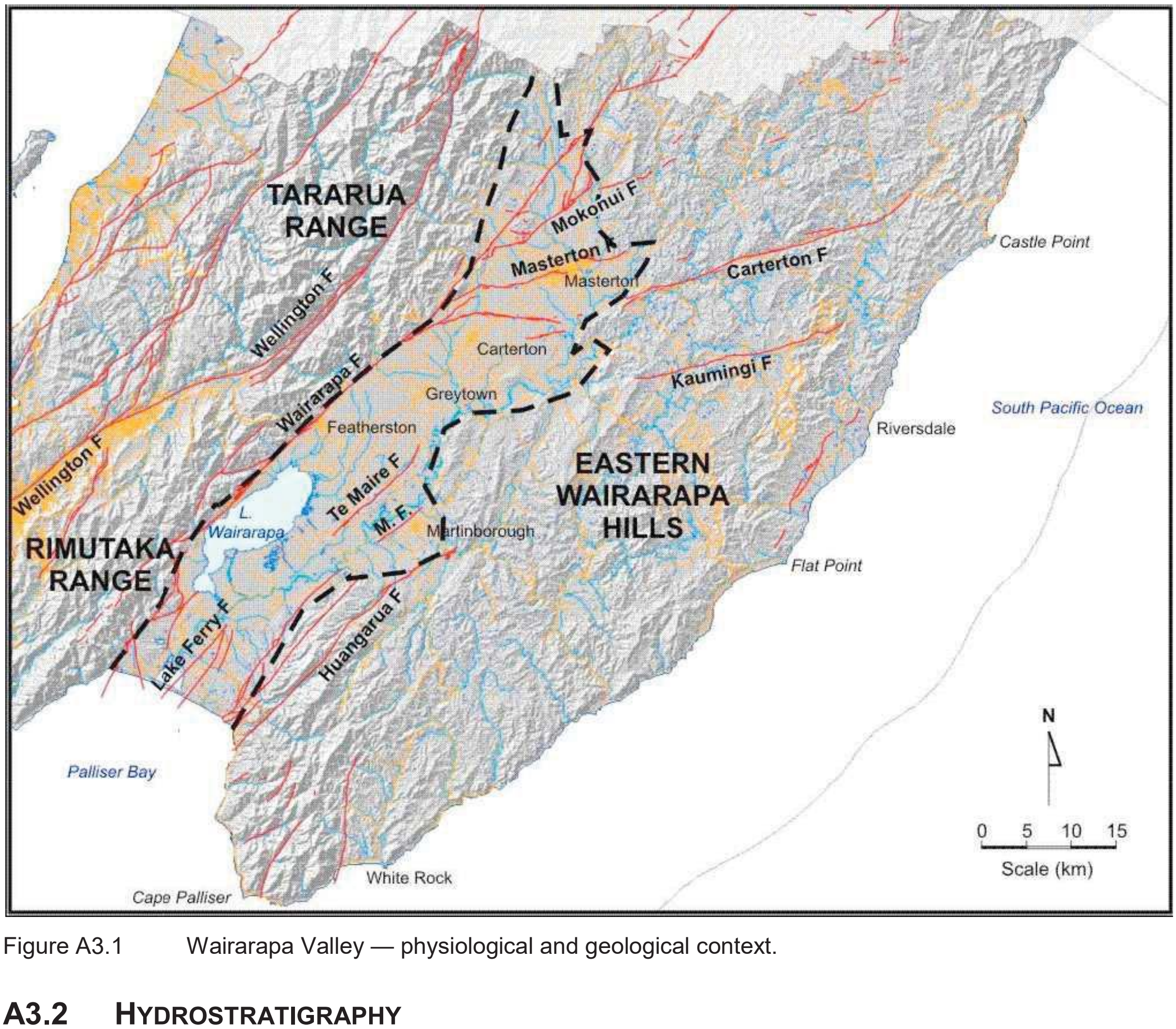

Figure A3.1 Wairarapa Valley — physiological and geological context.

A3.2 HYDROSTRATIGRAPHY

The Wairarapa sedimentary basin hosts a groundwater system within a heterogeneous sequence of unconsolidated late Quaternary age (Q1–Q8 age) fluvial, glacio-fluvial and marginal marine sediments. The deposits are dominated by aggradational alluvial and glacial outwash gravels laid down by the major rivers draining the Tararua Range (Ruamāhanga, Waoihine, Waingawa and Tauherenikau rivers). The youngest fluvial sediments are associated with the main drainage courses. Groundwater-bearing gravels tend to represent 'cold period' (glaciation) high energy, poorly sorted alluvial fan depositional environments. These are interdigitated with fine-grained overbank, swamp, lacustrine or estuarine deposits which broadly represent warmer (interglacial) climatic periods. Areas of enhanced sediment sorting locally along main former and modern drainage courses has resulted in the occurrence of highly productive aquifers.

Table A3.1 lists the late Quaternary stratigraphic sequence containing the productive and utilised aquifers in the Wairarapa valley. The units shown in Table A3.1 have been mapped out on the valley floor in Figure A3.2 relying upon stratigraphic principles to help constrain their three-dimensional distributions.

Table A3.1 Wairarapa Valley — modelled basin fill sequence. Aquifer zones = blue shading; predominantly aquitard material = grey shading. The orange shading indicates older sequences with poor groundwater potential (not modelled).

Relative age	Material	Name	Depositional environment	Map symbol[1]	Absolute age (ka)
Holocene	Mud and silt		Estuarine, lacustrine	Q1m Q1s	0–7
Holocene	Gravel and sand		Alluvial	Q1a	0–10
Late Quaternary Late Otiran	Gravel and sand	Waiohine *[Equivalent to Waiwhetu Gravel in L. Hutt Basin]*	Alluvial	Q2a	10–25
Late Quaternary Middle Otiran	Gravel and sand	Ramsley	Alluvial	Q3a	50–25
Late Quaternary Early Otiran	Gravel and sand	Waipoua	Alluvial	Q4a	70–50
Late Quaternary Kaihinu Interglacial	Mud, silt, sand and minor gravel	Francis Line	Swamp, lacustrine	Q5m	125–70
Late Quaternary Kaihinu Interglacial	Sand, some gravel	Eparaima	Marginal marine	Q5b	125–70
Middle Quaternary Waimea Glacial	Gravel and sand	*[Equivalent to Moera Gravel in L. Hutt Basin]*	Alluvial	Q6a – Q8	186–125
Middle Quaternary	Gravel, sand, silt, loess, tephra	Ahiaruhe	Alluvial, swamp	mQa	>500–186
Early Quaternary	Gravel, sand, silt, loess, tephra	Te Muna	Alluvial, swamp	eQa	c. 1000–500

[1] GNS Science QMap (1:250 000) of Wellington and Wairarapa areas.

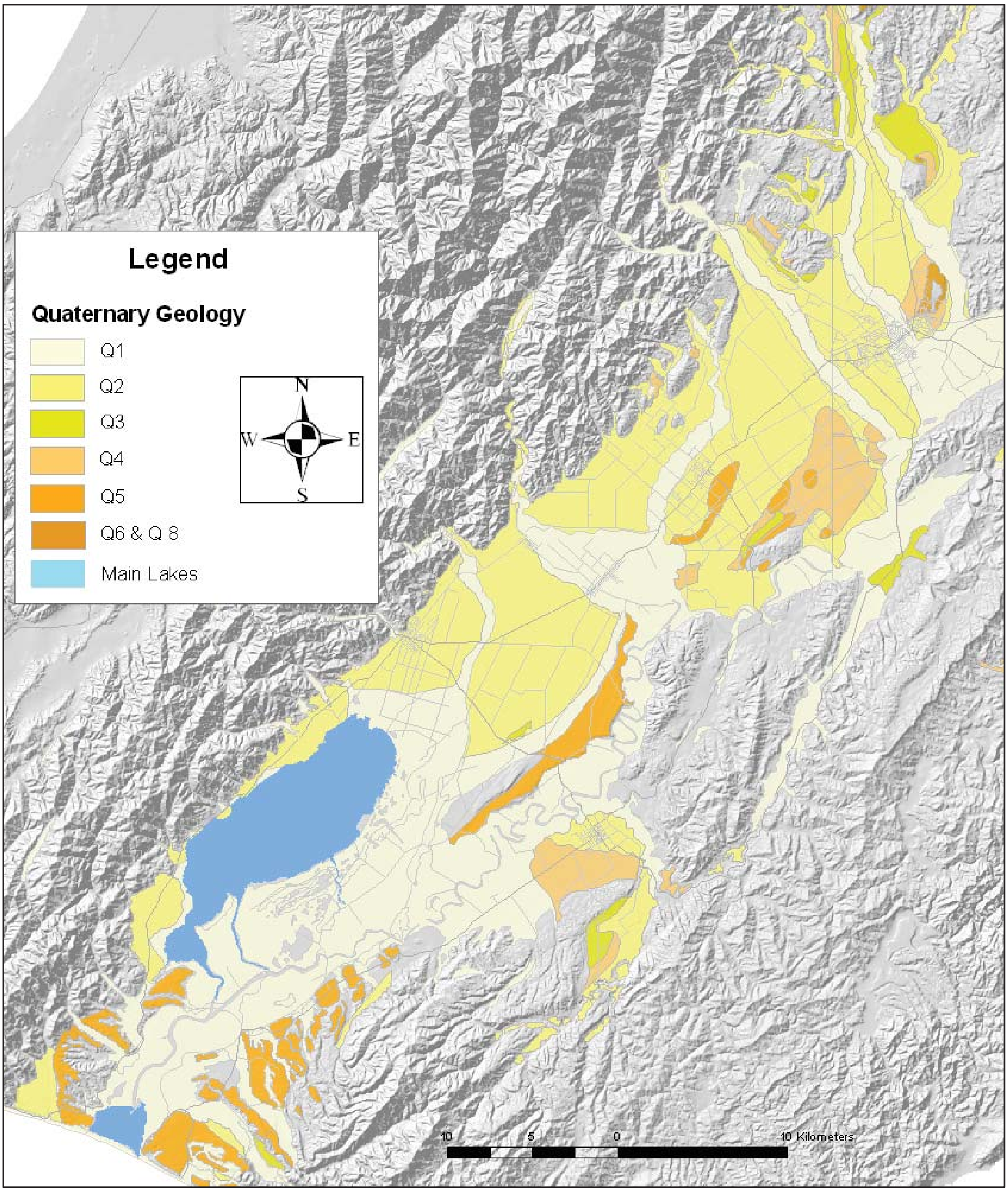

Figure A3.2 Simplified geological map of the Wairarapa Valley showing late Quaternary stratigraphy (Begg et al., 2005).

The late Quaternary deposits are dominated by aggradational alluvial and glacial outwash gravels laid down by the major rivers draining the Tararua Range (Ruamāhanga, Waingawa and Waipoua rivers). Two major glacial/high energy 'sediment packages' related to the last glacial (Otiran, Q2–4) and penultimate glacial (Waimea (Q6–Q8)) climate periods. The gravels generally represent high energy, poorly sorted alluvial fan depositional environments. These are interdigitated with fine-grained overbank, swamp, lacustrine or estuarine deposits.

Alluvial gravels are commonly clast-supported and rich in sand and silt, with frequent sandier or siltier horizons. As such, they generally represent poor aquifers except where they have been reworked. Broad areas of reworked, high-yielding gravels are recognisable near former and modern drainage courses (mostly mapped as Q1 age), and in the distal areas of fans at variable depths.

On the eastern margin of the Wairarapa Valley, deposits of late Quaternary age may be substantially more matrix-rich than in the central and western valley because many of the clasts within gravel deposits are derived from the fine-grained marine sediments of the eastern hill country (i.e., delivered by the Whangaehu River) and break down rapidly upon weathering.

The depositional environments of the late Quaternary sequence have been strongly influenced by subsidence, uplift and sea level changes. Post-deposition, the sequence has also been tectonically deformed by uplifting blocks of greywacke basement and older Quaternary and Tertiary sediments related to deep-seated faulting and folding. The region is intensely tectonically active and experiences exceptionally high rates of structural movement, including major earthquake events which have exerted a significant control on surface water drainage patterns and erosional and depositional processes, which in turn have influenced the groundwater environment.

A4.0 HYDROGEOLOGY

A4.1 CONCEPTUAL OVERVIEW

The Wairarapa Valley is a structurally controlled basin containing an accumulation of alluvial fan sequences built up by the Ruamāhanga River and its main tributaries — the Waingawa, Waiohine, Waipoua and Tauherenikau. In the subsiding lower valley beneath Lake Wairarapa, substantial thicknesses of Recent (Holocene) marine and estuarine deposits have also accumulated.

Late Quaternary sediments fill the upper levels of the basin to depths of between <10 m and about 100 m, the average thickness being about 50 m. These sediments host a dynamic groundwater flow system which exhibits a strong inter-relationship with the surface water environment. On a regional scale, the Wairarapa Valley can be hydrogeologically described as a heterogeneous unconfined to leaky-confined aquifer system, with greater degrees of confinement developing at depth within the sub-basins. The regional aquifer system is internally 'compartmentalised' by geological structures that have facilitated the development of flow barriers and sub-basins. In essence, the regional basin geometry is dominated by the major intra-basin cross-cutting faults, such as the Masterton and Carterton faults, which have tilted and folded older less permeable sediment sequences ('groundwater basement') towards the surface, thus impeding or blocking the flow of groundwater some areas. Uplift and subsidence processes have also created groundwater sub-basins such as Te Ore Ore, Parkvale, and the rapidly subsiding lower valley basin beneath Lake Wairarapa. Uplift of the coastal area has isolated the groundwater basin from the sea.

The top of the Middle Quaternary deposits (mQa) is assumed to be the base of the groundwater flow system (Table A4.1). Formations beneath the top of mQa are regarded to be largely isolated from the shallower actively recharged system since they are more compact and, because of their general lithological nature, are likely to be of significantly lower permeability. However, it should be appreciated groundwater also occurs where conditions are favourable within mQa and older formations and reasonable yields may be encountered locally.

The sediments within the active groundwater system, although connected, are highly heterogeneous and exhibit large variations in hydraulic conductivity, depending upon the lithological characteristics, specifically: grain size characteristics, gravel matrix composition, degree of sediment sorting/reworking, and degree of compaction.

Broad patterns of hydraulic conductivity are recognisable and in particular enhanced formation transmissivities (due to better sediment sorting and reworking) occur around the modern-day channels of major drainage systems where there is considerable interaction between surface water and groundwater. These highly transmissive sediments support the large-volume groundwater abstractions in the Wairarapa. At depth in some areas, there are also distinct horizons of variable spatial extent which exhibit enhanced transmissivity associated with historical drainage systems. These form a system of deeper leaky-confined or semi-confined productive aquifers separated by low permeability aquitards in areas such as Te Ore Ore, Parkvale, Carterton, Lower Ruamāhanga and Lake Wairarapa areas.

A4.2 PRINCIPAL GEOLOGICAL FEATURES CONTROLLING HYDROGEOLOGY

Conceptually, the principal structural and sedimentological features of hydrogeological significance in the Wairarapa Valley are shown in Figure A3.1 and Figure A4.1. They are:

- The regionally significant active Wairarapa Fault which penetrates the full thickness of the Australian Plate and controls and the western side of the basin. Greywacke basement forming the Tararua Range outcrops on the northwestern side on the fault.
- A series of major faults splaying from the Wairarapa Fault, including– the Mokonui, Masterton and Carterton faults, have disrupted and uplifted the sediment sequence. In places, the displacement along the faults has created partial groundwater flow barriers as shown by the common emergence of springs along the fault traces. For example, the Masterton Fault splays from the Wairarapa Fault near the southern end of Carterton Bush and raises Miocene–Pliocene mudstone to the surface at Lansdown and in the Ruamāhanga River. The Ruamāhanga and Waingawa rivers and their terraces are affected by the fault which appears to have impeded groundwater flow north of Masterton as indicated by spring emergence along the fault. The Carterton Fault is the southernmost of the three cross-valley faults, splaying from the Wairarapa Fault near Papaitonga Stream, and cutting across the Waiohine river gravels behind Carterton. Gravel units to the northeast of this fault are not as clearly back-tilted as observed along the two faults further to the north, and its influence on groundwater movement is less apparent.
- A number of structurally controlled sub-basins (Figure A4.1): Te Ore Ore, Parkvale, Carterton. These are generally more than 100 m deep and contain productive aquifers;
- A series of long-valley faults concentrated along the eastern side of the basin, including the Te Marie, Martinborough and Huangarua faults. The displacement on these structures place low permeability basement (or older Quaternary gravel in the case of Fernhill) against younger water bearing alluvial sediments in the Parkvale basin and on the lower portion of the Tauherenikau fan. The basement ridges form a groundwater divide between the Ruamāhanga River valley and alluvial fan and sub-basin deposits to the west. In the middle valley, Tiffen Hill diverts groundwater flowing through the alluvial fan deposits toward the confluence of the Waiohine and Ruamāhanga rivers where a considerable volume of baseflow discharge occurs. Similarly, in the lower valley, Te Maire ridge diverts groundwater flowing through the Tauherenikau fan southwards into the confined aquifer surrounding Lake Wairarapa where it merges with groundwater flowing through the lower section of the Ruamāhanga River valley.
- The northeast–southwest oriented fault-bounded uplifted basement blocks of Te Maire ridge and Tiffen Hill.
- Uplifted terraces of older Quaternary sediments beneath Martinborough and the associated Harris Anticline.
- Large alluvial fan systems draining the Tararua Range associated with the Ruamāhanga, Waingawa, Waiohine and Tauherenikau rivers.

- The Lake Onoke/coastal uplifted valley mouth area isolates the groundwater system from the ocean. The Miocene–Pliocene 'groundwater basement' occurs above sea level in the Lake Ferry – Palliser Bay area. At the western end of Palliser Bay, Early to Middle Quaternary mud, and some silt-bound gravel, are exposed in cliffs behind the bay. These uplifted and relatively impermeable rocks constrain the southern end of the Wairarapa Valley groundwater system. The Ruamāhanga River, despite having a very low gradient, continues to cut downwards through the rising rocks to maintain egress to the sea. The river enters the sea through Lake Onoke, which lies in a restricted opening ('The Narrows') between the uplifted hills. Permeable sediments must be present through this gap, but they are unlikely to be particularly thick because of the uplift since the last interglacial.

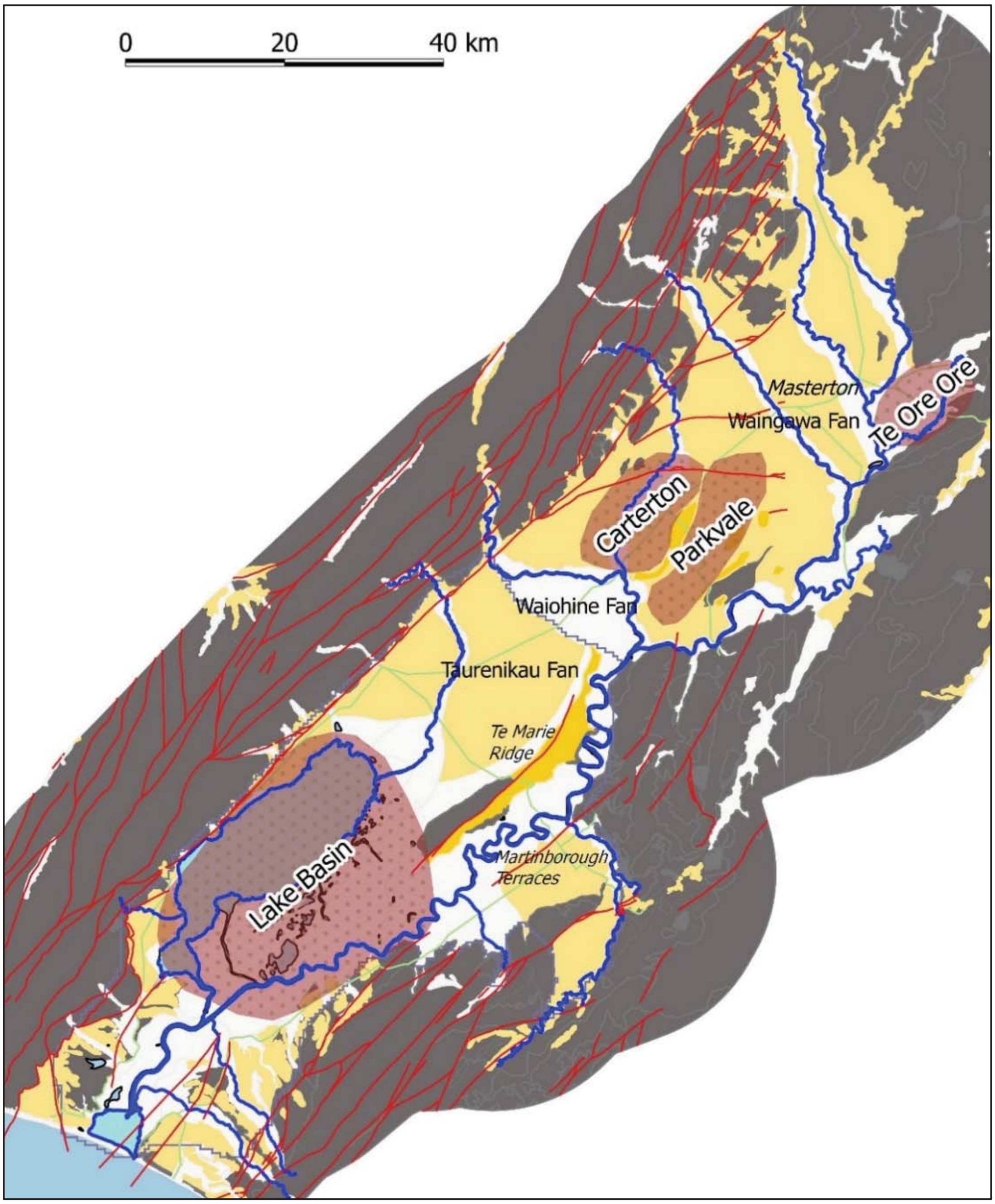

Figure A4.1 Principal hydrogeological features of the Wairarapa Valley. Major faults (red lines) and four sub-basin structures (shaded areas) shown.

A4.3 GROUNDWATER 'BASEMENT'

Indurated greywacke rocks comprising sandstone and interbedded mudstone of the Tararua, Rimutaka and Aorangi Ranges bound the Wairarapa basin and are faulted against the western margin of the basin by the Wairarapa Fault. These rocks belong to the Torlesse and Pahaoa Groups (230–120 Ma) and represent groundwater 'basement'. They have no primary porosity or permeability, but locally exhibit a secondary permeability along joint and fracture zones. On a regional scale, the greywacke is regarded to be impermeable.

The eastern hills comprise the Palliser and Onoke groups (25–2.3 Ma) which consist of marine sandstones, siltstones, mudstones and limestone. These deposits probably also underlie younger deposits within the Wairarapa plains alluvial basin. Regionally, these deposits are not an important groundwater resource and would tend to exhibit a low hydraulic conductivity although locally, aquifers may occur and yield relatively low quantities of water.

Early to Middle Quaternary (2.3 Ma–125 ka) alluvial sands, gravels and swamp deposits extend to the start of oxygen isotope stage 8 (Q6–8, Table A3.1). These sediments underlie the groundwater basin and generally have poor groundwater potential due to their silt and clay rich matrix, silt and loess interbeds, and structure. These sediments also outcrop along the eastern margin of the valley with some isolated outcrops on the western side. Waimea Glacial gravels (Q6a) probably form a viable aquifer and are included as part of the valley groundwater system.

A4.3.1 Hydrostratigraphic Units

The stratigraphy of the Wairarapa Valley (described above, Table A4.1) is highly heterogeneous and contains variable of aquifer productivity due to widely varying grain size distributions, gravel matrix compositions, degrees of sediment sorting/reworking, and degrees of compaction. Five broad hydrostratigraphic units are recognised based on formation lithology, well yield and aquifer properties. Table A4.1 lists the units, their spatial distribution and the general nature of their hydraulic properties. Figure A3.2 and Figure A4.1 also show their general distribution.

Table A4.1 Hydrostratigraphic units of the Wairarapa Valley.

Unit	General hydraulic nature	Distribution
Alluvial fan gravels (Q2–Q8)	Poor–moderate aquifers: generally low hydraulic conductivity, poorly sorted gravels with silts/clay and organic lenses. Improved sorting distally where higher well yields are obtained. Poor well yields generally on the upper fan areas.	Major fan systems on western valley side of Waipua, Waiohine, Waingawa, Mangatarere and Tauherenikau rivers. Also, Huangarua valley and Onoke area and side terraces.
Q1/Q2 Unconfined aquifers	Good aquifer: Shallow, highly permeable unconfined aquifers exhibiting a high degree of connectivity with surface water generally high hydraulic conductivity.	Main river channels – Ruamāhanga, Waingawa, Waiohine–Greytown floodplain, Tauherenikau, Huangarua.
Q2–4, Q6, Q8 aquifers In alluvial sub-basins	Aquifers: medium–high hydraulic conductivity, discreet, relatively continuous, confined or semi-confined units (generally <10 m thick).	All distal fan areas either at surface or below Q1 deposits. Te Ore Ore, Parkvale, Carterton, Lower Rumanhanga, Lake Basin and Onoke confined/semi-confined aquifers.
Q5 and Q7 silts/clay aquitards	Aquitards: very low hydraulic conductivity silty/clay swamp deposits.	Parkvale, Carterton, Ruamāhanga, Fernhill, Lake Bain, Te Ore Ore
Q6–mQa and Martinborough terraces	Low hydraulic conductivity, low yielding aquifers compact, silt/clay-rich gravels with silt aquitards.	Martinborough terraces.
Uplifted blocks	Aquitards: very low or low hydraulic conductivity. Form flow barriers.	Tiffen Hill, Fernhill. Te Marie Ridge, Harrise anticline, Lansdown Hill.

A4.3.2 Alluvial Fan Deposits

Large alluvial fans have developed where the major river systems emerge from the surrounding hills into the Wairarapa Valley. These include the extensive alluvial fans deposited by the Ruamāhanga, Waingawa, Waiohine and Tauherenikau rivers as well as those associated with some of the smaller river systems including the Mangatarere Stream and Waipoua River. These alluvial fans extend from the Tararua foothills eastward across the valley. Several smaller alluvial fans also extend into the Wairarapa Valley from eastern catchments including those of the Whangaehu, Huangarua, Tauanui and Turanganui rivers. These alluvial fan deposits comprise the present-day landform throughout much of the Wairarapa Valley.

The alluvial fan deposits represent accumulation of Q2 to Q8 gravels on an active depositional surface. These gravel deposits are typically poorly sorted with significant amounts of sand and silt present within the gravel matrix, although improved sorting and channelisation is evident in some distal areas. The alluvial fan deposits associated with the major river systems form relatively extensive, low to moderate permeability, stratified aquifer systems which extend across much of the western side of the Wairarapa Valley. Groundwater is found pervasively throughout these deposits where discrete layers of water bearing gravels are typically interspersed with lower permeability intervals forming a stratified aquifer system which may exhibit semi-confined (leaky) characteristics at depth due to the presence of the intervening lower permeability materials.

A4.3.3 Q1/Q2 Unconfined Aquifers

The most productive and utilised aquifer in the Wairarapa Valley are associated with recent Q1 gravels which have formed where the main river systems have reworked the older alluvial fan deposits since the last glacial period. These gravel deposits are typically restricted to the riparian margins of the major rivers and their lateral extent is often marked by prominent alluvial terraces which mark the lateral extent of postglacial river entrenchment. The Q1 gravels form shallow unconfined aquifers generally less than 15 metres in thickness which are highly permeable and exhibit a high degree of connectivity with surface water.

The Ruamāhanga River has entrenched into a relatively narrow valley which runs along the eastern side of the Wairarapa Valley between the eastern hills and the uplifted basement blocks associated with Tiffen Hill and Te Maire ridge. The Q1 and Q2 gravel deposits associated with river entrenchment are typically less than 15 metres deep forming a moderately to highly permeable unconfined (and locally semi-confined) aquifer system which is hydraulically connected to the Ruamāhanga River. South of the Huangarua River confluence the thickness of the alluvial sediments increases with individual gravel layers segregating out as wedges of silt-rich aquitard materials thicken down valley into the Lake Wairarapa basin. Due to the relatively restricted dimensions and high permeability of the Q1/Q2 aquifer system in the Ruamāhanga valley, groundwater in this area typically exhibits a high degree of connectivity with surface water.

A4.3.4 Alluvial Sub-Basin Deposits

Alluvial sub-basins occur in the Wairarapa Valley where structural deformation has allowed the accumulation of successive deposits associated with Quaternary glacial and interglacial cycles. In these areas, active subsidence has allowed differentiation of more permeable interglacial alluvial deposits (Q4, Q6 and Q8) from the intervening clay and silt dominated glacial deposits (Q3, Q5 and Q7) to form a sequence of semi-confined aquifers. Individual alluvial sub-basins are identified in the Te Ore Ore, Parkvale, Carterton and Lake Wairarapa areas. These individual sub-basins may be structurally complex due to internal deformation associated with faulting and folding.

Groundwater within the alluvial sub-basins typically exhibits limited direct interaction with surface water. However, vertical leakage induced by groundwater abstraction does have the potential to influence the water balance of overlying unconfined aquifers, by reducing discharge to local spring-fed stream and wetlands or intercepting a portion of groundwater throughflow which would have otherwise contributed to baseflow discharge in lower catchment areas.

Lake Wairarapa occupies a large, actively subsiding sub-basin at the southern end of the Wairarapa Valley. In this area reworked alluvial gravel deposits associated with the Tauherenikau and Ruamāhanga rivers merge to form a series of discrete confined aquifers which are separated by layers of fine-grained lacustrine and estuarine sediments associated with the lake. These confined aquifers are laterally continuous across a relatively wide area but pinch out before reaching the south coast due to the presence of a basement high across the valley in the vicinity of Lake Onoke. Due to the degree of confinement, confined aquifers in the lower valley exhibit limited direct interaction with surface water, although diffuse leakage from the upper confined aquifer is likely to contribute to the overall water balance of Lake Wairarapa.

A4.4 HYDROGEOLOGICAL CROSS-SECTIONS

A suite of geological cross sections has been constructed to assist with the three-dimensional characterisation of the Wairarapa Valley groundwater system. Six representative sections, the locations of which are shown in Figure A4.2, are provided in Figures A4.3 to A4.8. Further cross sections and more detailed descriptions of them can be found in Gyopari and McAlister (2010a, 2010b and 2010c). The cross sections have been constructed using a large number of geological bore logs, lithological interpretation and pumping test data. They show the interpreted aquifer sequence and the influence of faulting and folding which has resulted in a highly complex hydrogeological environment. The yellow areas on the cross-sections highlight the late Quaternary Q1–Q8 age sediments which host the bulk of the groundwater. Below these (shaded blue and purple), much lower permeability middle and early Quaternary material (mQa and eQa), or greywacke, predominate — although localised aquifers are encountered.

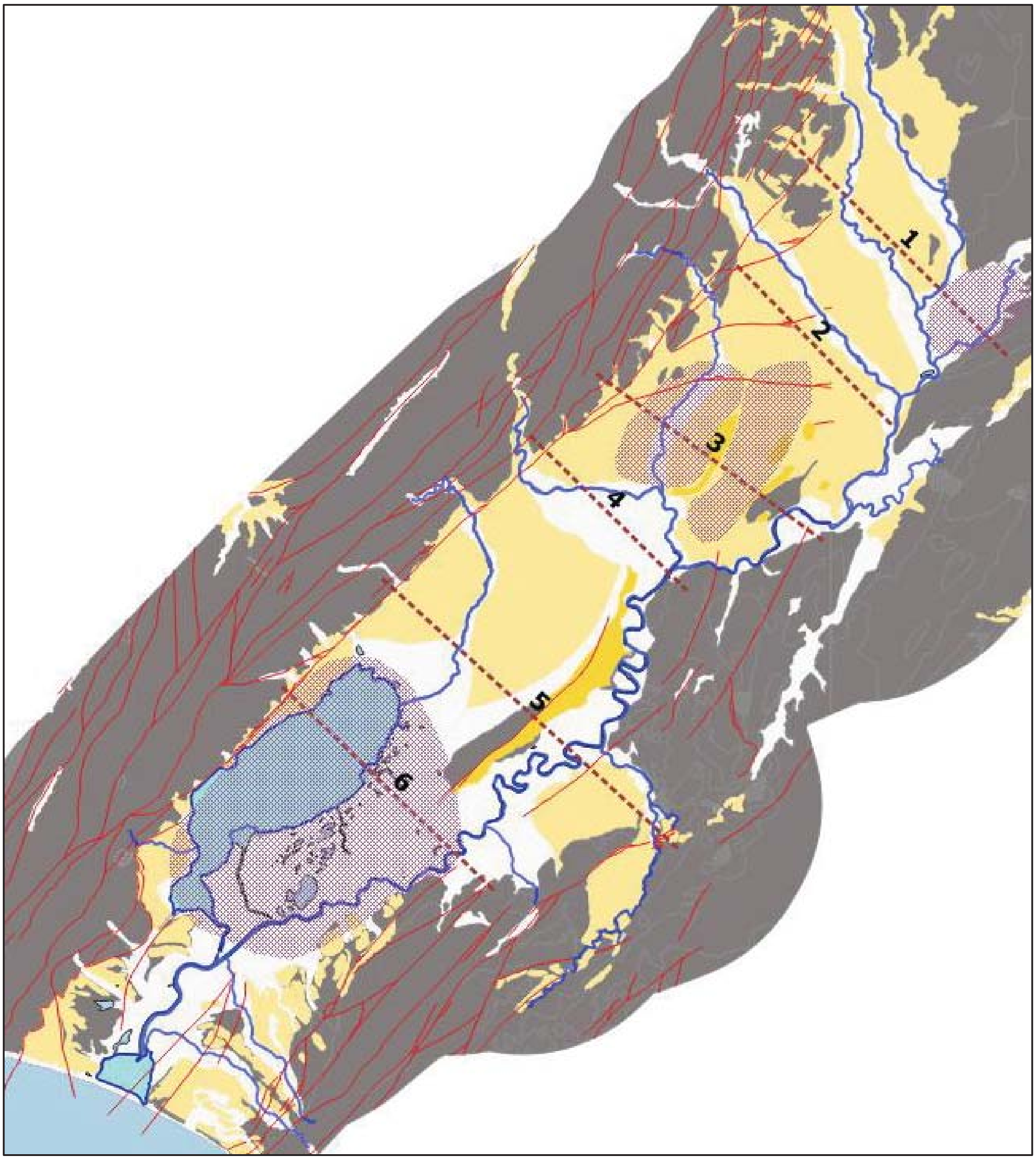

Figure A4.2 Locations of geological cross sections shown in Figures A4.3 to A4.8.

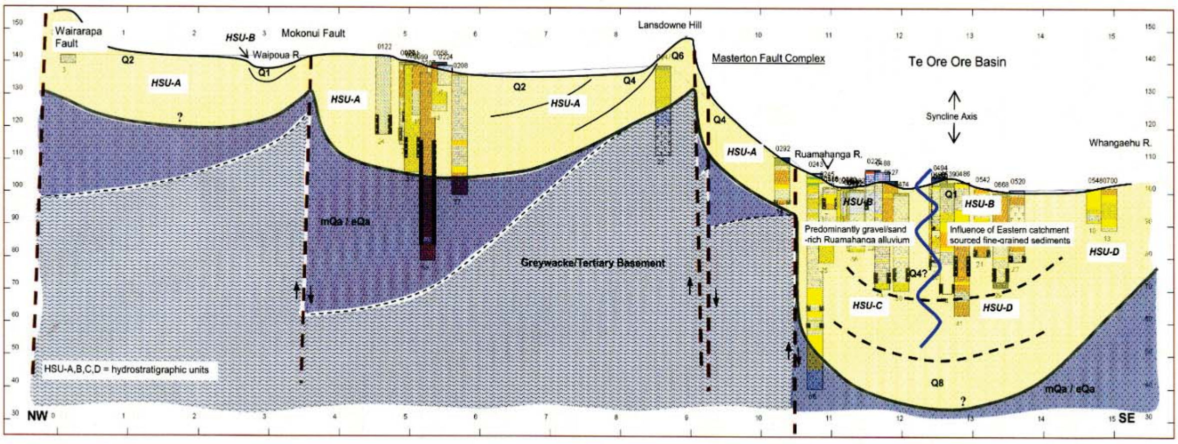

Figure A4.3 Geological cross section 1 (Te Ore Ore / Masterton). Vertical divisions = 10 m / horizontal = 1 km.

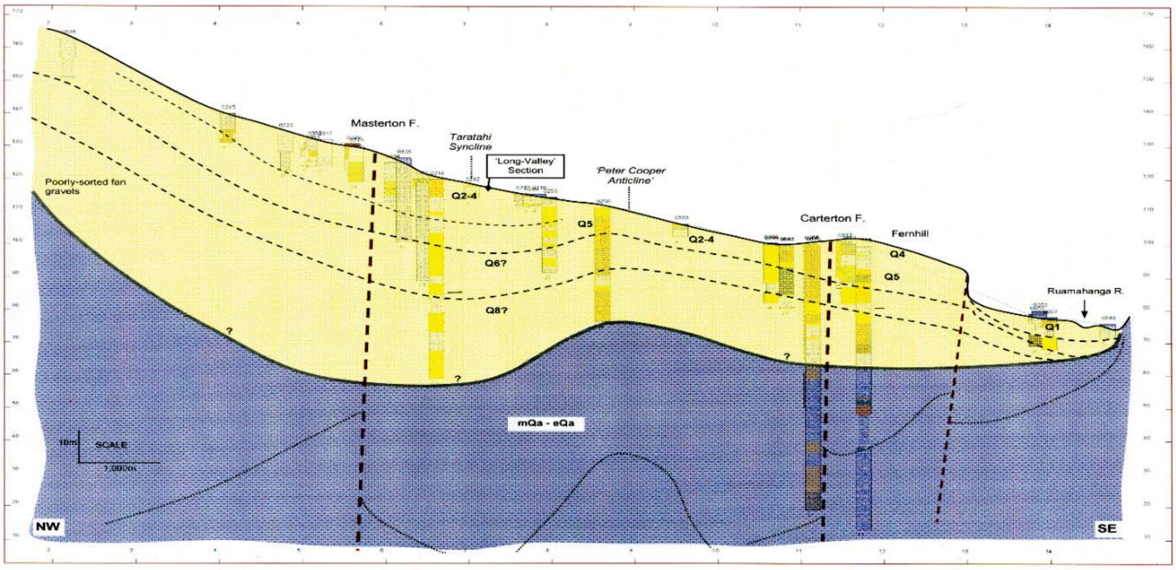

Figure A4.4 Geological cross section 2 (Waingawa fan). Vertical divisions = 10 m / horizontal = 1 km.

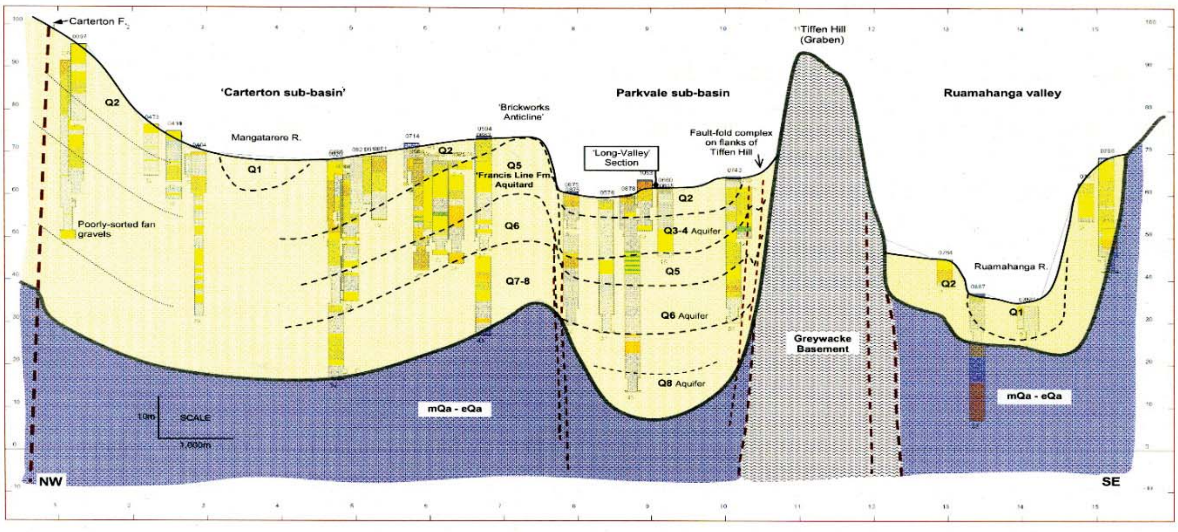

Figure A4.5 Geological cross section 3 (Parkvale – Carterton sub basins). Vertical divisions = 10 m / horizontal = 1 km.

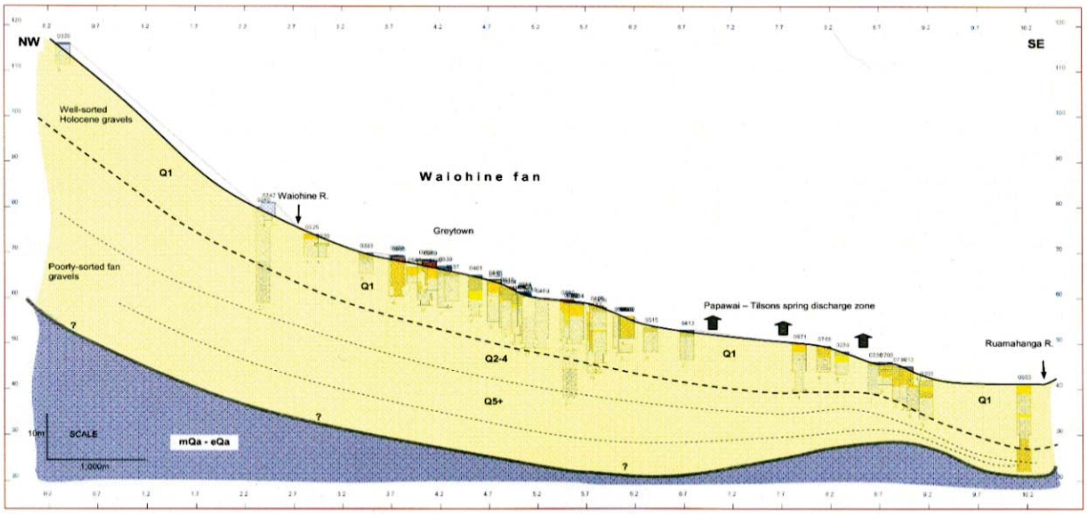

Figure A4.6 Geological cross section 4 (Waoihine fan – Greytown). Vertical divisions = 10 m / horizontal = 1 km.

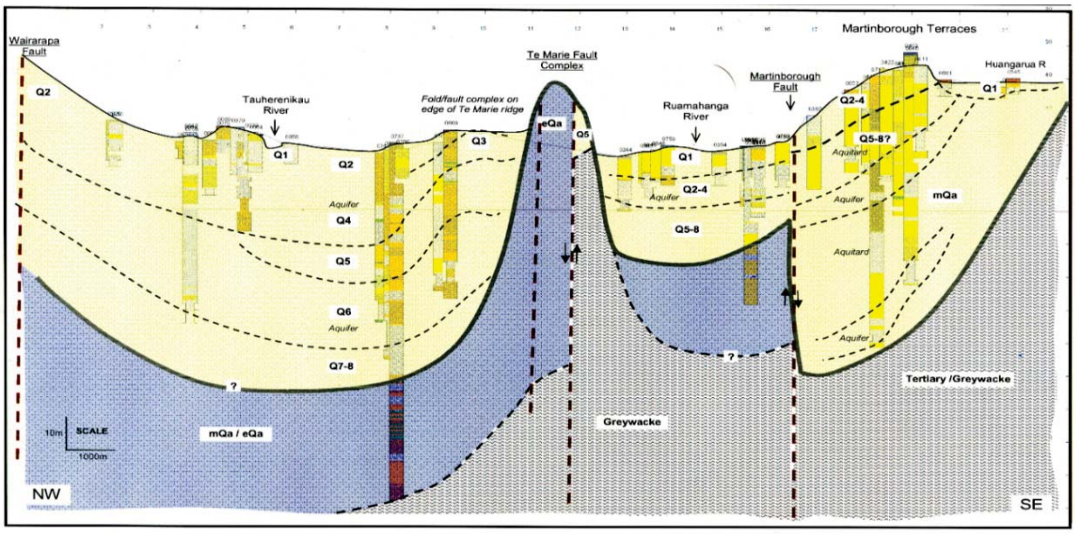

Figure A4.7 Geological cross section 5 (Tauherenikau fan–Te Marie Ridge–Huangarua). Vertical divisions = 10 m / horizontal = 1 km.

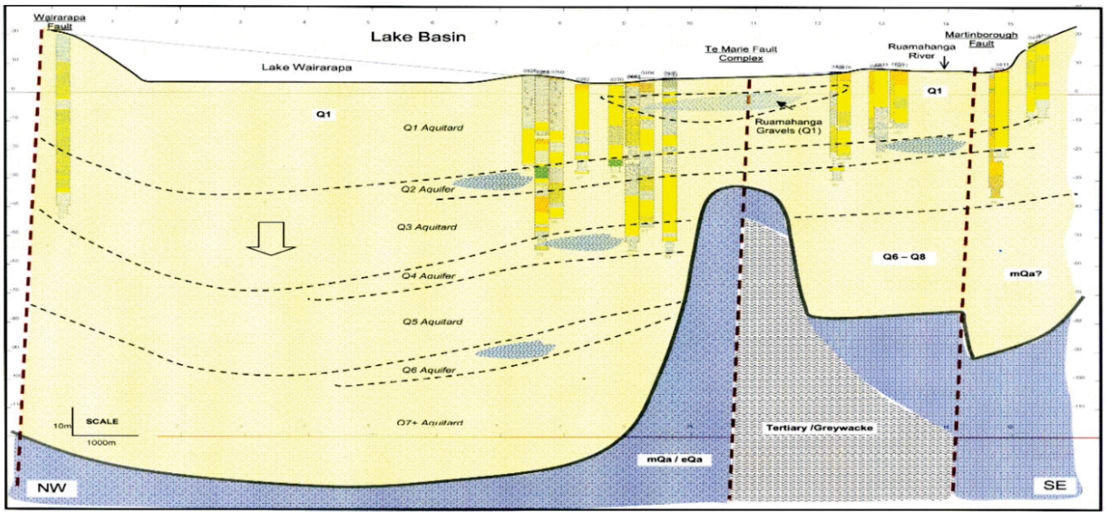

Figure A4.8 Geological cross-section 6 (Lake Wairarapa). Vertical divisions = 10 m / horizontal = 1 km.

A4.5 REGIONAL GROUNDWATER FLOW PATTERN

A4.5.1 Regional Flow Characteristics

Characterisation of regional groundwater flow patterns in the Wairarapa Valley can be achieved through the analysis of groundwater level data provided by a network of GWRC monitoring bores. GWRC operate 66 automatic and manual groundwater level monitoring bores in the Wairarapa Valley. The locations of the monitoring sites (surface water and groundwater) are shown in Figure A4.9.

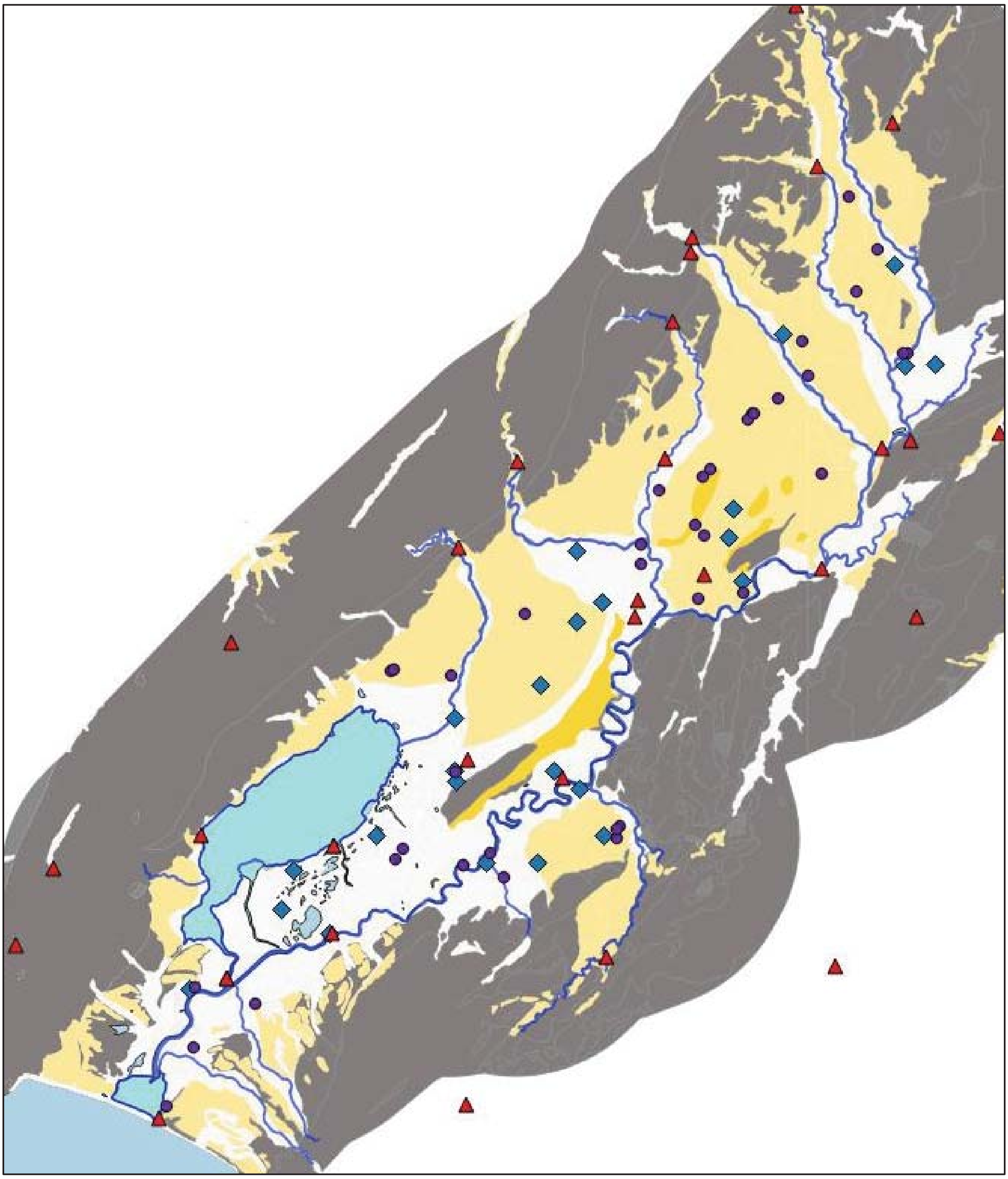

Figure A4.9 Locations of groundwater level monitoring sites (manual – circles; automatic – diamonds) and surface water gauge location (red triangles).

Figure A4.10 shows groundwater level contours based upon concurrent level measurements taken in March 2007. Although water levels have been measured in bores of different depths, a consistent regional groundwater flow pattern emerges when the data from all monitoring wells are contoured. It is only within the deep lower valley sub-basin that significant increases in head are observed with depth (these have been excluded in the construction of Figure A4.10). Within the other sub-basins (Parkvale, Carterton and Te Ore Ore) small changes in groundwater level occur with depth, but these are not significant.

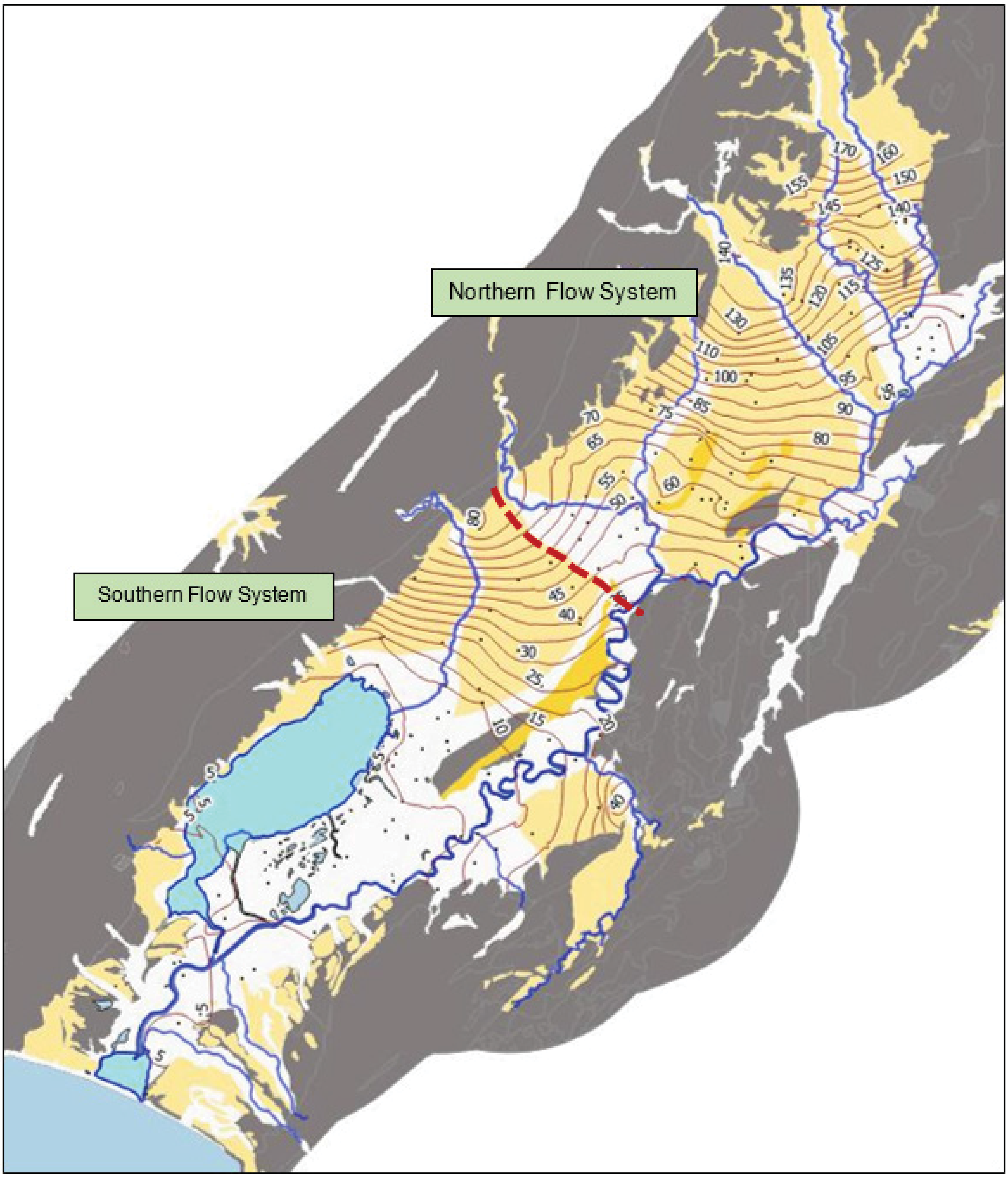

Figure A4.10 Shallow groundwater level contours (March 2007) for the Wairarapa Valley. Data points used to construct the map are also shown. Red dashed line indicates boundary between Northern and Southern Flow Systems along a flow line and geological boundary.

The flow pattern in Figure A4.10 generally reflects the regional topography with groundwater flowing in a southerly to south-westerly direction off the outwash fan areas and towards the Ruamāhanga River. The Ruamāhanga River and Lake Wairarapa control regional groundwater discharge. The rivers exert a significant influence on the flow patterns depending upon whether groundwater discharges to them (flow lines converge on the river), or whether the river recharges groundwater (flow lines diverge from the rivers). Further discussion on the interaction between shallow groundwater and the rivers is provided in Section 6.

In the lower valley area, around Lake Wairarapa and downstream of the Tauherenikau fan, a prominent flattening of the piezometric gradient is evident. The groundwater level contours appear to show that regional flow is focused on the area beneath the lake, and that the lower valley system is a ‘closed basin’. This concept is supported by groundwater age and chemistry data, which indicate old (>100 years) anaerobic water with elevated conductivity is present within deeper aquifers in the lower valley sub-basin (Morgenstern, 2005). The basin can only discharge by slow leakage through large thickness of low permeability lake sediment. However, although the contours indicate flow to the lake area, the rate of flow may be very small given the large thickness of lacustrine sediments.

A4.5.2 Temporal Groundwater Level Variations

GWRC maintains a network of manual and automatic groundwater level recording sites located in the main aquifer systems across the Wairarapa Valley. The temporal variation in groundwater levels at these sites typically reflects the nature of the hydraulic connection between the aquifer system and adjacent surface waterbodies.

Along the riparian margins of the main river systems groundwater levels typically exhibit a close relationship with variations in river stage. Figure A4.11 shows a plot of groundwater levels recorded in the shallow unconfined Q1 aquifer in the Greytown area in bore S26/0490, located approximately 1.5 kilometres from the Waiohine River. The figure shows groundwater levels respond rapidly to changes in river stage, typically peaking within 1 to 2 days after the peak river discharge.

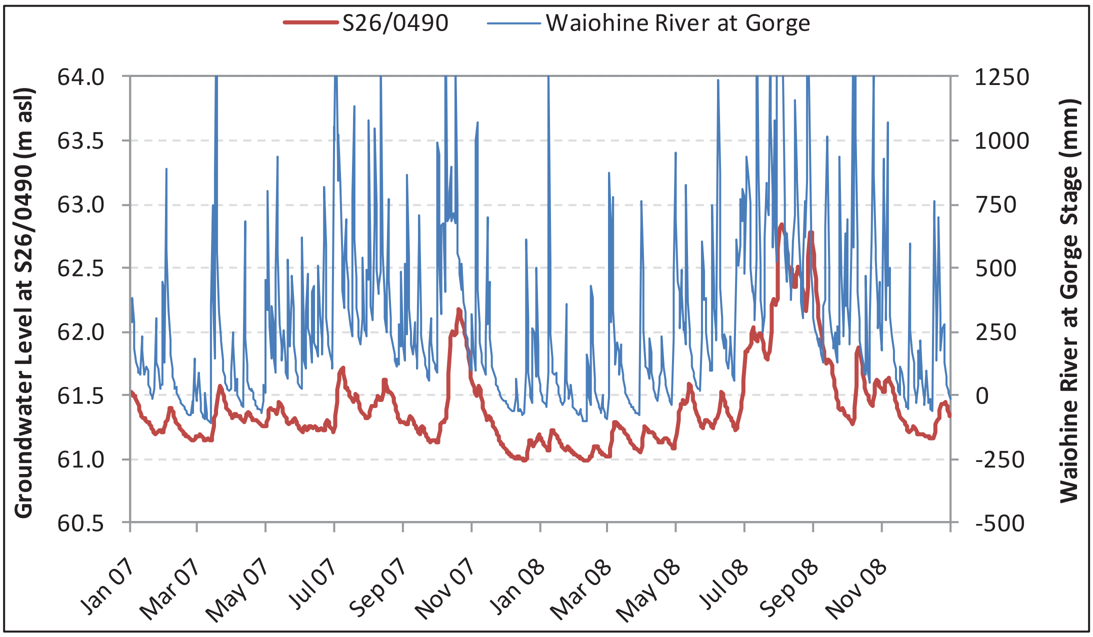

Figure A4.11 Temporal variations in groundwater levels in a shallow bore in the Greytown area (S26/0490) and Waiohine River stage.

A similar temporal groundwater level response to river stage variations is observed along the margins of the Ruamāhanga, Waipoua, Waingawa, Waiohine and Tauherenikau rivers reflecting significant interaction between the river and adjacent Q1 aquifers. In these areas groundwater level response to river stage variations typically becomes increasingly dampened with depth and distance from the river channel. However, in both the Greytown area and the lower Ruamāhanga Valley a clear relationship is observed between groundwater levels and river stage variations up to 4 kilometres from the river channel.

The amplitude of the observed variations in groundwater levels of up to one metre in response to individual high river stage events indicates significant transient flux between the river and aquifers. However, although groundwater levels in these aquifers exhibit considerable short-term variations in response to river stage, limited change in storage is observed on an inter-annual basis reflecting the relatively constant recharge contribution from the major rivers.

In contrast, groundwater levels in shallow unconfined aquifers on the alluvial fans away from the major river systems show little, if any, relationship with river stage. For example, groundwater levels in the unconfined aquifer in the Parkvale area (bore S26/0738) show little or no relationship with river flow, instead tracking seasonal variations in rainfall recharge (Figure A4.12).

Similarly, groundwater levels recorded in deeper, semi-confined aquifers typically show a distinct pattern of temporal variation which is influenced by seasonal recharge as well as the volume of groundwater abstraction. For example, Figure A4.13 shows groundwater levels recorded in semi-confined aquifers in the Te Ore Ore (bore T26/0494) and Parkvale (bore S26/0743) alluvial sub-basins over the period 2006 to 2008 inclusive. The plots show temporal groundwater level variations in these aquifer systems are dominated by drawdown resulting from abstraction during the summer months followed by a gradual water level recovery during the subsequent winter. This recovery is principally due to vertical leakage from overlying water bearing strata. This vertical leakage into deeper aquifers may contribute an overall reduction in groundwater baseflow discharge to surface water at a catchment scale.

More detailed analysis of spatial and temporal variations in groundwater level are provided in Gyopari and McAlister (2010a, 2010b and 2010c).

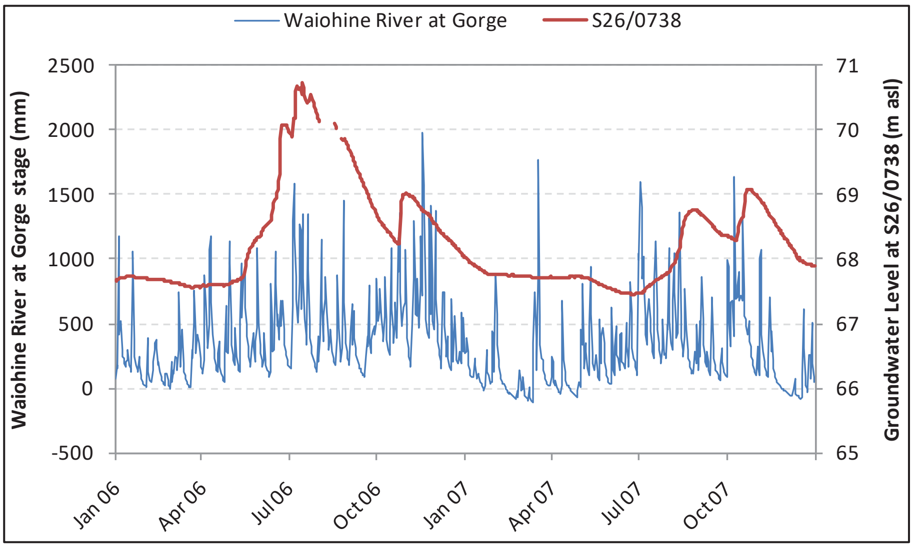

Figure A4.12 Temporal variations in groundwater levels in the unconfined aquifer in the Parkvale area (bore S26/0738) and stage height in the Waiohine River, 2006–07.

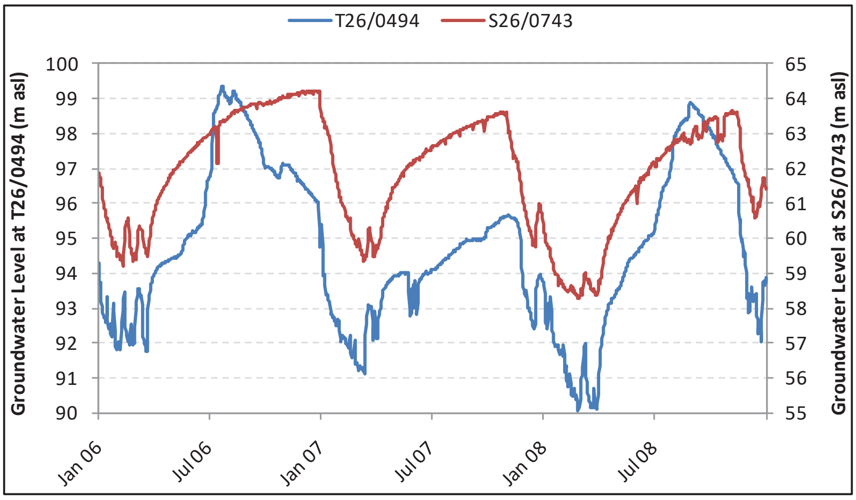

Figure A4.13 Groundwater levels in semi-confined aquifers in the Te Ore Ore (bore T26/0494) and Parkvale (bore S26/0743) alluvial sub-basins.

A4.5.3 Recognition of Sub-Regional Northern and Southern Flow Systems

For convenience and modelling requirements, the Wairarapa Valley groundwater system is recognised to comprise two sub-regional flow systems based on hydrogeological evidence. Figure A4.10 shows the location of a groundwater and surface water flow divide which also coincides with a geological boundary (red dashed line) between what has been termed a 'Northern Flow System' and a 'Southern Flow System'. The boundary follows a terrace along the southern edge of the Greytown Waiohine Q1 gravel plains and, although the line is not a physical barrier to the movement of water, regional groundwater flow does not cross this line – all groundwater in the northern area discharges to surface water and ultimately the Ruamāhanga River – prior to entering the southern area. The two groundwater flow systems can essentially be regarded as independent.

For reference, the Southern Flow System corresponds to the 'Lower Valley Catchment' in the previous FEFLOW modelling work whilst the Northern Flow System corresponds to the combined Middle and Upper Valley catchments (Gyopari and McAlister, 2010a, 2010b and 2010c). The Middle and Upper Valley catchments were combined in this study in order to create two roughly equal area groundwater catchments and the streamline the modelling process.

A4.6 Rainfall Recharge

A principal groundwater recharge process in the Lower Valley catchment is rainfall infiltration (or land surface recharge) — the portion of rainfall which is not diverted to runoff or lost to evapotranspiration but which seeps through the ground

The steep rainfall gradient across the valley from the Tararua Range to the eastern hills results in a considerable spatial variability in recharge. The highest annual rainfall of 1,800–1,900 mm occurs against the Tararua range, reducing to 800–900 mm on the eastern side of the valley. Because of the high rainfall gradient, rainfall recharge is expected to demonstrate a large spatial variability across the catchment. Soil type and underlying shallow geology also exert a significant influence on rainfall recharge processes.

Rainfall recharge has been calculated using a distributed soil moisture balance approach on a 500 m^2 grid. The soil moisture balance and irrigation water demand model IRRICALC (Aqualinc, 2016) has been used to calculate rainfall recharge, irrigation returns through the soil profile, crop water demand and surface runoff. Figure A4.14 shows the annual average recharge pattern for the Wairarapa Plains calculated by IRRICALC. There is a strong west to east recharge gradient ranging from about 800–1,000 mm/yr on the western side of the plains against the Tararua Range to 180–200 mm/yr on the eastern side which reflects the high rainfall gradient. The annual average rainfall on the western side of the valley is 1,000 mm and therefore the calculated recharge in this area represents about 50–60% of rainfall. On the drier eastern side of the valley rainfall recharge is estimated to be about 25% of rainfall.

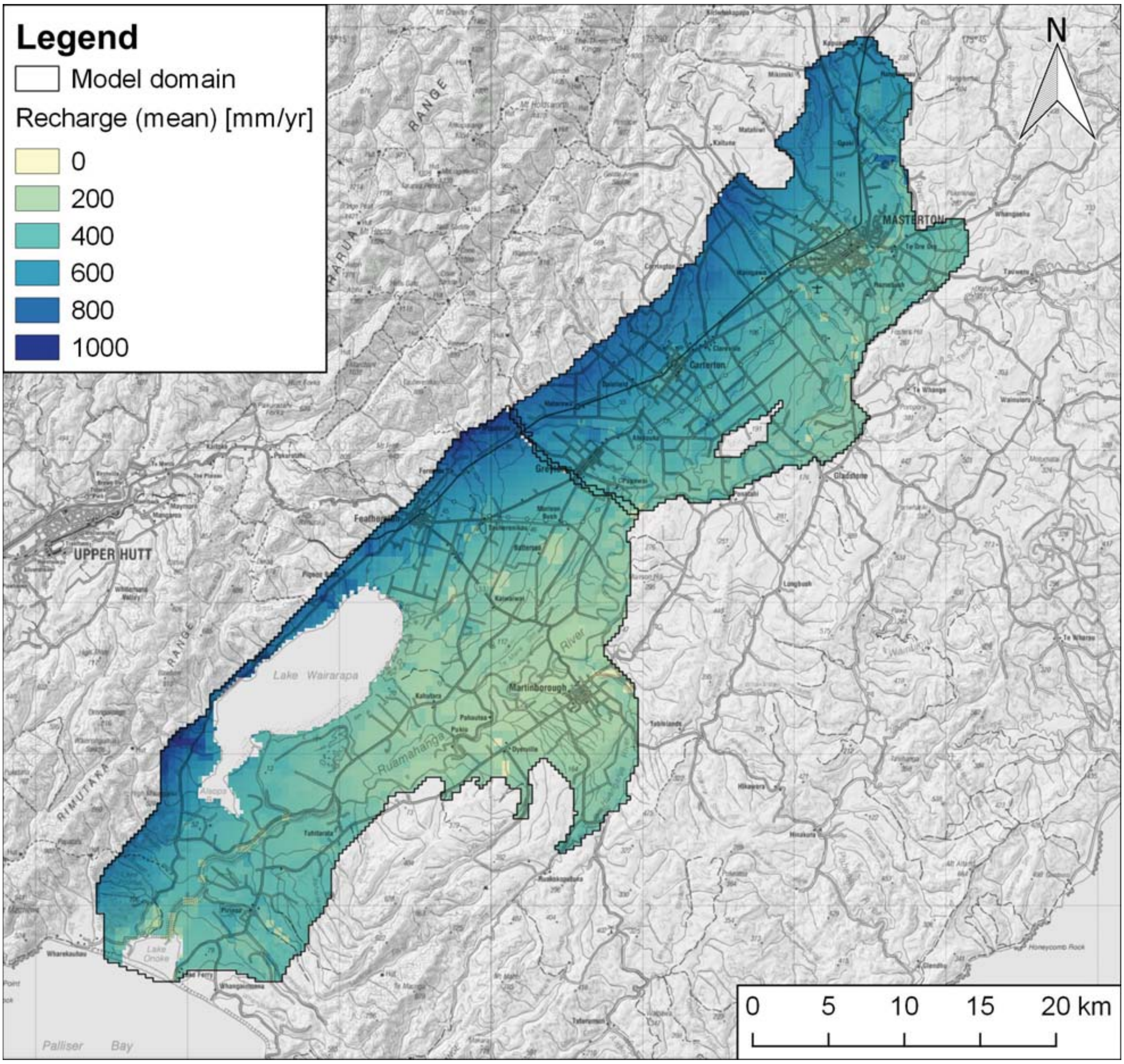

Figure A4.14 Calculated rainfall recharge using IRRICALC in mm/year.

A4.7 Groundwater Abstraction

Groundwater abstraction in the Wairarapa Valley has increased significantly over the past 20 years, and more than doubled over the past 10 years. Much of this growth is driven primarily by the dairy industry for seasonal pasture irrigation (generally November to April). Figure A4.15 illustrates the concentration of large shallow abstractions located within the Q1 unconfined aquifer adjacent to major drainage systems, particularly along the Ruamāhanga River. Many of these groundwater abstractions source water through the depletion of surface water flow.

The trends in groundwater abstraction and estimated actual abstractions based upon land use and crop water demands has been modelled using IRRICALC (Aqualinc, 2016). Figure A4.16 shows a groundwater irrigation demand time series for the period 1992 to 2007 which illustrates the considerable increase in irrigation water demand from the groundwater resource over this period.

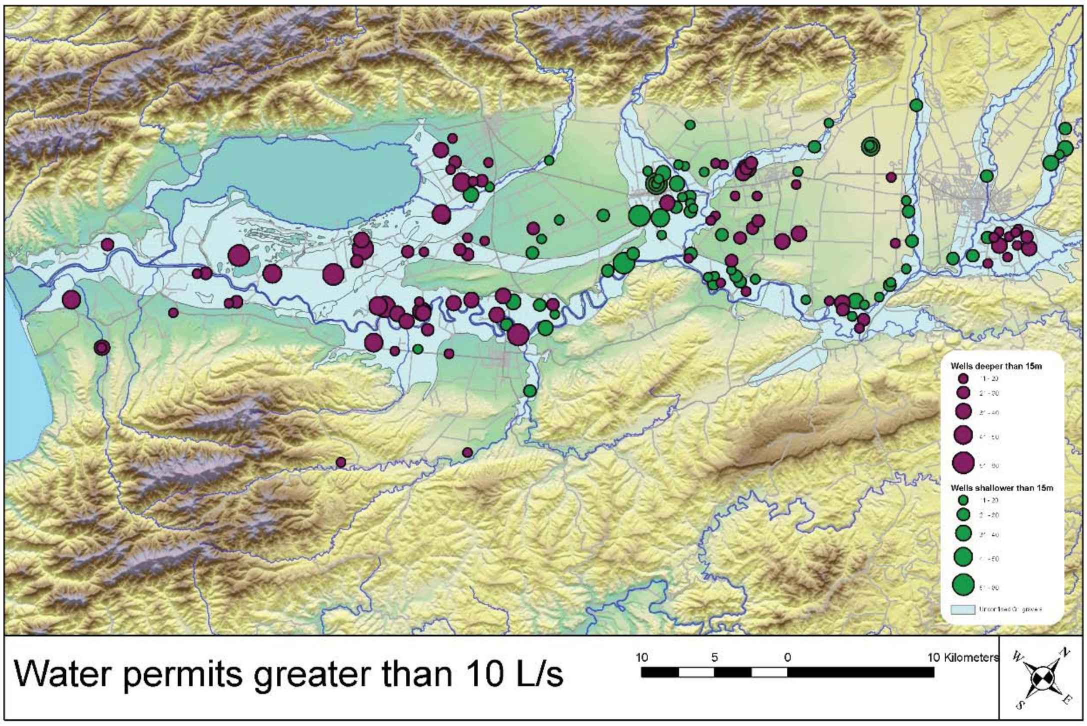

Figure A4.15 Location of groundwater take permits of >10 L/sec in the Wairarapa Valley. Circle size is proportional to take size; purple = wells greater than 15 m depth; green = wells less than 15 m depth.

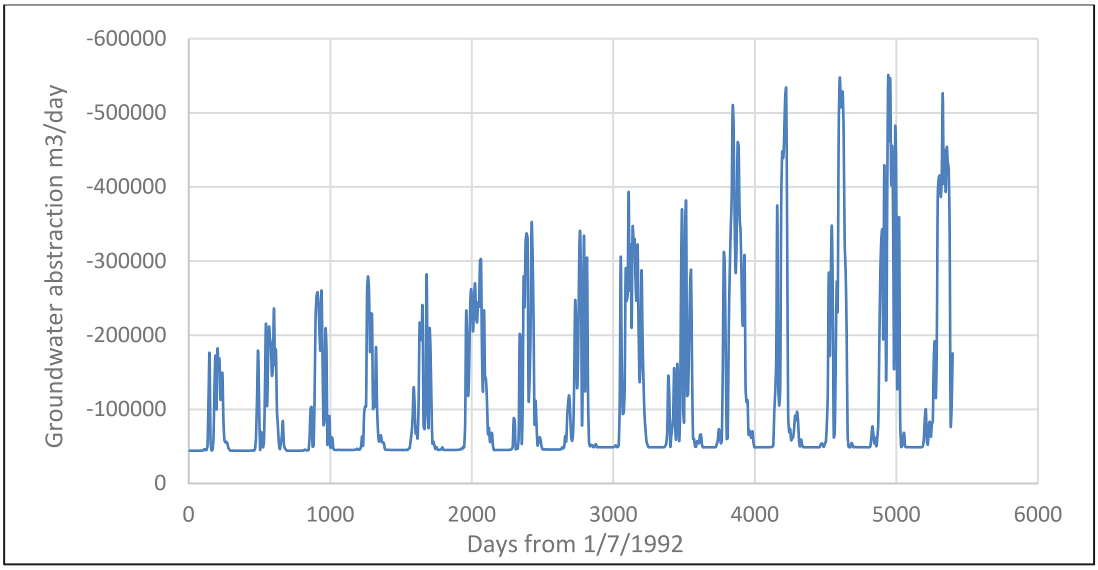

Figure A4.16 Simulated groundwater irrigation demand from groundwater abstraction bores using IRRICALC.

A4.8 AQUIFER HYDRAULIC PROPERTIES

The geological materials forming the main aquifer systems in the Wairarapa Valley exhibit a wide range of hydraulic properties which typically reflect their depositional origin and/or subsequent re-working.

Gravel materials (Q2–Q8) forming the alluvial fan deposits associated with the major river systems are highly heterogeneous reflecting their deposition on an actively aggrading alluvial fan surface. These materials tend to be poorly sorted with the relatively high percentage of sand and silt in the gravel matrix restricting aquifer permeability. However, vertical stratification of these materials into layers of higher and lower permeability occurs in some areas forming localised semi-confined aquifers which exhibit low to moderate permeability. In contrast, the alluvial gravel materials underlying the recent floodplains of the major rivers (Q1) have typically been extensively reworked during postglacial river entrenchment resulting in the removal of much of the finer material within the gravel matrix, significantly increasing aquifer permeability.

In the alluvial sub-basins, differentiation between the moderately permeable interglacial gravels and lower permeability silt-dominated glacial deposits is better defined than within the alluvial fan deposits. As a result, the Parkvale, Carterton and Te Ore Ore sub-basins host a series of relatively well-defined semi-confined aquifers which exhibit moderate transmissivity and a relatively low storage coefficient.

A large number of aquifer tests have been undertaken in the Wairarapa Valley to support historical resource consent applications. These aquifer tests show a degree of variability between individual test results which is primarily interpreted to reflect the overall heterogeneity of the alluvial gravel materials (although variability in aquifer test methodology and data quality are also likely to contribute to some of the observed variance). The main observation from these tests is the large (up to, and more than one order of magnitude) difference in aquifer transmissivity calculated for the Q1 gravel deposits compared to the older, more silt dominated Q2 to Q8 gravels comprising the alluvial fan and sub-basin aquifers. This pattern is illustrated in Figure A4.17 which shows the locations of aquifer tests and the interpreted hydraulic conductivities for all depths.

Gyopari and McAlister (2010a, 2010b and 2010c) undertook an analysis of available aquifer test data and derived the representative aquifer properties with respect to hydrostratigraphic units. Table A4.2 contains a summary of this work in the form of representative 'bulk' hydraulic properties of individual geological units to overcome some of the bias in available aquifer test results which tend to favour bores in areas exhibiting highest aquifer permeability.

Aquifer test results reflect the variability in hydrogeological settings and aquifer hydraulic properties across the various aquifer systems present in the Wairarapa Valley. Many results show evidence of the interception of recharge boundary conditions that may represent induced recharge from local surface waterways (in the case of tests from shallow unconfined aquifers) or vertical leakage from overlying water bearing layers (which may be hydraulically connected to surface water) in the case of tests from deeper semi-confined aquifers.

Overall, even given their restricted durations and common issues with data quality, aquifer test results in the Wairarapa Valley demonstrate direct effects on surface water in many shallow bores located in relative proximity to surface water. Many deeper tests also demonstrate that vertical leakage induced by pumping has the potential to draw water from overlying unconfined aquifers that may be hydraulically connected to surface water.

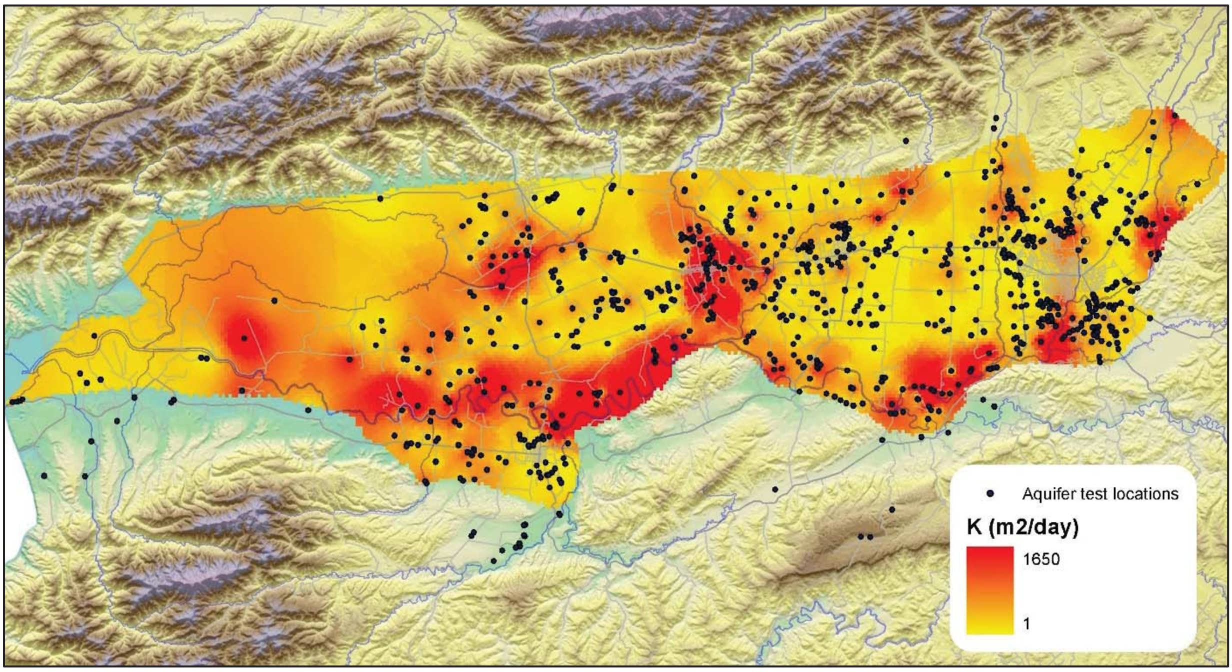

Figure A4.17 Hydraulic conductivity distribution from pumping test analyses in the Wairarapa Valley.

Table A4.2 Representative hydraulic characteristics of the main hydrostratigraphic units in the Wairarapa Valley.

Geological unit	Area	Transmissivity (m2/day)	Hydraulic conductivity (m/day)	Storage[2]
Holocene alluvium (Q1)	Waiohine	4,000–6,000	300–600	S_y = 0.05–0.15
	Ruamāhanga	3,000–4,000	300–400	S_y = 0.07–0.1
	Mangatarere	1,500–2,000	200–300	
	Waingawa	2,000–3,000	200–300	
	Te Ore Ore basin	2,000	200–300	S_y = 0.07–0.1
	Huangarua	1,100	100	S_y = 0.15
	Turanganui/Tauanui	2,000	200	S_y = 0.1–0.15
Alluvial fan gravels (Q2)	Taratahi/Parkvale	100–500	20–100	
	Tauherenikau	700		S_y = 0.05–0.1
	Waiohine /Mangatarere	100–500	10–50	S_y = 0.05–0.15 S = 1.5 x 10^{-4}
	Waingawa	600	60–00	S_y = 0.05–0.1
	Waipoua/Ruamāhanga	150	15–20	S_y = 0.03–0.05
	Kopuaranga	50	5–10	S_y = 0.03–0.05
Alluvial sub-basins (Q2–Q8)	Parkvale basin	500–1,000	50–150	S = 1.5 x 10^{-4}
	Te Ore Ore basin	1,000	100	S = 5 x 10^{-4}
	Lake basin	2,750		S = 1.5 x 10^{-4}
	Onoke	320		S = 1.3 x 10^{-4}
Martinborough Terraces	Upper (<60 m deep)	400–500		S = 0.0008
	Lower (>60 m deep)	50		S = 0.0002

[2] The storage coefficient (S) is presented as Sy (specific yield) for unconfined aquifers; specific yield is approximately equal to S for unconfined aquifers.

A5.0 GROUNDWATER SURFACE WATER INTERACTION

Fluxes between shallow groundwater and the surface water environment are an important and large component of the water balance for the Wairarapa Valley hydrologic system. Natural groundwater discharge occurs as baseflow to rivers and streams, spring discharge and diffuse seepage into wetlands and lakes. Some reaches of rivers and streams also loose flow to into adjacent aquifers. The patterns of flow loss and gain are highly variable and the direction of flow exchange can vary over short distances and change seasonally. The flux dynamics between these environments can also be influenced considerably by large groundwater abstractions near to open water ways. It is therefore critical to achieve a good level of understanding around the nature of groundwater-surface water interaction in the development of groundwater flow model.

The degree of the interaction between groundwater and surface water is dependent upon the head gradient between the aquifer and the river, and upon the degree of connectivity between both water bodies. The connectivity is a function of the permeability of the stream/river bed and aquifer, as well as the size and geometry of the contact area. Characterisation of groundwater surface water interaction is described below – for the Southern and Northern Flow Systems as defined in Section 5.5.3.

A5.1 SOUTHERN FLOW SYSTEM – CONNECTED SURFACE WATER ENVIRONMENTS

The principal surface water environments which are connected to groundwater in the Southern Flow System (Figure A4.10) are as follows:

- Tauherenikau River (above SH53).
- Huangarua River (relatively little information is available for this river).
- Main eastern side-valleys — Dry River, Tuanui and Tauranganui rivers (Onoke area) all loose flow to groundwater.
- Tauherenikau fan springs — Stonestead (Docks) Creek, Otakura/Battersea system, Abbotts/ Featherstone system.
- Water races — the Moroa water race is considered to both recharge groundwater and receive groundwater discharge.
- Ruamāhanga River — upstream of Huangarua confluence.
- Lake Wairarapa — gains inflow from Tauherenikau fan gravels and seepage from deeper aquifers.

To help understand and quantify the patterns of gain and loss, and thereby characterise groundwater-surface water interaction in the catchment, concurrent gauging surveys were carried out between 2006 and 2008. By measuring flow at various points along a river or stream on the same day during stable base flow (summer conditions) the gaining and losing patterns which characterise each of the river systems were observed. Full details and analyses of these surveys are contained in Gyopari and McAlister (2010c).

Figure A5.1 shows the results of the concurrent surveys in terms of losing, gaining or neutral (neither gaining nor losing) reaches highlighted in different colours. A river can have simultaneous gaining, losing and neutral reaches along its length in a seasonally varying pattern. It is important to recognise that Figure A5.1 represents the groundwater-surface water interaction during low flow and low groundwater level conditions. It is probable that under different flow regimes (i.e., high flows) that the pattern may be somewhat different.

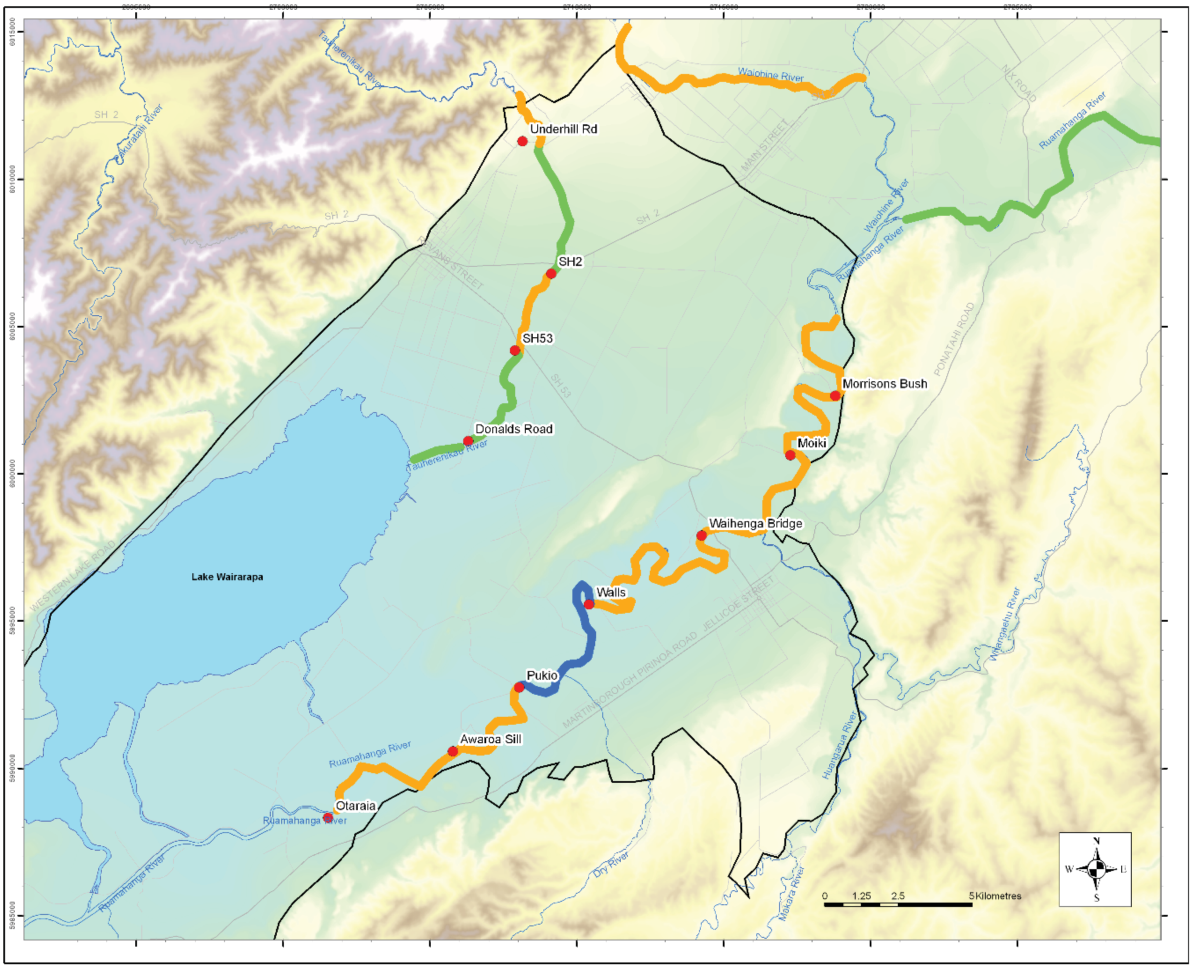

Figure A5.1 Southern Flow System (Lower Valley Catchment) — concurrent flow gauging sites on the Tauherenikau and Ruamāhanga rivers. Also shown are the flow loss and gaining patterns (orange = loss; blue = gain; green = neutral). From Gyopari and McAlister (2010c).

A5.1.1 Tauherenikau River

This river appears to have three different reaches in terms of groundwater-surface water interaction. From the Gorge to Underhill Road the river loses to groundwater. During low flow conditions, downstream of Underhill Road, the river crosses the fan and appears to neither lose nor gain water until SH2. Between SH2 and SH53 the river loses about 60% of its flow to groundwater. And below SH53, the river continues to lose water, but at a much lower rate. Figure A 5.2 shows the interpretation of the concurrent gauging survey for the Tauherenikau River. The plot shows an observed losing reach between the gorge (permanent gauging site) and the Racecourse-SH53 bridge area. Over this reach, the river consistently loses between 0.8 and 1.1 m^3/sec to groundwater. Most of this disappears over a 3-km section between the SH2 bridge and the SH53 bridge. The reason for the high bed-loss over this reach is probably due to the occurrence of channels filled with highly permeable gravel along a former course of the river. These gravels allow flow to be diverted to groundwater from the true left bank of the Tauherenikau River. The channels link into the Stonestead (Docks) Creek spring system and a large proportion of the loss from the river probably re-emerges in this vigorous spring systems which flows consistently at 600–800 L/s. Some of the loss may also re-emerge in springs and drains on the northern side of the river as it enters the delta area at Lake Wairarapa. Downstream from SH53 the flow in the Tauherenikau River remains stable, showing neither significant loss nor gain. Along this reach and down to the lake shore the river is generally elevated above the surrounding land and therefore the bed must have a relatively low hydraulic conductivity to prevent losses.

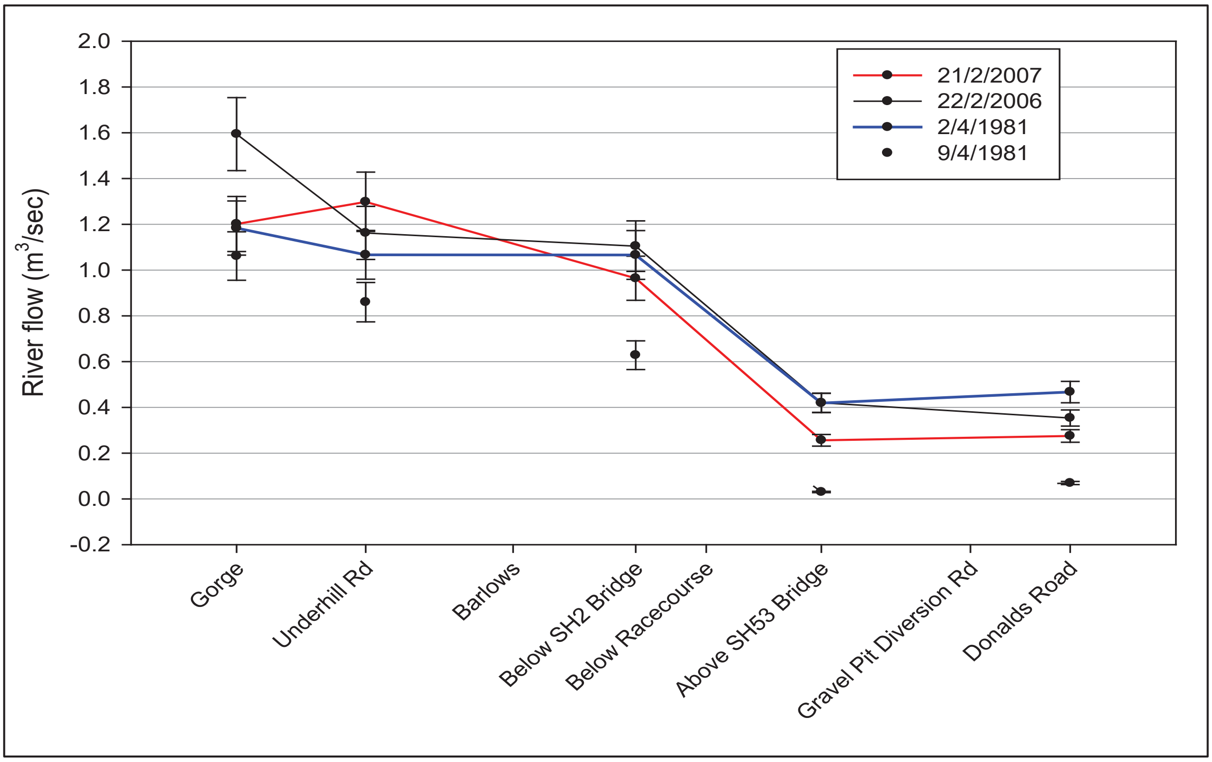

Figure A 5.2 Concurrent flow gauging surveys on the Tauherenikau River.

A5.1.2 Ruamāhanga River

The Ruamāhanga River exhibits considerable interaction with groundwater but the relatively large rates (mean annual low flow = 2.7 m^3/sec) mean that it is not possible to confidently identify losing and gaining patterns because the standard gauging error is too high at +/- 10%. However, data derived from concurrent gauging surveys carried out on 22/2/2006 showed very large losses of 1.3 m^3/sec between Morrisons Bush and Walls when considering inflow from the Huangarua River. This is consistent with the conceptual understanding that this reach of the Ruamāhanga River recharges both shallow and deeper aquifers and is a recharge sorce for deeper confined aquifers in the lake basin. Aquitard layers develop and thicken downstream from the Walls area and therefore the Ruamāhanga is not likely to recharge deep aquifers downstream of there. Towards Walls there are also recent gravel-filled palaeochannels of the Ruamāhanga River which may divert some flow from the river westwards towards Lake Wairarapa. Between Walls and Pukio both gauging surveys showed a large gain in flow of about 0.5–0.6 cumecs. The consistency between the sets of data suggests that the gain is real. The Dry River enters the Ruamāhanga River between these sites and, although there is no flow in the tributary during the summer at its confluence, it is probable that there is a significant shallow groundwater throughflow in the gravel fan deposits emanating from the eastern hills catchment. Together with shallow groundwater flowing off the Martinbourough Terraces, these throughflows could account for the gaining flow in the Ruamāhanga River between Walls and Pukio. Losses from the river on the reach below Pukio could relate to diversions from the river towards Lake Wairarapa via old gravel channel deposits. Gauging errors towards Otaraia are however likely to increase due to the higher flows and tidal influences on the flow.

A5.1.3 Groundwater Discharge on Tauherenikau Fan

Several extensive spring systems and diffuse groundwater discharge areas occur on the Tauherenikau fan. The most extensive discharge area is the Otakura/Battersea spring/drain system covering the eastern part of the fan, down to Te Maire ridge (Figure A5.3). The Battersea drainage system is highly modified and linked to the Moroa water race network making it very difficult to distinguish groundwater discharge from water race flows. The discharge area may extend as far up the fan as SH2 with much of the flow being channelled to the south. The flows in this spring system have not been quantified and it is likely that the water race system recharges the shallow groundwater during summer, whilst draining the water table during high winter levels. The Otakura spring system is also highly modified and is integrated with the agricultural drainage network. The main Otakura Stream channel (Figure A5.3) is fed by the Moroa water race at the northern end on Cross Line. Any groundwater gains downstream can thereby be attributed to groundwater inflow. During summer, it appears that there are no gains from groundwater and that the very small flows observed at the Otakura Stream weir of 30–50 L/s are entirely water race-derived. During summer, groundwater seepage may be strongly influenced by evapotranspiration and, although no flow is measured, there is probably a portion which is evaporated.

The other major spring discharge on the Tauherenikau fan is associated with the Stonestead (Docks) Creek system which is closely linked to the Tauherenikau River and discharge at a consistent 600–800 L/sec (as discussed previously). There is relatively sparse information on the Donalds/Abbotts creek system around Featherstone but some of the measured flows are regarded to be groundwater discharge from the fan alluvium. Spot gauging data suggest that the total summer base flow is in the order of 50–100 L/s. The total spring discharge on the Tauherenickau fan (Stonestead-Docks, Abbots and Otakura systems) may therefore approach 70,000–90,000 m^3 on an average daily basis (800–1000 L/sec).

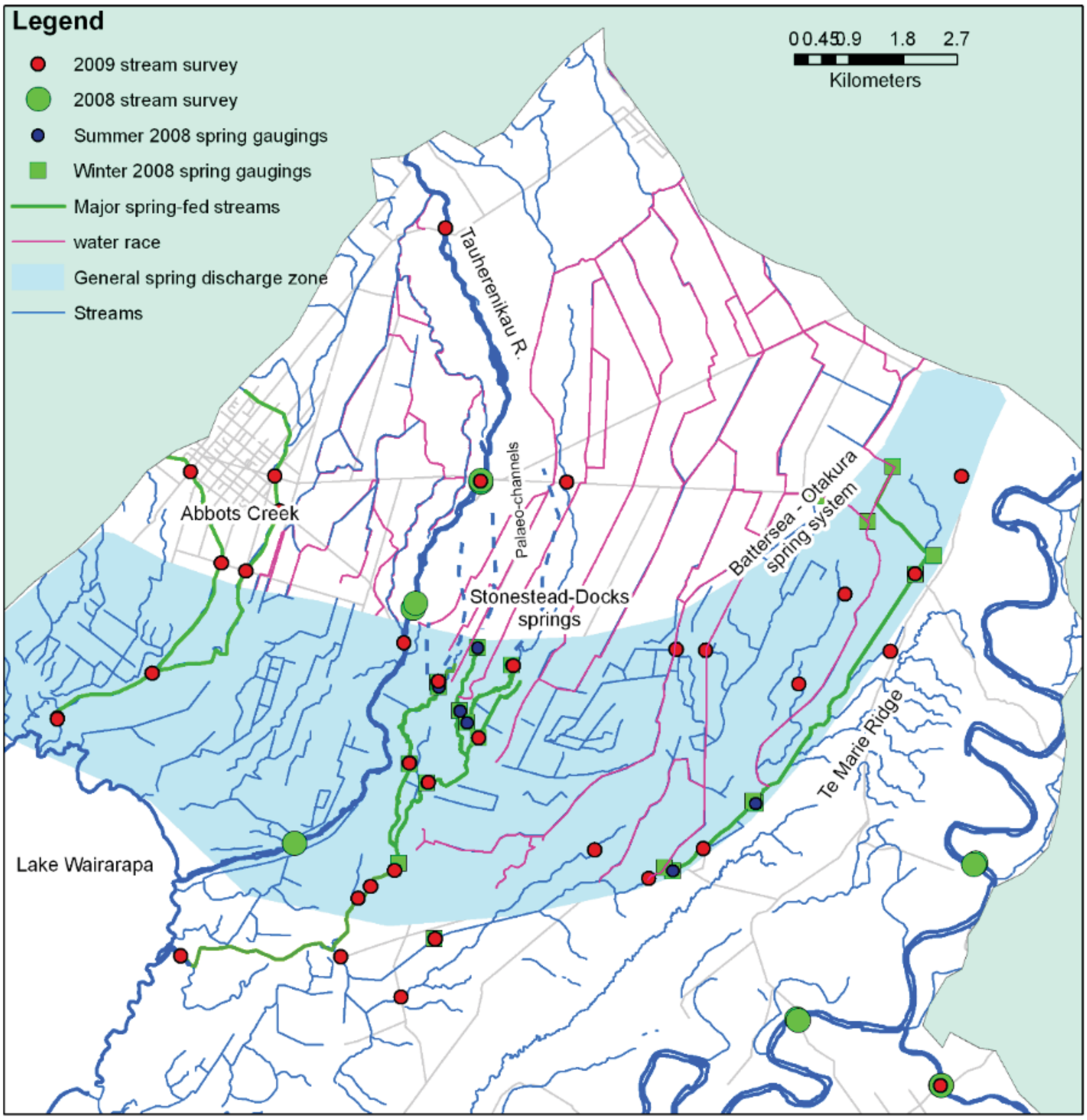

Figure A5.3 Groundwater discharge on the Tauherenikau fan — locations of stream and spring surveys, principal spring-fed streams and general groundwater discharge zone are shown. From Gyopari and McAlister (2010c).

A5.1.4 Lake Wairarapa

Very little information exists (other than anecdotal) with which to characterise the connection between Lake Wairarapa and groundwater. Conceptually, the lake is envisaged to receive groundwater inflow from the shallow Tauherenikau fan deposits and from groundwater stored in the superficial deposits around the lake; or from agricultural drains which are used to manage the water table in former lake margin wetland areas. Whether there is input from deep confined aquifers via seepage or discreet springs is unknown, although there are anecdotal reports of spring up-wellings in the lake bed. Piezometric contour lines for deeper aquifers in the lake basin converge on the lake (Figure A4.10) suggesting that there must be discharge from the deep aquifers (most probably as diffuse leakage) into the lake. Because the lake level is managed at the barrage and surface water inflows into the lake (principally the Tauherenikau River) and out of the lake have not be gauged, it is not possible to undertake water balance calculations for the lake at this time. The groundwater flow model has however proven very useful in terms of determining the functioning of the lake as a regional groundwater sink.

A5.2 NORTHERN FLOW SYSTEM – CONNECTED SURFACE WATER ENVIRONMENTS

Groundwater-surface interactions are described below for two sub areas in the in the Northern Flow System – the Upper and Middle valley catchments. These relate to the previous FEFLOW model areas (Gyopari and McAlister, 2010a, 2010b and 2010c) and refer to the area to the north of the Waingawa River (Upper Valley) and between the Waingawa River the boundary between the Northern and Southern Flow System (Middle Valley).

A5.2.1 Upper Valley Catchment Area

The principal surface water environments which exhibit complex interactions with groundwater are:

- Ruamāhanga River
- Waipoua River
- Waingawa River
- Spring discharge zones around Masterton and on the Te Ore Ore plains.

The Whangaehu and Kopuaranga rivers may also interact with groundwater although very little gauging information is available with which to characterise these systems.

Concurrent gauging surveys were carried out between 2006 and 2008 to characterise the loss and gain patterns of the rivers in this area. Figure A5.4 shows the locations of the gauge sites and the loss gain patterns identified during the surveys. Full details of which are documented in Gyopari and McAlister (2010a and 2010b).

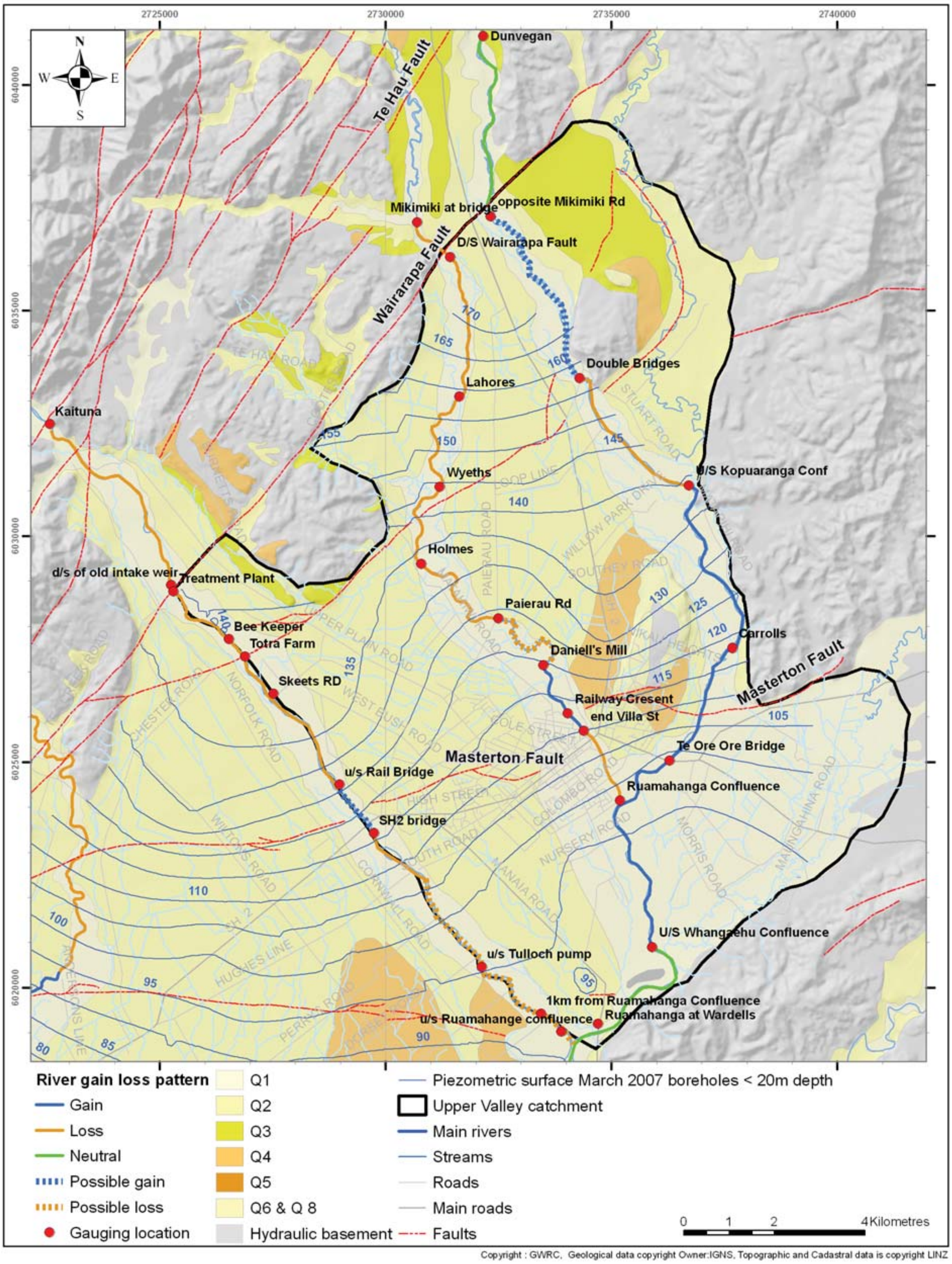

Figure A5.4 Summary of concurrent gauging data showing recognised river gain-loss patterns for the 'upper valley' catchment area of the Northern Flow System (north of the Waingawa River). Groundwater levels contours for March 2007 also shown (in metres above mean sea level). From Gyopari and McAlister (2010a).

A5.2.1.1 Ruamāhanga River

Figure A5.5 shows the results of three concurrent gauging surveys on the Ruamāhanga River between Mt Bruce and Wardells in February 2006, March 2006 and February 2007. The data show a complex and consistent pattern of flow losses and gains around the major fault systems. Flows appear constant above the Mokonui Fault, with a possible small gain before the fault of 3–400 L/s (March 2006). All three gauging runs indicate that there is a large loss of flow to groundwater (in the order of 1,000 L/s) immediately downstream of the fault. The flow pattern is consistent with the conceptual hydrogeological model which proposes a large uplift on the upstream side of the fault forcing groundwater discharge, and sudden thickening of the aquifer sequence on the downstream side creating conducive recharge conditions. From the Mokonui Fault there is a gradual increase in flow due to groundwater discharge. In February 2006, the gain between the Mokonui Fault and the Waingawa River confluence was measured at about 1,200 L/s. The other gaugings show a similar magnitude of gain. The Masterton Fault does not seem to impact the gaining pattern.

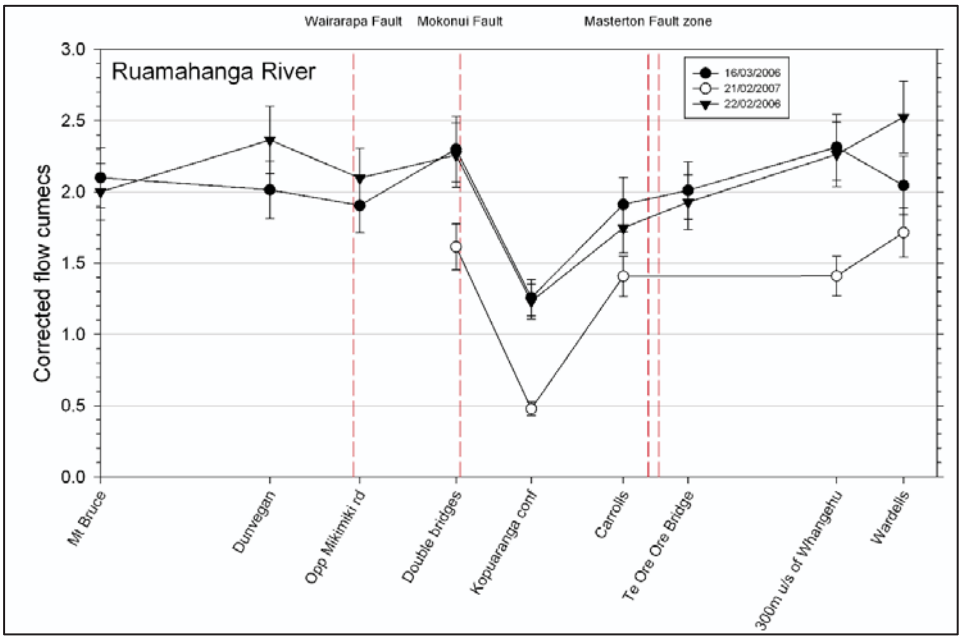

Figure A5.5 Concurrent flow gauging surveys on the Waingawa River.

A5.2.1.2 Waipoua River

This river has a complex pattern of losing and gaining reaches that appear to be controlled by the Mokonui and Masterton faults. The river gains water upstream of the faults and after crossing the fault traces water is lost to groundwater. There is a gradual flow loss to groundwater between the Wairarapa Fault and just upstream of the Masterton Fault where, in some years, the river can be dry. The magnitude of loss over this reach is about 150–300 L/s (Figure A5.6). A distinct gain in flow from groundwater in the order of 100–200 L/s occurs upstream of the Masterton Fault, followed by a flow loss in the reach down to the Ruamāhanga River confluence of about the same magnitude. This gain-loss pattern across the Masterton Fault mirrors the effect the Mokonui Fault has on the Ruamāhanga River. It is also consistent with the conceptual hydrogeological model of aquifer thinning upstream of the fault. Such thinning forces groundwater discharge and the rapid thickening of the younger sediment sequence on the downgradient side of the fault resulting in flow losses to the aquifer.

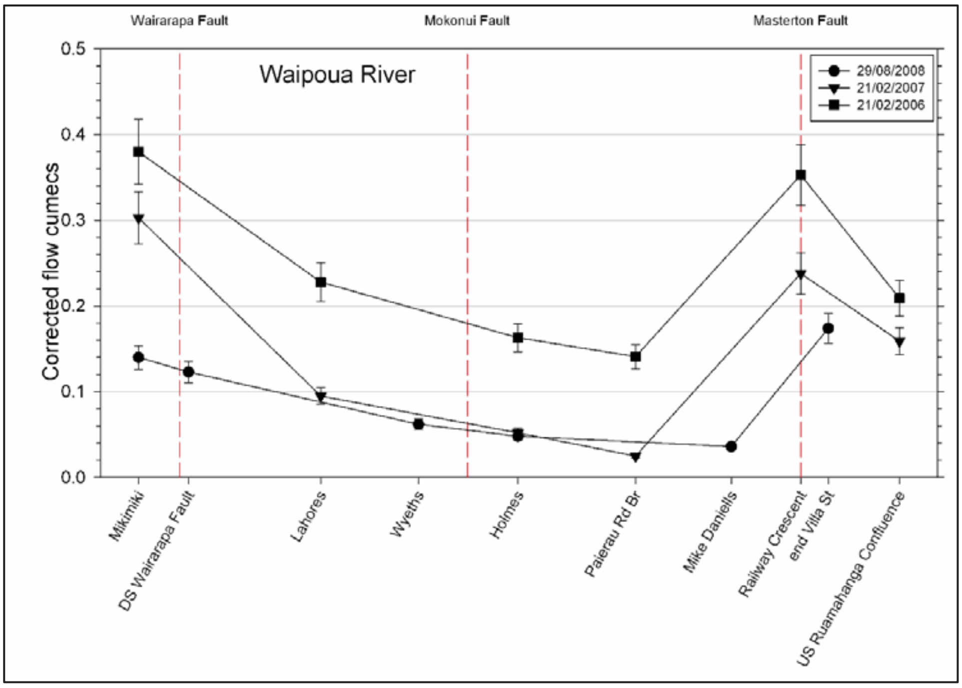

Figure A5.6 Concurrent flow gauging surveys on the Waipoua River.

A5.2.1.3 Waingawa River

Three distinct loosing and gaining reaches were identified on this river. The river loses water from the Gorge to Railway bridge, which is just below the Masterton Fault trace. Flow is then steady until the river crosses the Masterton fault, at which point it begins to lose water and continues to do so until the confluence with the Ruamāhanga River. Three concurrent gauging runs made during February 2006, 2007 and 2008 (Figure A5.7) indicate that the Waingawa River characteristically loses flow to groundwater over much of its length. The gaugings show a loss of up to about 800 L/sec but the rate of loss is highly dependent upon river stage and groundwater level conditions.

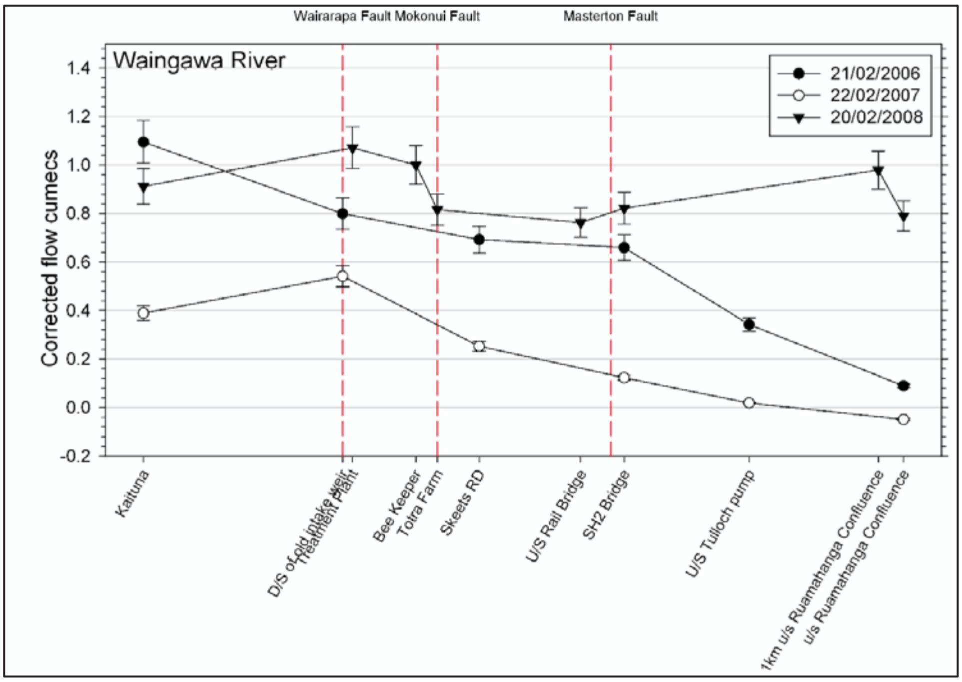

Figure A5.7 Concurrent flow gauging surveys on the Waingawa River.

A5.2.1.4 Spring discharges — Upper Valley area

Numerous springs emerge in the low-lying areas of the Upper Valley area of the Northern Flow System, in particular on the Te Ore Ore plain and in the Masterton area around the Masterton Fault. These areas were probably once extensive wetlands. They are now drained and a discreet network of spring-fed channels is all that remains. Figure A5.8 shows the locations of identified spring discharges in this area.

Masterton springs

The Masterton springs comprise an extensive channel network occupying the area between the Masterton Fault, Ruamāhanga River and Waingawa River (Figure A5.8). Many of the springs emerge around the Masterton Fault which appears to impede the flow of groundwater from the upstream alluvial fans and forcing it to the surface. The springs also seem to be associated with palaeochannels of the Waingawa River formed when it flowed through the Masterton area.

The Masterton springs comprise three main channel ‘arms’ – termed the Makoura, Kuripuni and Solway (Figure A5.8). In general flow in the springs tends to decrease with distance from the Waipoua River. The spring flows have been characterised using a series of summer gauging surveys carried out in the late 1970s and in 1981. Channel flow is sustained by groundwater discharge during dry periods but also via a surface water runoff component. The total summer measured flows from the spring channels is in the order of 150–200 L/s. Winter flow characteristics are difficult to ascertain due to the lack of gauging data and the influence of storm water runoff to the spring channels.

Poterau springs — Te Ore Ore plains

The Poterau Stream flows across the Te Ore Ore plain (Figure A5.8) and is spring-fed from an underlying gravel aquifer. The stream is located along a geological boundary between silt-rich alluvium sourced from the Whangaehu catchment and more gravel-rich alluvium associated with the Ruamāhanga River. Flows are highly seasonal with negligible flow occurring during the summer months. There has been a noticeable decrease in summer flows in recent years which may be due to increased groundwater abstraction for irrigation.

Flow in the Poterau Stream at the Whangaehu River confluence was gauged in March 2008 (17 L/s) and again in August 2008 (405 L/s). The Poterau seepage face during summer appears to be 400 to 550 m downstream of Morris Road. During winter, most flow gain occurs below Morris Road, with less than about 50 L/s inflow occurring above this point. The seepage face during winter was expected to be 250 to 300 m upstream of Watsons Road.

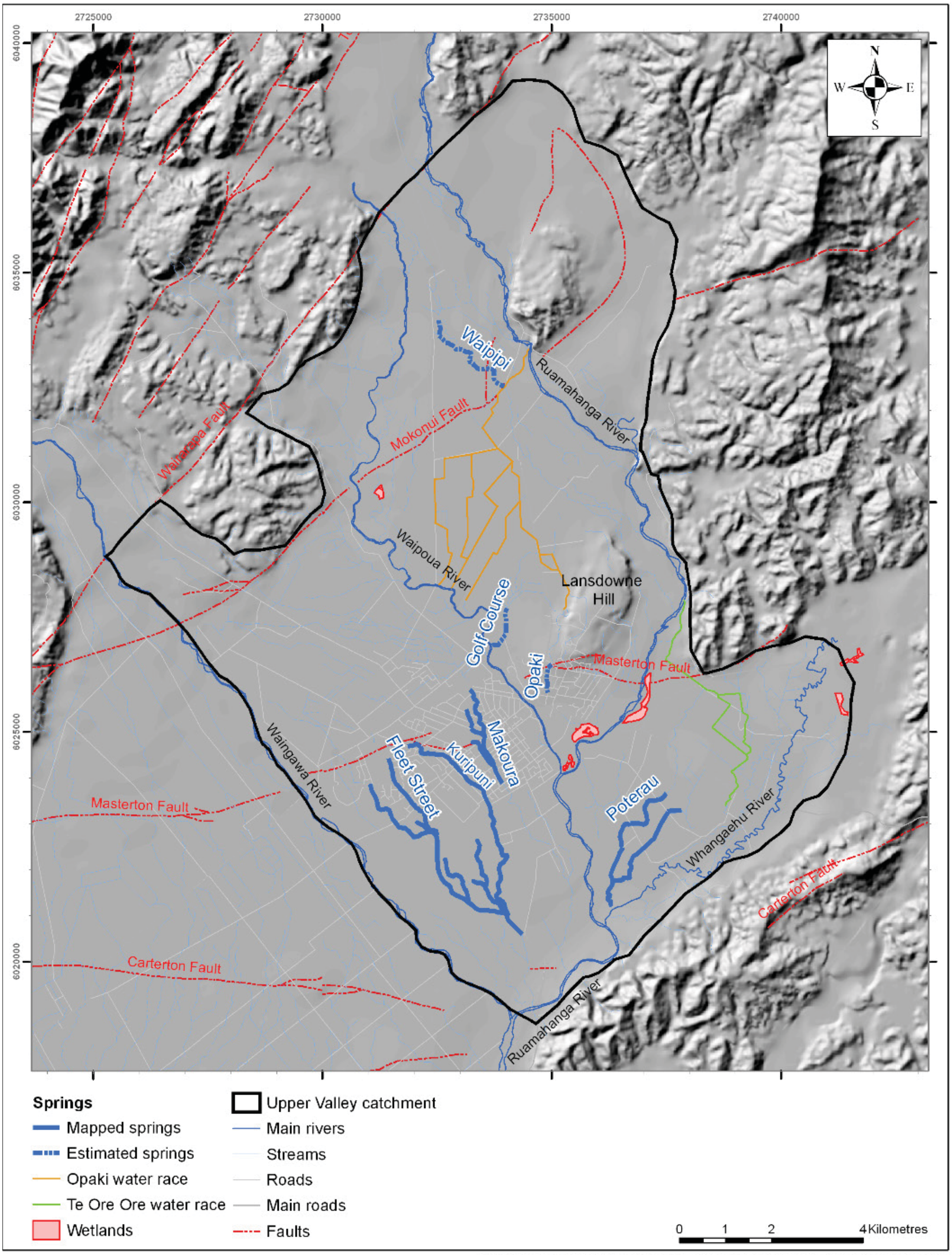

Figure A5.8 Spring discharges, wetlands and water races in the Upper Valley area of the Northern Flow System (Gyopari and McAlister, 2010a).

A5.2.2 Middle Valley Catchment Area

The principal surface water environments which exhibit complex interactions with groundwater are:

- Ruamāhanga River
- Waiohine River
- Mangatarere Stream
- Springs (Parkvale, Beef Creek/Enaki system, Papawai-Tilsons system, faultline springs, Otakura system).
- Water races (may recharge groundwater and receive groundwater discharge).

Concurrent gauging surveys were carried out between 2006 and 2008 to characterise the loss and gain patterns of the rivers in this area. Figure A 5.9 shows the locations of the gauge sites and the loss gain patterns identified during the surveys. Full details of which are documented in Gyopari and McAlister (2010a and 2010b).

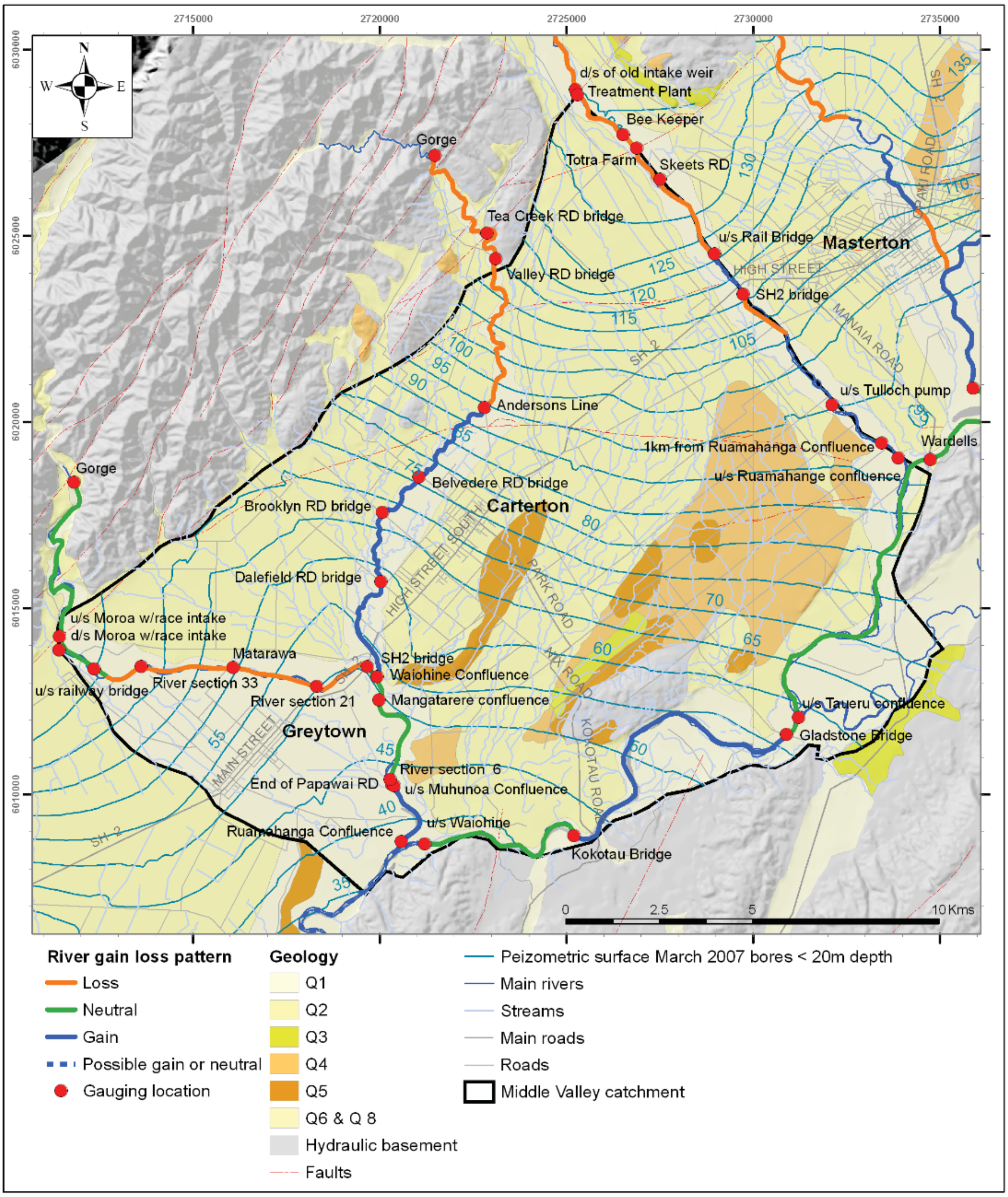

Figure A 5.9 Summary of concurrent gauging data showing recognised river gain-loss patterns for the 'middle valley catchment' of the Northern Flow System (south of the Waingawa River). Groundwater levels contours for March 2007 also shown (in metres above mean sea level). From Gyopari and McAlister (2010b)

A5.2.2.1 Waiohine River

Numerous concurrent gauging runs on the Waiohine River in 1981, 2006 and 2007 (Figure A 5.10) show a losing stretch of river between the Railway bridge and the SH2 bridge (upstream from the confluence with the Mangatarere Stream). The loss is in the order of 0.5 to 1.5 m^3/s during summer low flow conditions. This losing stretch of river coincides with the river passing over highly permeable Q1 gravels and aquifers associated with the Waiohine plain.

Supplementary gauging data (see Gyopari and McAlister, 2010b) shows that the Waiohine River loses flow to groundwater up until the flow (measured at the Gorge and SH2) reaches about 8 m^3/s. Above this, it appears that the river begins to gain flow from groundwater (during winter conditions when groundwater levels are higher). The river is neutral between SH2 bridge and the confluence of the Muhunoa Stream. No significant groundwater discharges from either the Carterton or Parkvale aquifers are evident from gauging data along this stretch of the Waiohine River. Most of the water lost from the upper stretches of the Waiohine River migrates through the highly permeable aquifers in the Greytown area and emerges as discharge at the Greytown area springs. This is substantiated by hydrochemistry data presented in Section 8 of this report.

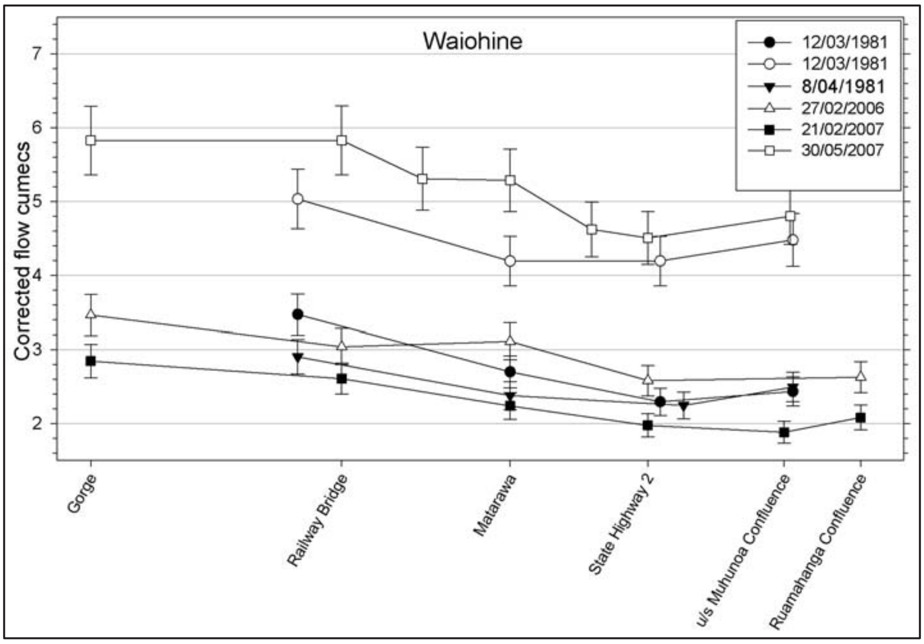

Figure A 5.10 Corrected concurrent gauging plots for the Waiohine River. Where possible, estimated major surface inputs and outputs have been excluded to gain and loss from adjacent groundwater systems.

A5.2.2.2 Mangatarere Stream

Like many Tararua-sourced easterly flowing rivers and streams in the Wairarapa, the Mangatarere Stream loses water in its upper reaches as it travels across the upper parts of the Waingawa alluvial fan. The gauged loss is up to about 0.15 m^3/s between the Valley Road Bridge and Andersons Line (Figure A5.11). In some dry summers the stream is known to dry up completely around Andersons Line but flow is usually permanent below the Belvedere Road Bridge. The Mangatarere Stream and its major tributaries (Beef Creek, Enaki Stream and Kaipaitangata Stream) gain from groundwater in the lower half of the catchment between Andersons Line and Belvedere Road Bridge. The Mangatarere gains up to 0.25 m^3/s over this lower stretch of stream to the confluence with the Waiohine River.

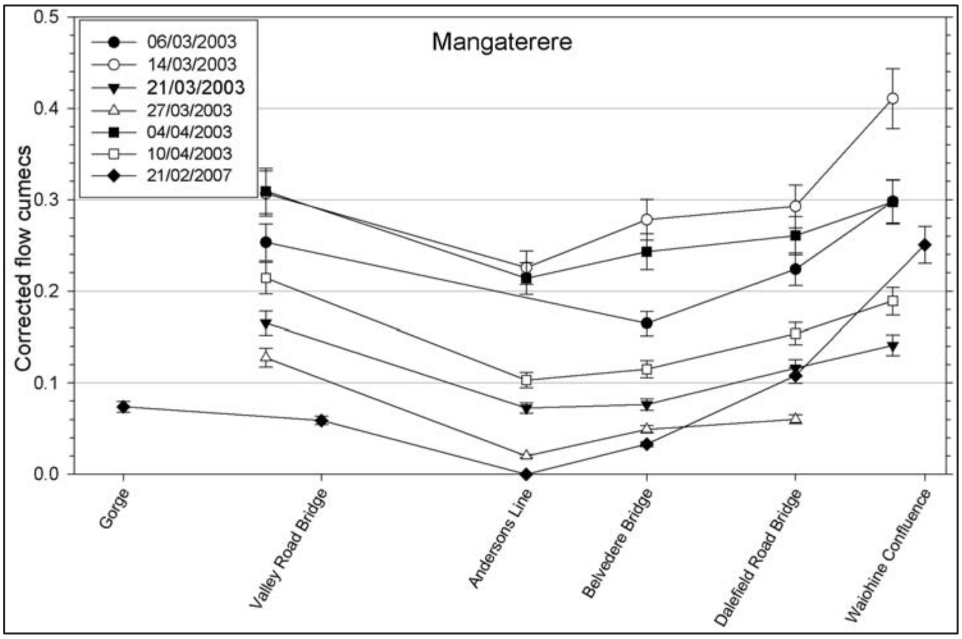

Figure A5.11 Corrected concurrent gauging plots for the Mangatarere Stream.

A5.2.2.3 Ruamāhanga River

The relatively large rates of flow in this river (mean annual low flow = 2.7 m3/s) means that it only possible to detect general losing and gaining patterns given the standard gauging error of +/- 10%. Figure A5.12 shows that between the Waingawa River confluence and Gladstone Bridge the river neither significantly gains nor loses flow (it is 'neutral'). Between Gladstone bridge and Kokotau bridge the river gains approximately 1 m3/s of flow (during summer) from groundwater seepage. Downstream to the Waiohine River confluence, there is conflicting data from gauging indicating this stretch of river is either neutral or gains over 1 m3/s during summer.

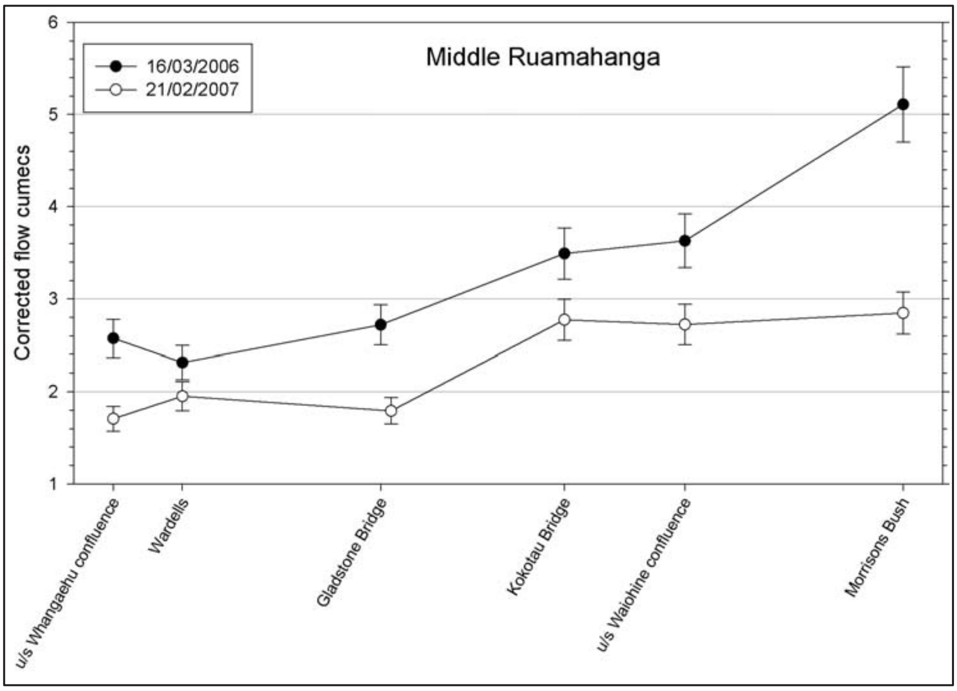

Figure A5.12 Corrected concurrent gauging plots for the Ruamāhanga River.

A5.2.3 Spring Discharges — Middle Valley Area

There is considerable interaction between "natural" spring-fed streams and the artificial water race systems in this area. Although this interaction often makes it difficult to accurately quantify natural flows from groundwater discharge, distinct areas of groundwater discharge areas are shown on Figure A5.13. Table A5.1 shows the estimated flows from the identified spring systems.

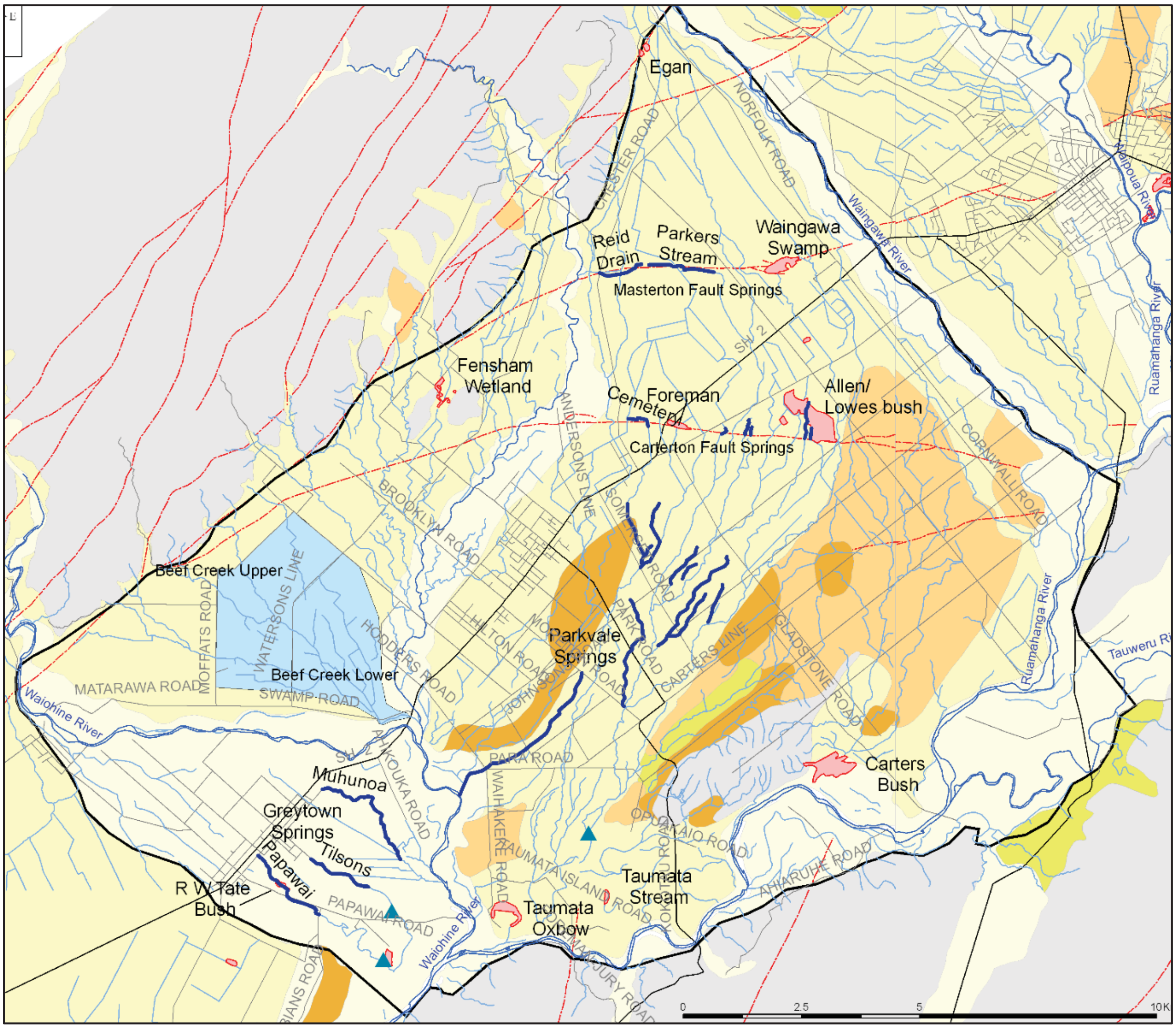

Figure A5.13 Main spring and wetland systems and water races in the middle valley catchment of the Northern Flow System. Heavy blue lies — spring-fed streams; shaded light blue area — widespread spring discharge (Beef Creek system), shaded red area spring-fed wetlands (source: Gyopari and McAlister 2010b)

Table A5.1 Estimated spring flows — Middle Valley catchment.

Location	Mean annual flow (L/s)	Mean annual low flow (L/s)
Papawai Stream	380	200**
Tilsons Creek	235	140
Muhunoa Stream	800	550
Masterton Fault*	120	30
Carterton Fault*	110	230
Parkvale Springs*	70	150
Beef Creek	1,900	60

* Approximations based upon very limited data

** From Keenan (2009)

A5.2.3.1 Greytown springs (Papawai, Tilsons, Muhunoa)

Substantial quantities of groundwater discharge into the roughly parallel Papawai, Tilsons and Muhunoa streams from the shallow alluvial aquifers on the Greytown–Waiohine plain (Figure A5.13). The combined mean outflow from this spring system is estimated to be in the order of 1.5 m^3/s (1,500 L/s). The springs flow to the southeast and discharge either into the Waiohine River (Muhunoa Stream) or Ruamāhanga River (Papawai Stream and Tilsons Creek). The flow characteristics of the Papawai Stream and Tilsons Creek are provided by a recent instream flow assessment for the Papawai Stream (Keenan, 2009).

A5.2.3.2 Parkvale springs

Groundwater discharge in the Parkvale area occurs along drainage systems rather than as discrete springs. These spring-fed streams merge with the Taratahi Water Race system making it difficult to quantify spring flow. The mean flow for the entire Parkvale spring system has been estimated to be about 150 L/s. Flow has been continuously monitored at the outflow of the Parkvale Stream system since January 2002 but represents a combination of spring discharge and flow in the Taratahi Water Race.

A5.2.3.3 Masterton and Carterton fault springs

Figure A5.13 shows the locations of the principal spring discharges associated with the Masterton and Carterton faults. The fault structures create topographic breaks and appear to impede the flow of groundwater in some areas resulting in the emergence of springs along the fault traces. There is very limited information regarding the flow rates from these springs but estimates have been made using historic spot gauging data and visual flow estimates (Table A5.1).

A5.2.3.4 Beef Creek, Enaki and Kaipaitangata diffuse springs

Widespread, diffuse spring discharges occur towards the base of Waiohine–Mangatarere fan system west of Carterton. The principal base flow-dominated streams here are the lower reaches of Beef Creek and the Enaki and Kaipaitangata streams. The lower reaches of these streams, prior to discharging into the Mangatarere Stream, appear to be the main discharge zones.

Flow in Beef Creek at SH 2 was measured at 60 L/s and 1,880 L/s for March and August 2008 respectively. Another spot gauging on Beef Creek at SH 2 in February 2005 provided a flow of 97 L/s. During winter, the creek gains by over 1,000 L/s between Jervois Road and Watersons Line.

A5.2.4 Wetlands

Two types of wetland occur within the Middle Valley catchment – those associated with spring discharge zones along faults and riparian wetlands which are associated with the main river channel systems. Figure A5.13 shows the locations of the principal wetland systems. Spring-fed wetlands include the Waingawa Swamp on the Masterton Fault, and Lowes/Allen's Bush (on the Carterton Fault). Linear wetland systems occur along the lengths of both faults.

A6.0 CONCEPTUAL HYDROGEOLOGICAL MODEL

A6.1 PURPOSE

The numerical groundwater modelling process draws together large quantities of data from different sources from which a conceptual interpretation for a groundwater system is developed. This conceptual framework is subsequently translated into a quantitative numerical model relying upon the hydrogeological analysis to build and calibrate the model under a range of climatic conditions. Emphasis has therefore been placed on producing a sound and realistic conceptualisation of the groundwater system as a basis for numerical analysis.

The Murray Darling Basin Commission (MDBC) modelling guidelines (Middlemis, 2001) provide the following guidance on the purpose, form and significance of a conceptual model:

- Development of a valid conceptual model is the most important step in a computer modelling study.
- The conceptual model is a simplified representation of the essential features of the physical hydrogeological system and its hydrogeological behaviour, to an adequate degree of detail.
- Conceptual models are subject to simplifying assumptions which are required because a complete reconstruction of the field system is not feasible, and because there is rarely sufficient data to completely describe the system in comprehensive detail.
- The conceptualisation is developed using the principle of parsimony such that the model is as simple as possible while retaining sufficient complexity to adequately represent the physical elements of the system and to reproduce system behaviour.

The conceptual hydrogeological model has been tailored to ensure it can adequately address key modelling objectives.

A6.2 CONCEPTUAL FRAMEWORK SUMMARY

The Wairarapa Valley is a structurally controlled basin containing an accumulation of alluvial fan sequences built up by the Ruamāhanga River and its main tributaries – the Waingawa, Waiohine, Waipoua and Tauherenikau rivers. In the subsiding lower valley beneath Lake Wairarapa, substantial thicknesses of Recent (Holocene) marine and estuarine deposits have also accumulated. The groundwater basin structure is dominated by the major intra-basin cross-cutting faults, such as the Masterton Fault, which have tilted and folded older less permeable sediment sequences (‘groundwater basement’) towards the surface, thus impeding or blocking the flow of groundwater in some areas. Uplift and subsidence processes have also created groundwater sub-basins such as Te Ore Ore, Parkvale, and the rapidly subsiding lower valley basin beneath Lake Wairarapa. Uplift of the coastal area has isolated the groundwater basin from the sea. Geological structures have also caused blocks of older less permeable sediments and basement greywacke to be upthrown and placed against younger water-bearing strata in some areas (e.g., Te Marie Ridge, Tiffen Hill, Lansdown Hill).

Late Quaternary sediments fill the upper levels of the basin to depths of between <10 m and about 100 m, the average thickness being about 50 m. The top of the Middle Quaternary deposits (mQa) is assumed to be the base of the groundwater flow system. Formations beneath the top of mQa are regarded to be largely isolated from the shallower actively recharged system since they are more compact and, because of their general lithological nature, are likely to be of significantly lower permeability.

The sediments within the active groundwater system, are highly heterogeneous and exhibit large variations in hydraulic conductivity, depending upon the lithological characteristics, specifically: grain size characteristics, gravel matrix composition, degree of sediment sorting/reworking, and degree of compaction. Broad patterns of hydraulic conductivity are recognisable on a regional scale relating to depositional environments. Gravel-rich aquifers exhibiting enhanced formation transmissivities due to better sediment sorting and reworking occur around the modern-day channels of major drainage systems where there is a strong groundwater-surface water interaction, and in distal fan and sub-basin areas. These highly conductive sediments support the large-volume groundwater abstractions in the Wairarapa.

On a regional scale, the Wairarapa Valley basin contains an unconfined to leaky-confined aquifer system with greater degrees of confinement occurring at depth within the sub- basins. The regional aquifer system is internally ‘compartmentalised’ by geological structures that have facilitated the development of flow barriers and sub-basins. The Wairarapa Valley groundwater basin is ultimately ‘closed’ in that all groundwater is forced to discharge to the surface water environment and there is no significant groundwater connection to the sea.

A6.3 Hydrostratigraphic Units and Connectivity to Surface Water Environment

Table A6.1 lists the principal recognised hydrostratigraphic units identified in the Wairarapa Valley together with the perceived nature of their connectivity with the surface water environment. The distribution geometry and hydraulic properties of these units has been modelled using geological information (mapping and bore log interpretation and cross section construction – see Figure A4.2), bore yield and pumping test analyses.

A6.4 Groundwater Flow and Identification Sub-Regional Flow Systems

A southerly to south-westerly regional groundwater flow pattern (Figure A4.10) generally reflects topography and is strongly influenced by the main river systems depending upon whether groundwater discharges to them (flow lines converge on the river), or whether the river recharges groundwater (flow lines diverge from the rivers). General groundwater level patterns suggest a single leaky or interconnected aquifer system. In the lower valley area, around Lake Wairarapa and downstream of the Tauherenikau fan, a prominent flattening of the piezometric gradient is evident. The groundwater level contours show that regional flow is focused on the area beneath the lake, and that the lower valley system is a ‘closed basin’. Geological controls mean that there is minimal connection between the groundwater system and the sea and there is no (or only minor) offshore flow.

Internally, the regional groundwater basin can be divided into two sub-regional flow systems. A groundwater and surface water flow divide occurs along the southern edge of the Waoihine plains (Figure A4.10) separating a ‘Northern Flow System’ (425 km^2). and a larger ‘Southern Flow System’ (680 km^2). Although this is not a physical barrier to the movement of groundwater, regional flows do not cross this line – all groundwater in the northern area discharges to surface water and ultimately the Ruamāhanga River – prior to entering the southern area. The two groundwater flow systems can essentially be regarded as independent, and closed (i.e., groundwater must exit via surface water within each flow system).

Table A6.1 Modelled hydrostratigraphic units of the Wairarapa Valley and nature of connectivity to the surface water environment.

Unit	Distribution	Physical characteristics	Nature of surface water/groundwater interaction
Alluvial fans (Q2–Q8)	Alluvial fans extending from the Tararua foothills associated with the Waipoua, Ruamāhanga, Waiohine Tauherenikau rivers and Mangatarere Stream.	Poorly sorted alluvial gravels in a silt-rich matrix which form moderate to low permeability stratified unconfined to semi-confined aquifers.	Alluvial fan aquifers provide a significant contribution to baseflow discharge in lower catchment areas via throughflow into Q1 gravel aquifers. Some local discharge to spring-fed streams in mid to lower fan areas and adjacent to faults. Potential for groundwater abstraction along outer margin of Q1 gravels to result in direct stream depletion effects on main rivers as well as localised effects on spring-fed streams and wetlands. Abstraction from alluvial fan aquifers also has the potential to contribute to cumulative reduction in baseflow discharge at a catchment scale.
Recent alluvial gravels (Q1)	Recent floodplains of the major river systems.	Shallow, highly permeable unconfined aquifers exhibiting a high degree of connectivity with surface water.	Extensive interaction with main river systems. Significant flow loss to groundwater in upper reaches with discharge back to lower reaches including in some areas extensive spring-fed stream systems. Potential for groundwater abstraction to result in significant stream depletion effects on main stem rivers and spring-fed streams.
Alluvial sub-basins (Q6–Q8)	Te Ore Ore, Parkvale, Carterton, Lake and Onoke sub-basins.	Moderately permeable water bearing gravel units interspersed with lower permeability sand silt deposits forming a sequence of semi-confined aquifers.	Limited direct interaction with surface water. However, groundwater abstraction from semi-confined aquifers may induce vertical leakage from overlying unconfined aquifers and ultimately contribute to cumulative reduction in baseflow discharge.
Ruamāhanga valley (Q1–Q2)	Narrow, elongate river valley extending from Opaki to the Lake Wairarapa basin.	Shallow moderate to high permeability unconfined aquifer system exhibiting high degree of connectivity with surface water.	Extensive interaction with surface water with flow loss/gain occurring according to relative river stage and groundwater levels. Potential for groundwater abstraction to result in direct depletion of river flow.
Lake Wairarapa basin	Lower Wairarapa Valley area south of Featherston.	Extensive confined aquifer system consisting of water bearing alluvial gravel layers associated with the Ruamāhanga River or Tauherenikau fan separated by thick silt aquitards.	Limited interaction with surface water.

This page left blank on purpose.

A6.5 CONCEPTUAL AND ESTIMATED WATER BALANCES

It is useful to independently calculate the water balance for the flow systems to provide a high-level check on the veracity of modelled balances. Even though such calculations are inherently very broad-brush, they provide an order of magnitude estimate of the different fluxes into and out of the system.

The conceptual components of the regional water balance for the Wairarapa groundwater basin are as follows:

- Inputs:
  - rainfall recharge;
  - runoff recharge — surface water inflow from rivers, streams, water races;
  - irrigation returns.
- Outputs:
  - groundwater discharge into river beds, streams, water races;
  - diffuse seepage to wetlands and evapotranspiration losses;
  - spring flow;
  - abstraction from bores.

It has been possible to calculate an independent 'steady state' water balance to provide a basic 'order of magnitude' assessment of the various system inflows and outflows. This provides a valuable check on the numerical model flow balance predictions. Table A6.2 and Table A6.3 contain the estimated water balances for the Northern and Southern Flow Systems respectively. The fluxes through the Southern Flow System, although larger in area, are significantly smaller than the Northern Flow System because much of the area is occupied by Lake Wairarapa (80 km^2) and lower valley confining layers which isolate the underlying confined artesian aquifers.

Table A6.2 Estimated steady state water balance for the Northern groundwater flow system.

Water balance component	In (m3/day)	Out (m3/day)
Rainfall recharge	450,000	
River flow loss/groundwater recharge	240,000	
Water race loss	30,000	
River flow gain/ groundwater discharge		520,000
Springs and diffuse evapotranspiration		140,000
Abstraction		60,000
Total	*720,000*	720,000

Table A6.3 Estimated steady state water balance for the Southern groundwater flow system.

Water balance component	In (m^3/day	Out (m^3/day)
Rainfall recharge	540,000	
River flow loss/groundwater recharge	210,000	
Water race recharge (Moroa)	10,000	
River flow gain/groundwater discharge		300,000
Springs and diffuse evapotranspiration from water table		300,000
Abstraction		60,000
Lake Wairarapa discharge (and Onoke)		100,000
Totals	760,000	760,000

The sources of the various balance quantities presented in Table A6.2 and Table A6.3 are as follows:

- Rainfall recharge: based upon average annual rainfall of the sub-areas (Northern Flow System: 1200 mm; Southern Flow System: 1100 mm) and assuming 30% of the rainfall over each area becomes rainfall recharge. The recharge area for the Northern Flow System is 425 km^2 and for the Southern Flow System is 600 km^2 (excluding the lakes).
- River inflow: concurrent gaugings average values.
- River discharge: concurrent gauging data.
- Springs/evapotranspiration (ET): combination of gauging data and balance differential.
- Abstraction: 60% of consented abstraction.
- Water race loss: estimated to be 25% of consented race take.

Bearing in mind the limitations of the estimated equilibrium water balances, it is interesting to note that rainfall recharge dominates the inflow to the groundwater system and is significantly higher than river leakage. The Southern Flow System has significantly less rainfall recharge (even though is a much larger area than the Northern Flow System) because much of the lower valley lake area has a very low permeability aquitard near to the surface and underlying aquifers are artesian. Discharge from the groundwater system is dominated by flows back to the surface water environment (rivers, streams and springs). Abstraction appears as a relatively minor component of the balance only because the balance calculation represents average conditions. The peak summer daily consented abstraction rates are considerably higher.

A7.0 MODEL SET UP SCRIPTS

A7.1 STREAMFLOW-ROUTING PACKAGE

The Streamflow-Routing Package (SFR) for MODFLOW defines streams based on segment and reach numbers. The North model has 110 segments, and the South model has 165 segments. Each segment has a variable number of reaches, numbered from 1 on the upstream end. Segments are linked to each other using OUTSEG. The south model links segments to the Lake Package using negative lake IDs set to OUTSEG. All stream segments calculate stream depth using Manning's equation assuming a wide rectangular channel (ICALC=1) with a roughness coefficient of 0.03 and width of 30 m.

A7.2 SFR NETWORK FOR SOUTH MODEL

The original SFR network prepared by Greater Wellington Regional Council (GWRC) had several issues, including discontinuities (where there were gaps up to 1.2 km) and implausible reaches inherited from REC2. The SFR network for the South model was redesigned by GNS Science by redrafting the stream sections from the 1:50k topographic map series (Land Information New Zealand) with guidance from the original SFR network. The SFR network for the North model was not modified, as the issues were not as severe.

The vector network of streams was converted for MODFLOW SFR using GMS 10.0.

A7.3 STREAMFLOW OBSERVATIONS

Streamflow observations were provided for the Wairarapa Valley by GWRC at over 400 locations, including 18 continuous and 5 derived locations. The majority of locations were spot measures with one or two measures on different dates. From the locations, 189 were selected to use for streamflow calibration, and the nearest MODFLOW stream segment and reach were assigned based on the site name description and spatial location.

The streamflow observations were uniquely named for PEST using a pattern: "*TSSS*r*RR*t*PPPP*", where:

- T is a single character to indicate the streamflow observation type (c=continuous, d=derived or s=spot measure type).
- SSS is the SFR segment number.
- *RR* is the SFR reach number.
- *PPPP* is the model stress period.

For example, "c029r06t0242" describes a continuous streamflow observation from stream segment 29, reach 6 at weekly stress period 242, which is 12–18 February 1997.

Weekly model stress period numbers start at on 1 July 1992, and average flows were determined using any observations within the 7-day period. Calculations were performed using SQL aggregates with data stored in a relational database management system (RDMS).

A7.4 PYTHON SCRIPTING

Data was processed using the Python programming language with several common packages, such as NumPy and H5py. Additionally, an in-house developed Python module for MODFLOW and MT3DMS was used to read and write files. This package is similar to FloPy (Bakker et al., 2016), but is simpler to adapt and expand due to in-house control.

Python scripts written by GNS Science were used for many aspects of the project, such as preparing input datasets for MODFLOW, or processing data in a PEST simulation.

A7.4.1 Data Preparation Scripts

Several data SOURCEs were converted to HDF5 file structures to enable faster array access to the raw data SOURCEs. HDF5 is a versatile data format that can store multidimensional array data which can be read much quicker than from the original text-based data SOURCE formats obtained by GNS Science.

REC2 data described daily simulated flows from the TOPNET model from the National Institute of Water and Atmospheric Research. This data originated as CSV files. The script “christain_to_h5.py” reads each of the CSV files, and stores arrays of stream flows, dates and REC2 IDs.

IRRICALC was used to determine irrigation rates, abstracted from both groundwater and surface water SOURCEs. The script “julian_GW_SW_to_h5.py” processes the text files from RAR archive files to HDF5 array files for each model. The SWPumping dataset, indexed by stream segment and reach, describe surface water extractions. The GWRC Pumping dataset, indexed by grid row and column, describe groundwater extractions from wells.

Land surface recharge and quick-flow rates were determined by GWRC for the top of the model grid. The script “julian_LSR_QKF_to_h5.py” reads these data from RAR archive files to HDF5 array files for each model as 3D grids (2D grid and time dimensions).

Each script also aggregates temporal data from daily to weekly averages (7 day), starting on 1 July 1992, which is also stored in the HDF5 file structures.

Conversion of MODFLOW/MT3D outputs for inputs to eSOURCE has a number of steps:

The catchments defined by Jacobs for their zones is "SOURCE_subcatchments_v3.shp" showing 237 polygons. And the MODFLOW SFR segment/reach are in the two files named with "*sfr_seg*", which are aligned with the structures in the MODFLOW SFR package (Data Set 2), and have a Jacobs ID that can be joined for the catchments. These two files describe the spatial correponsdance between the flow regime representation in the two respective mdoels.

The cell by cell flow terms from the MODFLOW unformatted budget file (cbb) and the cell by cell concentration terms from the MT3DMS unformatted concentration file (ucn) are then interrogated, to output CSV files for input into eSOURCE. Each csv file has daily timesteps from 1 July 1992 to 31 December 2014 (8219 values). Values are linearly interpolated if the model timestep is larger (e.g., 7 days), and extrapolated at starting and/or ending parts by simply repeating the nearest value. This makes a contestant file structure for Jacobs to process, regardless of the model's time stepping approach. Furthermore, catchments that don't intersect any SFR boundaries are filled with zeros to maintain a consistent structure.

The script processes each catchment by doing the following:

Select the cells that describe the segment, reach for the Jacobs ID

Process component flow budgets for the selected cells from the "STREAM LEAKAGE", based on the IN (positive), OUT (negative) and NET.

Multiply each cells concentration by the OUT component. This a cell-by-cell calculation where the concentration is constant (not time-varying) and the flows are transient, and provide the mass OUT.

Write a simple CSV file.

A7.4.1.1 MODFLOW File Generation Scripts

h5_to_rch.py reads the time-varying recharge on the 2D model grids, and write a MODFLOW Recharge Package (RCH) file. The option NRCHOP=3 was used to apply recharge to the highest active cell in each vertical column.

h5_to_sfr.py prepares data from several SOURCEs and produces a Streamflow-Routing Package (SFR) file. MODFLOW SFR packages index stream locations based on a segment and reach number (data set 2), found in either a Shapefile or simplified CSV SOURCE. The principle datasets this script determines is time-varying flow and runoff for each stream segment (FLOW and RUNOFF in data set 6a). Incoming stream flows are provided by TOPNET at segments identified by GWRC, with additional corrections by GNS Science and Jacobs. The segments with streamflows are generally on the perimeter of the model region. The streamflow time series in the Ruamāhanga entering the South model was synthesised by GWRC. Surface water takes from IRRICALC were subtracted from the flow reaches. Additional surface water takes were manually assigned for consented water races at constant rates, subtracted from their nearest stream segments. Runoff was determined from quick-flow to each segment, as determined by GWRC.

h5_to_wel.py prepares specified fluxes for the Well Package (WELL) file. The primary fluxes are from groundwater wells as determined by GWRC using IRRICALC. Other GWRC pumping consents were identified by John Drewry, and pump at a constant rate on 1 January of the year that was specified. Injections were also included from water races, assigned with constant rate injections.

Each of the MODFLOW generation scripts also produce a file that have average stress rates for each stress period. Additionally, the scripts were also designed to prepare a PEST template file to allow parameterization of model variables. Time-varying SOURCE datasets were also stored in high-precision CSV files for simulation scripts, were needed.

A7.4.1.2 Simulation Scripts

Several Python scripts were used within simulations to prepare or read files for PEST, MODFLOW and MT3DMS.

A7.4.1.3 Pre-processing Scripts

“rewritesfr.py” reads custom parameters of hydraulic conductivity of the streambed (HCOND), and scaling parameters for flow and runoff for each stream segment, and rewrites a new Streamflow-Routing Package (SFR) file. The scaling parameters are multiplied with a high-precision CSV copy of the time-varying flow and runoff datasets (data set 6a).

“rewritewel.py” reads scaling parameters three specified flux datasets: groundwater pumping from IRRICALC, groundwater pumping from other groundwater consents, and injection from water races. High-precision CSV copies of the time-varying stresses for the three parameter groups are used to re-assemble the rates for the Well Package (WELL) with the applied scaling parameters.

A7.4.1.4 Post-processing Scripts

"get_sfr_streamflows.py" extracts simulated streamflow rates at observation locations along streams, at specified times. This data is written to the binary Budget file, even though it consists of streamflows simulated by the Streamflow-Routing Package, and is not a budget component. This script write a text file used by PEST as instruction files to compare against observed streamflows.

"gwrc_bud2txt.py" extracts MODFLOW budget components from written to the binary output file, and writes a simplified text file for PEST to process as instruction files to compare against observed budgets. Zones are defined by rows and columns in external text files, and are used to define sections of stream locations. Net stream leakage is calculated for each zone, and budgets at specific model times are determined. Similar calculations are also determined for drain cells.

A8.0 GROUNDWATER LEVEL MODEL OUTPUTS AND MEASUREMENTS FOR MONITORING WELLS IN THE NORTH MODEL

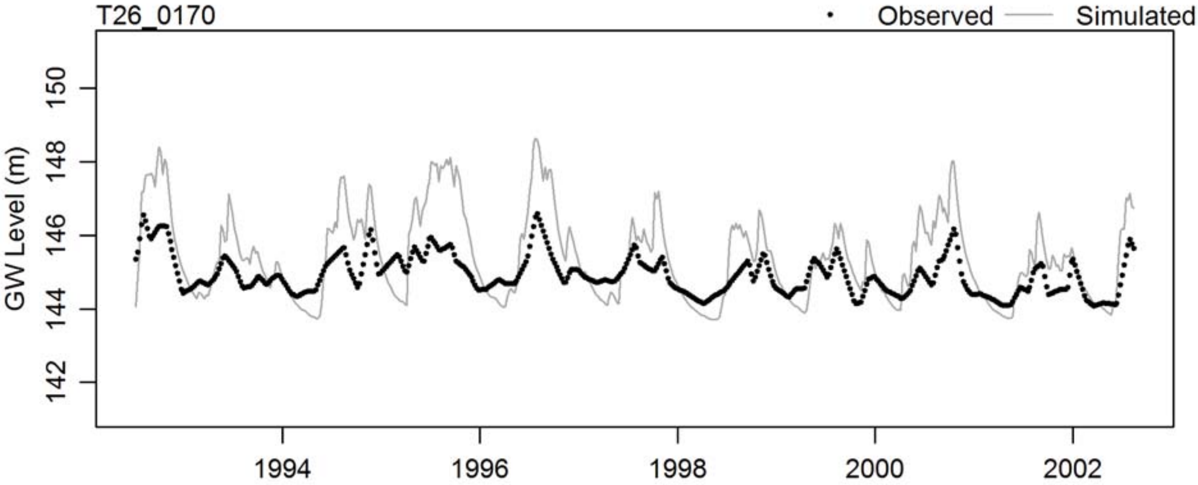

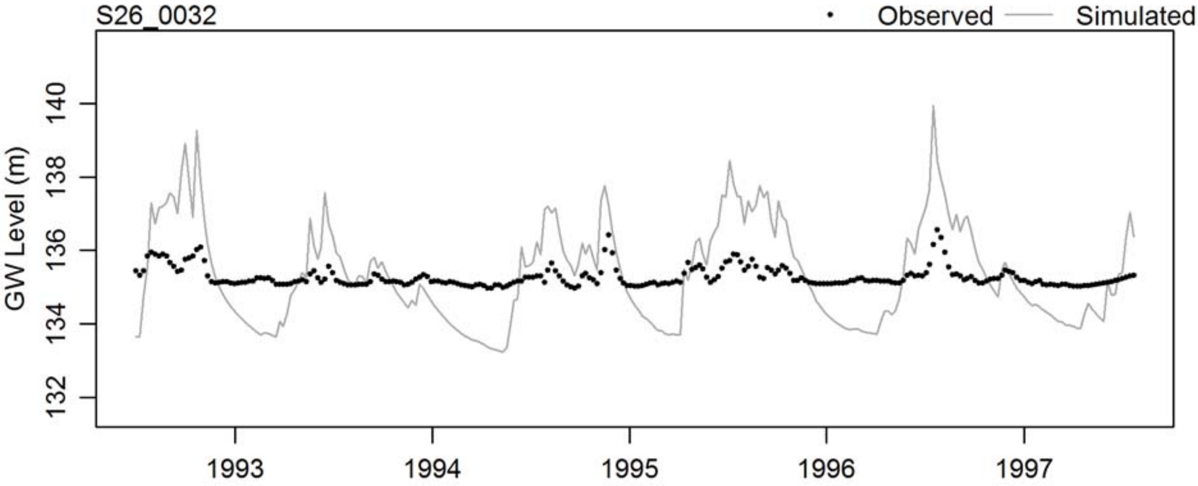

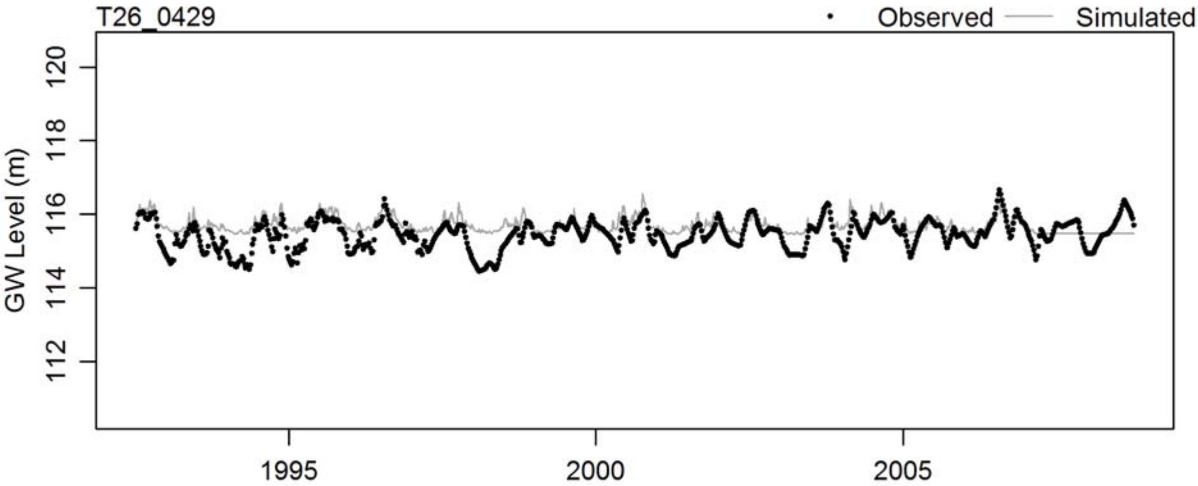

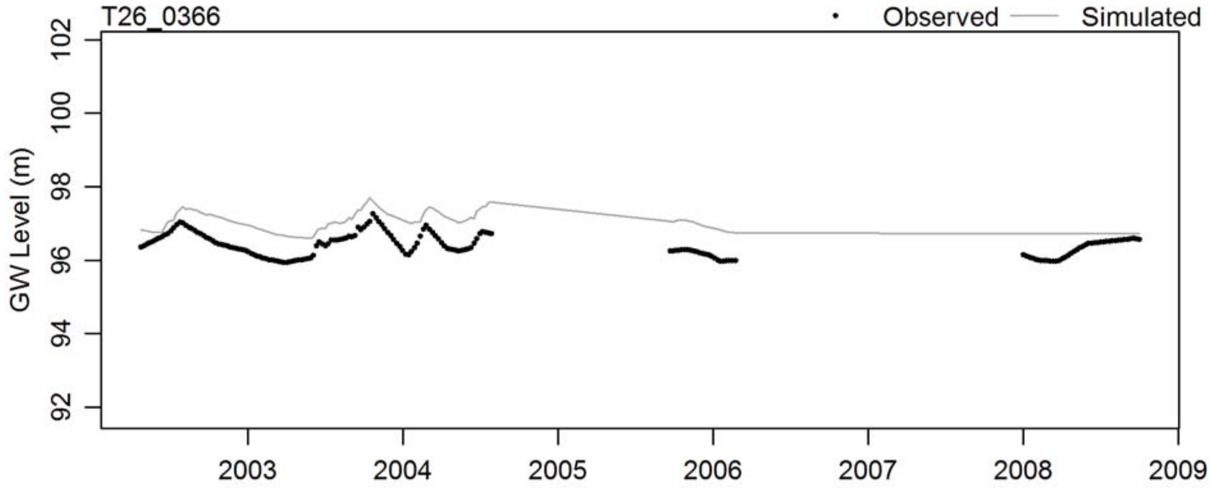
T26_0366
Observed
Simulated
GW Level (m)
102
100
98
96
94
92
2003
2004
2005
2006
2007
2008
2009

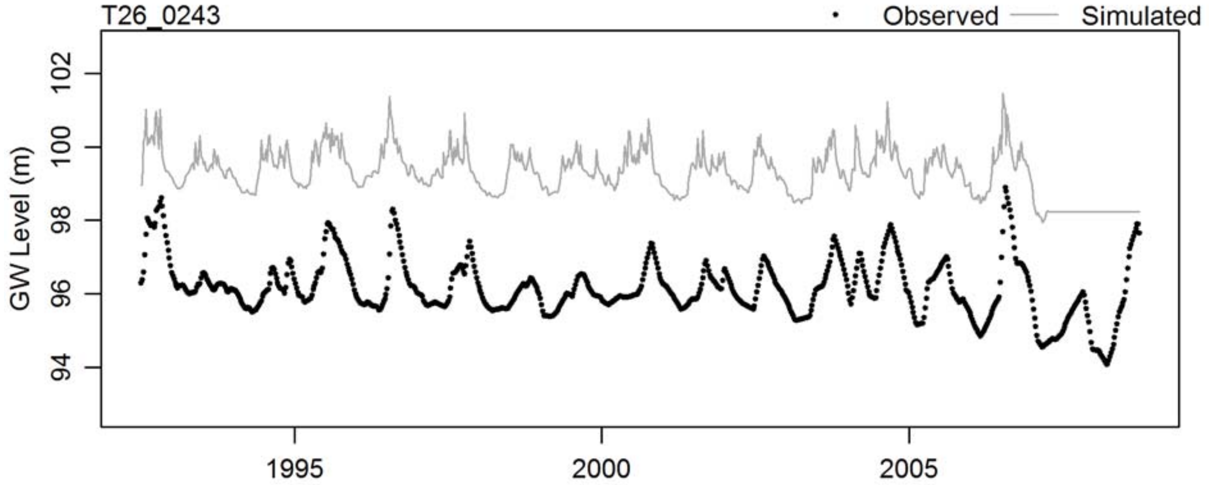
T26_0243
Observed
Simulated
GW Level (m)
102
100
98
96
94
1995
2000
2005

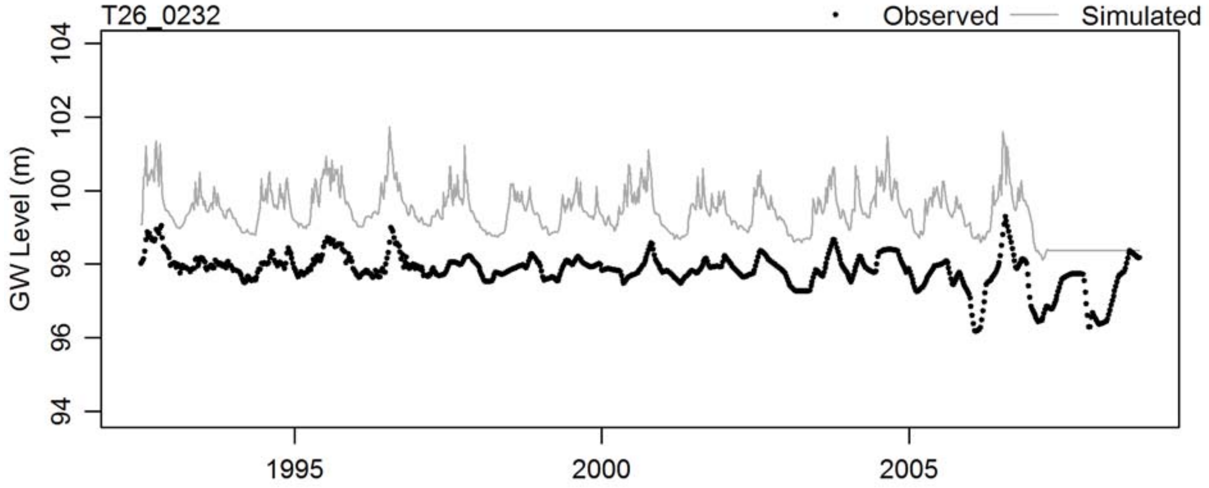
T26_0232
Observed
Simulated
GW Level (m)
104
102
100
98
96
94
1995
2000
2005

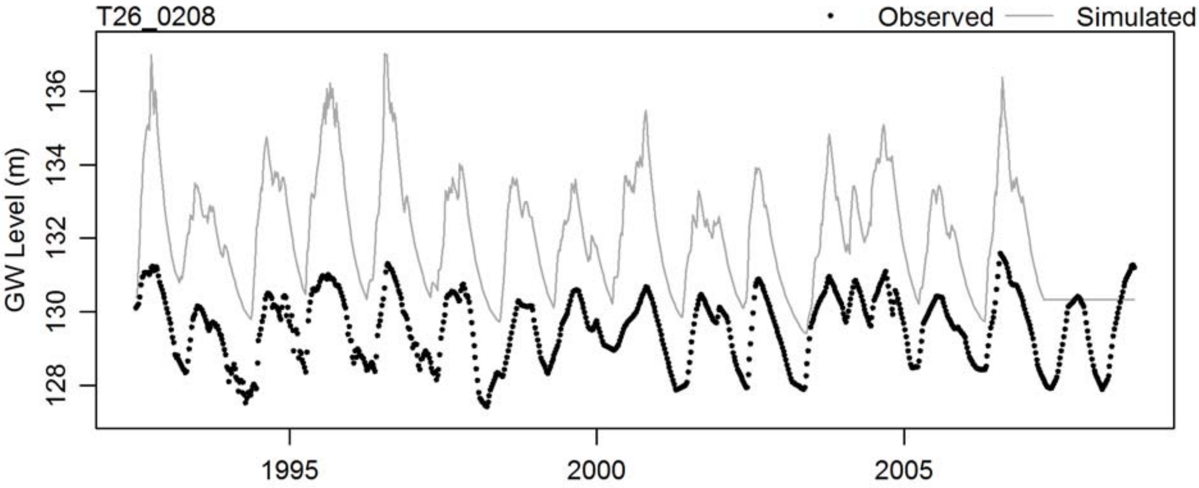
T26_0208
Observed
Simulated
GW Level (m)
128
130
132
134
136
1995
2000
2005

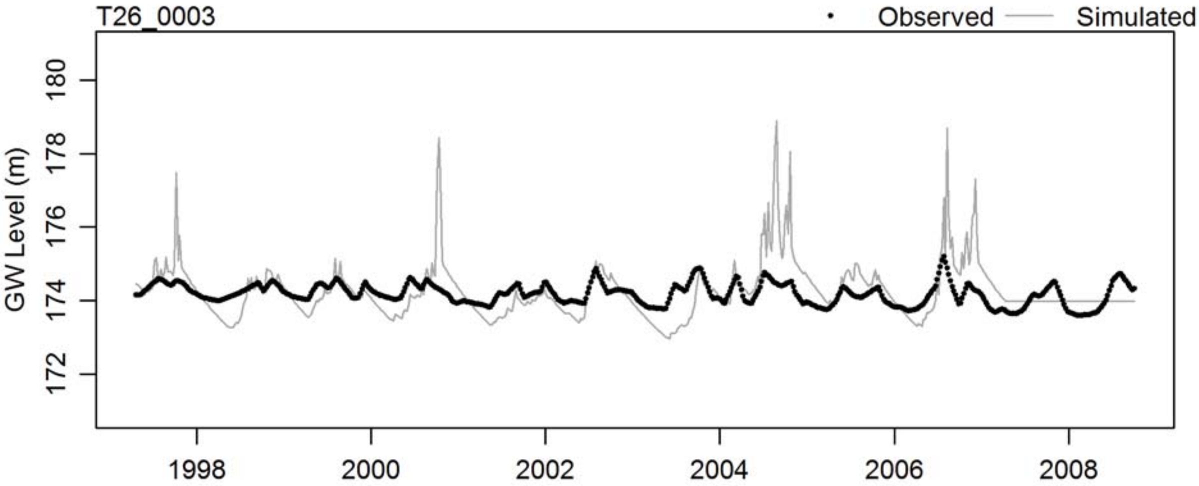
T26_0003
Observed
Simulated
GW Level (m)
172
174
176
178
180
1998
2000
2002
2004
2006
2008

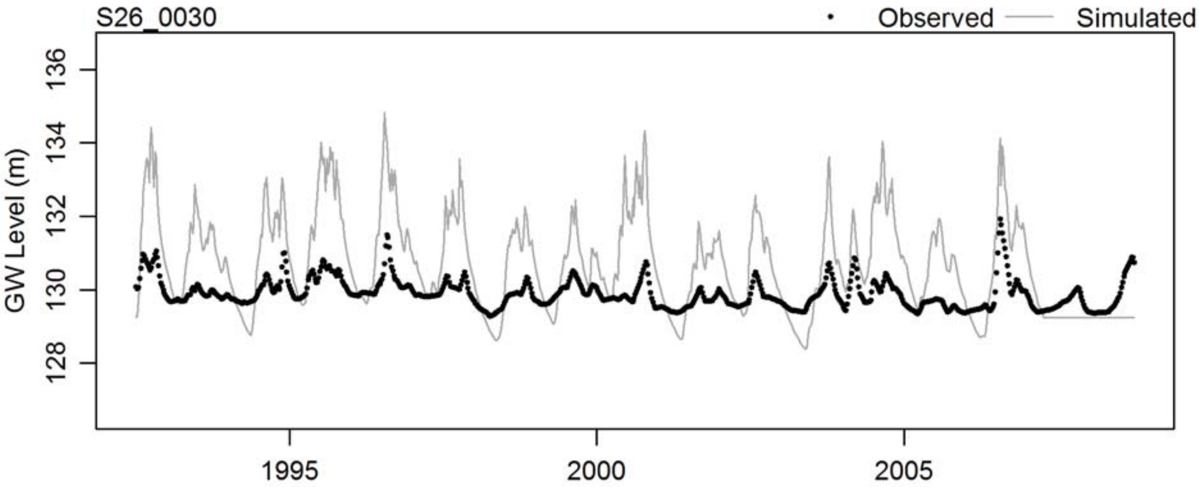
S26_0030
Observed
Simulated
GW Level (m)
128
130
132
134
136
1995
2000
2005

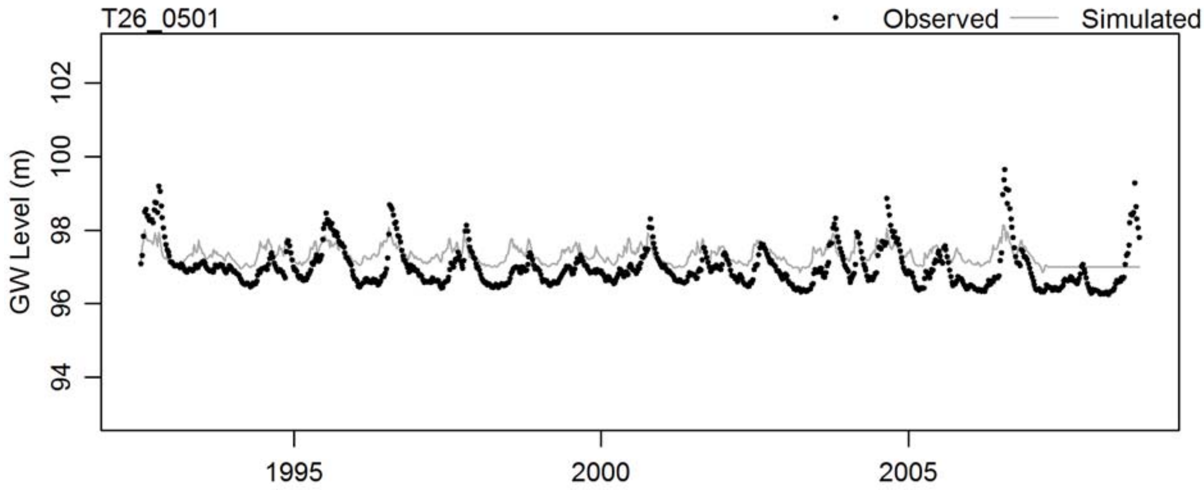
T26_0501
Observed
Simulated
GW Level (m)
94
96
98
100
102
1995
2000
2005

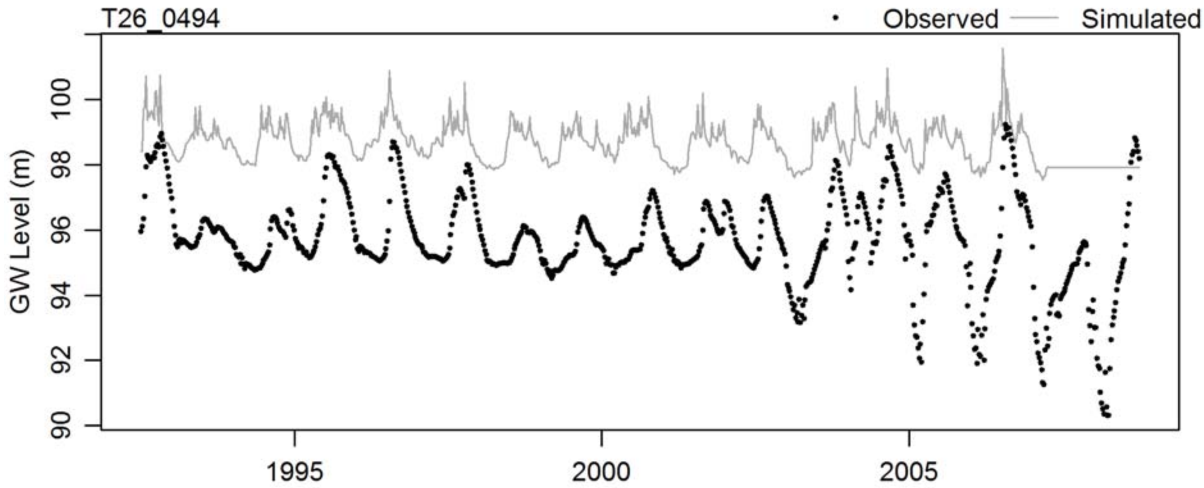
T26_0494
Observed
Simulated
GW Level (m)
90
92
94
96
98
100
1995
2000
2005

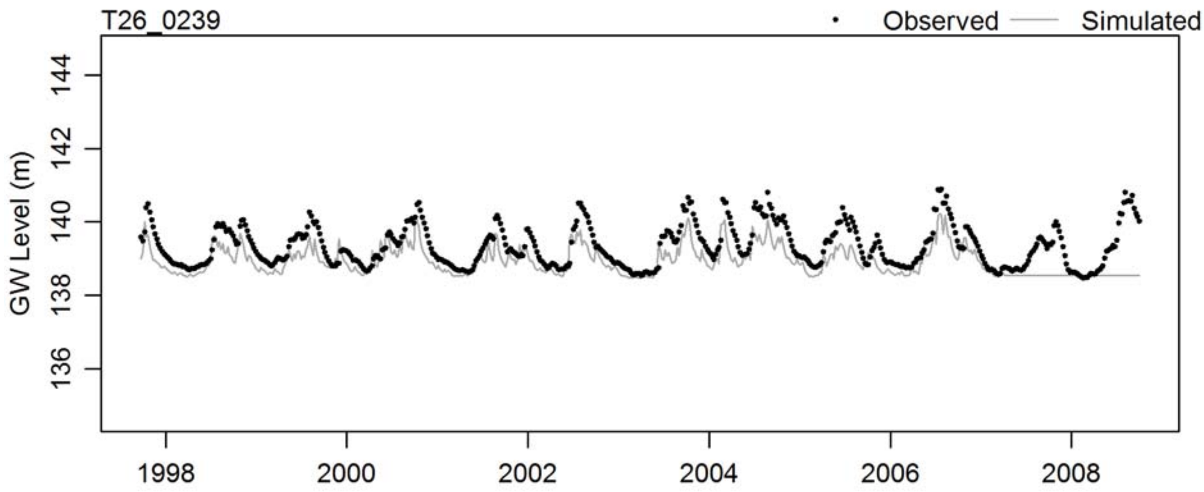
T26_0239
Observed
Simulated
GW Level (m)
136
138
140
142
144
1998
2000
2002
2004
2006
2008

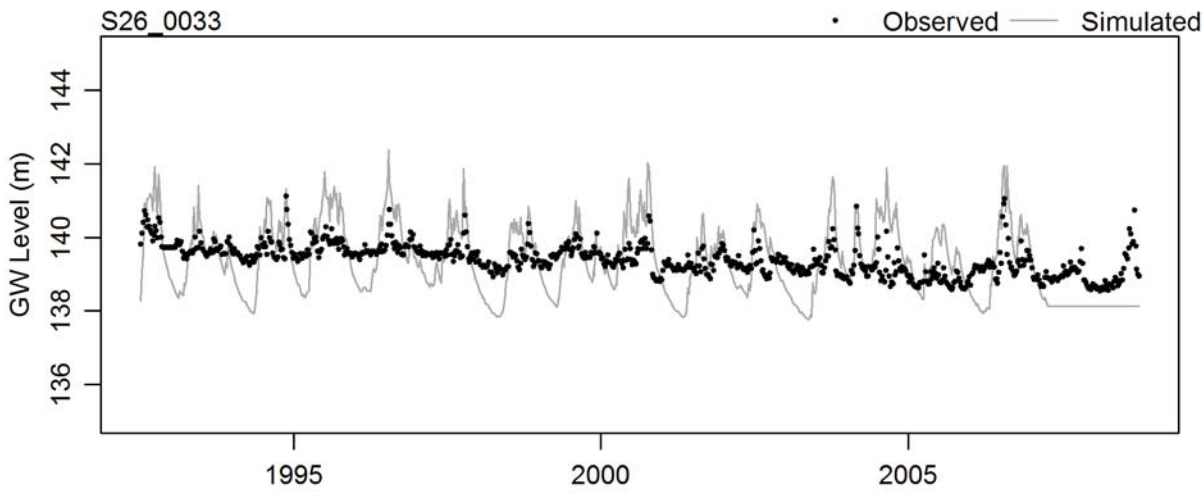
S26_0033
Observed
Simulated
GW Level (m)
136
138
140
142
144
1995
2000
2005

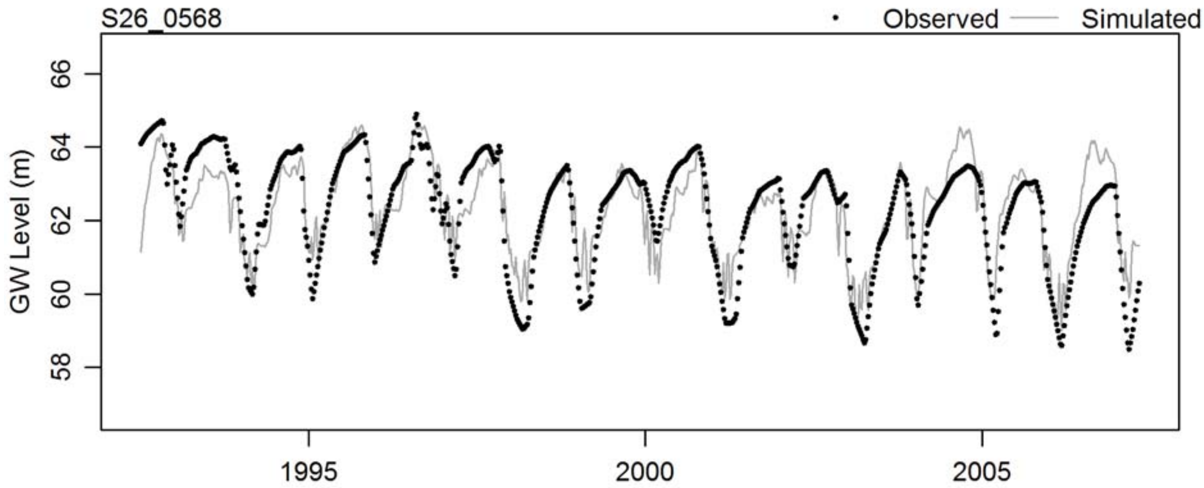
S26_0568
Observed
Simulated
GW Level (m)
58
60
62
64
66
1995
2000
2005

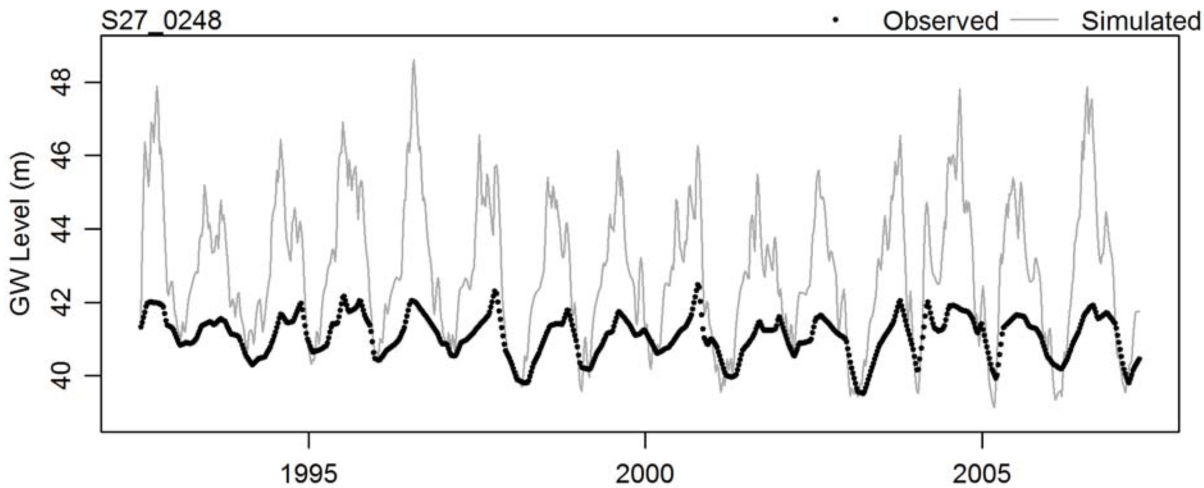
S27_0248
Observed
Simulated
GW Level (m)
40
42
44
46
48
1995
2000
2005

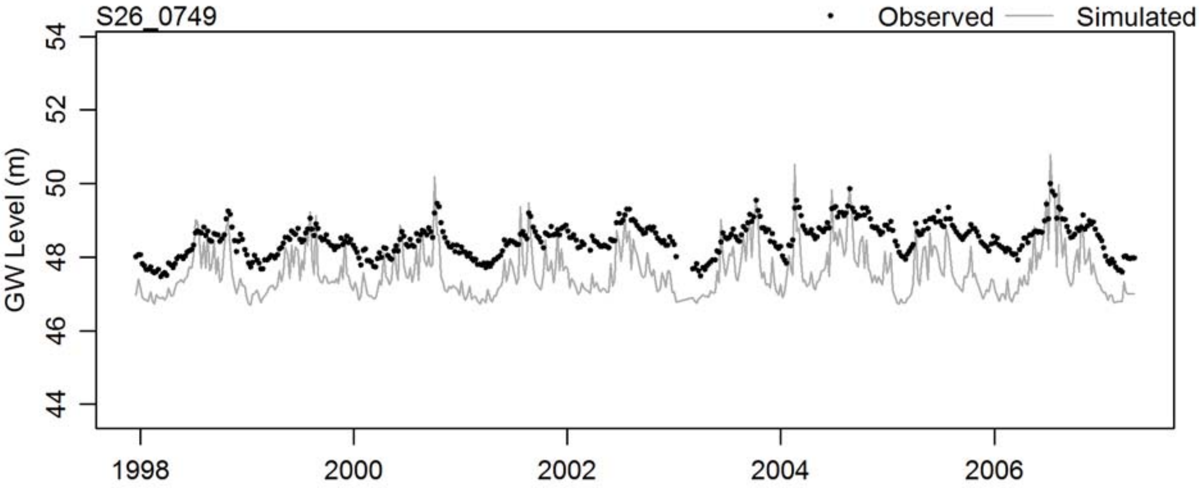
S26_0749
Observed
Simulated
GW Level (m)
54
52
50
48
46
44
1998
2000
2002
2004
2006

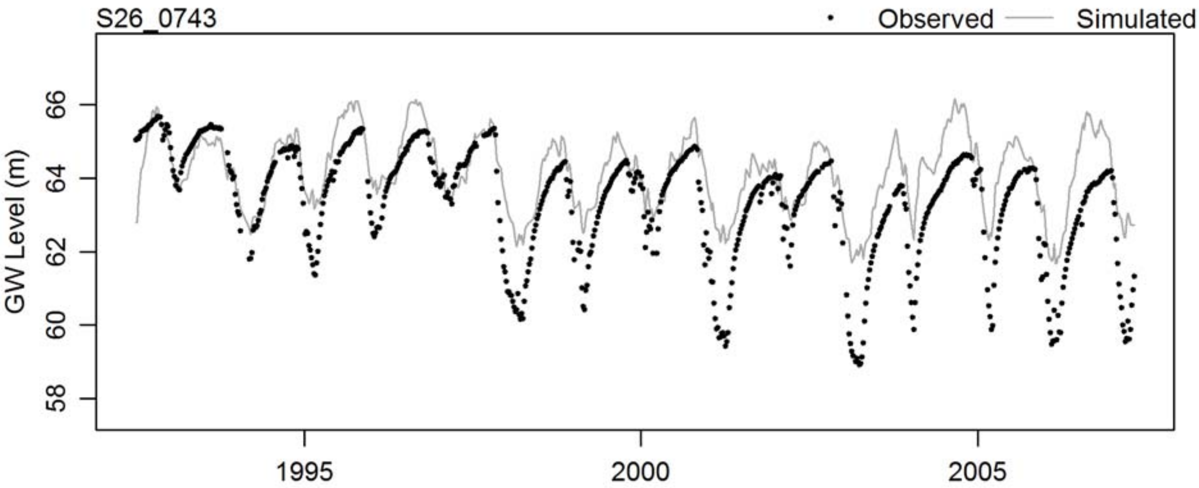
S26_0743
Observed
Simulated
GW Level (m)
66
64
62
60
58
1995
2000
2005

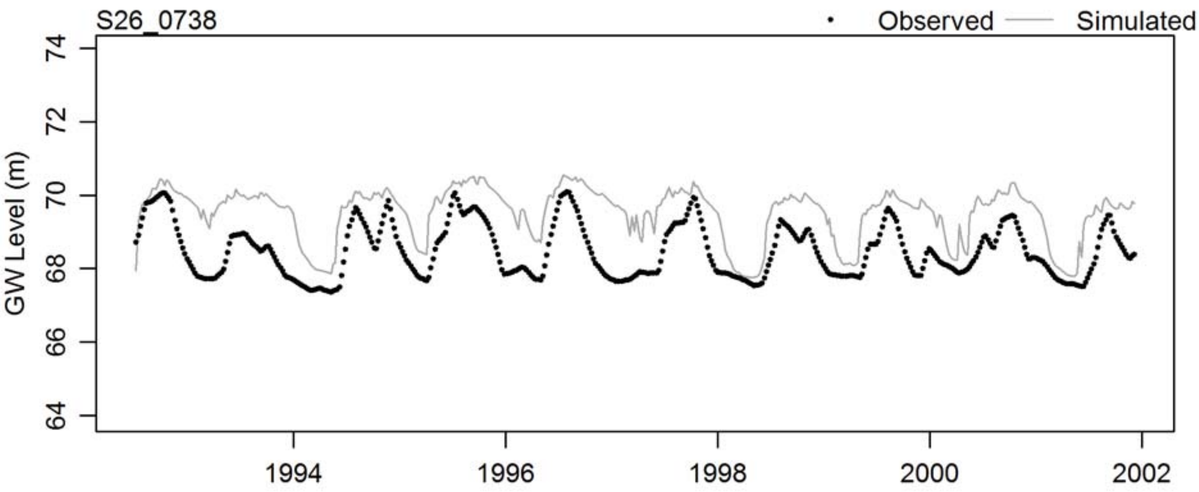
S26_0738
Observed
Simulated
GW Level (m)
74
72
70
68
66
64
1994
1996
1998
2000
2002

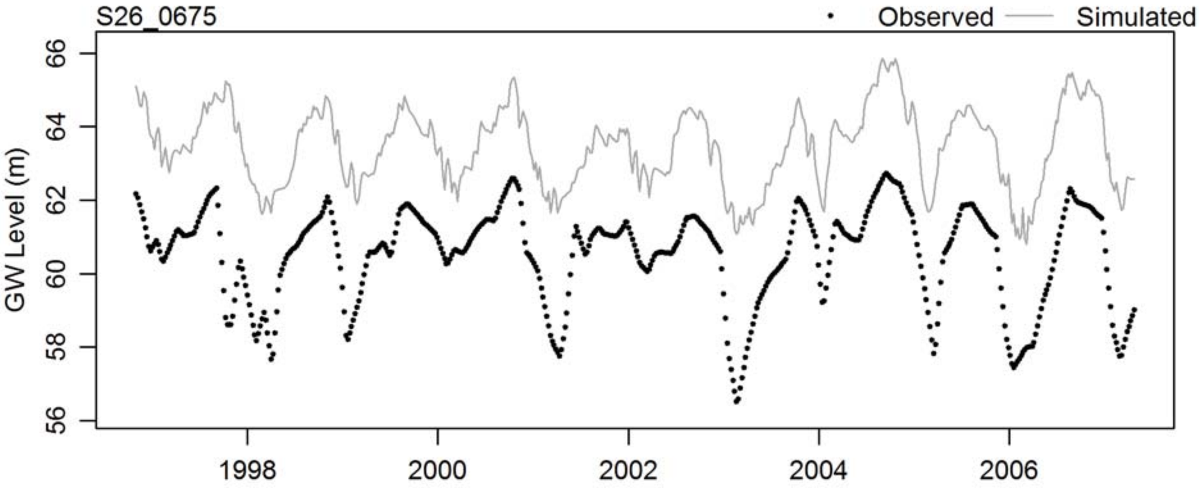

S26_0675
Observed
Simulated
GW Level (m)
56
58
60
62
64
66
1998
2000
2002
2004
2006

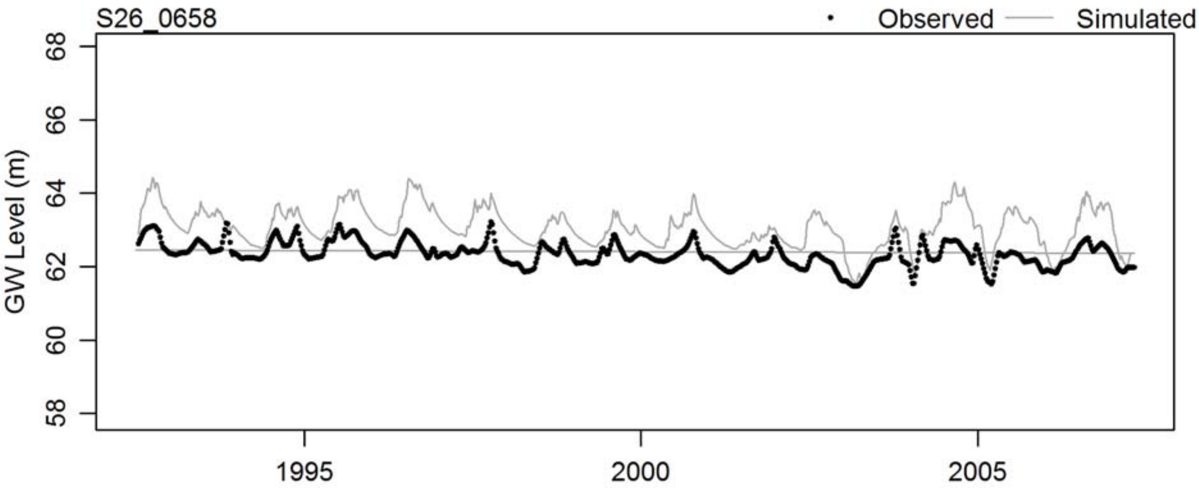

S26_0658
Observed
Simulated
GW Level (m)
58
60
62
64
66
68
1995
2000
2005

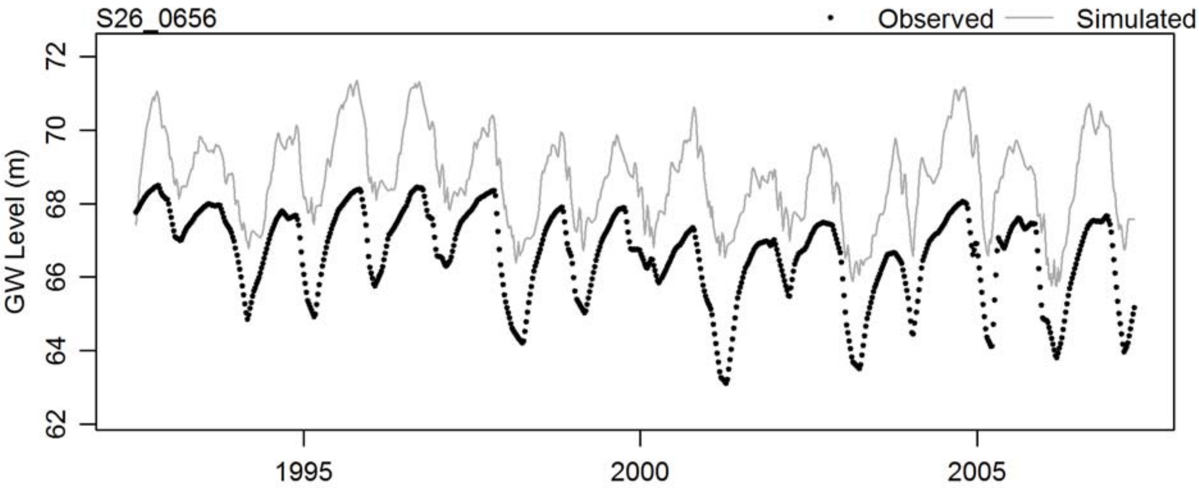

S26_0656
Observed
Simulated
GW Level (m)
62
64
66
68
70
72
1995
2000
2005

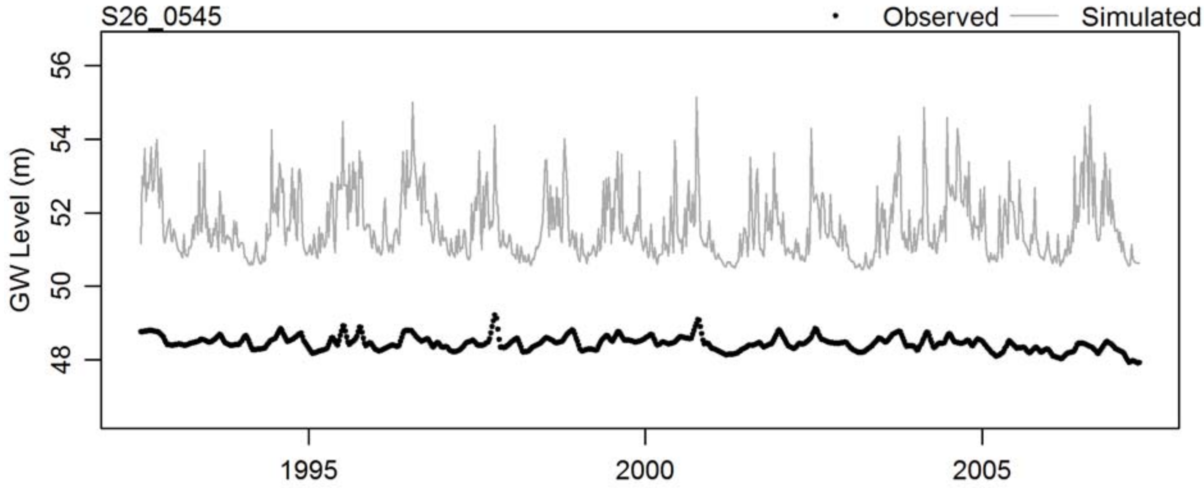
S26_0545
Observed
Simulated
GW Level (m)
56
54
52
50
48
1995
2000
2005

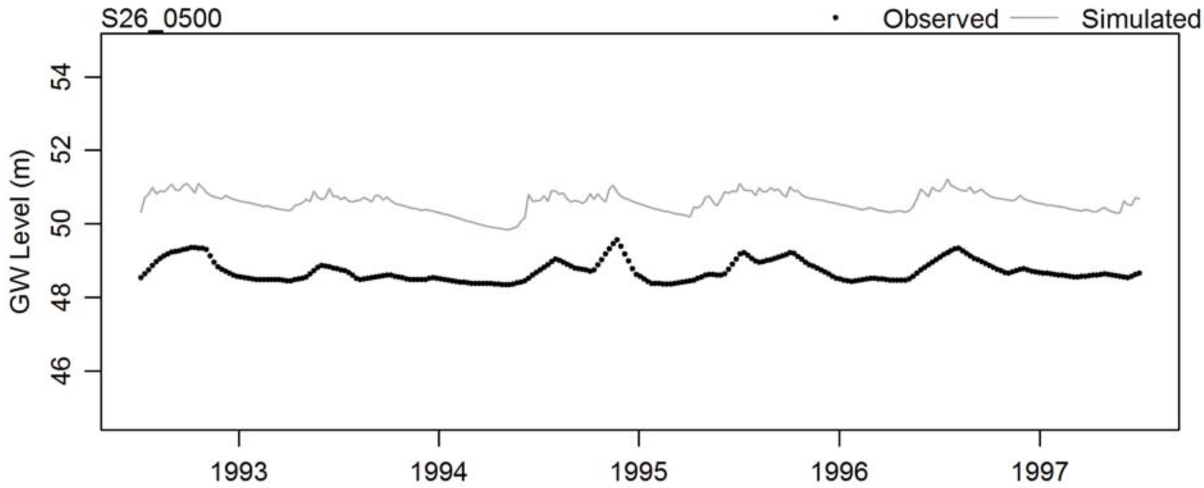
S26_0500
Observed
Simulated
GW Level (m)
54
52
50
48
46
1993
1994
1995
1996
1997

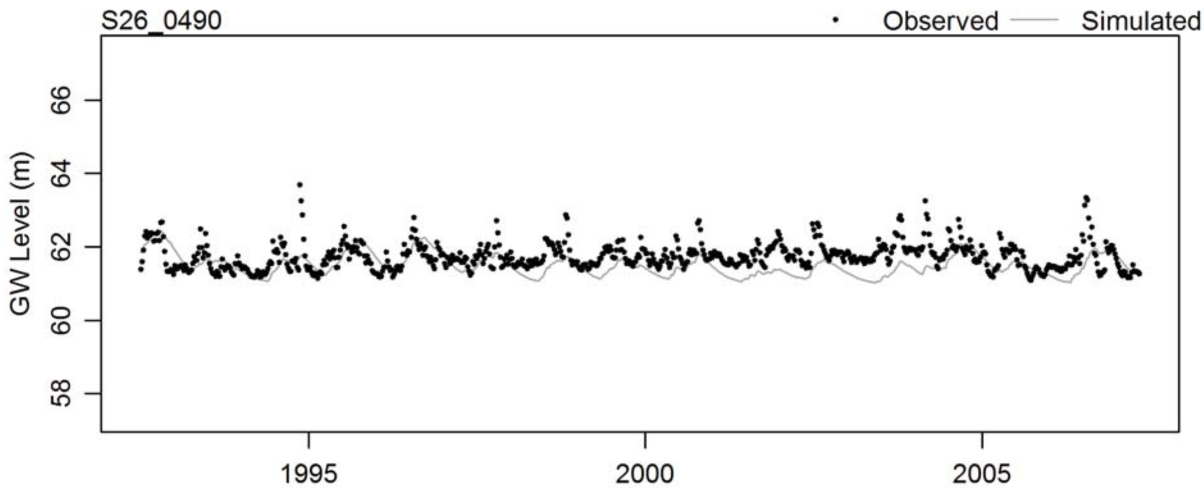
S26_0490
Observed
Simulated
GW Level (m)
66
64
62
60
58
1995
2000
2005

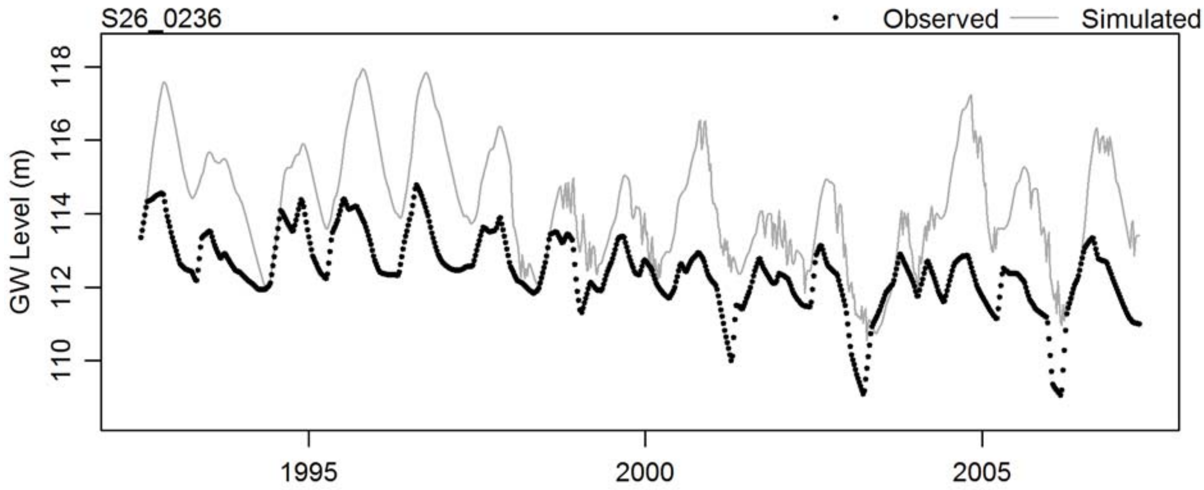
S26_0236
Observed
Simulated
GW Level (m)
110
112
114
116
118
1995
2000
2005

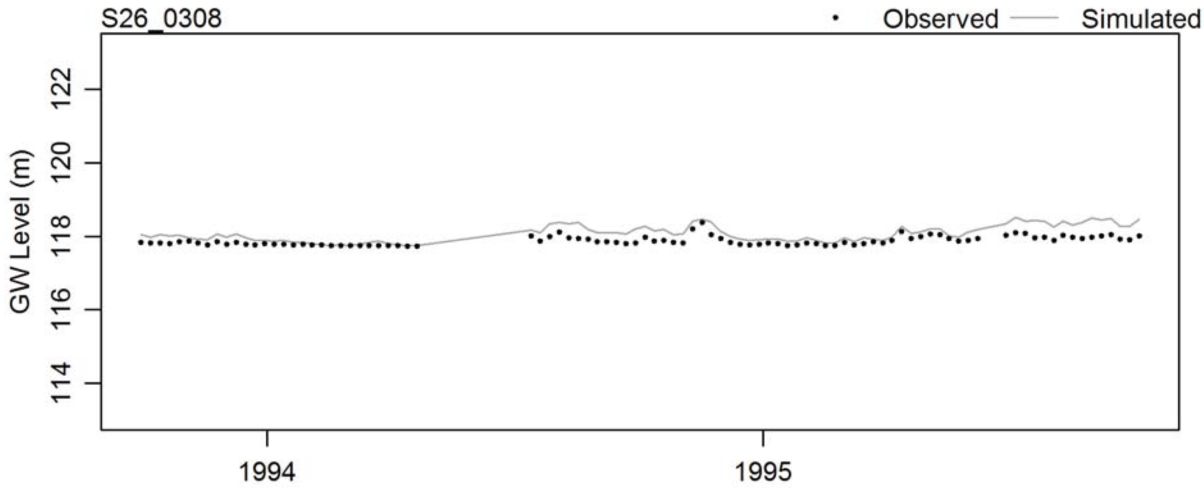
S26_0308
Observed
Simulated
GW Level (m)
114
116
118
120
122
1994
1995

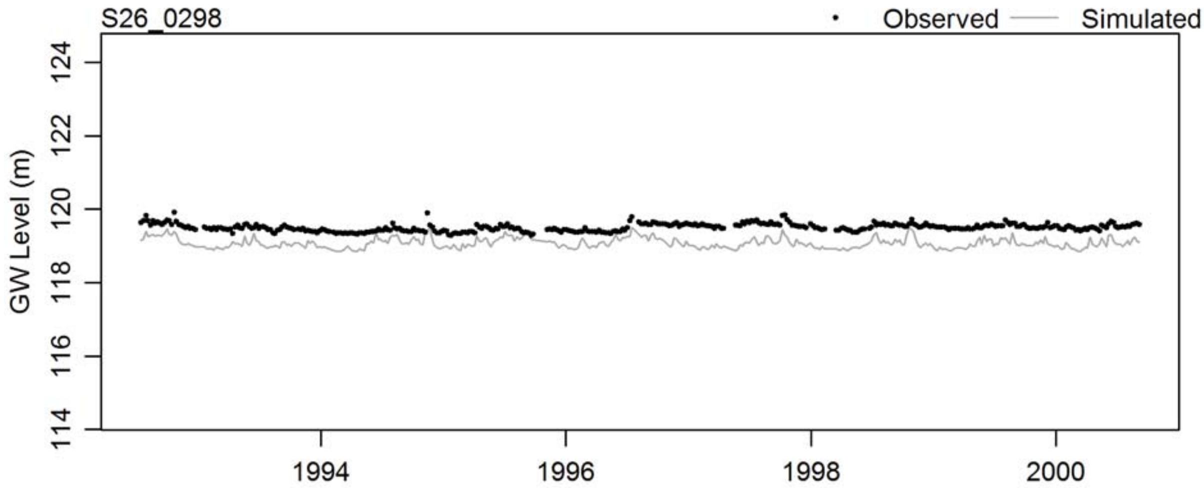
S26_0298
Observed
Simulated
GW Level (m)
114
116
118
120
122
124
1994
1996
1998
2000

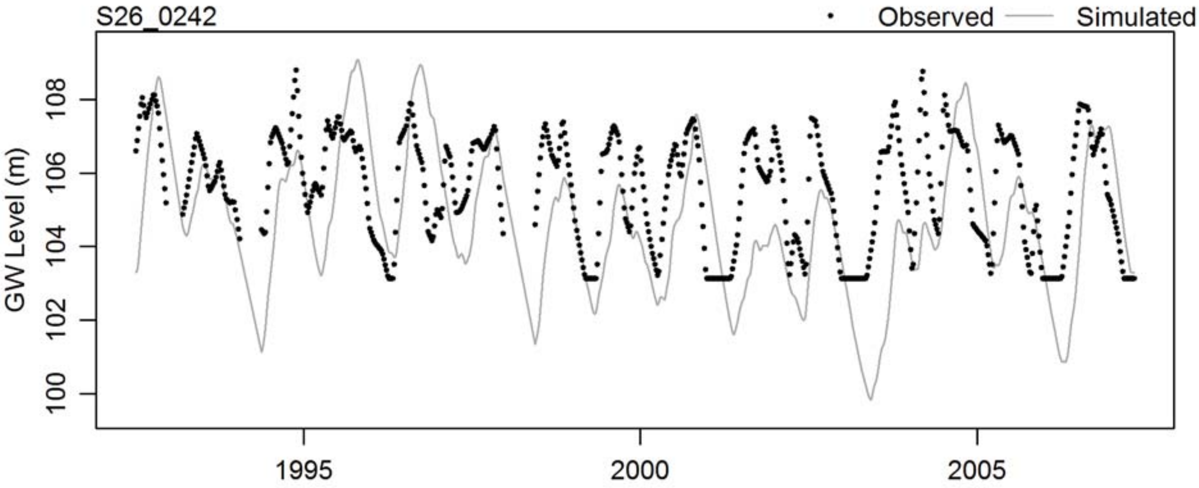
S26_0242
Observed
Simulated
GW Level (m)
100
102
104
106
108
1995
2000
2005

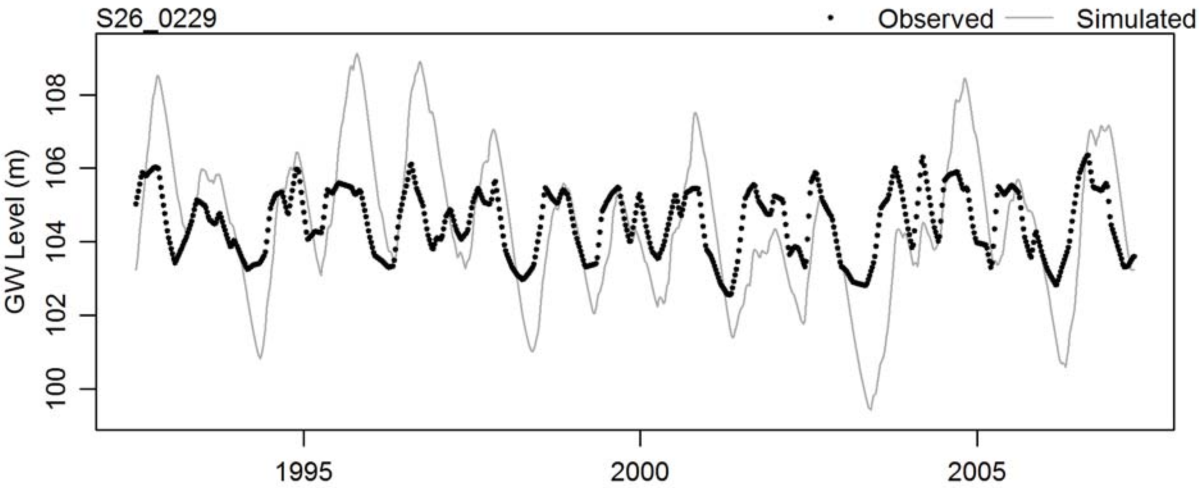
S26_0229
Observed
Simulated
GW Level (m)
100
102
104
106
108
1995
2000
2005

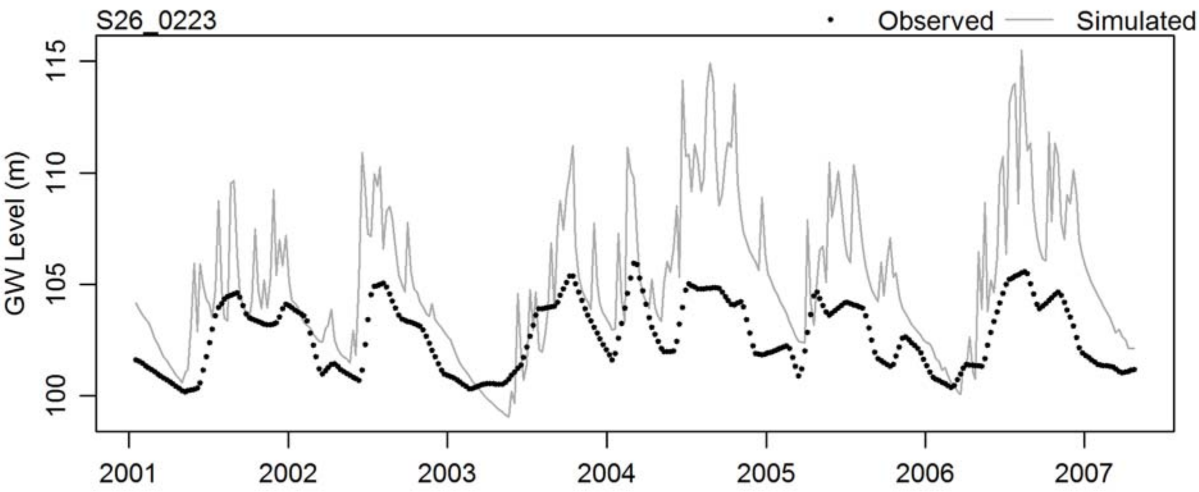
S26_0223
Observed
Simulated
GW Level (m)
100
105
110
115
2001
2002
2003
2004
2005
2006
2007

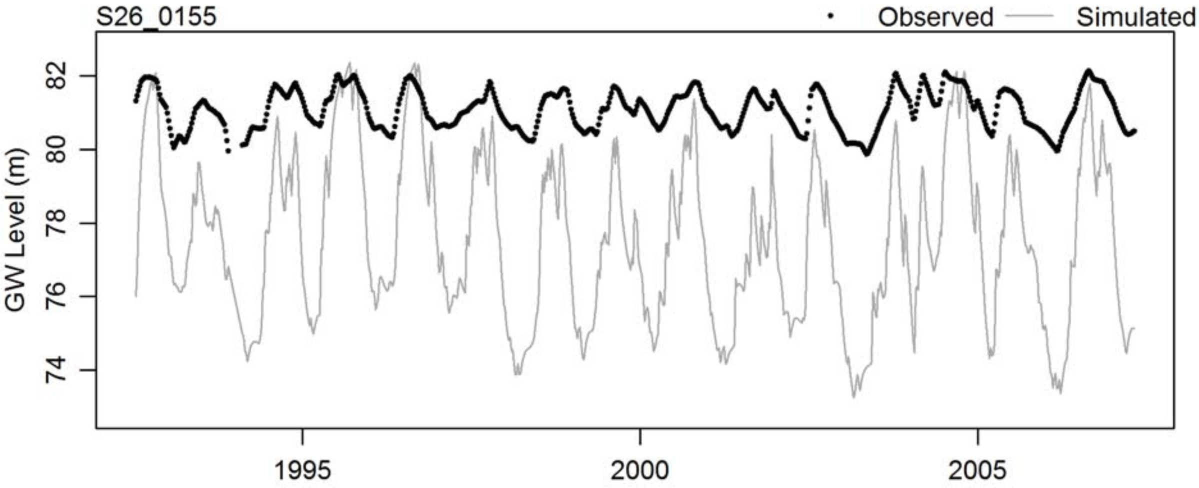
S26_0155
Observed
Simulated
GW Level (m)
82
80
78
76
74
1995
2000
2005

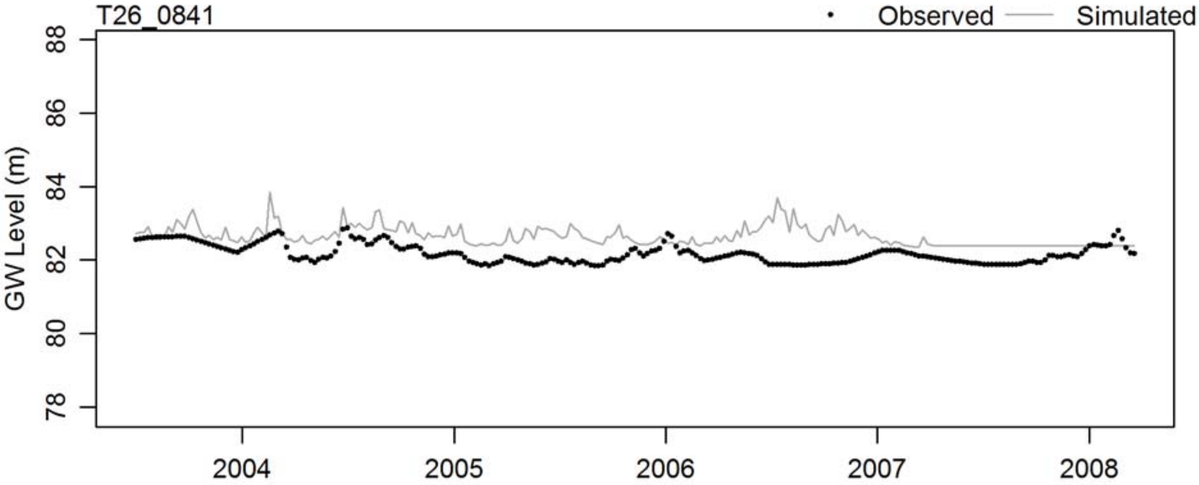
T26_0841
Observed
Simulated
GW Level (m)
88
86
84
82
80
78
2004
2005
2006
2007
2008

A9.0 GROUNDWATER LEVEL MODEL OUTPUTS AND MEASUREMENTS FOR MONITORING WELLS IN THE SOUTH MODEL

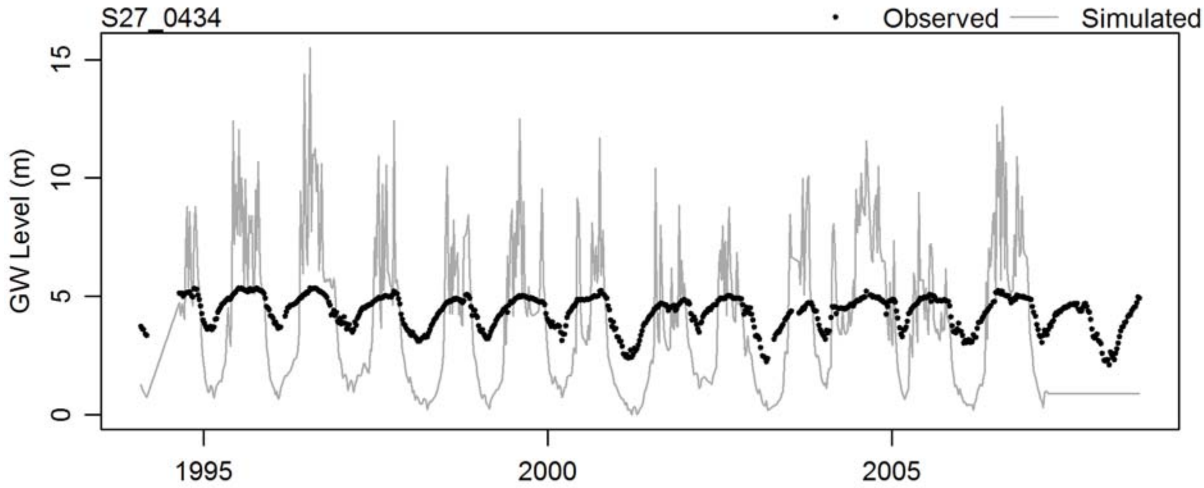

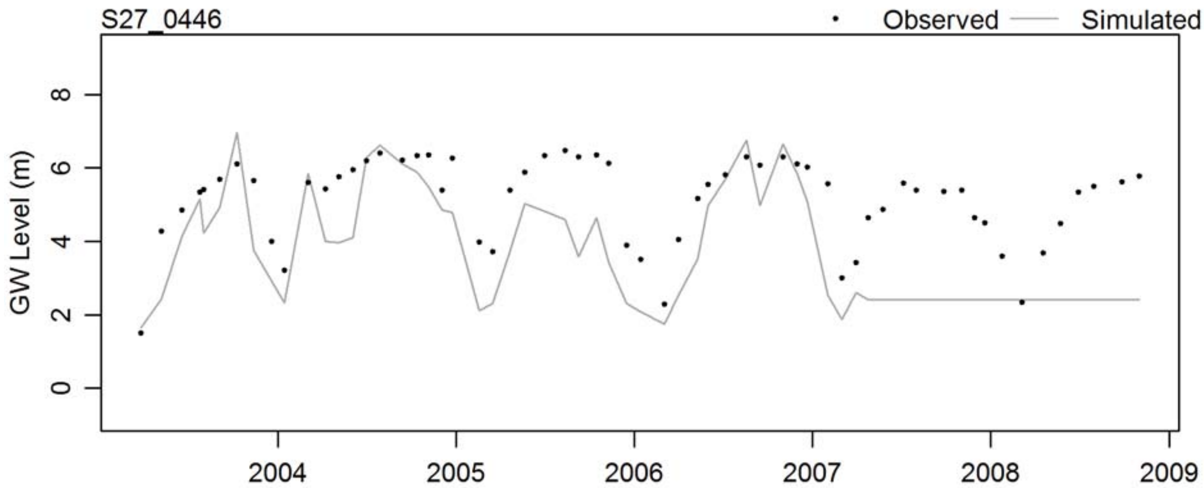

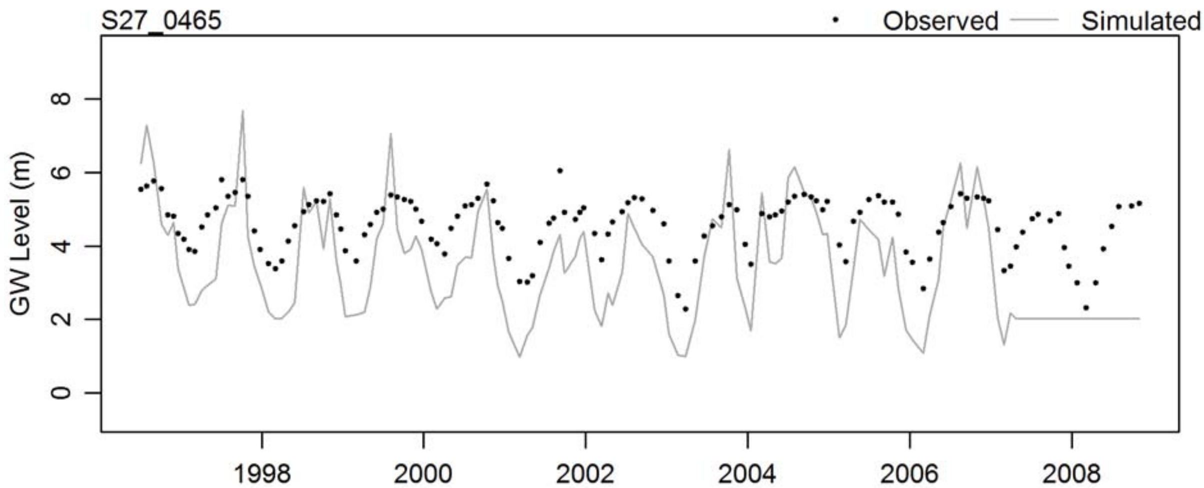

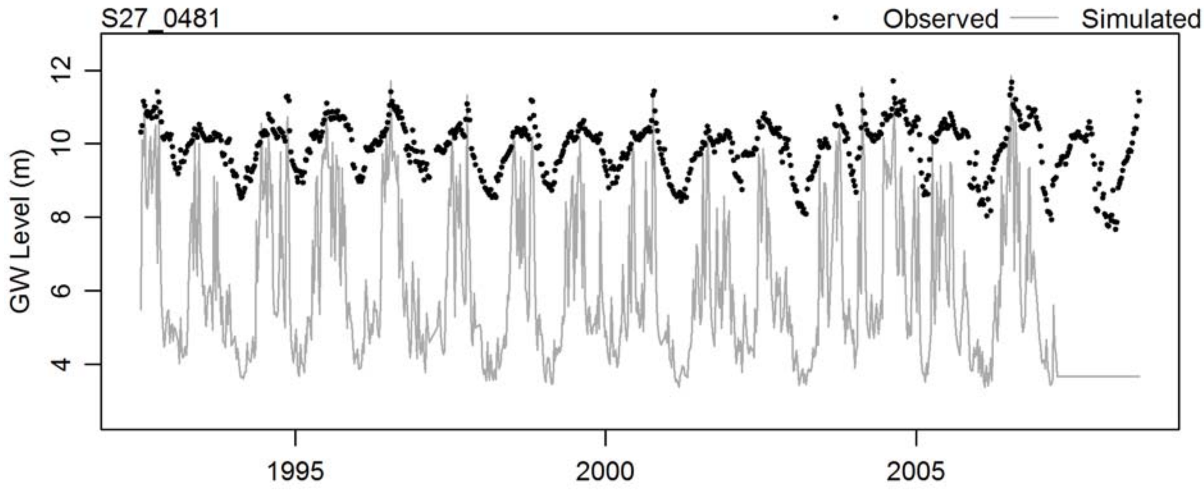
S27_0481
Observed
Simulated
GW Level (m)
12
10
8
6
4
1995
2000
2005

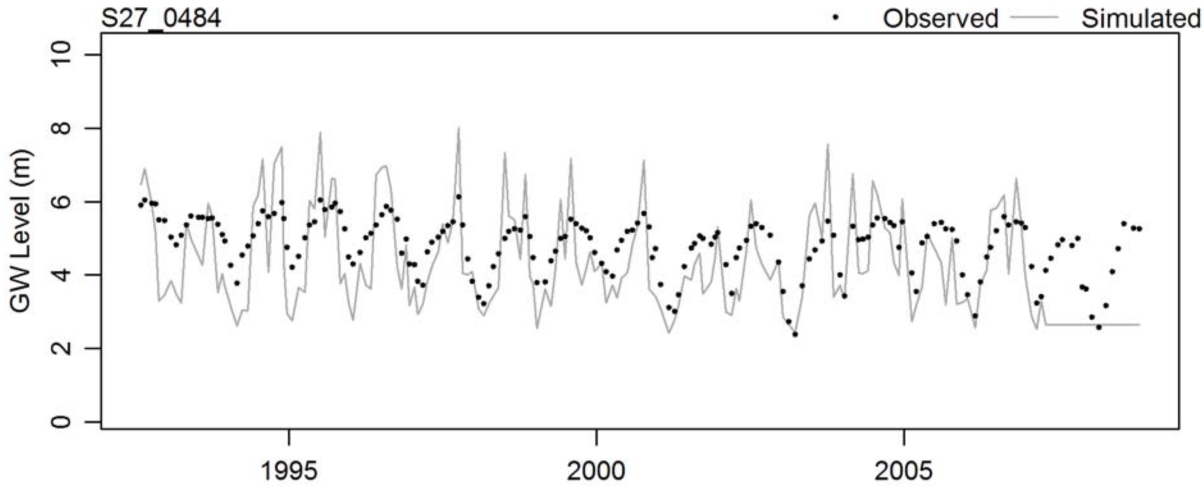
S27_0484
Observed
Simulated
GW Level (m)
10
8
6
4
2
0
1995
2000
2005

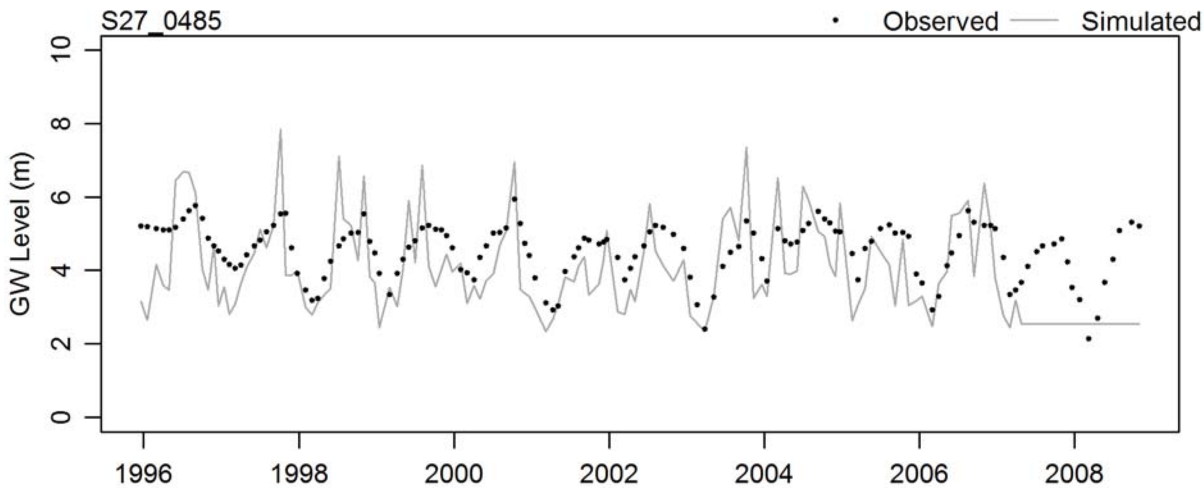
S27_0485
Observed
Simulated
GW Level (m)
10
8
6
4
2
0
1996
1998
2000
2002
2004
2006
2008

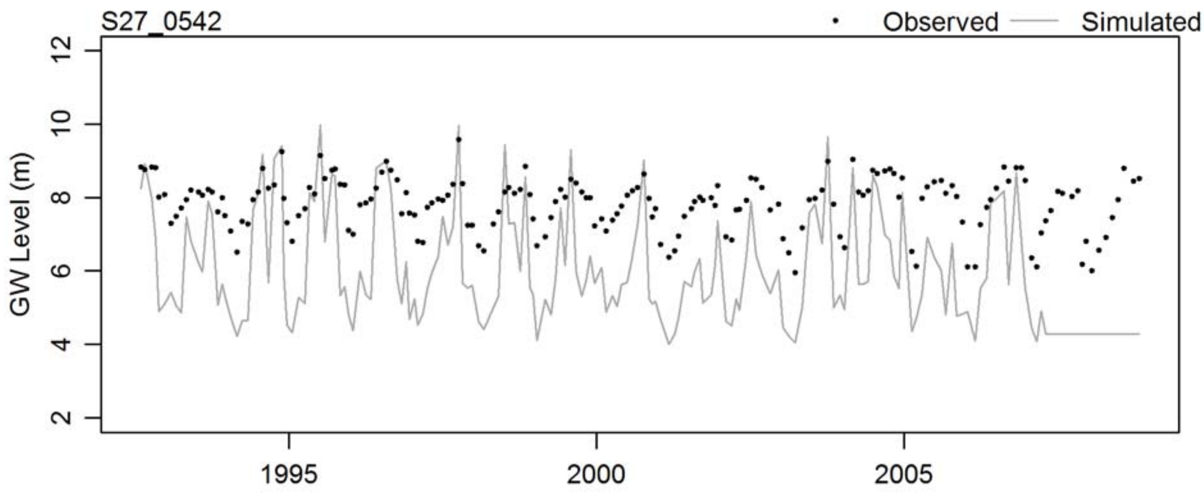
S27_0542
Observed
Simulated
GW Level (m)
2
4
6
8
10
12
1995
2000
2005

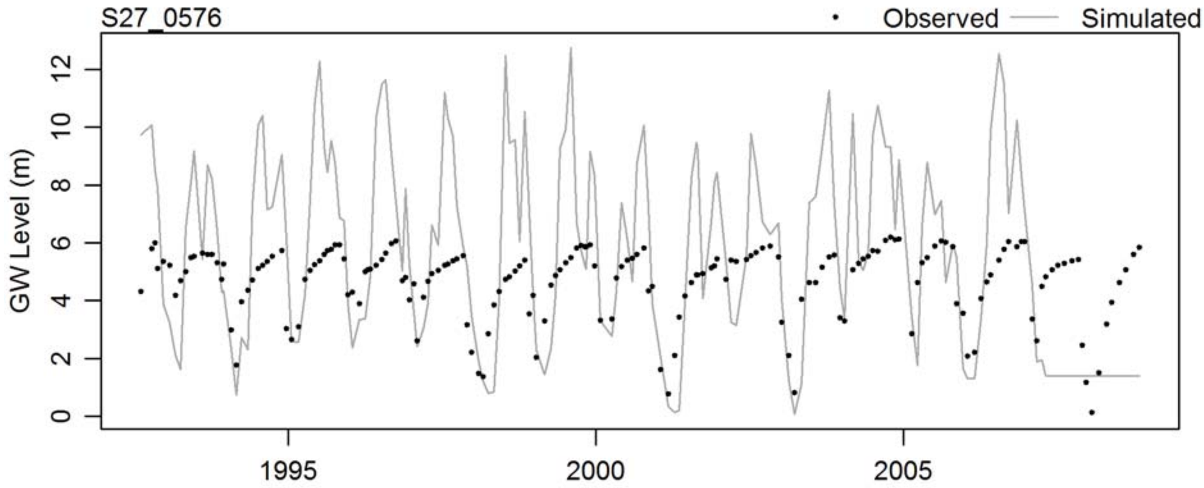
S27_0576
Observed
Simulated
GW Level (m)
0
2
4
6
8
10
12
1995
2000
2005

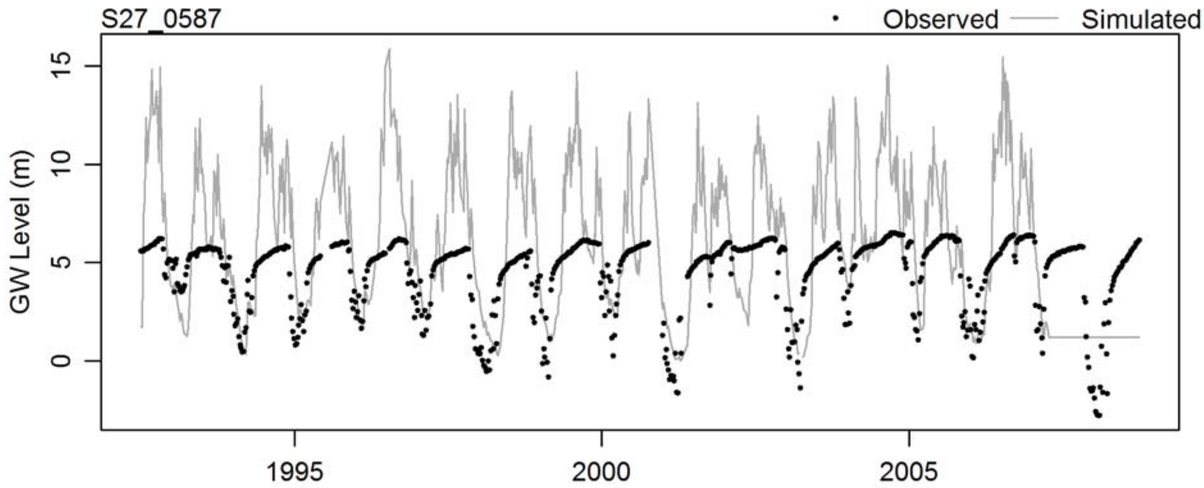
S27_0587
Observed
Simulated
GW Level (m)
0
5
10
15
1995
2000
2005

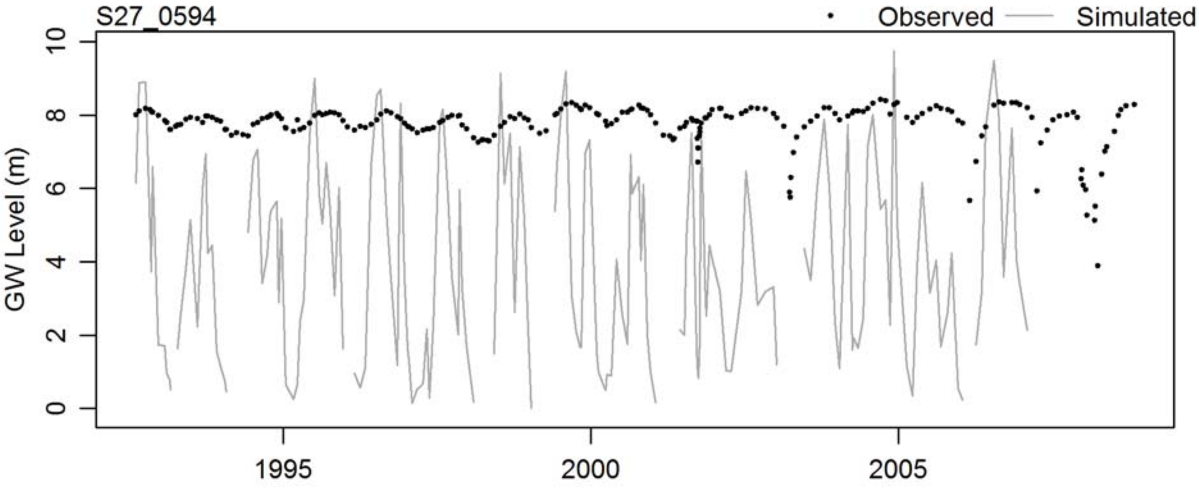
S27_0594
Observed
Simulated
GW Level (m)
0
2
4
6
8
10
1995
2000
2005

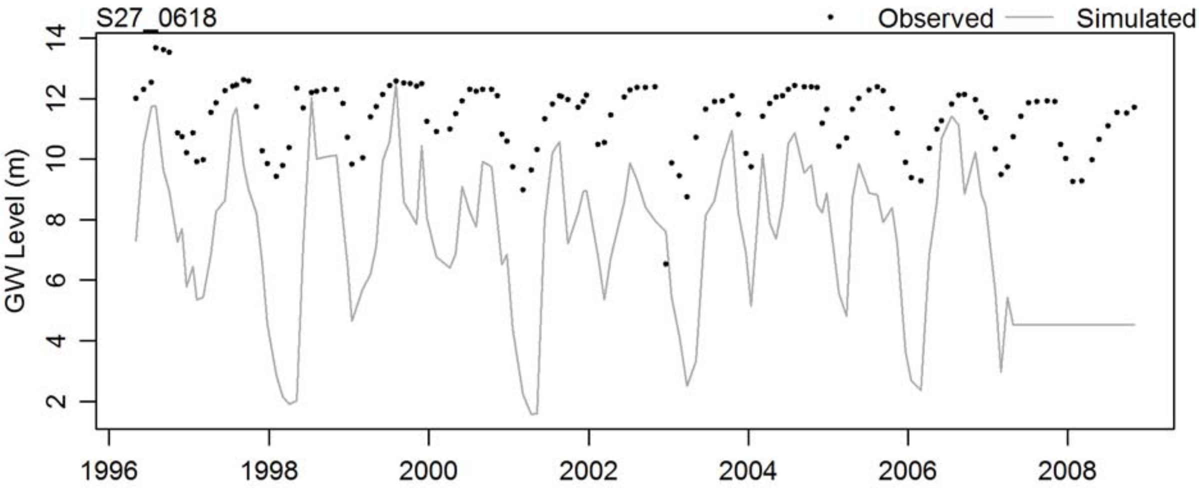
S27_0618
Observed
Simulated
GW Level (m)
2
4
6
8
10
12
14
1996
1998
2000
2002
2004
2006
2008

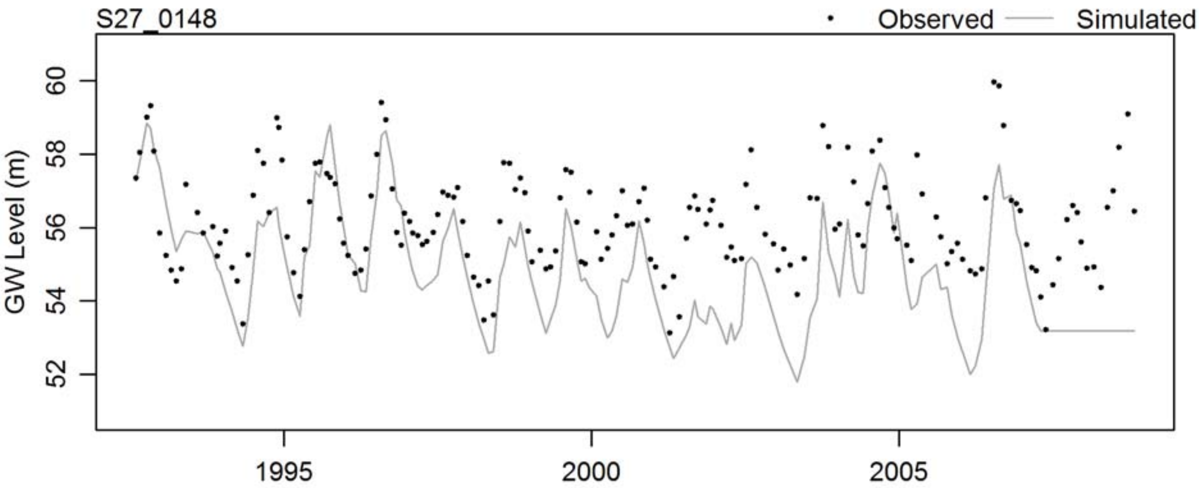
S27_0148
Observed
Simulated
GW Level (m)
52
54
56
58
60
1995
2000
2005

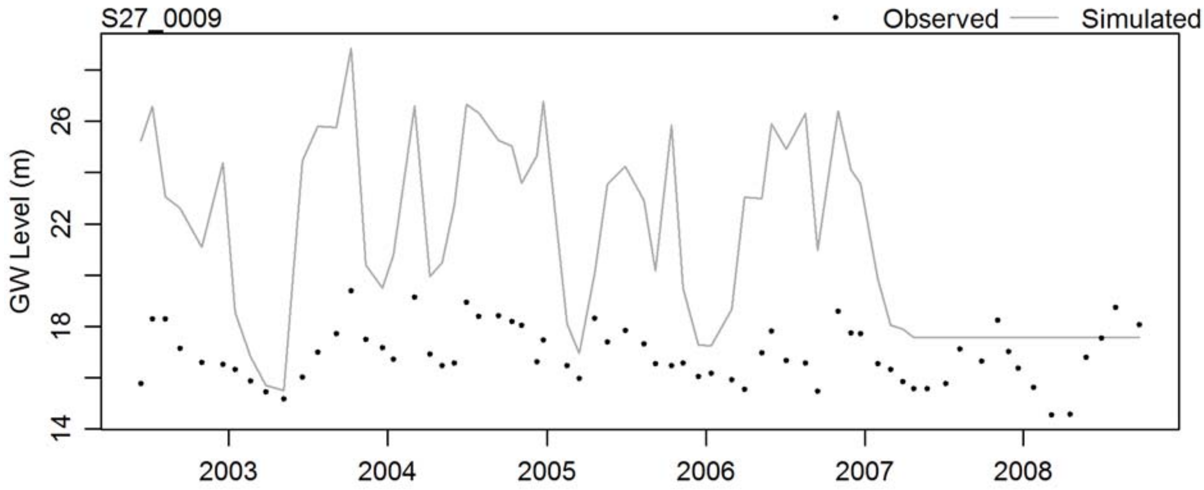
S27_0009
Observed
Simulated
GW Level (m)
14
18
22
26
2003
2004
2005
2006
2007
2008

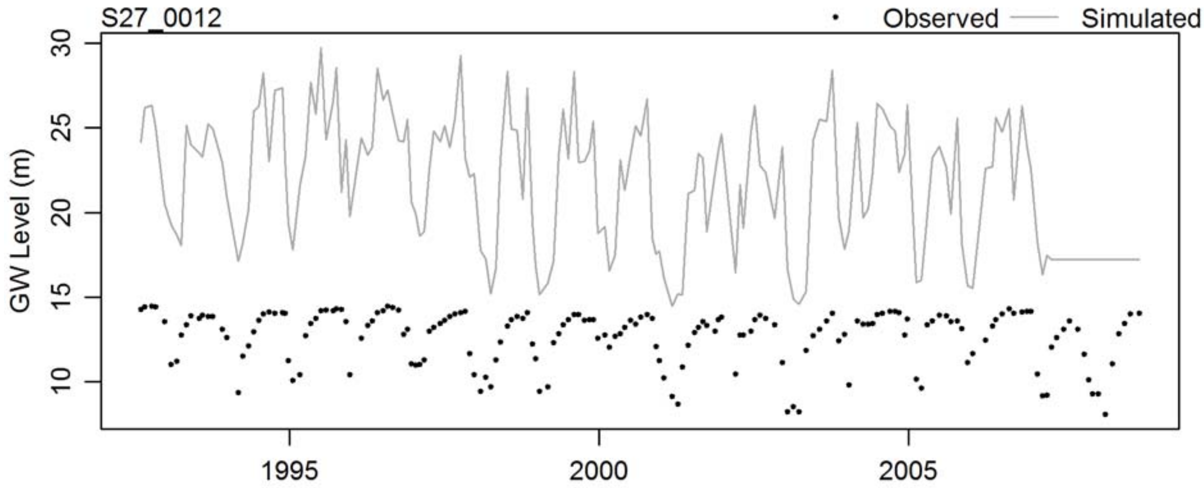
S27_0012
Observed
Simulated
GW Level (m)
10
15
20
25
30
1995
2000
2005

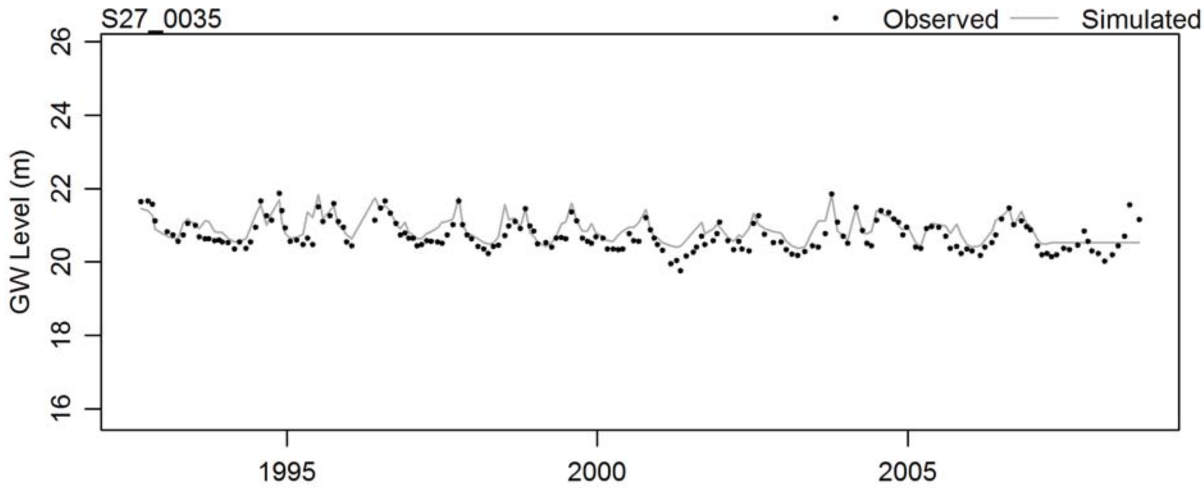
S27_0035
Observed
Simulated
GW Level (m)
16
18
20
22
24
26
1995
2000
2005

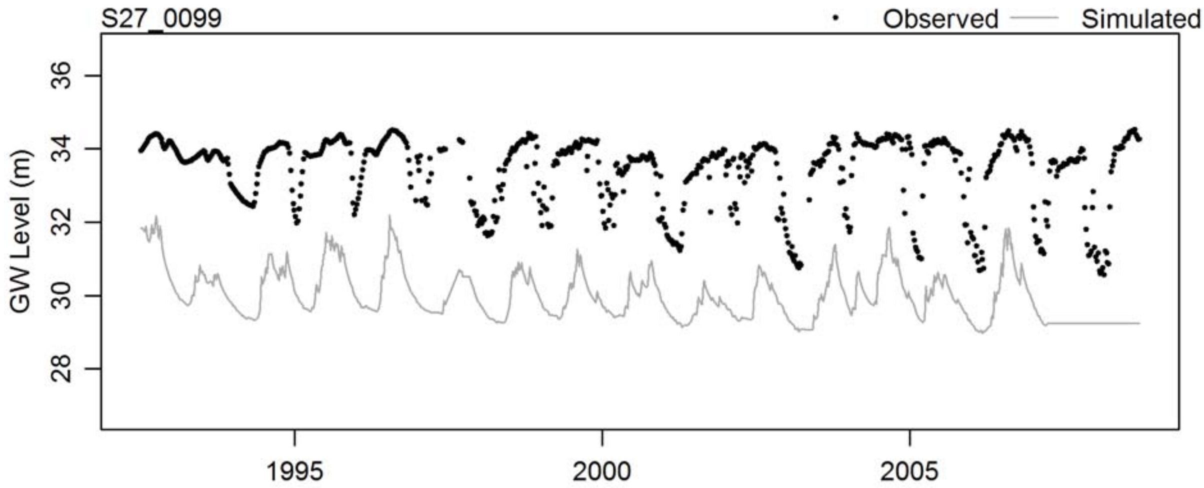
S27_0099
Observed
Simulated
GW Level (m)
28
30
32
34
36
1995
2000
2005

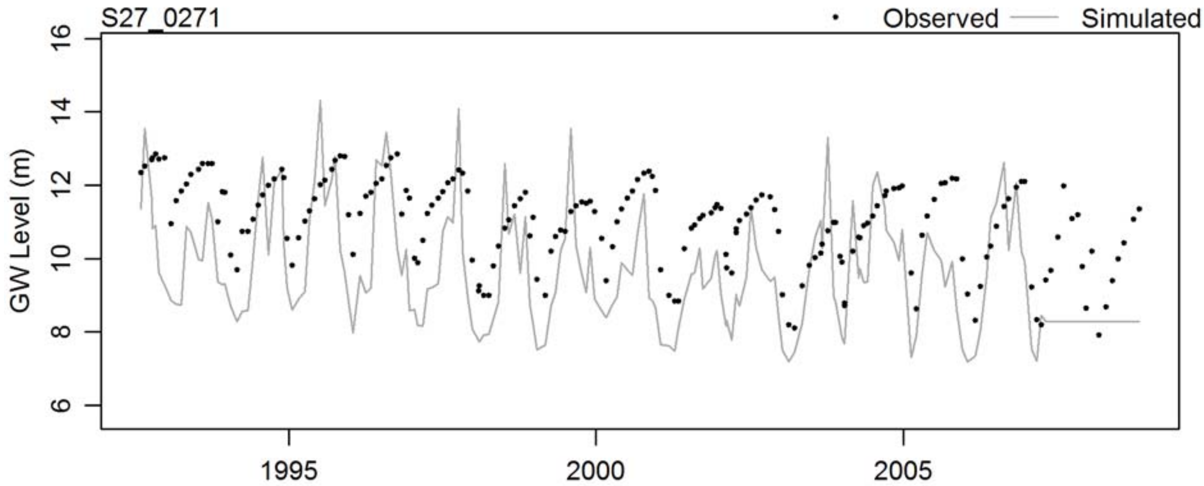
S27_0271
Observed
Simulated
GW Level (m)
6
8
10
12
14
16
1995
2000
2005

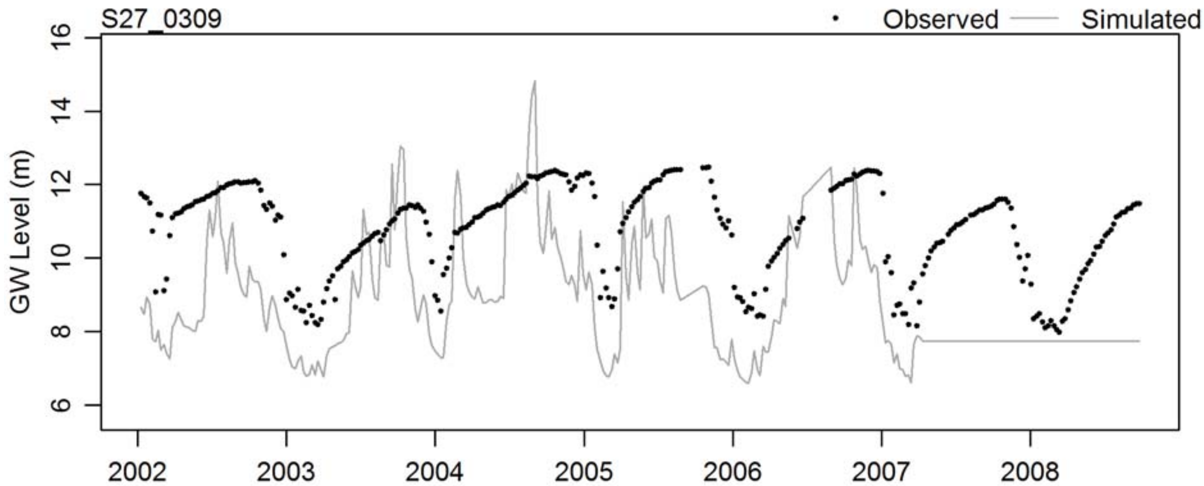
S27_0309
Observed
Simulated
GW Level (m)
6
8
10
12
14
16
2002
2003
2004
2005
2006
2007
2008

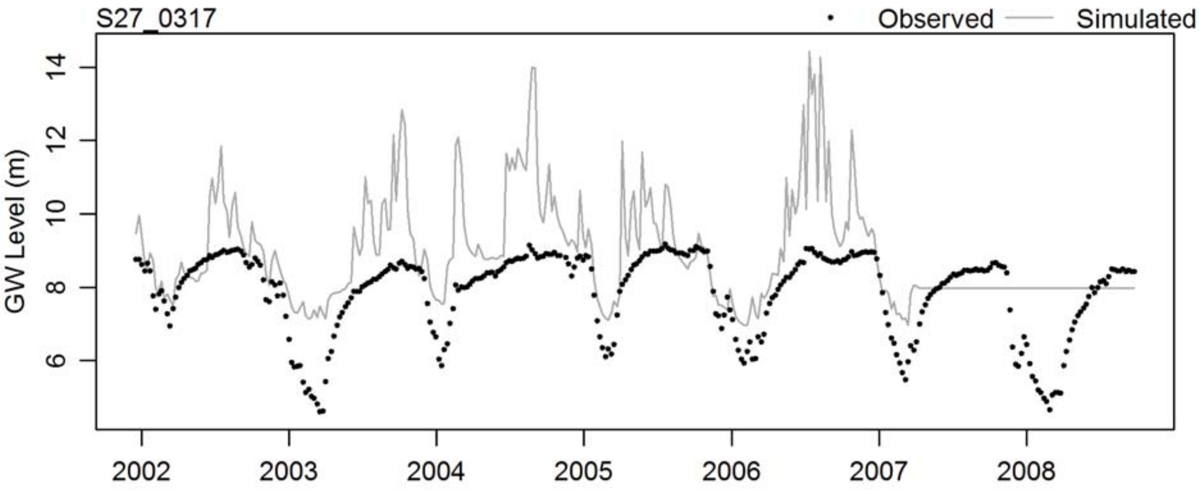
S27_0317
Observed
Simulated
GW Level (m)
6
8
10
12
14
2002
2003
2004
2005
2006
2007
2008

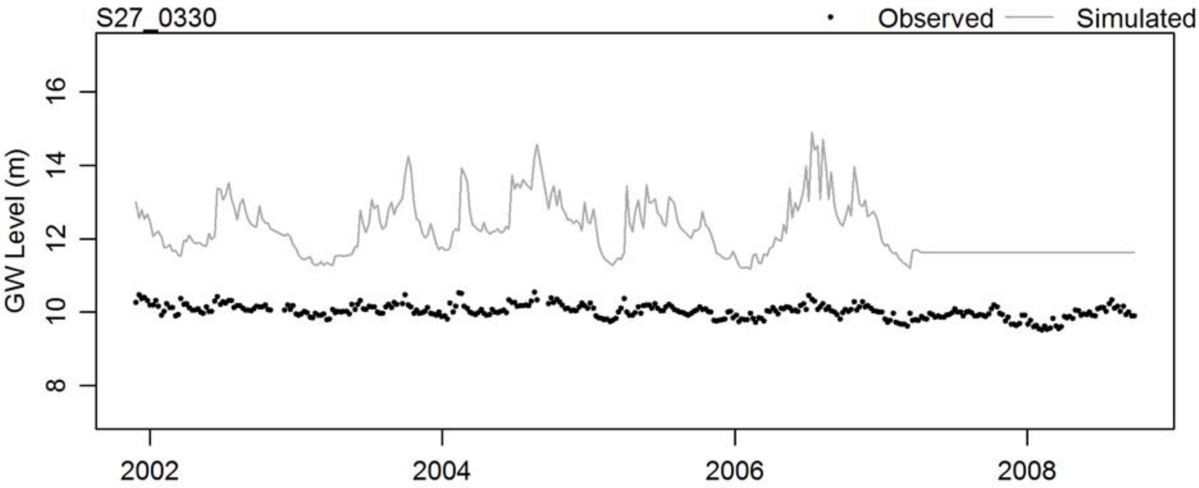
S27_0330
Observed
Simulated
GW Level (m)
8
10
12
14
16
2002
2004
2006
2008

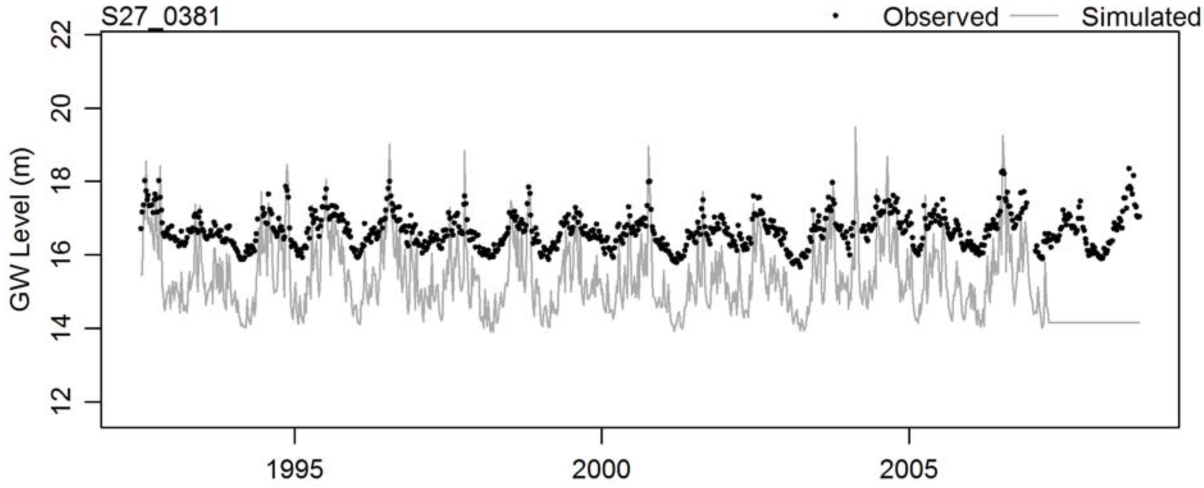
S27_0381
Observed
Simulated
GW Level (m)
22
20
18
16
14
12
1995
2000
2005

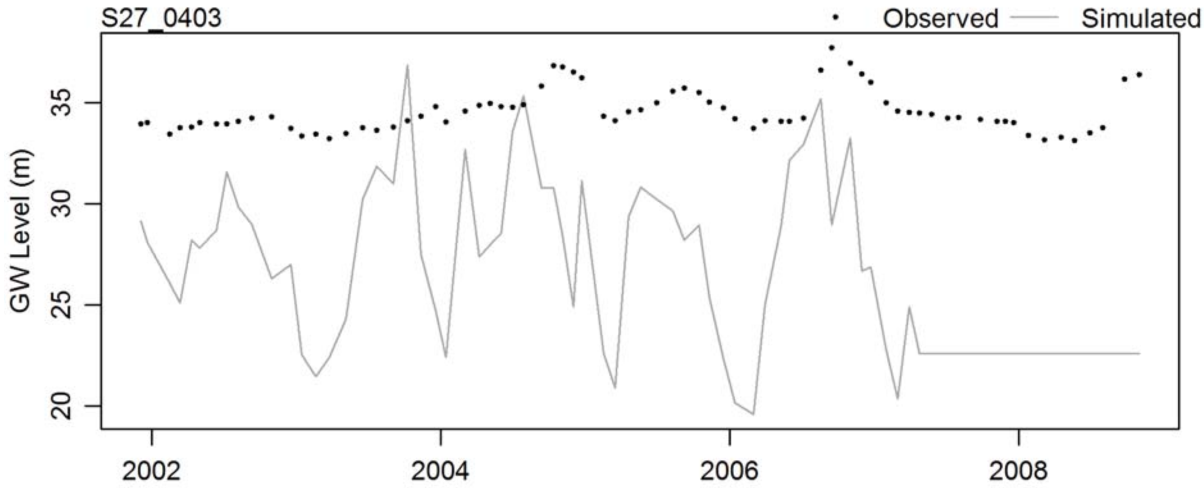
S27_0403
Observed
Simulated
GW Level (m)
35
30
25
20
2002
2004
2006
2008

A10.0 MODELLED AND MEASURED STREAM FLOWS IN THE NORTH MODEL

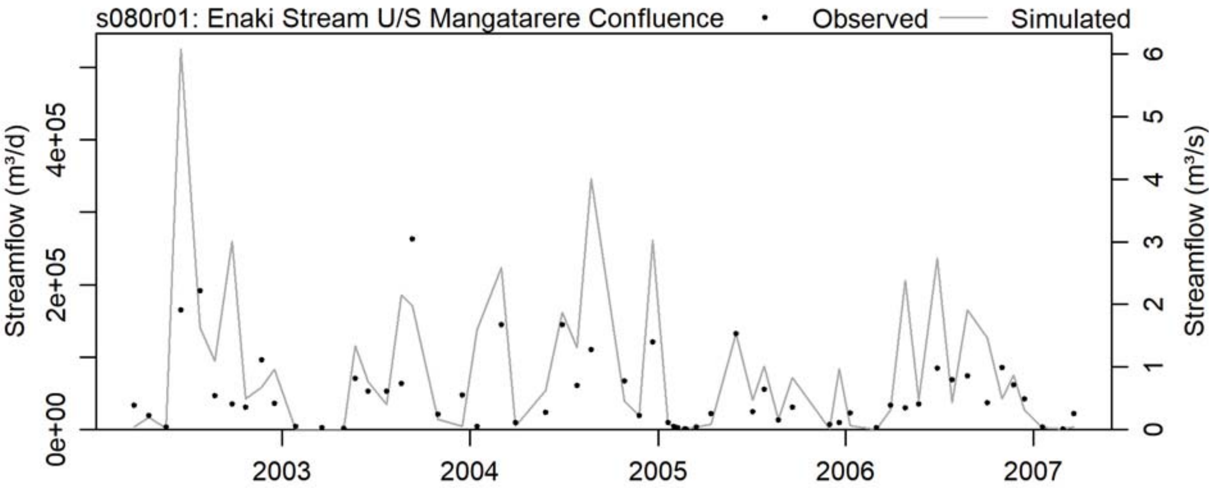

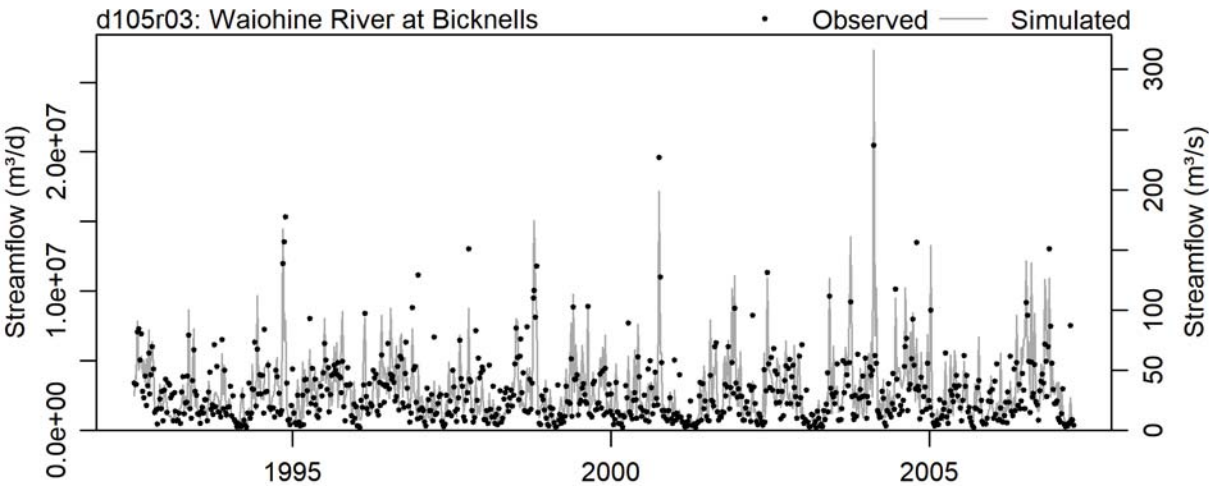

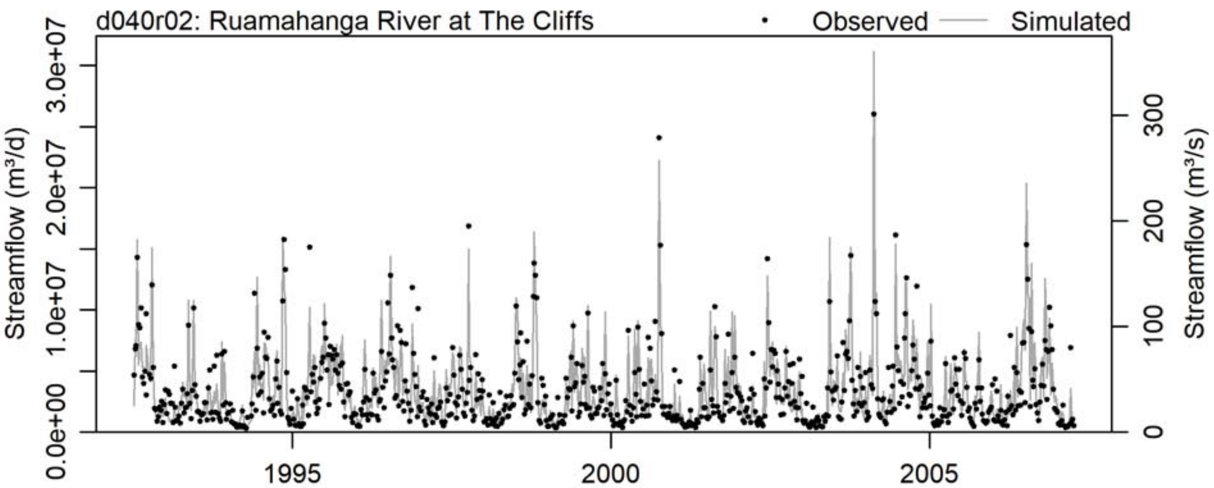

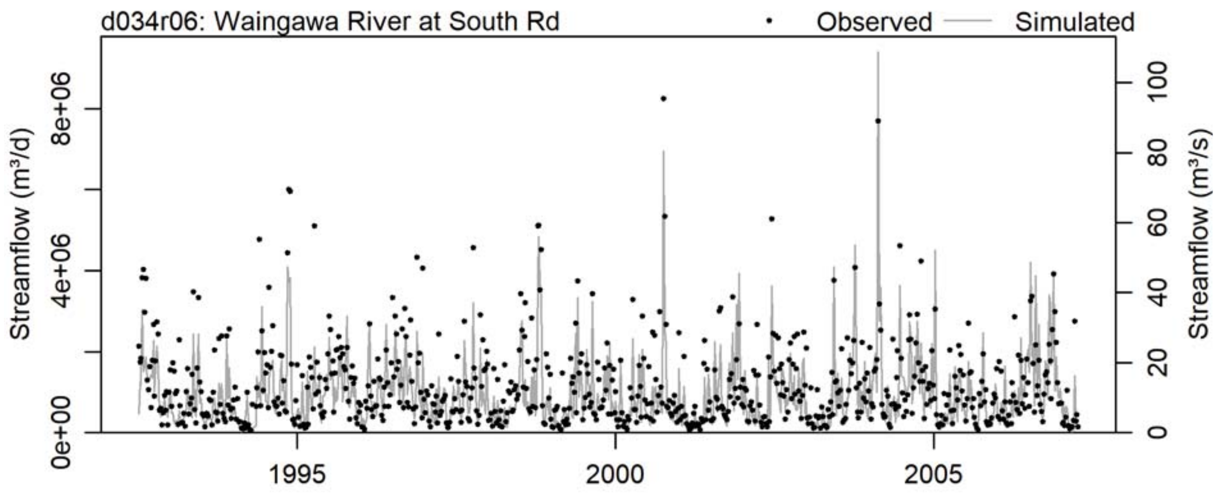
d034r06: Waingawa River at South Rd
Observed
Simulated
Streamflow (m³/d)
Streamflow (m³/s)
0e+00
4e+06
8e+06
0
20
40
60
80
100
1995
2000
2005

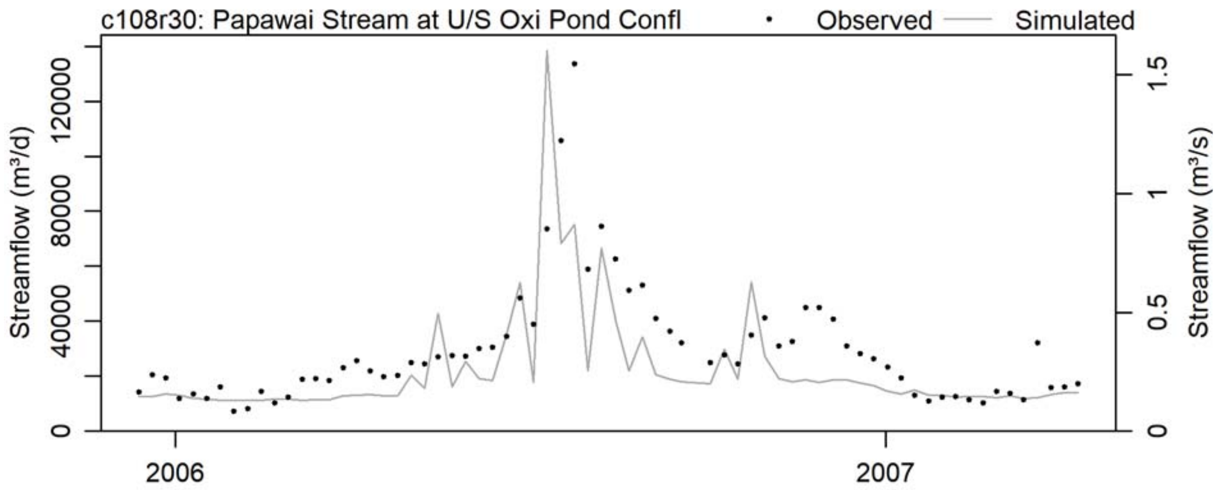
c108r30: Papawai Stream at U/S Oxi Pond Confl
Observed
Simulated
Streamflow (m³/d)
Streamflow (m³/s)
0
40000
80000
120000
0
0.5
1
1.5
2006
2007

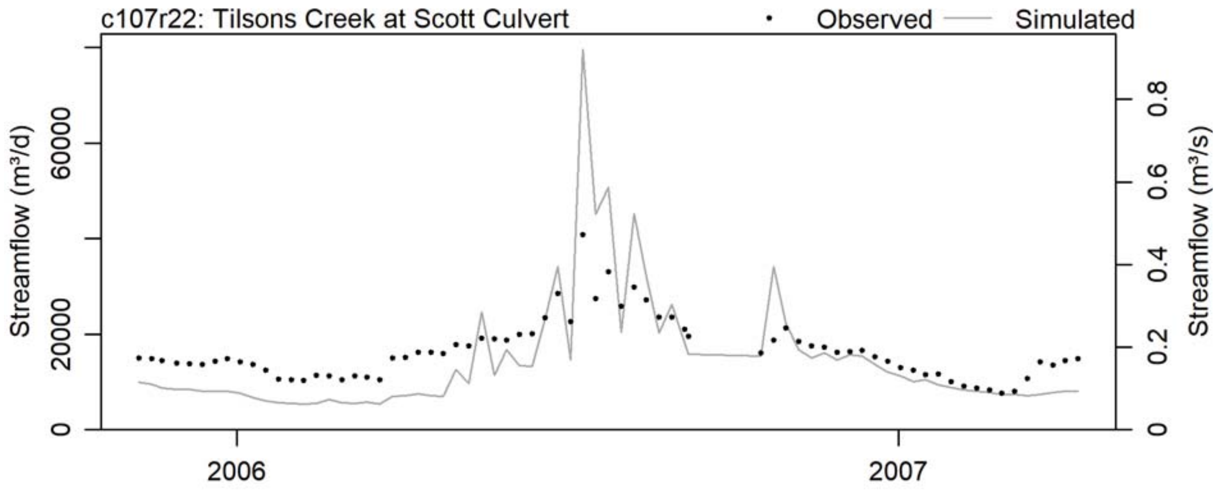
c107r22: Tilsons Creek at Scott Culvert
Observed
Simulated
Streamflow (m³/d)
Streamflow (m³/s)
0
20000
60000
0
0.2
0.4
0.6
0.8
2006
2007

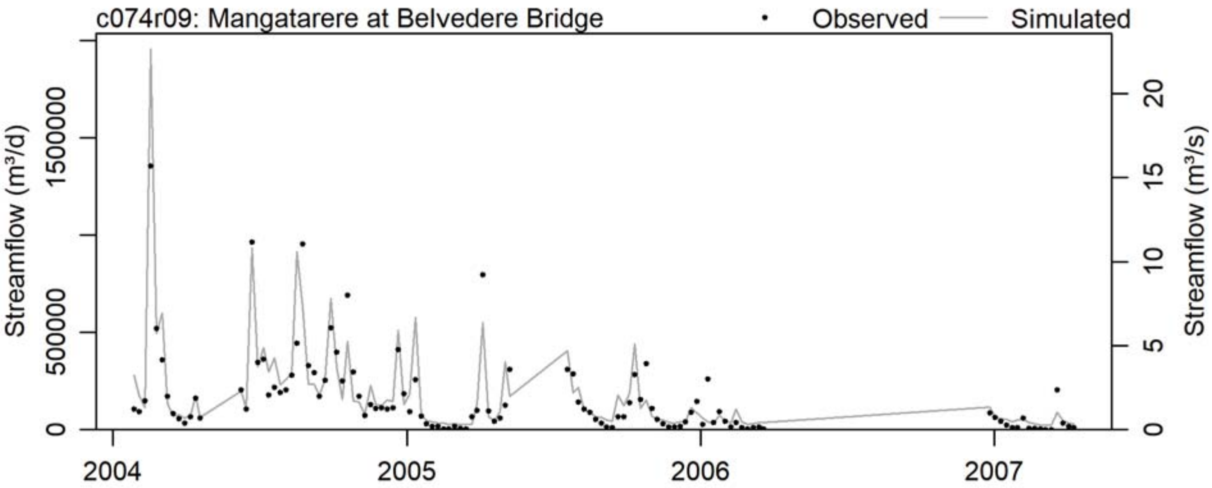
c074r09: Mangatarere at Belvedere Bridge
Observed
Simulated
Streamflow (m³/d)
Streamflow (m³/s)
0
500000
1500000
0
5
10
15
20
2004
2005
2006
2007

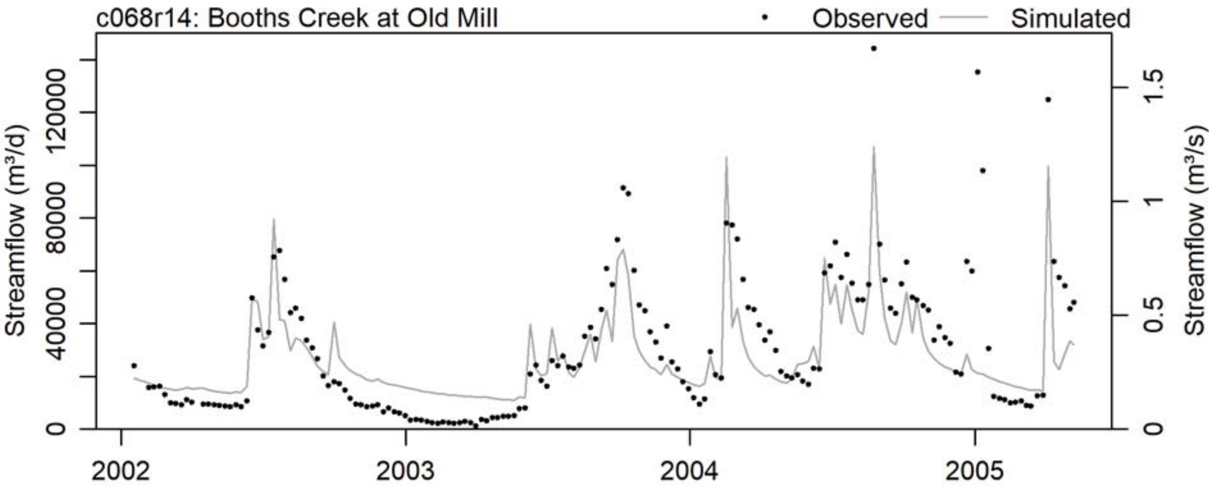
c068r14: Booths Creek at Old Mill
Observed
Simulated
Streamflow (m³/d)
Streamflow (m³/s)
0
40000
80000
120000
0
0.5
1
1.5
2002
2003
2004
2005

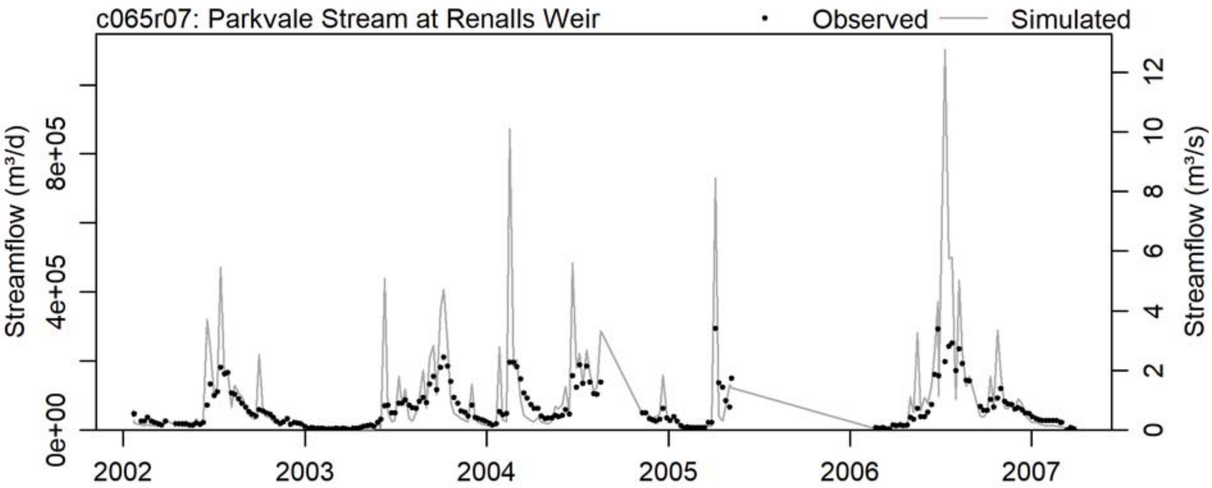
c065r07: Parkvale Stream at Renalls Weir
Observed
Simulated
Streamflow (m³/d)
Streamflow (m³/s)
0e+00
4e+05
8e+05
0
2
4
6
8
10
12
2002
2003
2004
2005
2006
2007

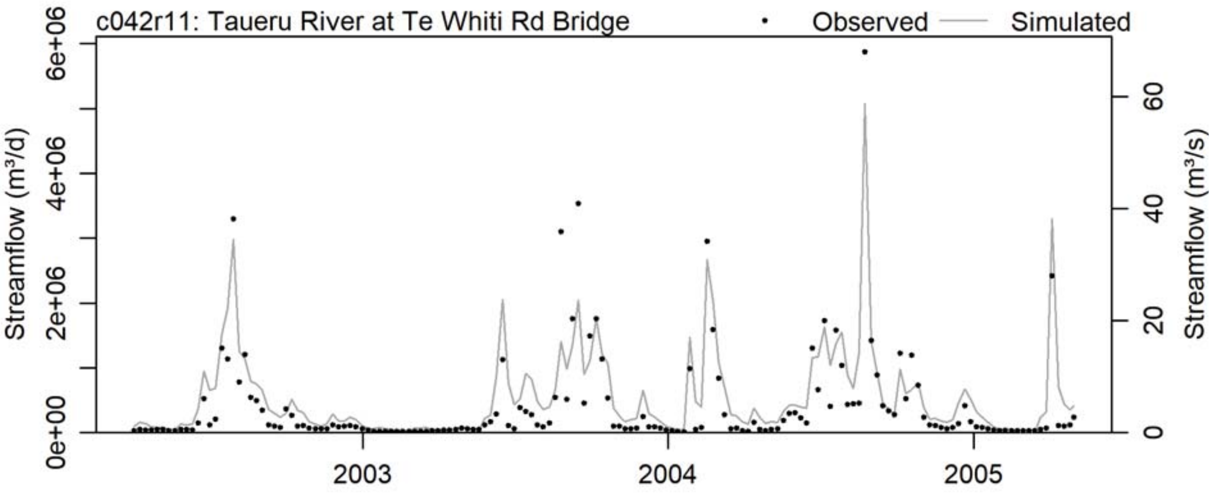
c042r11: Taueru River at Te Whiti Rd Bridge
Observed
Simulated
Streamflow (m³/d)
Streamflow (m³/s)
0e+00
2e+06
4e+06
6e+06
0
20
40
60
2003
2004
2005

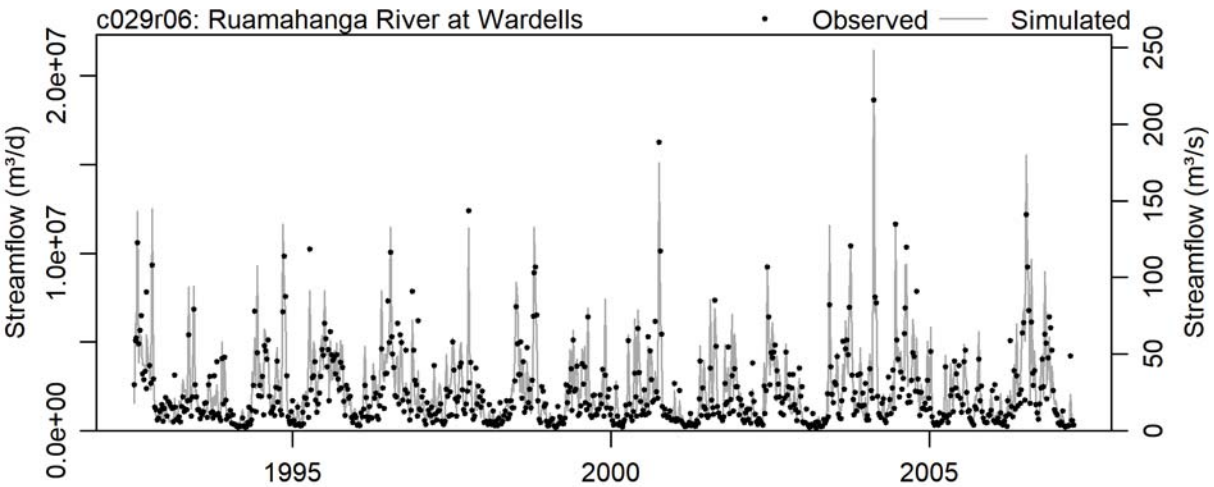
c029r06: Ruamahanga River at Wardells
Observed
Simulated
Streamflow (m³/d)
Streamflow (m³/s)
0.0e+00
1.0e+07
2.0e+07
0
50
100
150
200
250
1995
2000
2005

A11.0 MODELLED AND MEASURED STREAM FLOWS IN THE SOUTH MODEL

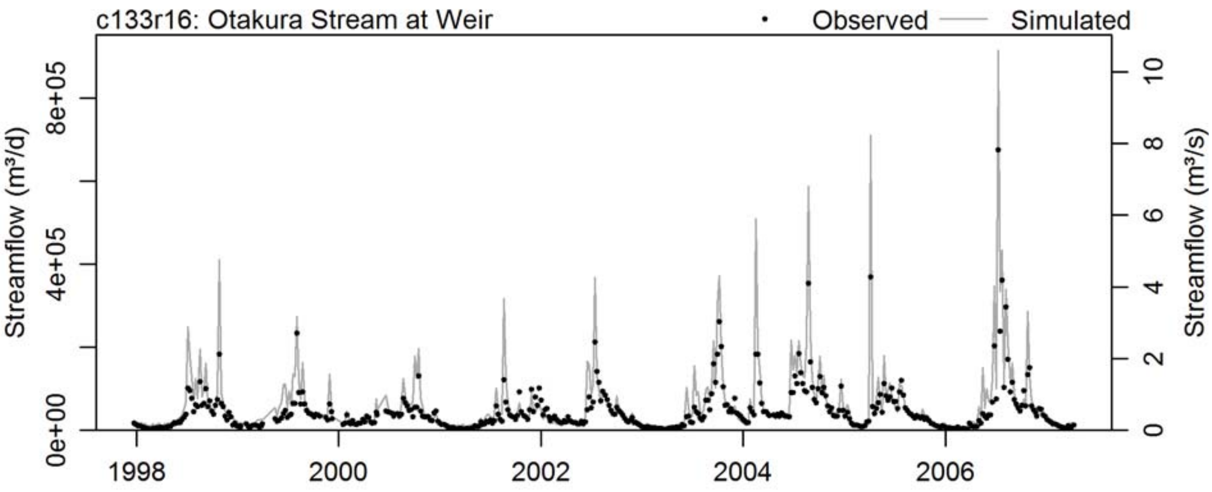

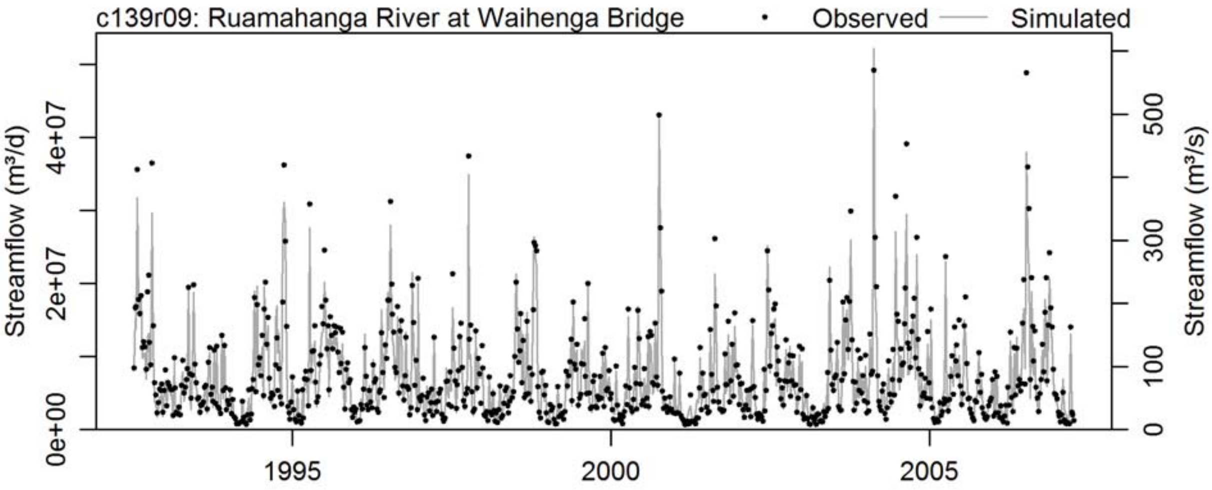

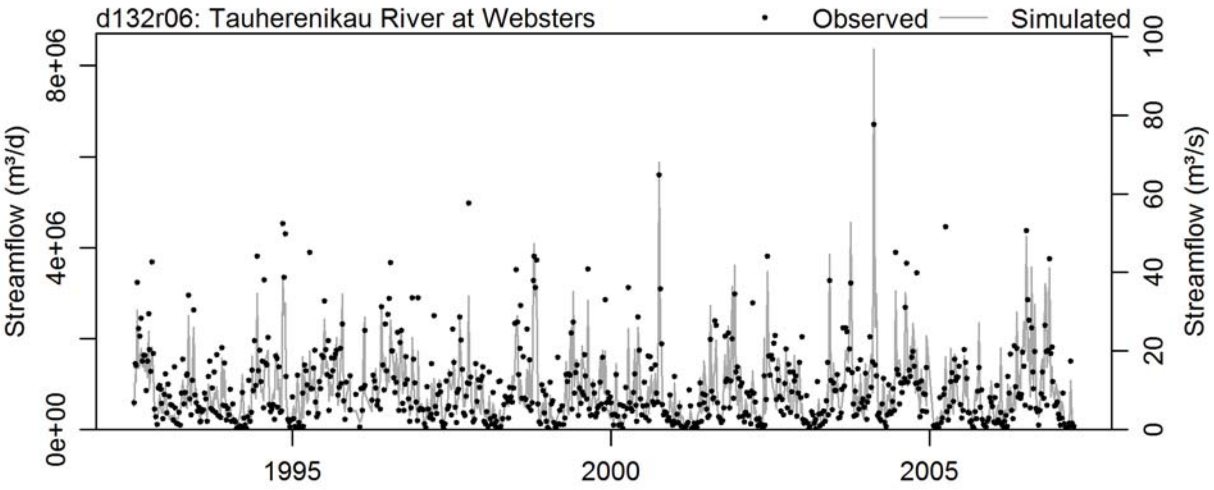
d132r06: Tauherenikau River at Websters
Observed
Simulated
Streamflow (m³/d)
Streamflow (m³/s)
0e+00
4e+06
8e+06
0
20
40
60
80
100
1995
2000
2005

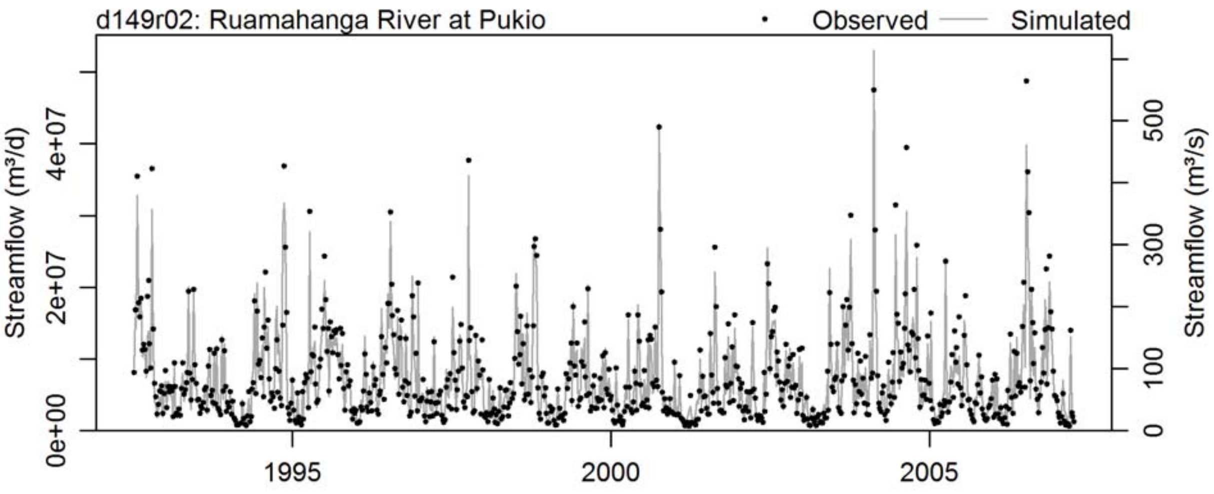
d149r02: Ruamahanga River at Pukio
Observed
Simulated
Streamflow (m³/d)
Streamflow (m³/s)
0e+00
2e+07
4e+07
0
100
300
500
1995
2000
2005

A12.0 FLOW DURATION CURVES FOR STREAM FLOW MONITORING SITES IN THE NORTH MODEL.

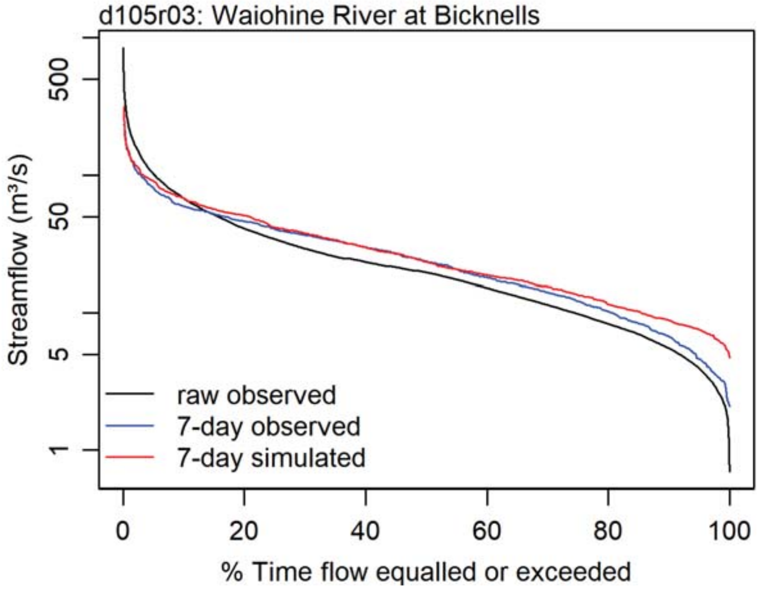

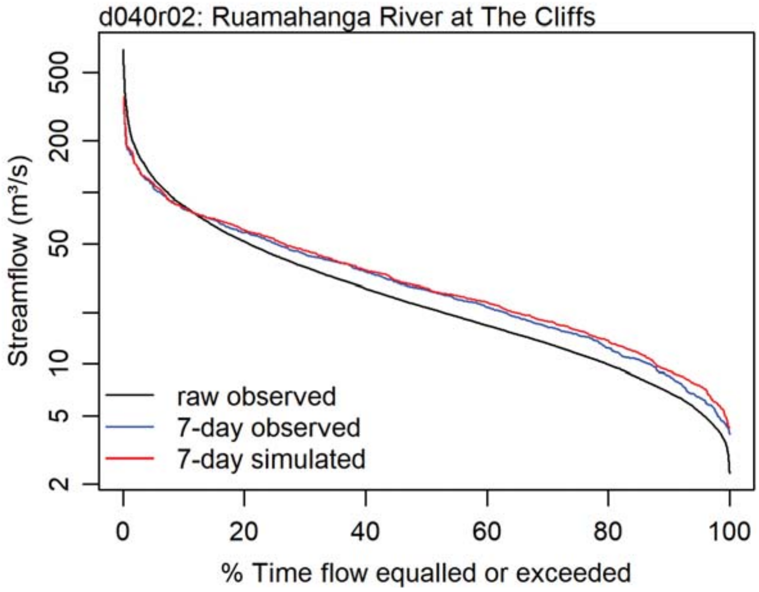

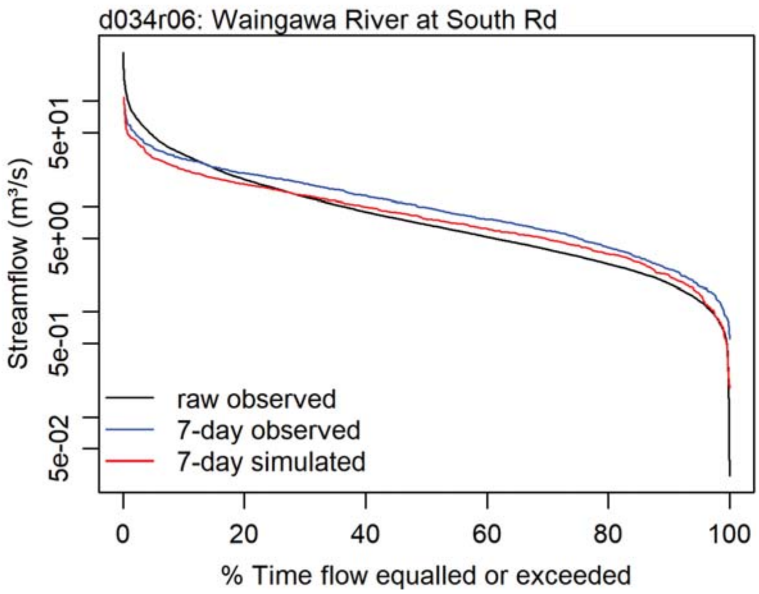
d034r06: Waingawa River at South Rd
Streamflow (m³/s)
5e-02
5e-01
5e+00
5e+01
raw observed
7-day observed
7-day simulated
0
20
40
60
80
100
% Time flow equalled or exceeded

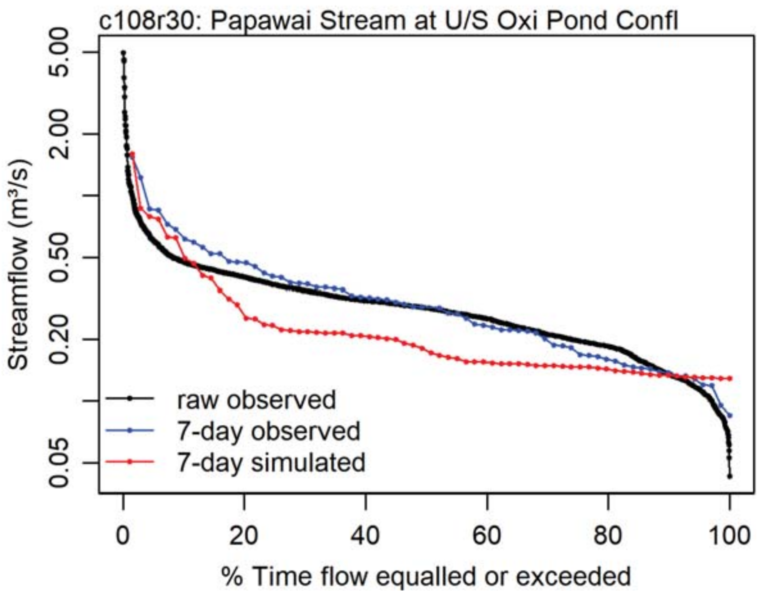
c108r30: Papawai Stream at U/S Oxi Pond Confl
Streamflow (m³/s)
0.05
0.20
0.50
2.00
5.00
raw observed
7-day observed
7-day simulated
0
20
40
60
80
100
% Time flow equalled or exceeded

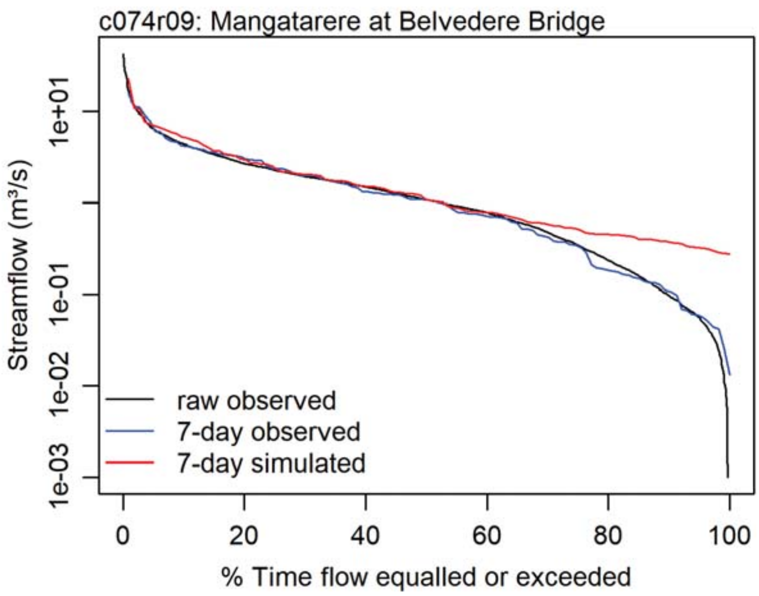
c074r09: Mangatarere at Belvedere Bridge
Streamflow (m³/s)
1e-03
1e-02
1e-01
1e+01
raw observed
7-day observed
7-day simulated
0
20
40
60
80
100
% Time flow equalled or exceeded

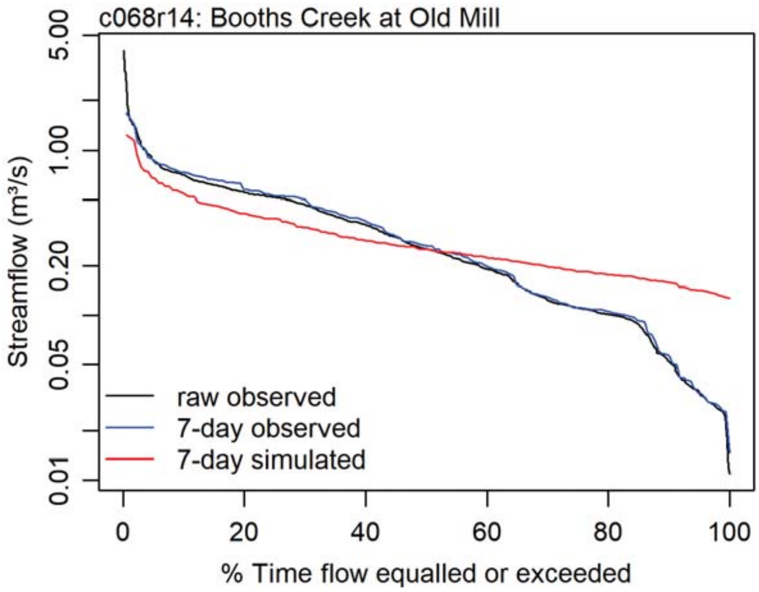
c068r14: Booths Creek at Old Mill
Streamflow (m³/s)
5.00
1.00
0.20
0.05
0.01
raw observed
7-day observed
7-day simulated
0
20
40
60
80
100
% Time flow equalled or exceeded

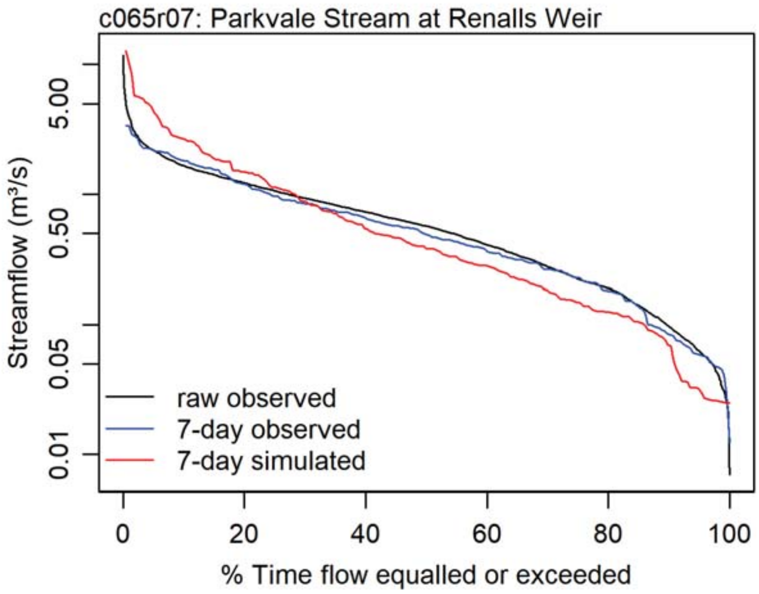
c065r07: Parkvale Stream at Renalls Weir
Streamflow (m³/s)
5.00
0.50
0.05
0.01
raw observed
7-day observed
7-day simulated
0
20
40
60
80
100
% Time flow equalled or exceeded

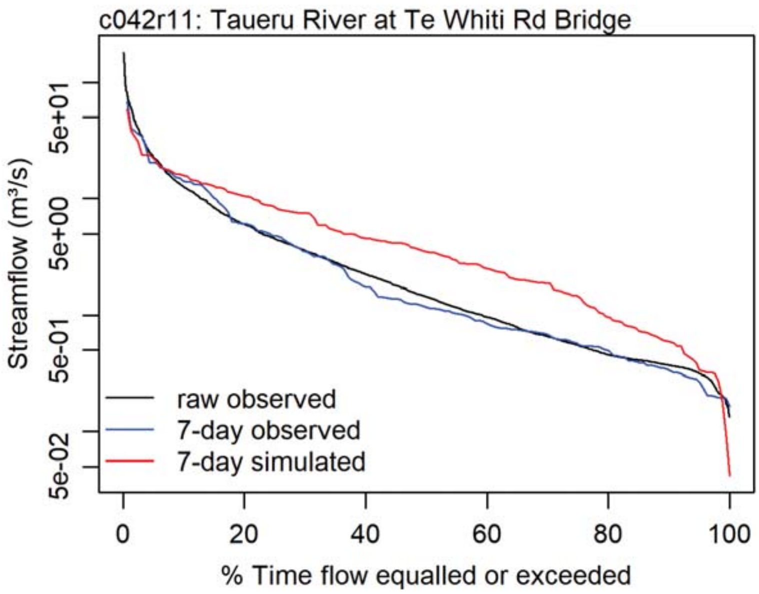
c042r11: Taueru River at Te Whiti Rd Bridge
Streamflow (m³/s)
5e+01
5e+00
5e-01
5e-02
raw observed
7-day observed
7-day simulated
0
20
40
60
80
100
% Time flow equalled or exceeded

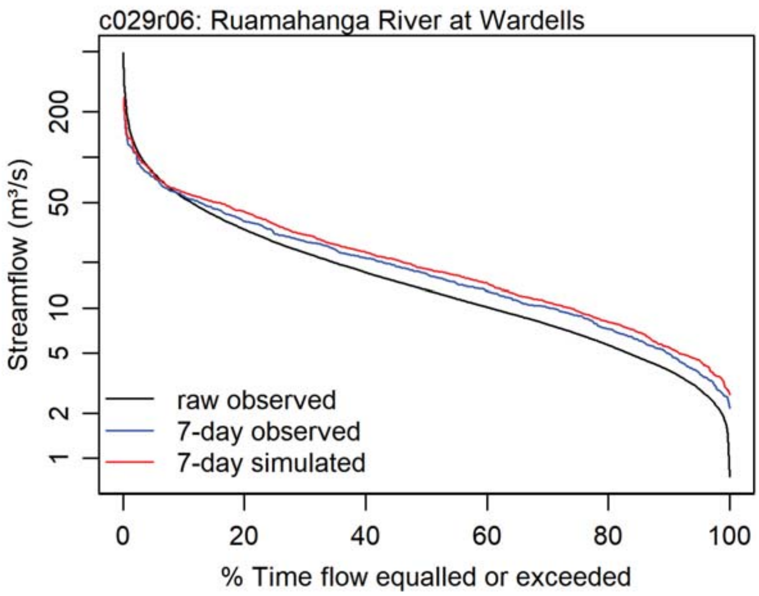
c029r06: Ruamahanga River at Wardells
Streamflow (m³/s)
200
50
10
5
2
1
raw observed
7-day observed
7-day simulated
0
20
40
60
80
100
% Time flow equalled or exceeded

A13.0 FLOW DURATION CURVES FOR STREAM FLOW MONITORING SITES IN THE SOUTH MODEL.

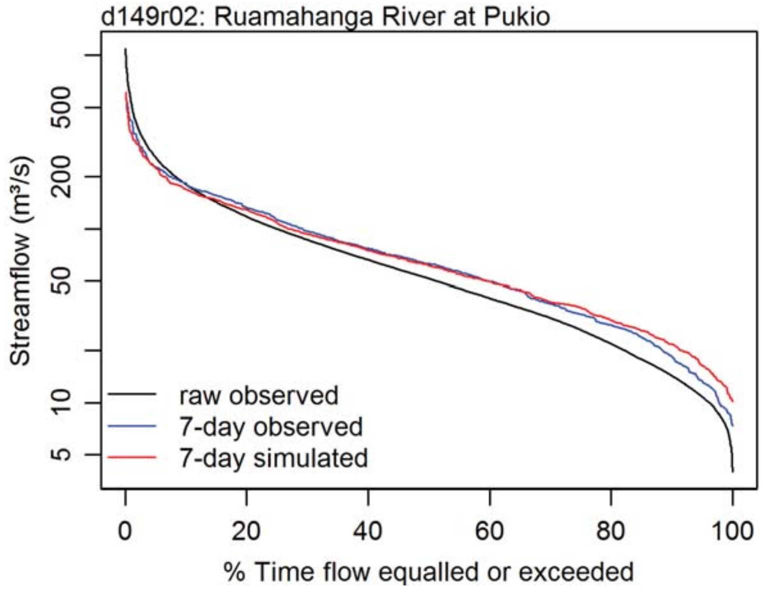

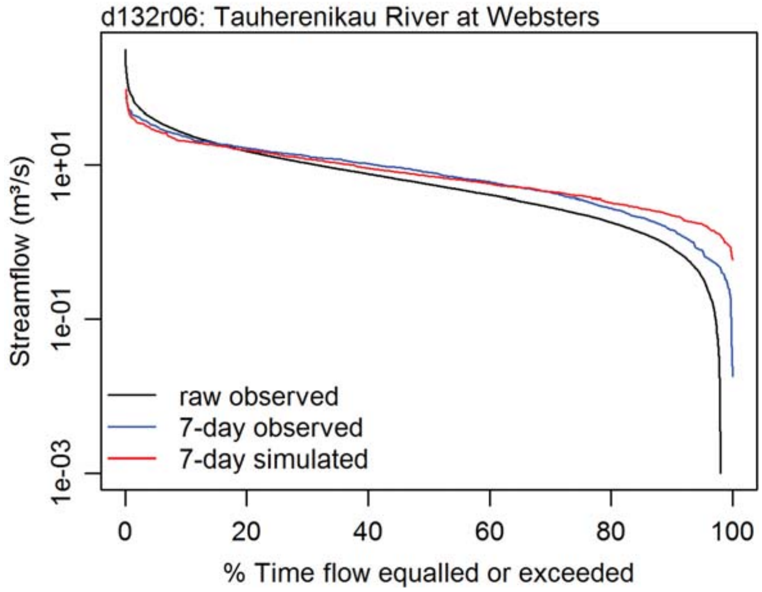

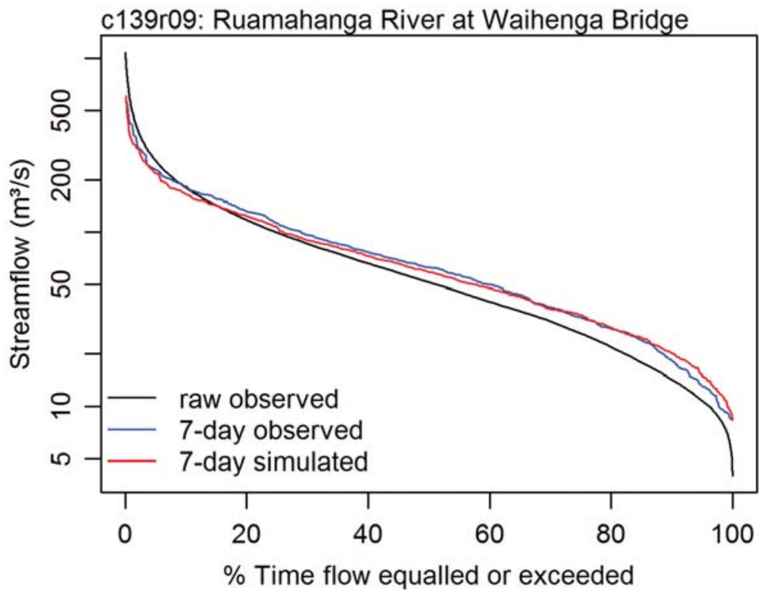
c139r09: Ruamahanga River at Waihenga Bridge
Streamflow (m³/s)
500
200
50
10
5
raw observed
7-day observed
7-day simulated
0
20
40
60
80
100
% Time flow equalled or exceeded

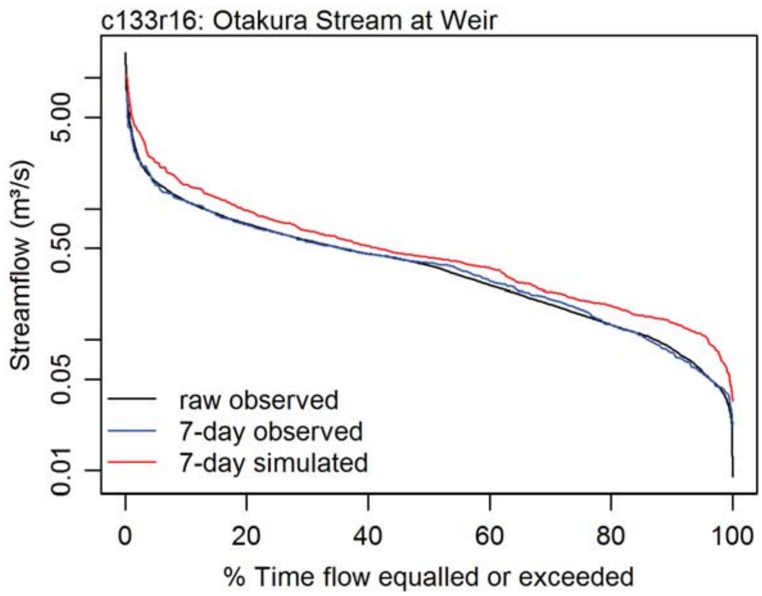
c133r16: Otakura Stream at Weir
Streamflow (m³/s)
5.00
0.50
0.05
0.01
raw observed
7-day observed
7-day simulated
0
20
40
60
80
100
% Time flow equalled or exceeded

A14.0 TABLES OF SURFACE WATER FLOW STATISTICS

Table A14.1 Simulated mean annual low flows for gauging sites in the northern groundwater model.

Site gauging details	Measured mean annual low flow (L/s)	Simulated mean annual low flow (L/s)
Ruamahanga River at Wardells (c029r06)		
1992	6031	4470.81
1993	2480.14	2959.63
1994	3488.57	3733.47
1995	3586	4630.37
1996	4101.57	4856.70
1997	3260.42	3808.72
1998	2402.14	3512.12
1999	2561.85	3552.99
2000	2837.57	3281.22
2001	3880.85	4870.66
2002	2158	2639.46
2003	5436.57	5949.00
2004	3768.28	3402.92
2005	2824	3818.59
2006	2639.57	2838.11
Taueru River at Te Whiti Rd Bridge (c042r11)		
2001	348.8	544.09
2002	193	318.94
2003	164.57	443.59
2004	313.57	42.08
Parkvale Stream at Renalls Weir (c065r07)		
2001	180.14	90.32
2002	29.14	24.80
2003	185.42	115.13
2004	76.14	88.28
2005	47.14	25.02
2006	12.33	76.56
Booths Creek at Old Mill (c068r14)		
2001	97.86	157.52
2002	14.57	127.47

Site gauging details	Measured mean annual low flow (L/s)	Simulated mean annual low flow (L/s)
2003	111	189.04
2004	101.33	168.53
Mangatarere at Belvedere Bridge (c074r09)		
2003	375.14	477.92
2004	50.57	296.87
2005	43.33	312.88
2006	13	276.71
Tilsons Creek at Scott Culvert (c107r22)		
2005	119.29	61.92
2006	88.14	81.73
Papawai Stream at U/S Oxi Pond Confl (c108r30)		
2005	85.14	128.52
2006	119.57	139.02
Waingawa River at South Rd (d034r06)		
1992	1852.43	1423.73
1993	548.14	292.89
1994	1284.00	877.17
1995	908.43	1659.27
1996	1547.57	731.63
1997	1726.00	1528.61
1998	903.43	693.67
1999	857.43	501.94
2000	802.29	596.42
2001	1690.29	1170.41
2002	1259.00	189.20
2003	1511.00	1612.51
2004	1712.86	733.70
2005	840.29	995.61
2006	1173.71	250.22
Ruamahanga River at The Cliffs (d040r02)		
1992	8523.14	7365.97
1993	3871.71	4695.05

Site gauging details	Measured mean annual low flow (L/s)	Simulated mean annual low flow (L/s)
1994	5654.57	6108.96
1995	5330.57	7926.87
1996	6446.29	7183.76
1997	5780.29	7006.89
1998	4275.43	5601.24
1999	4305.57	5467.80
2000	4500.14	5301.48
2001	6440.71	7621.59
2002	4222.71	4298.81
2003	7750.00	9239.38
2004	6216.57	5483.36
2005	5554.14	6647.81
2006	4621.71	4259.16
Waiohine River at Bicknells (d105r03)		
1992	5593.29	6971.96
1993	2527.29	5295.27
1994	3733.86	7749.32
1995	2083.29	8462.09
1996	3465.00	7303.33
1997	5081.43	6502.03
1998	3323.43	5986.85
1999	2827.86	6080.81
2000	2311.00	5231.46
2001	4446.71	7886.07
2002	2196.86	4719.20
2003	3735.86	10390.01
2004	4074.57	6891.99
2005	2315.71	7824.47
2006	3225.71	5580.99

Table A14.2 Simulated mean annual low flows for gauging sites in the southern groundwater model.

Site gauging details	Measured mean annual low flow (L/s)	Simulated mean annual low flow (L/s)
Tauherenikau River at Websters (d132r06)		
1992	1134.14	1839.29
1993	240.00	888.78
1994	459.86	1263.41
1995	628.00	1856.57
1996	189.86	1204.80
1997	320.67	1675.44
1998	255.33	937.02
1999	412.00	945.40
2000	18.00	865.76
2001	376.71	1721.46
2002	190.33	584.31
2003	819.29	2155.85
2004	543.50	974.89
2005	394.00	1239.93
2006	318.33	679.45
Ruamahanga River at Pukio (d149r02)		
1992	22714.29	20000.92
1993	8569.00	10117.32
1994	9223.43	13168.78
1995	12589.29	11159.02
1996	13713.29	12602.04
1997	12009.00	13373.76
1998	9191.71	10556.41
1999	9102.71	16286.53
2000	7309.71	12790.79
2001	13457.43	14939.85
2002	8627.71	12091.16
2003	16881.29	24854.81
2004	11953.29	16536.12
2005	10807.43	12291.23
2006	7693.00	14720.76

Site gauging details	Measured mean annual low flow (L/s)	Simulated mean annual low flow (L/s)
Otakura Stream at Weir (c133r16)		
1997	39.71	0.00
1998	68.14	0.00
1999	159.00	0.00
2000	31.29	0.00
2001	182.86	0.00
2002	29.43	0.00
2003	217.71	0.00
2004	112.00	0.00
2005	22.00	0.00
2006	53.57	0.00
Ruamahanga River at Waihenga Bridge/ Ruamahanga River at Waihenga Troll (c139r09)		
1992	22372.86	18521.39
1993	8464.71	8453.62
1994	9861.43	11520.95
1995	12416.14	9793.22
1996	13653.00	10986.94
1997	11758.00	12285.55
1998	9239.57	9316.85
1999	8993.29	14950.16
2000	8343.43	11804.52
2001	13448.43	13251.98
2002	8520.14	10947.32
2003	16739.86	23081.55
2004	11848.00	15261.63
2005	10827.86	10583.85
2006	9575.57	13387.68

Table A14.3 Simulated and measured 7-day period below partial and full low flow restrictions for gauging sites in the northern groundwater model.

Site gauging details	Measured number of 7 day periods below partial low flow restriction	Measured number of 7 day periods below full low flow restriction	Simulated number of 7 day periods below partial low flow restriction	Simulated number of 7 day periods below full low flow restriction
Ruamahanga River at Wardells (c029r06)				
1992	0	0	0	0
1993	2	0	0	0
1994	0	0	0	0
1995	0	0	0	0
1996	0	0	0	0
1997	0	0	0	0
1998	2	0	0	0
1999	1	0	0	0
2000	0	0	0	0
2001	0	0	0	0
2002	3	1	1	0
2003	0	0	0	0
2004	0	0	0	0
2005	0	0	0	0
2006	1	0	0	0
Parkvale Stream at Renalls Weir (c065r07)				
2001	0	0	2	1
2002	16	15	21	21
2003	0	0	1	0
2004	6	6	5	2
2005	5	5	14	12
2006	3	3	6	3
Papawai Stream at U/S Oxi Pond Confl (c108r30)				
2005		7		22
2006		8		11

Table A14.4 Simulated and measured 7-day period below partial and full low flow restrictions for gauging sites in the southern groundwater model.

Site gauging details	Measured number of 7 day periods below partial low flow restriction	Measured number of 7 day periods below full low flow restriction		Measured number of 7 day periods below partial low flow restriction
Otakura Stream at Weir (c133r16)				
1997		12		0
1998		3		0
1999		0		0
2000		14		1
2001		0		0
2002		17		8
2003		0		0
2004		0		0
2005		13		9
2006		6		1
Ruamahanga River at Waihenga Bridge/ Ruamahanga River at Waihenga Troll (c139r09)				
1992	0	0	0	0
1993	1	1	2	1
1994	0	0	0	0
1995	0	0	0	0
1996	0	0	0	0
1997	0	0	0	0
1998	0	0	0	0
1999	1	0	0	0
2000	2	1	0	0
2001	0	0	0	0
2002	2	0	0	0
2003	0	0	0	0
2004	0	0	0	0
2005	0	0	0	0
2006	0	0	0	0